Catalysis by Metal Complexes 38
Series Editors:
D.J. Cole-Hamilton · P.W.N.M. van Leeuwen

Pedro J. Pérez *Editor*

Alkane C–H Activation by Single-Site Metal Catalysis

Springer

Catalysis by Metal Complexes

Volume 38

For further volumes:
http://www.springer.com/series/5763

Catalysis by Metal Complexes

This book series covers topics of interest to a wide range of academic and industrial chemists, and biochemists. Catalysis by metal complexes plays a prominent role in many processes. Developments in analytical and synthetic techniques and instrumentation, particularly over the last 30 years, have resulted in an increasingly sophisticated understanding of catalytic processes.

Industrial applications include the production of petrochemicals, fine chemicals, and pharmaceuticals (particularly through asymmetric catalysis), hydrometallurgy, and waste-treatment processes. Many life processes are based on metallo-enzyme systems that catalyze redox and acid–base reactions.

Catalysis by metal complexes is an exciting, fast developing, and challenging interdisciplinary topic which spans and embraces the three areas of catalysis: heterogeneous, homogeneous, and metallo-enzyme.

Catalysis by Metal Complexes deals with all aspects of catalysis which involve metal complexes and seeks to publish authoritative, state-of-the-art volumes which serve to document the progress being made in this interdisciplinary area of science.

Series Editors

Prof. D. J. Cole-Hamilton
EaStChem, School of Chemistry
University of St Andrews
Purdie Building, North Haugh
St Andrews, Fife KY16 9ST
Scotland, UK

Prof. Piet W. N. M. van Leeuwen
Institute of Chemical Research of Catalonia
Av. Paisos Catalans 16
43007 Tarragona
Spain

Volume 38:
Alkane C–H Activation by Single-Site Metal Catalysis

Volume Editor

Pedro J. Pérez
Laboratorio de Catálisis Homogénea
Departamento de Química y Ciencia de los Materiales
Unidad Asociada al CSIC, Centro de Investigación en Química Sostenible
Universidad de Huelva Campus de El Carmen
21007 Huelva, Spain
E-mail: perez@dqcm.uhu.es

Pedro J. Pérez
Editor

Alkane C–H Activation by Single-Site Metal Catalysis

Springer

Editor
Pedro J. Pérez
Laboratorio de Catálisis Homogénea
Departamento de Química y Ciencia de los Materiales
Unidad Asociada al CSIC
Centro de Investigación en Química Sostenible
Universidad de Huelva
Huelva
Spain

ISSN 0920-4652
ISBN 978-90-481-3697-1 ISBN 978-90-481-3698-8 (eBook)
DOI 10.1007/978-90-481-3698-8
Springer Dordrecht Heidelberg New York London

Library of Congress Control Number: 2012943629

© Springer Science+Business Media Dordrecht 2012
This work is subject to copyright. All rights are reserved by the Publisher, whether the whole or part of the material is concerned, specifically the rights of translation, reprinting, reuse of illustrations, recitation, broadcasting, reproduction on microfilms or in any other physical way, and transmission or information storage and retrieval, electronic adaptation, computer software, or by similar or dissimilar methodology now known or hereafter developed. Exempted from this legal reservation are brief excerpts in connection with reviews or scholarly analysis or material supplied specifically for the purpose of being entered and executed on a computer system, for exclusive use by the purchaser of the work. Duplication of this publication or parts thereof is permitted only under the provisions of the Copyright Law of the Publisher's location, in its current version, and permission for use must always be obtained from Springer. Permissions for use may be obtained through RightsLink at the Copyright Clearance Center. Violations are liable to prosecution under the respective Copyright Law.
The use of general descriptive names, registered names, trademarks, service marks, etc. in this publication does not imply, even in the absence of a specific statement, that such names are exempt from the relevant protective laws and regulations and therefore free for general use.
While the advice and information in this book are believed to be true and accurate at the date of publication, neither the authors nor the editors nor the publisher can accept any legal responsibility for any errors or omissions that may be made. The publisher makes no warranty, express or implied, with respect to the material contained herein.

Printed on acid-free paper

Springer is part of Springer Science+Business Media (www.springer.com)

Dedicated
to María, Pedro L. and Jose M.;
to Rosario and Ezequiel

Foreword

The field of carbon–hydrogen bond activation has changed dramatically since Alexander Shilov's profoundly important discovery of platinum-catalyzed hydrocarbon functionalization many years ago. In contrast to this intermolecular C–H activation chemistry, subsequent research published during the 1960s and early 1970s involved intramolecular cyclometallation reactions—often of aromatic C–H bonds, but in a few cases aliphatic C–H bonds were also found to undergo this reaction. Glimmers of future breakthroughs in this field were provided by work on "agostic" C–H/metal interactions, the finding that C–H bonds adjacent to aromatic and silicon groups could undergo oxidative addition reactions, and early dehydrogenation reactions that were among the few after the early Shilov work to report this transformation in catalytic processes. However, it was not until the early 1980s that direct observation of an overall oxidative addition of a metal to an aliphatic C–H bond was demonstrated. Later in that decade, important further advances were published, such as gas phase and solution flash kinetic studies on alkane complexes that were later corroborated by direct NMR detection.

While these experiments renewed interest in the field, it is probably fair to say that the activity which occurred in the 1980s and 1990s pales in light of the explosion of C–H activation chemistry that has occurred in the past decade. Much of the early work in this area focused on the discovery of stoichiometric organometallic reactions and gaining an understanding of the basic mechanistic principles behind C–H oxidative addition. These initial studies were crucial to overcoming the criticisms that many of us in the field heard in the early days—for example, that C–H bond activation would always be plagued by poor selectivity, and that it would be impossible to carry out C–H bond functionalization reactions catalytically. That these have proven to be overly pessimistic prognostications is demonstrated by the discoveries summarized in Brent Gunnoe's comprehensive Introduction and the chapters that follow it in this book. In the organic area, it is clear that synthetic methods chemists have developed many catalytic C–H activation reactions, for example methods for the addition of aromatic and vinyl C–H bonds to multiple bonds in partner reactants. Several of these processes have been accepted into the lexicon of truly useful transformations that can be applied in drug

synthesis and the total synthesis of complex natural products. The discovery of catalytic borylation of alkanes and arenes represents another important landmark. The application of C–H activation catalysis to a useful, large-scale industrial conversion of alkane feedstocks such as methane to a transportable fuel such as methanol remain to be achieved, but the finding that it is possible to attain substantial conversion for catalytic methane oxygenation, by protecting the product methanol from further oxidation by in situ derivatization, provides hope that this problem will ultimately be solved. These discoveries are an important complement to metal-catalyzed organic oxidations, coupling reactions, and metathesis reactions that have received Nobel Prize recognition during the past decade. Concurrently, chemical biologists and bioinorganic chemists have begun to reveal the importance that C–H activation reactions play in biological systems and have made substantial progress in elucidating their mechanisms and modeling these processes in synthetic biomimetic systems.

The history of C–H bond activation, and the current research described in this book, provides a hint of the understanding and applications that lie before us as this field continues to be explored by an increasingly visionary and enthusiastic group of organic, organometallic, biological, and physical chemists.

Berkeley, CA, 2012 Robert G. Bergman

Preface

Over the past decade, carbon–hydrogen bond activation has been probably one of the most studied fields in Chemistry, as demonstrated by the increasing amount of publications on the subject.

Thirty years ago, the activation of carbon–hydrogen bonds of hydrocarbons by transition metal complexes led researchers to believe that the development of catalytic systems could convert the readily available alkanes into value added products. However, despite the simplicity and affordability of these raw materials, to date their use in industrial chemistry is still very limited.

Alkane C–H Activation by Single-Site Metal Catalysis presents the current state-of-the-art development in the catalytic systems for the catalytic transformations of alkanes under homogeneous conditions. Its six chapters follow the timeline of achievements in the field. Chapter 1 summarizes the overall vision of the subject. Chapter 2 reviews the so-called electrophilic activation, initiated by Shulpín in the late 1960s, and the base for the Catalytica system. Chapter 3 examines the catalytic borylation of alkanes, discovered by Hartwig, whereas Chap. 4 provides an updated vision of the alkane dehydrogenation reaction. Chapter 5 covers the oxygenation of C–H bonds, a field of enormous interest with bioinorganic implications, and finally Chap. 6 presents the functionalization of alkane C–H bonds by carbene or nitrene insertion.

Each chapter concludes with a perspective of the topics discussed to inspire future works on alkanes and to motivate more and more researchers to take part in the challenge of converting alkanes into practical raw materials for industrial chemistry.

Huelva, Spain, 2012 Pedro J. Pérez

Contents

Contributors

Chulsung Bae Department of Chemistry, University of Nevada Las Vegas, 4505 Maryland Parkway, Box 454003, Las Vegas, NV 89154-4003, USA, e-mail: chulsung.bae@unlv.edu

Maurice Brookhart Department of Chemistry, University of North Carolina at Chapel Hill, Chapel Hill, NC 27599, USA, e-mail: mbrookhart@unc.edu

Ana Caballero Laboratorio de Catálisis Homogénea, Departamento de Química y Ciencia de los Materiales, Unidad Asociada al CSIC, Centro de Investigación en Química Sostenible, Universidad de Huelva, Campus de El Carmen, 21007 Huelva, Spain, e-mail: ana.caballero@dqcm.uhu.es

Jongwook Choi Department of Chemistry and Chemical Biology, Rutgers, The State University of New Jersey, New Brunswick, NJ 08903, USA, e-mail: Jongwook@rci.rutgers.edu

Anna Company Department de Química, Universitat de Girona, Campus de Montilivi, 17071 Girona, Spain, e-mail: anna.company@udg.edu

Miquel Costas Department de Química, Universitat de Girona, Campus de Montilivi, 17071 Girona, Spain, e-mail: miquel.costas@udg.edu

M. Mar Díaz-Requejo Laboratorio de Catálisis Homogénea, Departamento de Química y Ciencia de los Materiales, Unidad Asociada al CSIC, Centro de Investigación en Química Sostenible, Universidad de Huelva, Campus de El Carmen, 21007 Huelva, Spain, e-mail: mmdiaz@dqcm.uhu.es

Michael Findlater Department of Chemistry, University of North Carolina at Chapel Hill, Chapel Hill, NC 27599, USA, e-mail: findlate@email.unc.edu

Manuel R. Fructos Laboratorio de Catálisis Homogénea, Departamento de Química y Ciencia de los Materiales, Unidad Asociada al CSIC, Centro de Investigación en Química Sostenible, Universidad de Huelva, Campus de El Carmen, 21007 Huelva, Spain, e-mail: manuel.romero@dqcm.uhu.es

Alan Goldman Department of Chemistry and Chemical Biology, Rutgers, The State University of New Jersey, New Brunswick, NJ 08903, USA, e-mail: alan.goldman@rutgers.edu

T. Brent Gunnoe Department of Chemistry, University of Virginia, McCormick Road, P.O. Box 400319, Charlottesville, VA 22904-4319, USA, e-mail: tbg7h@virginia.edu

Laura Gómez Department de Química, Universitat de Girona, Campus de Montilivi, 17071 Girona, Spain, e-mail: laura.gomez@udg.edu

Jay A. Labinger Beckman Institute, California Institute of Technology, 139-74, Pasadena, CA 91125, USA, e-mail: jal@its.caltech.edu

Julio Lloret Department de Química, Universitat de Girona, Campus de Montilivi, 17071 Girona, Spain, e-mail: julio.lloret@udg.edu

Pedro J. Pérez Laboratorio de Catálisis Homogénea, Departamento de Química y Ciencia de los Materiales, Unidad Asociada al CSIC, Centro de Investigación en Química Sostenible, Universidad de Huelva, Campus de El Carmen, 21007 Huelva, Spain, e-mail: perez@dqcm.uhu.es

Chapter 1
Introduction: Alkane C–H Activation by Single-Site Metal Catalysis

T. Brent Gunnoe

Abstract An overview of the importance and potential impact of catalysts for the selective functionalization of hydrocarbons is given. The presentation includes a brief history of metal-mediated C–H activation and review of various transformations by which metals induce the cleavage of C–H bonds. An introduction to some of the prominent strategies to develop transition metal catalysts for alkane functionalization is presented.

1.1 Introduction

The selective functionalization of carbon-hydrogen bonds is one of the foremost challenges for synthetic chemists. In particular, controlled transformations of hydrocarbons derived from fossil resources have been highly sought, but accessing selective routes to convert hydrocarbons to functionalized materials has been challenging. The development of low temperature ($\leq$250 °C) and selective processes that provide high yields for alkane derivatization is one of, if not the, most challenging goals in the field of catalysis. With some exceptions (e.g., allylic or benzylic C–H bonds), typical C–H bond dissociation energies (BDEs) of hydrocarbons fall in the range of $\sim$95–110 kcal/mol. As a result, synthetic strategies for the manipulation of hydrocarbons that rely on homolytic C–H bond cleavage require high-energy reactants, and such substrates can be tedious to prepare and impractical for scale-up. Also, achieving selectivity for radical

T. B. Gunnoe (✉)
Department of Chemistry, University of Virginia, McCormick Road, 400319, Charlottesville, VA 22904-4319, USA
e-mail: tbg7h@virginia.edu

P. J. Pérez (ed.), *Alkane C–H Activation by Single-Site Metal Catalysis*, Catalysis by Metal Complexes 38, DOI: 10.1007/978-90-481-3698-8_1,
© Springer Science+Business Media Dordrecht 2012

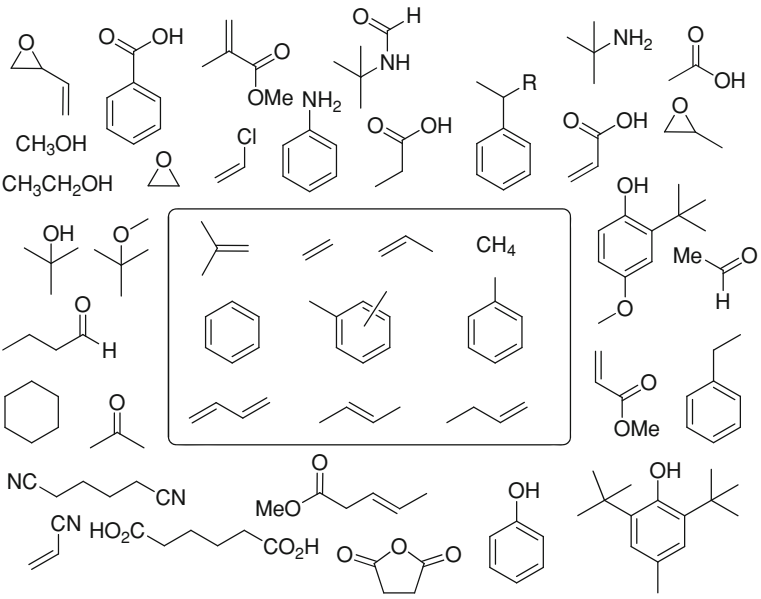

Scheme 1.1 Important hydrocarbons that are derived from fossil resources (shown in *box*) and examples of compounds that are produced from them

processes is often not feasible. In addition to the substantial homolytic bond dissociation energies, the covalent nature of the typical C–H bond is perhaps an equally important factor that renders C–H functionalization difficult. In general, hydrocarbons are neither basic nor acidic, and they are not typically susceptible to reactions with nucleophiles or electrophiles with the exception of extremely reactive substrates (e.g., super acids) [1].

Recently, several catalytic methods for C–H functionalization of substrates that possess heteroatoms have been developed [2–8]. The C–H bond activation of hetero-functionalized substrates has two advantages over manipulation of hydrocarbons: (1) the hetero-functionality can serve to coordinate the substrate to the catalyst, and (2) the functional group can activate the C–H bond toward cleavage. Catalysts that selectively functionalize hydrocarbons, especially alkanes, represent a more substantial challenge. Thus, extension of the exciting achievements in the C–H functionalization of hetero-substituted systems to hydrocarbons has evolved at a slower pace. Scheme 1.1 shows the primary hydrocarbons used in the chemical industry and several compounds that are produced from them. This scheme illustrates the central importance of methodologies for hydrocarbon hetero-functionalization for the petrochemical industry [9, 10].

Synthetic manipulation of unsaturated hydrocarbons is more facile than transformations of saturated substrates. As a result, the primary building blocks of the petrochemical industry are mainly composed of unsaturated compounds that possess one or more carbon–carbon double bonds (Scheme 1.1). Some of these

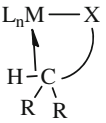

Fig. 1.1 Carbon-hydrogen agostic interaction

unsaturated substrates are accessed by cracking, which is an energy intensive process (generally 650–900 °C) [10]. Although methane is listed as a feedstock, it is most commonly used indirectly by conversion to syngas, a mixture of CO and H_2, which is then converted in a second step to higher value compounds (e.g., by Fischer–Tropsch chemistry). The development of efficient catalysts for direct alkane functionalization could open the door to increased use of alkanes as precursors for the petrochemical industry. Additionally, catalysts for low temperature hydrocarbon functionalization could result in less energy intensive processes for the use of fossil feedstocks.

1.2 Brief History and Description of Metal-Mediated C–H Activation

For several decades, chemists have been pursuing the development and understanding of systems that activate C–H bonds. Focused efforts in this area began with the discovery of C–H agostic bonds, which are chelated C–H units that bond with a metal (Fig. 1.1) [11, 12]. In addition, examples of transition metal-mediated cleavage of C–H bonds, which were rare at that time, spurred additional interest in this area [13, 14].

Reports of catalytic transition metal-mediated reactions with hydrocarbons, including methane, prompted activity to develop and understand well-defined transformations of metal-mediated C–H bond cleavage. For example, Shilov et al. disclosed the use of Pt(II) salts to catalytically functionalize methane [15–17]. In addition, in the late 1960s and early 1970s, H/D exchange reactions between metal hydrides and deuterated hydrocarbons were reported [18–20]. In the late 1970s and 1980s, examples of well defined transition metal-mediated activation of C–H bonds appeared [15, 21−25] Work by Bergman, Graham, Jones, Periana et al. demonstrated that Ir(I) and Rh(I) complexes could break strong C–H bonds of arenes and alkanes through oxidative addition reactions that produce Ir(III) or Rh(III) hydrocarbyl hydride products (Scheme 1.2) [21, 22, 26−33]. The ability to study these systems in detail has resulted in substantial information about these and related C–H activation reactions. Other early examples of metal-mediated C–H activation by oxidative addition included reactions of low valent W, Fe, Ru and Re systems [13, 14, 34–38].

Concomitant with the study of oxidative addition processes were studies of high oxidation state d^0 complexes that facilitate C–H activation by σ-bond metathesis as well as the use of late transition metal complexes that are thought to break C–H

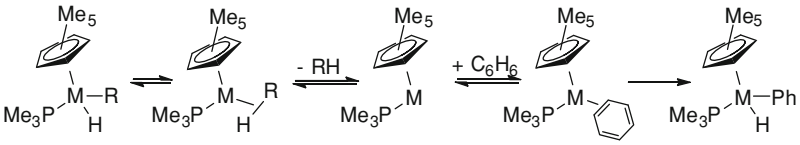

Scheme 1.2 Oxidative addition reactions via Rh(I) and Ir(I) intermediates (M = Rh or Ir; R = H or alkyl)

bonds by electrophilic substitution [39–43]. Although distinction between various mechanisms and reaction pathways can be difficult [44–46], after three decades of intense effort toward metal-mediated C–H bond breaking, several general categories of metal-based C–H bond rupture have emerged (Scheme 1.3). It has been argued that the term C–H activation should be reserved for cases in which the metal directly interacts with the C–H bond. By this definition, some of the reactions presented in Scheme 1.3 would not be classified as a metal-mediated C–H activation.

1.3 The Alkane Challenge

Although the selective functionalization of hydrocarbons is challenging, synthetic transformations of alkanes are particularly difficult. Relative to alkanes, the activation and functionalization of aromatic or olefinic substrates can be more facile due to the presence of π-electrons as well as vacant π^* molecular orbitals. The π-electrons often enhance the nucleophilicity (relative to alkanes) of the hydrocarbon substrate and can facilitate coordination to metal centers. Furthermore, the presence of relatively low energy π^* molecular orbitals (i.e., when compared to σ^* molecular orbitals) can promote metal-to-ligand dπ-backbonding, which can enhance substrate coordination.

In contrast to unsaturated substrates, alkanes are poor nucleophiles and hence coordinate only weakly to metals. In fact, in some cases hydrocarbon coordination is the rate limiting step in overall C–H activation sequences (Scheme 1.4) [28, 47]. Typical metal-alkane bond enthalpies are <15 kcal/mol, [48–50] and isolation of these complexes is a substantial challenge. In most cases coordinated alkanes have only been observed using special spectroscopic techniques [49, 51, 52]. Thus, a primary challenge in the field of catalytic conversion of alkanes is a coordination chemistry problem, and with so few examples of systems that are amenable to study by spectroscopy, detailed structure/activity studies have been difficult to achieve. In fact, it is only recently that alkanes coordinated to transition metals have been observed using NMR spectroscopy [53–57].

Another substantial challenge for the functionalization of alkanes is selectivity. In general, the order of CH bond dissociation energies is H_2C–H > R(H) C–H > R_2C–H with a range of approximately 100–95 kcal/mol. For example, the

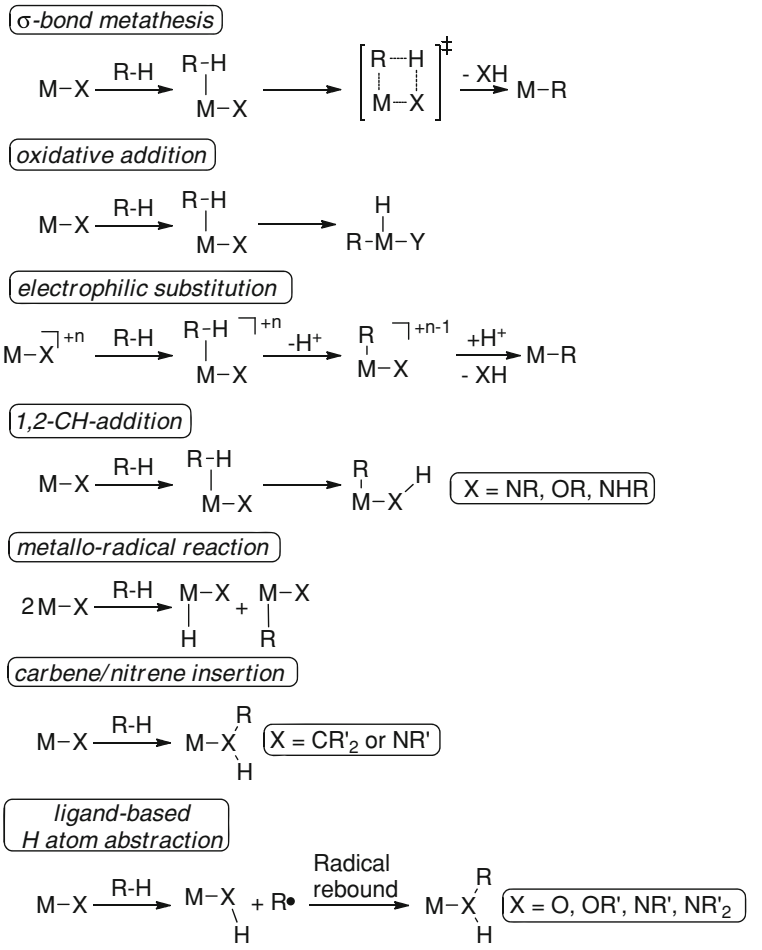

Scheme 1.3 Various mechanisms for C–H bond breaking by transition metal complexes

BDE of the CH_3 group of butane is ~101 kcal/mol while the CH_2 BDE is ~98 kcal/mol (Scheme 1.5). For 2-methylbutane, the methine CH BDE is ~96 kcal/mol [58]. For alkanes, in many cases, it is the "linear" functionalized product that is most desirable. However, the difference in C–H BDEs makes preferential cleavage of terminal alkane CH bonds difficult. One prominent example where terminal functionalization can be desirable is the production of alcohols, which are commonly used as solvents either directly or as the corresponding acetate. Because of their more favorable solvent properties, unbranched linear alcohols are often more valuable than branched alcohols. Currently, linear alcohols are typically produced via the generation of syngas ($CO + H_2$) and α-olefins with subsequent olefin hydroformylation and hydrogenation of the

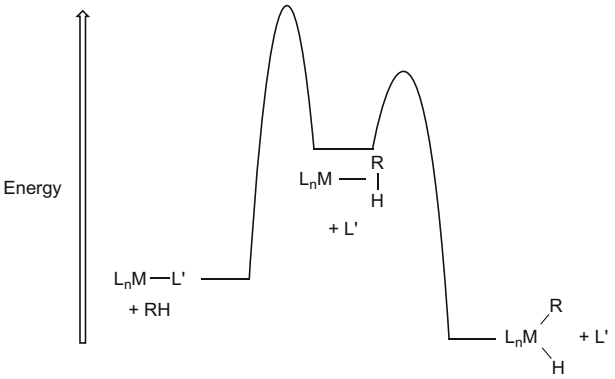

Scheme 1.4 Reaction coordinate showing ligand exchange between L′ and hydrocarbon RH and subsequent C–H oxidative addition. Hydrocarbon coordination to the metal is often the rate limiting step in overall metal-mediated C–H activation and bond breaking

Scheme 1.5 Representative bond dissociation energies of alkanes

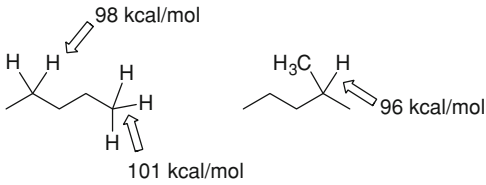

aldehyde (Scheme 1.6). A more direct route would involve the selective partial oxidation of alkanes at the terminal position.

Transition metal-mediated C–H activation has provided the means to control selectivity for C–H bond cleavage, including examples of selective activation of stronger C–H bonds in preference to weaker C–H bonds as is often observed for oxidative addition reactions. Transition metal-mediated C–H activation of arenes is often more rapid than alkanes, which possess weaker C–H bonds than the arene substrates, and aryl hydride products are often thermodynamically preferred over alkyl hydride systems. For example, the Ir(I) intermediate {Cp*Ir(PMe_3)} , which is accessed from Cp*Ir(PMe_3)$(H)_2$, reacts nearly 4 times faster with the aromatic C–H bonds of *p*-xylene than with the benzylic C–H bonds (Scheme 1.7) [27].

In addition to aromatic C–H activation in preference to alkane activation, selective C–H activation of stronger CH_3 over CH_2 and CH units has been reported for alkanes. For example, studies of the reactivity of Rh(I) complexes with alkanes reveal that the C–H activation of primary C–H bonds is both kinetically and thermodynamically favored over secondary and tertiary C–H bonds [21, 59, 60]. After substantial study, the generally accepted pathway for alkane C–H activation typically involves initial alkane coordination followed by C–H bond cleavage by oxidative addition (Scheme 1.8). In addition, detailed mechanistic studies have suggested that, for some systems, the selectivity is a result of a lower activation barrier for rupture of the stronger C–H bond compared with weaker internal CH_2

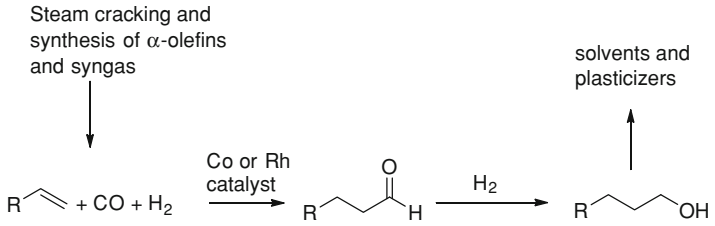

Scheme 1.6 Synthesis of linear aldehydes and alcohols

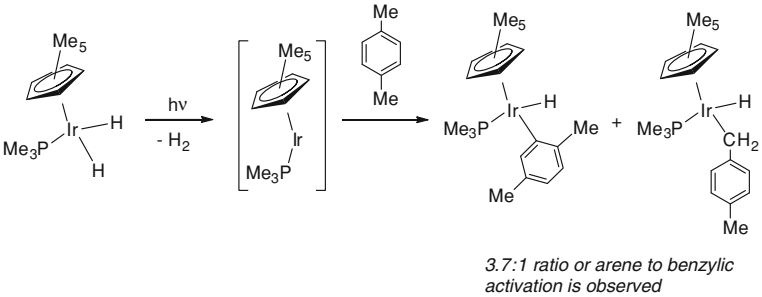

Scheme 1.7 Aromatic C–H activation is observed in preference to benzylic C–H activation by Ir(I) system

Scheme 1.8 Metal-mediated alkane oxidative addition is often selective (kinetically and thermally) for the stronger terminal C–H bond (product shown in *box*)

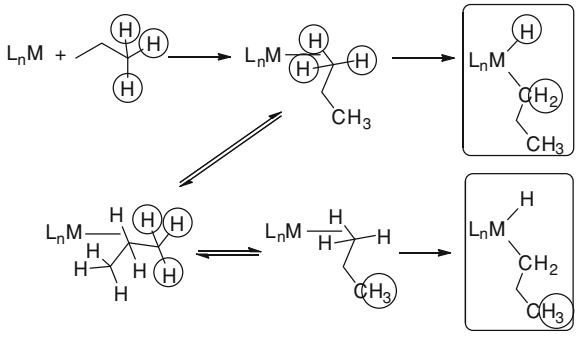

groups. For example, monitoring isotopic scrambling for the complex [(1,4,7-trimethyl-1,4,7-triazacyclononane)Rh{P(OMe)$_3$}(hexyl)(D)] [BAr′$_4$] {Ar′ = 3,5-(CF$_3$)$_2$C$_6$H$_3$} at 4 °C shows deuterium incorporation into the α-CH$_2$ group and the terminal methyl group. Incorporation of deuterium at the terminal position occurs at a slower rate compared to H/D exchange at the α-position [59]. Also, detailed studies of Tp*Rh(CNR′)(R)(H) systems (Tp* = hydridotris-3,5-dimethylpyrazolylborate; R′ = neopentyl; R = alkyl) reveal similar results [60, 61]. Importantly, the selectivity for activation of stronger C–H bonds, even in the presence of weaker C–H bonds, provides opportunity for the development of pathways for the selective manipulation of alkanes.

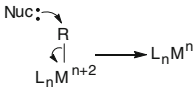

Scheme 1.9 Reductive nucleophilic addition to electrophilic hydrocarbyl ligand of late transition metals

While several examples of metal-mediated activation of strong C–H bonds, such as aromatic C–H bonds and terminal positions on linear alkanes, have been reported, extension to catalytic hydrocarbon *functionalization* remains a challenge. In order to achieve active catalysts, it is necessary to combine the C–H activation step with a functionalization step, which presents several obstacles. Despite these difficulties, significant progress has been made in recent years. This book provides a review of recent achievements in the progress toward catalysts for alkane functionalization.

1.4 Alkane Functionalization via Electrophilic Activation

One of the earliest examples of metal-mediated functionalization of alkanes was the use of aqueous solutions of Pt(II) salts as catalysts as reported by Shilov et al. in the 1960s [15]. Although not practical for scale up, the Shilov catalyst and related systems, which together form a class of electrophilic catalysts that likely function by closely related pathways [15, 16, 62–64] remain among the best examples in terms of selectivity, activity and catalyst longevity. The original work in this area sparked significant interest, and detailed studies have revealed substantial information about the Shilov (and related) systems [15–17, 65, 66].

Alkane functionalization reactions have been observed with Pt, Pd, Hg, Tl, Au, Cu, Ir and Rh catalysts. These late metal systems are often referred to as electrophilic catalysts since, in many cases, it is believed that the C–H bond breaking step involves the formation of a metal alkyl (or aryl) by alkane (or arene) coordination and subsequent liberation of a proton (i.e., the metal serves as an electrophile to displace a proton from the alkane or arene, see Scheme 1.3). Other features in common with many of these catalysts include carbon–oxygen bond formation (or carbon-halide) by nucleophilic addition to an electrophilic hydrocarbyl ligand (Scheme 1.9) and the use of acidic media. Despite the achievements with this class of catalysts, several challenges impede the development of practical catalysts for hydrocarbon functionalization, including reaction rates, the incorporation of scalable oxidants, and catalysts that give high conversion *and* high selectivity. Chapter 2 provides an overview of alkane (and other hydrocarbon) C–H functionalization by electrophilic systems including a detailed overview of the Shilov Pt systems as well as results from studies of other late transition metals.

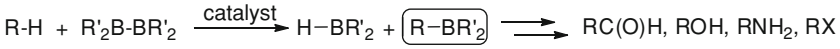

Scheme 1.10 Strategy for functionalization of hydrocarbons via formation of hydrocarbylboranes

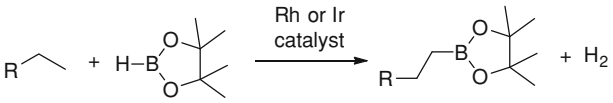

Scheme 1.11 Catalytic conversion of alkanes to linear alkyl boranes

1.5 Catalytic Carbon-Boron Bond Formation via Activation of Alkane C–H Bonds

Organoboron compounds are susceptible to a diverse range of reactions and are useful synthetic precursors. As a result, the selective conversion of C–H bonds of alkanes to substrates that possess C–B functionalization is an attractive strategy *en route* to aldehydes, amines, alcohols or alkyl halides (Scheme 1.10). Another attractive feature of the C–H → C–B transformation is the thermally favorable nature of alkane borylation.

Catalysts for the conversion of C–H bonds to C–B bonds must be able to combine selective C–H activation, activation of the boron precursor and selective C–B bond formation without scrambling of regioselectivity achieved in the metal-mediated C–H bond breaking step. In 1995, Hartwig et al. reported the photo-induced conversion of metal-boryls and hydrocarbons to boranes [67]. Kinetic isotope effects for a series of Fe, Ru and W systems are consistent with metal-mediated alkane activations and suggest that boryl radicals are not likely involved [68]. The use of rhenium complexes allowed catalytic conversion under photolytic conditions [69]. Subsequently, Rh and Ir catalysts for the selective conversion of alkanes and pinacolate boranes to linear alkyl boranes under thermal conditions were reported (Scheme 1.11) [70]. Work in this area has now been extended to an array of transition metal catalysts as well as studies of substrate scope. Chapter 3 provides a comprehensive summary of this work, including discussion of various catalysts, results and interpretation of mechanistic studies, and an overview of substrate scope for different catalyst systems.

1.6 Alkane Dehydrogenation

Olefins are an important substrate for the chemical industry [10]. Given the synthetic versatility of olefins, the catalytic dehydrogenation of alkanes is an attractive strategy to facilitate the utilization of saturated hydrocarbons (Scheme 1.12);

Scheme 1.12 Catalytic alkane dehydrogenation to produce a terminal olefin

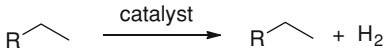

Scheme 1.13 Catalytic dehydrogenation of cyclic alkanes using tert-butylethylene as the hydrogen acceptor

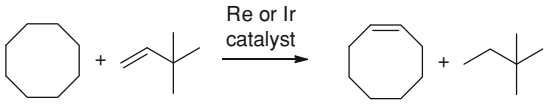

however, alkane dehydrogenation is an endothermic process, which places substantial constraints on the development of these reactions. Although the dehydrogenation of hydrocarbons is endothermic, it is practiced on a commercial scale at high temperatures (usually between 650 and 900 °C) [71].

Transition metal catalysts for alkane dehydrogenation that operate at moderate temperatures have been reported and studied. Most of these systems require an "acceptor" that is hydrogenated to render the overall process exothermic. In 1979, Crabtree et al. reported an Ir catalyst that dehydrogenates cyclic hydrocarbons including cyclic alkanes [72]. Using *tert*-butylethylene as the hydrogen acceptor, the groups of Felkin and Crabtree reported catalytic Re- and Ir-mediated processes (Scheme 1.13). Using $(PMe_3)_2Rh(CO)Cl$ as catalyst, Goldman et al. found that cyclic and linear alkanes are dehydrogenated under photolytic conditions [73]. This four-coordinate bis-phosphine/chloride d^8 catalyst precursor [i.e., $(PMe_3)_2Rh(CO)Cl$] set the stage for the next development, which involved the use of monoanionic tridentate bisphosphine "pincer" ligands coordinated to Ir(I). These complexes are thermally robust and provide a suitable framework for highly active and stable homogeneous catalysts for alkane dehydrogenation (Fig. 1.2) [74–76]. Chapter 4 summarizes the development of transition metal catalysts for low temperature alkane dehydrogenation with a focus on recent developments.

1.7 Alkane C–H Oxygenation Catalyzed by Transition Metal Complexes

Several enzymes functionalize C–H bonds by generating transition metal complexes with oxo, methoxy or aryloxo ligands [77–80]. Many of these catalysts function by an initial net hydrogen atom abstraction followed, in some cases, by C–O bond formation through a "rebound" step. The net hydrogen atom abstraction, including examples of substrates that possess strong C–H bonds such as methane, is driven by the favorable reduction of the metal center (Scheme 1.14). Substantial effort has been devoted to understanding the function of these enzymes, including those to mimic reactivity with synthetic models.

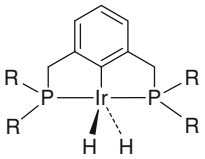

Fig. 1.2 Ir(I) catalyst precursors for alkane dehydrogenation supported by tridentate "pincer" ligands

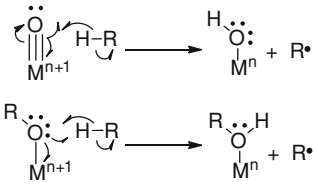

Scheme 1.14 Net hydrogen atom abstraction by high valent metal oxo or alkoxide

The use of transition metal catalysts in the presence of oxidants to functionalize C–H bonds is a well-studied area. These efforts span a large portion of the transition series and a range of catalyst types. The combination of oxidants in the presence of transition metal salts can give systems that catalyze hydrocarbon oxidation. For example, iron salts and hydrogen peroxide (the Fenton system) oxidize a range of substrates that possess C–H bonds. Such reactions commonly involve free radical reaction pathways and are often difficult to study in detail. In order to better understand C–H functionalization by metal oxo complexes and to generate systems that are active for more inert hydrocarbons and that exhibit enhanced selectivity, substantial effort has been put toward the isolation and study of well-defined metal oxo complexes and related systems (e.g., $L_nM{=}NR$, L_nM-OR, etc.) [81]. There are two primary challenges with development of useful catalysts based on metal oxo (and related intermediates such as metal hydroperoxides): (1) generating metal oxo complexes with sufficient reactivity to transform substrates that possess C–H BDEs >100 kcal/mol and (2) controlling selectivity. Recently, electrocatalytic methods have provided a strategy to generate highly reactive metal oxo systems; [82] however, these processes have to this point been mostly focused on water oxidation catalysts. In Chap. 5 a thorough overview of alkane oxidation, organized by catalyst identity, is provided.

1.8 Catalytic Insertion of Carbenes and Nitrenes into C–H Bonds

Over 50 years ago, the insertion of organic carbenes into C–H bonds was reported; [83] however, achieving selective and synthetically useful variants with these organic reactions is difficult. Subsequently, Cu systems were found to catalyze the intramolecular insertion of carbenes, which are typically generated from diazoalkanes, into C–H bonds [84]. These reactions opened the door to the possibility of useful metal-mediated carbene insertion into C–H bonds, which provides an

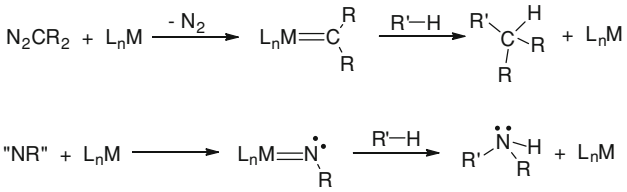

Scheme 1.15 Metal-catalyzed insertion of carbenes and nitrenes into C–H bonds

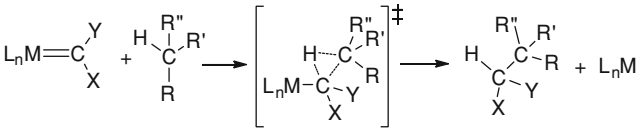

Scheme 1.16 Proposed mechanism for insertion of metal-coordinated carbene into C–H bond

Scheme 1.17 Silver catalyzed functionalization of methane (Tp^X = various hydridotris(indazolyl)borates)

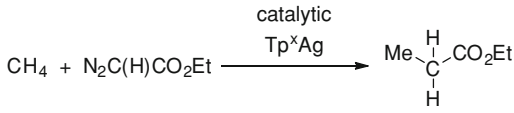

avenue to control selectivity. Extension of these reactions to nitrene complexes provides a strategy for C–H → C–N transformations (Scheme 1.15).

Using dirhodium catalyst precursors, intermolecular insertions of carbenes into alkanes (cyclic and acyclic) were achieved [85, 86]. These early studies of Rh catalysts sparked a series of studies aimed at developing useful catalysts and understanding the mechanism of C–H bond cleavage [84]. In 1993, Doyle et al. proposed a mechanism for C–H activation in which the carbene unit inserts into the C–H bond without direct interaction with the metal center (Scheme 1.16) [87]. This model was used to rationalize the variation in selectivity as a function of the electron-donor strength of ancillary ligands. A recent DFT study provides additional support for this proposed pathway for carbene insertion [88].

After several years of development, it is understood that catalysts for carbene insertion into C–H bonds are typically constrained to those systems that possess highly electrophilic carbene moieties. Metal-mediated carbene insertion into C–H bonds has been observed with catalysts based on Ag, Au, Co, Cu, Fe, Rh and Ru [84, 86]. Recently, the range of reactivity has been extended to functionalization of methane and other alkanes using Ag catalysts (Scheme 1.17) [89].

Similar to metal-catalyzed carbene insertions, but somewhat different from a mechanistic point of view, nitrene insertion into C–H bonds can be catalyzed by late transition metal complexes. An early report from Breslow and Gellman disclosed catalytic tosylamidation of cyclohexane by Mn and Fe catalysts [90], and subsequent work has included catalysts based on Fe, Ru, Mn, Rh, Mn, Pd, Cu and Ag [86, 91–95] These reactions offer great promise, particularly in the synthetic

organic area, if easily accessible nitrene sources can be developed in tandem with efficient and stereoselective transition metal catalysts. Chapter 6 provides an overview of metal catalyzed carbene and nitrene insertion into C–H bonds.

1.9 Conclusions

The development of general synthetic methods for the selective functionalization of C–H bonds could have a broad impact on chemical synthesis spanning synthetic organic chemistry, including pharmaceutical and agricultural sectors, as well as the petrochemical industry. The 2001 Nobel Prize in chemistry (William Knowles, Ryoji Noyori and Barry Sharpless) was awarded for the development of asymmetric catalysis, the 2005 Nobel Prize in chemistry (Yves Chauvin, Robert Grubbs and Richard Schrock) was awarded for the development of catalysts for olefin metathesis, and the recent 2010 Nobel Prize (Richard Heck, Ei-ichi Negishi and Akira Suzuki) was awarded for Pd-catalyzed cross coupling reactions. All of these developments have facilitated the synthesis of high value organic molecules and are of great importance. The development of selective catalysts that functionalize the C–H bonds of organic substrates would be likely to have an equally substantial influence on the field of synthetic chemistry, and catalysts that efficiently and selectively convert hydrocarbons (especially alkanes) could impact the petrochemical industry.

Acknowledgments T.B.G. acknowledges support for work on the development of catalysts for alkane functionalization from the Center for Catalytic Hydrocarbon Functionalization, an Energy Frontier Research Center funded by the US Department of Energy, Office of Science, Office of Basic Energy Sciences under Award Number DE-SC0001298.

References

1. Olah GA, Rasul G (1997) Acc Chem Res 30:245–250
2. Daugulis O, Do H-Q, Shabashov D (2009) Acc Chem Res 42:1074–1086
3. Bellina F, Rossi R (2010) Chem Rev 110:1082–1146
4. Chen MS, White MC (2010) Science 327:566–570
5. Chen MS, White MC (2007) Science 318:783–787
6. Kakiuchi F, Murai S (2002) Acc Chem Res 35:826–834
7. Murai S, Kakiuchi F, Sekine S, Tanaka Y, Kamatani A, Sonoda M, Chatani N (1993) Nature 366:529–531
8. Colby DA, Bergman RG, Ellman JA (2010) Chem Rev 110:624–655
9. Wittcoff HA, Reuben BG, Plotkin JS (2004) Industrial organic chemicals, 2nd edn. John Wiley and Sons, Hoboken, New Jersey
10. Chenier PJ (1992) Survey of industrial chemistry, 2nd edn. Wiley-VCH, New York
11. Brookhart M, Green MLH, Parkin G (2007) Proc Nat Acad Sci 104:6908–6914
12. Brookhart B, Green MLH, Wong L–L (1988) Prog Inorg Chem 36:1–124
13. Chatt J, Davidson JM (1965) J Chem Soc (A) 843–855

14. Cotton FA, Frenz BA, Hunter DL (1974) Chem Commun 755–756
15. Shilov AE, Shul'pin GB (1997) Chem Rev 97:2879–2932
16. Stahl SS, Labinger JA, Bercaw JE (1998) Angew Chem Int Ed 37:2180–2192
17. Lersch M, Tilset M (2005) Chem Rev 105:2471–2526
18. Barefield EK, Parshall GW, Tebbe FN (1970) J Am Chem Soc 92:5234–5235
19. Chatt J, Coffey RS (1969) J Chem Soc A 1963–1972
20. Garnett JL, Hodges RJ (1967) J Am Chem Soc 89:4546–4547
21. Jones WD, Feher FJ (1989) Acc Chem Res 22:91–100
22. Arndtsen BA, Bergman RG, Mobley TA, Peterson TH (1995) Acc Chem Res 28:154–162
23. Labinger JA, Bercaw JE (2002) Nature 417:507–514
24. Green MLH (1984) Pure Appl Chem 56:47–58
25. Green MLH, O'Hare D (1985) Pure Appl Chem 57:1897–1910
26. Janowicz AH, Bergman RG (1982) J Am Chem Soc 104:352–354
27. Janowicz AH, Bergman RG (1983) J Am Chem Soc 105:3929–3939
28. Jones WD, Feher FJ (1984) J Am Chem Soc 106:1650–1663
29. Jones WD, Feher FJ (1982) J Am Chem Soc 104:4240–4242
30. Hoyano JK, McMaster AD, Graham WAG (1983) J Am Chem Soc 105:7190–7191
31. Hoyano JK, Graham WAG (1982) J Am Chem Soc 104:3723–3725
32. Buchanan JM, Stryker JM, Bergman RG (1986) J Am Chem Soc 108:1537–1550
33. Periana RA, Bergman RG (1986) J Am Chem Soc 108:7332–7346
34. Berry M, Elmitt K, Green MLH (1979) Dalton Trans 12:1950–1958
35. Parkin G, Bercaw JE (1989) Organometallics 8:1172–1179
36. Gould GL, Heinekey DM (1989) J Am Chem Soc 111:5502–5504
37. Baker MV, Field LD (1986) J Am Chem Soc 108:7433–7434
38. Ittel SD, Tolman CA, English AD, Jesson JP (1978) J Am Chem Soc 100:7577–7585
39. Watson PL (1983) J Am Chem Soc 105:6491–6493
40. Lin Z (2007) Coord Chem Rev 251:2280–2291
41. Thompson ME, Baxter SM, Bulls AR, Burger BJ, Nolan MC, Santarsiero BD, Schaefer WP, Bercaw JE (1987) J Am Chem Soc 109:203–219
42. Sadow AD, Tilley TD (2003) J Am Chem Soc 125:7971–7977
43. Jordan RF, Taylor DF (1989) J Am Chem Soc 111:778–779
44. Balcells D, Clot E, Eisenstein O (2010) Chem Rev 110:749–823
45. Niu S, Hall MB (2000) Chem Rev 100:353–405
46. Vastine BA, Hall MB (2007) J Am Chem Soc 129:12068–12069
47. Chen GS, Labinger JA, Bercaw JE (2007) Proc Nat Acad Sci 104:6915–6920
48. Hall C, Perutz RN (1996) Chem Rev 96:3125–3146
49. Brown CE, Ishikawa Y-I, Hackett PA, Rayner DM (1990) J Am Chem Soc 112:2530–2536
50. Sun X-Z, Grills DC, Nikiforov SM, Poliakoff M, George MW (1997) J Am Chem Soc 119:7521–7525
51. Wasserman EP, Moore CB, Bergman RG (1992) Science 255:315–318
52. McNamara BK, Yeston JS, Bergman RG, Moore CB (1999) J Am Chem Soc 121:6437–6443
53. Bernskoetter WH, Schauer CK, Goldberg KI, Brookhart M (2009) Science 326:553–556
54. Geftakis S, Ball GE (1998) J Am Chem Soc 120:9953–9954
55. Lawes DJ, Geftakis S, Ball GE (2005) J Am Chem Soc 127:4134–4135
56. Lawes DJ, Darwish TA, Clark T, Harper JB, Ball GE (2006) Angew Chem Int Ed 45:4486–4490
57. Ball GE, Brookes CM, Cowan AJ, Darwish TA, George MW, Kawanami HK, Portius P, Rourke JP (2007) Proc Nat Acad Sci 104:6927–6932
58. Luo Y-R (2003) Handbook of bond dissociation energies in organic compounds. CRC Press, Boca Raton
59. Flood TC, Janak KE, Iimura M, Zhen H (2000) J Am Chem Soc 122:6783–6784
60. Northcutt TO, Wick DD, Vetter AJ, Jones WD (2001) J Am Chem Soc 123:7257–7270
61. Jones WD (2003) Acc Chem Res 36:140–146
62. Fekl U, Goldberg KI (2003) Adv Inorg Chem 54:259–319

63. Periana RA, Taube DJ, Evitt ER, Löffler DG, Wentrcek PR, Voss G, Masuda T (1993) Science 259:340–343
64. Periana RA, Taube DJ, Gamble S, Taube H, Satoh T, Fujii H (1998) Science 280:560–564
65. Conley BL, Tenn IWJ, Young KJH, Ganesh SK, Meier SK, Ziatdinov VR, Moronov O, Oxgaard J, Gonzales J, Goddard WA III, Periana RA (2006) J Mol Catal A 251:8–23
66. Labinger JA (2004) J Mol Catal A 220:27–35
67. Waltz KM, He X, Muhoro C, Hartwig JF (1995) J Am Chem Soc 117:11357–11358
68. Waltz KM, Hartwig JF (2000) J Am Chem Soc 122:11358–11369
69. Chen H, Hartwig JF (1999) Angew Chem Int Ed 38:3391–3393
70. Chen H, Schlecht S, Semple TC, Hartwig JF (2000) Science 287:1995–1997
71. Olah GA, Molnár Á (2003) Hydrocarbon chemistry, 2nd edn. Wiley-Interscience, Hoboken
72. Crabtree RH, Mihelcic JM, Quirk JM (1979) J Am Chem Soc 101:7738–7740
73. Maguire JA, Boese WT, Goldman ME, Goldman AS (1990) Coord Chem Rev 97:179–192
74. Xu W–W, Rosini GP, Gupta M, Jensen CM, Kaska WC, Krogh-Jespersen K, Goldman AS (1997) Chem Commun 2273–2274
75. Liu F, Pak EB, Singh B, Jensen CM, Goldman AS (1999) J Am Chem Soc 121:4086–4087
76. Gupta M, Hagen C, Flescher RJ, Kaska WC, Jensen CM (1996) Chem Commun 2083–2084
77. Ortiz de Montellano PR (2010) Chem Rev 110:932–948
78. Baik M-Y, Newcomb M, Friesner RA, Lippard SJ (2003) Chem Rev 103:2385–2419
79. Mirica LM, Ottenwaelder X, Stack TDP (2004) Chem Rev 104:1013–1045
80. Goldsmith CR, Jonas RT, Stack TDP (2002) J Am Chem Soc 124:83–96
81. Gunay A, Theopold KH (2010) Chem Rev 110:1060–1081
82. Paul A, Hull JF, Norris MR, Chen Z, Ess DH, Concepcion JJ, Meyer TJ (2011) Inorg Chem 50:1167–1169
83. Doering WvE, Buttery RG, Laughlin RG, Chaudhuri N (1956) J Am Chem Soc 78:3224
84. Doyle MP, Duffy R, Ratnikov M, Zhou L (2010) Chem Rev 110:704–724
85. Demonceau A, Noels AF, Hubert AJ, Teyssie P (1981) J Chem Soc Chem Commun 688–689
86. Díaz-Requejo MM, Pérez PJ (2008) Chem Rev 108:3379–3394
87. Doyle MP, Westrum LJ, Wolthuis WNE, See MM, Boone WP, Bagheri V, Pearson MM (1993) J Am Chem Soc 115:959–964
88. Nakamura E, Yoshikai N, Yamanaka M (2002) J Am Chem Soc 124:7181–7192
89. Caballero A, Despagnet-Ayoub E, Díaz-Requejo MM, Díaz-Requejo A, González-Núñez ME, Mello R, Muñez BK, Ojo W-S, Asensio G, Etienne M, Pérez PJ (2011) Science 332:835–838
90. Breslow R, Gellman SH (1982) Chem Commun 1400–1401
91. Müller P, Fruit C (2003) Chem Rev 103:2905–2919
92. Au S-M, Huang J-S, Yu W-Y, Fung W-H, Che C-M (1999) J Am Chem Soc 121:9120–9132
93. Davies HML (2006) Angew Chem Int Ed 45:6422–6425
94. Yu X-Q, Huang J-S, Zhou X-G, Che C-M (2000) Org Lett 2:2233–2236
95. Liang C, Collet F, Robert-Peillard F, Müller P, Dodd RH, Dauban P (2007) J Am Chem Soc 130:343–350

Chapter 2
Alkane Functionalization via Electrophilic Activation

Jay A. Labinger

Abstract Electrophilic activation, which may be defined as the substitution of a transition metal center for a proton to generate a new metal–carbon bond, is the basis of a number of promising approaches to selective catalytic functionalization of alkanes. The field was introduced by the groundbreaking chemistry exhibited by aqueous chloroplatinum complexes, reported by Shilov in the early 1970s. Since then the field has expanded greatly, and electrophilic alkane activation has been demonstrated using a wide variety of species. These include ligand-supported platinum complexes; complexes of additional late transition metals, most commonly palladium but also iridium, gold and others; and even post-transition metals such as mercury. That body of work is surveyed here, with particular emphasis on mechanistic understanding, examples of actual functionalization at sp^3-hybridized C–H bonds in alkanes and related compounds, and assessment of the further development that will be needed for practical applications.

2.1 Definition and Scope

What do we mean by electrophilic activation of alkanes? It *seems* as though the term should have mechanistic implications. The obvious antecedent is electrophilic substitution of arenes, which classically proceeds via a delocalized carbocationic Wheland intermediate, as shown in Scheme 1; the electrophile E^+ may be metal-centered, such as Hg^{2+}. Of course, there is no *classical* analog of the

J. A. Labinger (✉)
Beckman Institute, California Institute of Technology,
139-74, Pasadena, CA 91125, USA
e-mail: jal@its.caltech.edu

P. J. Pérez (ed.), *Alkane C–H Activation by Single-Site Metal Catalysis*,
Catalysis by Metal Complexes 38, DOI: 10.1007/978-90-481-3698-8_2,
© Springer Science+Business Media Dordrecht 2012

Scheme 2.1 Electrophilic mechanisms for substitution of an arene (top) and metallation of an alkane (bottom)

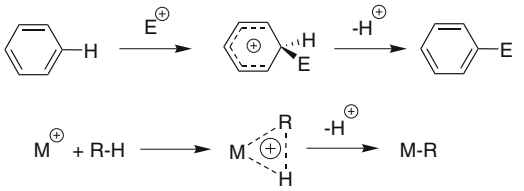

Wheland intermediate for alkane activation; but we now know that alkane σ complexes of transition metals are ubiquitous and, in many cases, remarkably stable, so the "non-classical" analog in Scheme 1 might be reasonable. But it appears that most if not all cases of alkane activation by transition metals *start* with formation of the σ complex, although they proceed therefrom in a variety of ways, rarely (if ever) exactly as in Scheme 2.1. Such a consideration would imply we should call *all* alkane activations electrophilic,[1] even oxidative additions which require very electron-rich metal centers, and which formally involve electron flow from the metal to the alkane. Clearly, then, it will be much more useful to use the term to signify stoichiometry, not mechanism.

Accordingly, for the purpose of this review, we define "electrophilic activation" as formation of an alkyl-metal complex according to Eq. 2.1. This chemistry was first established for aqueous chloroplatinate complexes—the so-called Shilov system—and has been extended to a number of late- and post-transition metal species, typically in protic and/or highly polar media. It should be emphasized that this is not, and cannot be, an unambiguous mechanistic designation. The proton may well be lost *along with* another ligand, a situation described by Eq. 2.2; but that stoichiometry also corresponds to the sigma bond metathesis reactions characteristic of d^0 early transition metal alkyl complexes [2]. Indeed, a similar route—sometimes termed a "sigma complex-assisted metathesis" or σ-CAM [3]—has been invoked for some late transition metal activations as well. Or the net stoichiometry of Eq. 2.2 may proceed via an oxidative addition/reductive elimination sequence (Eq. 2.3). But neither alkane activation by sigma bond metathesis at early transition metals nor oxidative addition at electron-rich late transition metal

[1] Periana and Goddard have recently offered an alternate perspective [1]. According to their theoretical studies, reactions may be classified as electrophilic, ambiphilic or nucleophilic based on the calculated transfer of charge from alkane to metal complex, or the reverse, in the transition state for C–H activation. Many of the systems classified as ambiphilic or nucleophilic involve simultaneous interaction of the C–H bond with both the metal center and another ligand, but even if only the metal center is involved, the net transfer can still be from metal to C–H bond, if π back-donation from a filled metal orbital to the C–H σ^* orbital is more important than donation from the C–H σ orbital to a vacant metal orbital. It is not clear how general or useful this approach might be (a possible illustration is discussed in Sect. 4.7); for one thing, a stated goal is to develop methods for combining C–H activations with compatible functionalization reactions, but (as we will see) in many cases the species that effects functionalization differs substantially from that responsible for the activation, so the nature of the activation (even assuming the methodology can accurately describe it) may well be entirely disconnected from potential functionalization chemistry. In any case, we will not make any use of these distinctions here.

centers commonly leads on to net alkane functionalization; the systems that favor those two pathways tend to be incompatible with many thermodynamically allowed transformations, particularly those involving oxidations [4]. In contrast, net overall oxidation often *can* be achieved via electrophilic activation (as defined by Eq. 2.1 or 2.2), often by reaction of the organometallic intermediate with a nucleophilic substituent, accompanied (at some point in the sequence) with a change in metal oxidation state, resulting in the overall stoichiometry of Eq. 2.4.

$$M^+ + R\text{-}H \longrightarrow M\text{-}R + H^+ \tag{2.1}$$

$$M\text{-}X + R\text{-}H \longrightarrow M\text{-}R + H\text{-}X \tag{2.2}$$

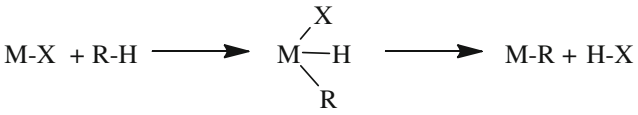

(2.3)

$$R\text{-}H + X^- \longrightarrow R\text{-}X + H^+ + 2e^- \tag{2.4}$$

The main focus of this review is electrophilic functionalization of alkanes.[2] We will allow a rather loose definition of what counts as an alkane, generally including functionalization of a saturated (sp^3-hybridized) C–H bond even though it may be part of a more complex molecule, so long as the chemistry involved could reasonably be applicable to simple alkanes. Reactions that *only* activate C–H bonds, without leading on to functionalization, will be considered only insofar as they shed important light on mechanism or reactivity patterns, with no attempt at comprehensive coverage (particularly of the *immense* body of literature concerning cyclometallation!). The same criterion will apply to the functionalization of aryl C–H bonds, for which there is a large body of recent work, especially involving *directed* activation by palladium (which effects a number of directed activations at sp^3 carbon as well see Sect. 4.1.2) [9]; only those examples that provide mechanistic lessons will be examined in any detail. The chapter is organized primarily according to the activating species, although in a few instances results are presented in the "wrong" section to facilitate comparisons.

[2] This subject has been reviewed before, far too often to cite all of them. Some particularly relevant ones; an earlier, but considerably shorter, review of electrophilic oxidations [5]; a much more thorough coverage of Pt-mediated C–H activation and functionalization [6]; a more recent review of oxidative functionalization of alkanes in protic media [7]; a general review of transition metal catalyzed oxidative functionalization of C–H bonds [8].

2.2 The Shilov System

C–H activation by a soluble transition metal complex was first reported by Garnett and Hodges in 1967: they found that a solution of $[PtCl_4]^{2-}$ in aqueous acetic acid, with added HCl, catalyzed H/D exchange between a variety of arenes and D_2O, at temperatures around 100–120 °C [10]. Exchange of aryl C–H bonds may not have appeared remarkable, possibly just another example of (reversible) electrophilic metallation of arenes as in Scheme 2.1; but the paper also noted some activity for exchange at the benzylic positions of toluene and mesitylene, and even in cyclohexane. More details on the aliphatic activations appeared shortly afterward, from Hodges [11] as well as the group of Alexander Shilov in the (then) USSR [12]. The first demonstration of actual functionalization came in a follow-up paper from the Shilov group: a combination of $[PtCl_4]^{2-}$ and $[PtCl_6]^{2-}$ in water or aqueous trifluoroacetic acid, under conditions similar to those used to effect H/D exchange, oxidized alkanes to a mixture of products, primarily alcohols and alkyl chlorides [13]. This combination of aqueous Pt(II) and Pt(IV) salts has become known as the Shilov system.

2.2.1 General Features

Shilov (in collaboration with his colleague Georgiy Shul'pin) has published comprehensive surveys of this chemistry as parts of two major review articles [14, 15] and two books [16, 17], the most recent dating from 2000; only highlights of the earlier work will be presented here. (Specific findings that are not explicitly referenced here have been taken from those surveys.) Initial studies by the Shilov group on the oxidations, and by both the Shilov and Hodges groups on H/D exchange, focused on two features of this novel chemistry: the effect of changing Pt speciation by varying $[Cl^-]$ and/or adding other anionic ligands, and the relative reactivities of different C–H bonds. In essentially all regards the two reactions show parallel features and trends, strongly indicating that they start off the same way, via C–H activation at a Pt(II) center. Reversal of that process results in H/D exchange, while Pt(IV) intervenes to divert some intermediate to a species leading to oxidative functionalization. The similarity of conditions to those needed for aryl H/D exchange suggests that arene and alkane reactions are closely related mechanistically. In general C–H bond reactivity follows the order primary > secondary > tertiary, which is the opposite of what would be predicted by considering bond strength; it is also the opposite of how one might guess a *mechanistically* electrophilic reaction would behave, since alkyl substitution is electron-releasing. Dependence of the rates of both H/D exchange and oxidation on $[Cl^-]$ implicated the reactivity order $[PtCl_4]^{2-} < [PtCl_3(H_2O)]^- < [PtCl_2(H_2O)_2] > [PtCl(H_2O)_3]^+ > [Pt(H_2O)_4]^{2+}$, which also seems incompatible with an electrophilic mechanism: the cationic species would be expected to be most electrophilic.

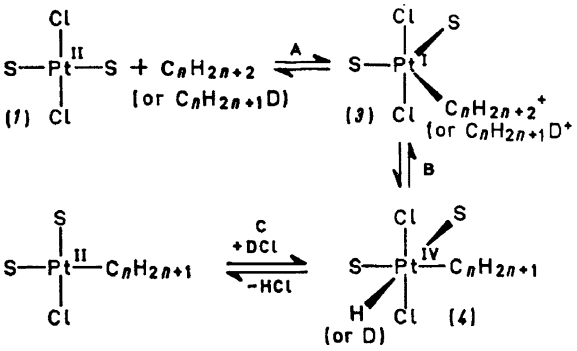

Scheme 2.2 Early mechanistic proposal for C–H activation by Pt(II). Reproduced from Ref. [11] with kind permission of © The Royal Society of Chemistry (1971)

Two additional observations gave important clues. C–H positions adjacent to quaternary centers are much less reactive, suggesting an important steric component in determining reactivity; and the distribution of $C_nH_{2n+2-x}D_x$ isotopologues was not statistical, but rather revealed a propensity for multiple exchange during each alkane-Pt encounter. To explain all of this, Hodges offered the C–H activation mechanism shown in Scheme 2.2 [11], which proceeds via rate-determining coordination of the alkane to Pt(II), followed by oxidative addition of a C–H bond to give an (alkyl)Pt(IV) hydride that can exchange with D^+; multiple exchange would be explained by assuming that intermediate ***3*** is sufficiently stable to allow steps **B** and **C** to take place (in both directions) a number of times before alkane dissociates (the reverse of step **A**). As we shall see, this proposal was in many ways remarkably prescient, especially considering that at the time there was no understanding at all of how an alkane might coordinate (Hodges described it as "electron transfer from delocalized molecular orbitals in the alkane to the platinum atom in the complex"), or how such an interaction could possibly give rise to a relatively long-lived species. Indeed, the feeling that such species were highly unlikely gave rise to alternate interpretations, involving intermediate olefin or carbene complexes, in a number of papers.

The preference for primary site oxidation is potentially useful, since many desirable alkane oxidation targets are those derived from terminal functionalization. For example, terminal alcohols used in detergents are currently obtained via hydroformylation of olefins; alkanes would constitute a much cheaper feedstock. As noted above, most oxidations involve homolytic pathways and disfavor the stronger C–H bonds. However, Shilov chemistry exhibits fairly modest selectivity: primary H/D exchange is perhaps a factor of 2-5 or so faster than at secondary positions [11].

Of even greater import is the relative reactivity of the initial alkane and its functionalization product. C–H bonds adjacent to oxygen-centered substituents, as well as most other functional groups likely to be introduced, are significantly weaker than those in simple alkanes, so that in traditional radical-based oxidations the products will be much more reactive than the starting material, severely limiting the yields attainable. For example, it has been estimated that these considerations would restrict the yield of methanol via *any* oxidation of methane that proceeds via a radical path to no more than a few percent, a prediction that so far has not been exceeded in

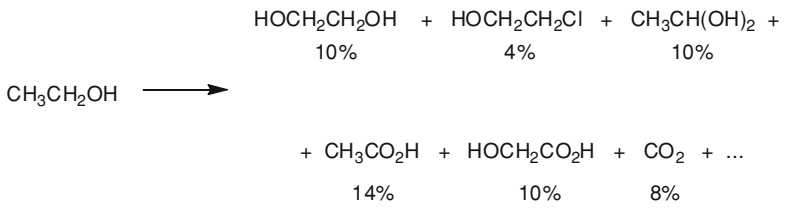

Scheme 2.3 Typical product distribution resulting from reaction of ethanol (at about 50 % conversion) under standard Shilov conditions

any reliable experimental report [18]. Since the selectivity trends for Shilov oxidation of alkanes argue strongly against anything resembling a radical mechanism, it seems possible that the same constraints might not apply. Experimental evidence that this is indeed so was first obtained for the oxidation of *p*-toluenesulfonic acid (a substrate chosen to permit detailed study in pure water, without the added complications of carboxylic acid co-solvents). Under the standard Shilov conditions, oxidation took place at the methyl group to give a mixture of the corresponding alcohol and aldehyde, but none of the carboxylic acid; analysis of the product distribution indicated that the methyl group is about 1.5 times as reactive as the hydroxymethyl group (uncorrected for statistical factors), as shown in Eq. 2.5. No significant oxidation at aryl positions was observed [19].

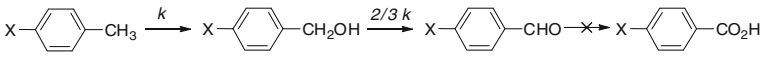

(2.5)

An even more dramatic demonstration of the unusual reactivity preferences demonstrated by this chemistry was obtained from the reaction of ethanol: all previously known oxidation methods lead to oxidation at the hydroxymethyl end of the molecule, to give acetaldehyde or acetic acid. In contrast, Shilov oxidation gave significant yields of the products resulting from oxidation at the methyl end—ethylene glycol and 2-chloroethanol—along with additional products attributable to initial hydroxymethyl oxidation and sequential further oxidation of the initial products (Scheme 2.3) [19]. Again, the product distribution turns out to be consistent with the methyl group being approximately 1.5 times as reactive as the hydroxymethyl group.

An estimate of the relative reactivity of methane and methanol, based on the attainable yields of the latter, and taking into account the limited solubility of the former, also gave a value on the order of 1.5 [20]. A more direct measurement was attempted by allowing the Shilov reaction of *both* methane and methanol to proceed to a steady-state product distribution, from which a reactivity ratio of about 0.17:1 was deduced [21]. However, that result is complicated by the tendency of platinum metal to precipitate from Shilov reactions, especially when carried out in pure water. (The use of a carboxylic acid co-solvent appears to retard Pt deposition considerably; a possible explanation will be discussed later.) Sen and others have shown that metallic platinum is an excellent catalyst for oxidation of alcohols by a

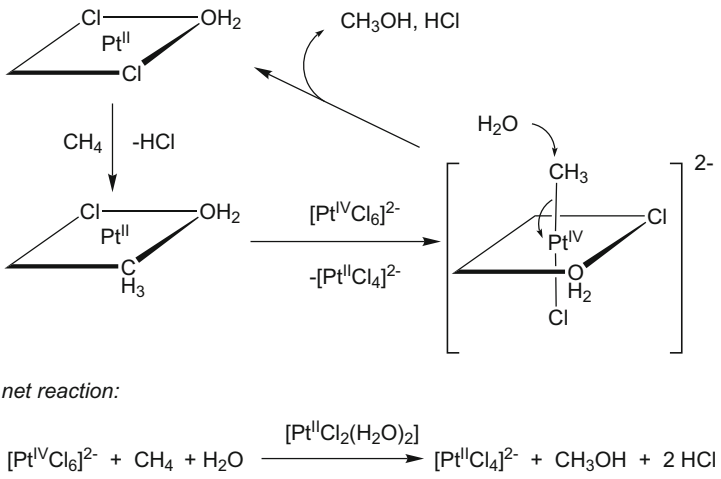

net reaction:

$$[Pt^{IV}Cl_6]^{2-} + CH_4 + H_2O \xrightarrow{[Pt^{II}Cl_2(H_2O)_2]} [Pt^{II}Cl_4]^{2-} + CH_3OH + 2\,HCl$$

Scheme 2.4 Proposed three-step Shilov oxidation sequence for the oxidation of methane to methanol/methyl chloride

variety of oxidants, including $[PtCl_6]^{2-}$ [22], so that if colloidal (and hence not visible) Pt were present during this experiment (and, likewise, in any of those discussed above), the apparent reactivity of methanol would be artificially high. Hence the measured ratio must be taken as a lower limit; at a minimum we can say that for all of these experiments, C–H bonds in methyl and hydroxymethyl groups are of comparable reactivity. If that conclusion holds in general, then the yield (that is, one-pass conversion times selectivity) for direct oxidation of an alkane to an alcohol could be as high as $\sim$30 %, an order of magnitude better than the quasi-theoretical limit for a radical mechanism [18]. Such findings understandably excited renewed interest in the potential of electrophilic functionalization methods.

Thorough mechanistic understanding of this chemistry is obviously a desirable target. The conditions of the reaction (especially when pure water is used as the solvent, rendering most substrates insoluble and promoting deposition of Pt metal), along with the general inability to observe any reaction intermediates, make it necessary to use indirect methods to get at many of the most interesting details; a less-detailed model for the overall reaction was formulated at early stages. As noted above, the close parallels between H/D exchange and oxidation strongly support the hypothesis that both begin the same way, with activation of the C–H bond at a Pt(II) center (exactly *how* that takes place will be addressed in the following section). The independent synthesis of (alkyl)Pt(IV) complexes can be achieved, most readily by the oxidative addition of alkyl iodides to $[PtCl_4]^{2-}$; the insolubility of PtI_2 drives ligand redistribution to afford $[RPtCl_5]^{2-}$ (or $[RPtCl_4(H_2O)]^{-}$, depending on exact conditions). The latter species, when exposed to Shilov conditions, undergo reductive elimination to ROH/RCl plus Pt(II), at a rate fully compatible with that of the overall oxidation of alkanes. All of this leads directly to the three-step sequence (exemplified for methane oxidation) in Scheme 2.4.

2.2.2 Mechanistic Details

Although the above scheme has held up through the ensuing years, it is incomplete: there are multiple possibilities for the precise mechanism (or, perhaps, mechanisms) involved in each of these three sequential steps. In the next three sections we will examine how the steps have been studied separately in order to elucidate their mechanisms in detail, followed by a brief revisit to consider how they fit together to account for the overall behavior of the intact Shilov system.

2.2.2.1 C–H Activation

The close similarity between the H/D exchange and Shilov oxidation processes, in terms of kinetics, site preferences, and other parameters, strongly implies that this first step is both rate- and selectivity-determining, and hence essential to understand as thoroughly as possible. It is also the most *difficult* to study, however, since the reaction of Pt(II) with RH to give RPt(II) cannot be isolated from the rest of the steps. Hence most of the detailed mechanistic studies have involved model complexes, an approach which is always subject to uncertainty, as the changes needed to generate a model for which the necessary observations can be made may well also cause the mechanism to change. Nonetheless, an extensive body of investigations on such models has led to a mechanistic picture that is (at least) self-consistent, as well as accounting reasonably well for the more limited set of findings on the actual Shilov system. As before, we will only highlight some of the more revealing experiments here; a much more extensive review of C–H activation at Pt has appeared [23].

Two clearly differing mechanisms for C–H activation at Pt(II) have been considered from the beginning: oxidative addition, an established process for late-transition metal centers, followed by proton loss; or direct deprotonation of a σ-alkane complex, by analogy to the well-known acidity of σ-dihydrogen complexes. The so-called σ-CAM mechanism, in which the hydrogen is abstracted by a ligand on Pt, may be considered as a close variant of direct deprotonation. Scheme 2.5 shows these three alternatives; the σ-alkane complex is shown as a likely intermediate on the oxidative addition route, and might well be on the σ-CAM route as well.

The fact that most well-defined examples of oxidative addition involve very electron-rich metal centers—*not* an obvious characteristic of these Pt(II) species—was taken by some as an argument for direct deprotonation; but as noted above, experimental evidence on the actual system proved elusive. In one study, Zamashchikov examined the behavior of the (dimethyl)Pt(IV) complex $[PtCl_4(CH_3)_2]^{2-}$, which under Shilov-like conditions (aqueous chloride solution containing $[PtCl_6]^{2-}$at 95 °C) decomposes to give ethane and ethyl chloride (as well as methyl chloride and methane). Those two products were also generated by Shilov oxidation of ethane, and comparison of the isotope effects on the product distributions in the two cases implicated a common intermediate, which

Scheme 2.5 C–H activation at Pt(II) by oxidative addition (top), direct deprotonation (middle), or σ-CAM (bottom) routes

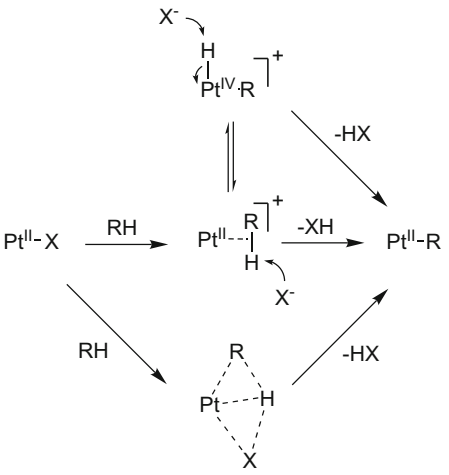

Scheme 2.6 Reactions used to argue for the oxidative addition mechanism

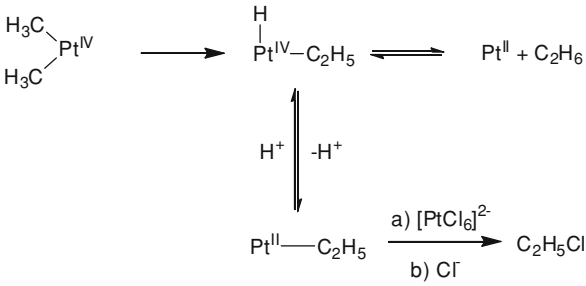

(they argued) had to be the oxidative addition adduct (Scheme 2.6), since they assumed σ-alkane complex formation would not be subject to any isotope effect [24]. However, there is considerable evidence in other systems that invalidates the latter assumption, so this attempt at a direct answer does not necessarily hold up.

Computational methods have been brought to bear on this question, but they are problematic. In aqueous media, the contributions of solvation and specific hydrogen bonding interactions will surely be very important, and it is not clear how reliable the methodology for handling them is likely to be. In an early study, Siegbahn and Crabtree examined the activation of methane by *cis*-$PtCl_2(H_2O)_2$ by DFT, and found the lowest overall activation energy for a σ-CAM-like route; the calculated transition state (Fig. 2.1) includes specific solvation by a water molecule in the secondary coordination sphere, hydrogen bonded to both coordinated water and chloride. While the calculated transition state for an oxidative addition route came out very close in energy, the authors preferred the σ-CAM, feeling that a Pt(IV) intermediate was unlikely [25]. Subsequent calculations by Ziegler included all possible chloro(aquo)Pt(II) species; they concluded that the neutral $PtCl_2(H_2O)_2$ is the most reactive, but depending on conditions it may be present in

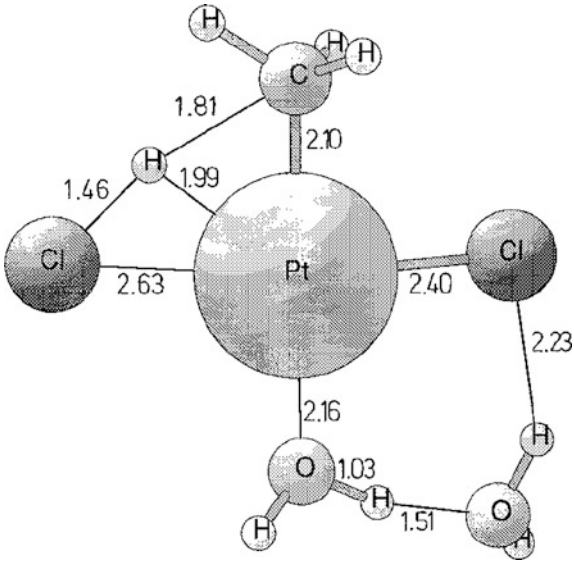

Fig. 2.1 Calculated transition state for activation of methane by $PtCl_2(H_2O)_2$. Reprinted from Ref. [25] with kind permission of © The American Chemical Society (1996)

such low concentration that most of the activation proceeds via anionic $[PtCl_3(H_2O)]^-$. Coordination of methane by associative displacement of water was calculated to be the rate-determining step; the actual C–H activation (assumed to be oxidative addition) had a much lower barrier [26].

In the absence of a direct experimental approach, researchers turned to indirect methods—specifically, examination of the microscopic reverse reaction, protonolysis of an (alkyl)Pt(II) complex. It was hoped that the alternatives (which correspond to running the reactions in Scheme 2.5 from right to left) could be more conclusively distinguished, perhaps even by observation of an intermediate. Here too there is a problem, though: the postulated Pt(II) complexes $[PtCl_3R]^{2-}$ are quite unstable. Attempts to synthesize such a species, either by methylation of $[PtCl_4]^{2-}$ or by reduction of $[PtCl_5(CH_3)]^{2-}$, were unsuccessful, leading to decomposition, formation of dimethyl species, and/or instantaneous liberation of methane by protonolysis. (There was one exception: reduction of $[PtCl_5(CH_3)]^{2-}$ by cobaltocene in a *nonprotic* solvent gave a mixture of salts including the desired species, which was used in studies described below) [27]. Hence model complexes were required even for this indirect approach.

The reaction summarized in Eq. 2.6 was carried out for several ligands L (amines and phosphines were used) under a variety of conditions of solvent, temperature and acid, with two key findings. First, several cases generated an NMR-observable alkyl(hydrido)Pt(IV) species, which was stable at low temperature and decomposed to alkane on warming; second, in deuterated acidic media many of the reactions displayed multiple H/D exchange in both the liberated alkane and the remaining unreacted alkyl group(s) [28].

$$L_2PtRX \xrightarrow{HY(DY)} L_2PtXY + RH(RD) \tag{2.6}$$

$L_2 = Me_2NCH_2CH_2NMe_2$ or $L = PEt_3$; $R = CH_3$ or $PhCH_2$; $X = Cl$ or CH_3

These findings point clearly to the overall reaction network shown in Scheme 2.7; both σ-alkane complex and alkyl(hydrido)Pt(IV) species are intermediates (to account for the H/D exchange), but proton loss takes place from the latter. If microscopic reversibility applies, then, C–H activation in the Shilov system would proceed by the oxidative addition route (reading Scheme 2.7 from bottom to top). But *does* it apply? The model complexes used in these studies do not themselves exhibit C–H activation chemistry, and it is certainly conceivable that the introduction of ligands perturbs the system sufficiently to alter the mechanism, so uncertainties remain. At a minimum, a system that *does* effect C–H activation and exhibits the same behavior needed to be demonstrated. That was eventually achieved for several model Pt(II) complexes, all having a common feature: at least one readily displaceable ligand, usually a solvent molecule, to facilitate the initial coordination of the alkane. That process corresponds to the step shown in the lower left corner of Scheme 2.7 (reading up). The reaction shown schematically in Eq. 2.7 was accomplished first for S = pentafluoropyridine [29]; subsequently the introduction of trifluoroethanol as solvent[30] led to an extremely versatile and richly informative model system. And there are even some cases, notably that of Scheme 2.8, where a *stable* alkyl(hydrido)Pt(IV) can be obtained via C–H activation [31].

$$[L_2Pt(CH_3)(S)]^+ + RH \longrightarrow [L_2Pt(R)(S)]^+ + CH_4 \tag{2.7}$$

A number of studies on the trifluoroethanol-based system have significantly increased our detailed understanding of the C–H activation process. The dependence of the rate of benzene activation on the electronic and steric nature of the diimine ligands in Scheme 2.9 [32], along with the observation of extensive H/D scrambling in both the initial protonolysis of the dimethyl compound and the subsequent C–H activation, demonstrates that the rate-determining step in alkane activation[3] is coordination of the alkane to give the σ-complex; (reversible) C–H cleavage to give the alkyl(hydrido)Pt(IV) complex is faster. Experiments on these model systems further indicate that alkane (or arene) coordination proceeds via *associative* displacement of solvent [32, 33].

[3] For benzene activation the C–H activation step may be rate-determining, in cases where the steric constraints are not too severe; presumably the much more favorable interaction arene-metal π complex, compared to the σ alkane complex, lowers the barrier to complexation below that of C–H cleavage. This situation does not appear to arise in alkane activation by Pt(II); it is usually straightforward to decide which step is rate-determining by examining isotope exchange.

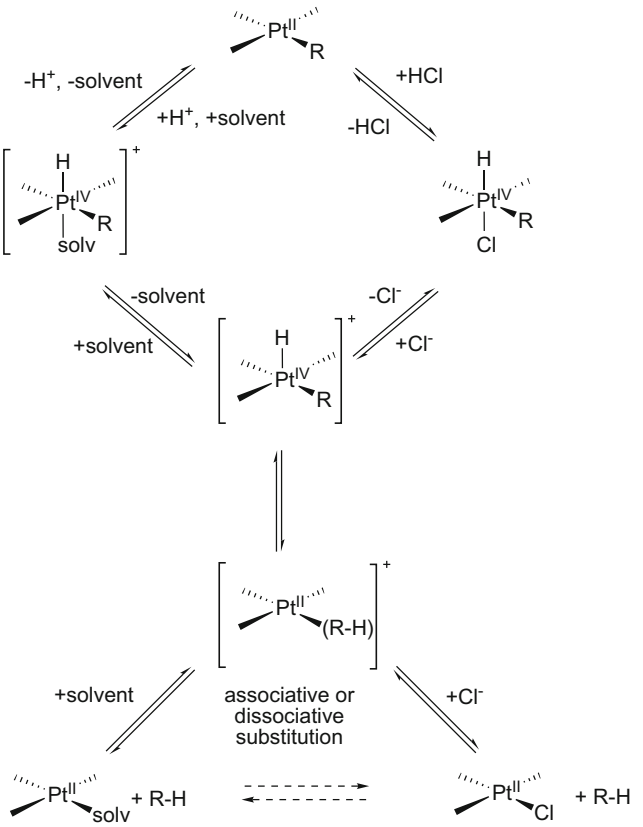

Scheme 2.7 Mechanism for protonolysis of (alkyl)Pt(II) complexes

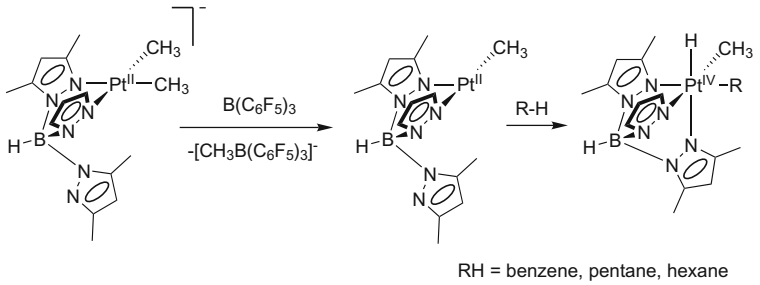

Scheme 2.8 Formation of a stable alkyl(hydrido)Pt(IV) complex via oxidative addition of alkane

Another important conclusion from this study is that electronic effects are manifested primarily in how tightly the ligand to be displaced is bound to the metal. This helps resolve some of the observations that appear at first to be at odds with the description of this chemistry as "electrophilic" (although it should be

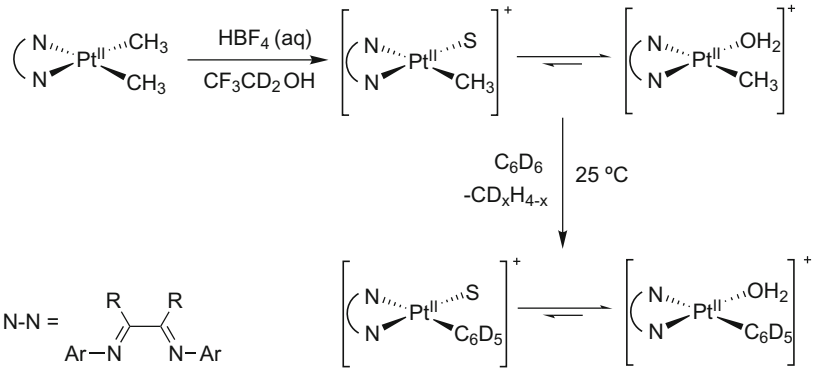

Scheme 2.9 Trifluoroethanol-based model for C–H activation studies

pointed out, once again, that we are not necessarily ascribing any mechanistic content to the term). Whereas one might expect the most electrophilic complexes—those with the highest positive charge and/or most electron-withdrawing ligands—to be the most reactive, in fact that is rarely what is found. Most of the reactivity trends in Scheme 2.9, as the N–N ligand is varied, reflect changes in the equilibrium between the aquo and solvento complexes (only the latter reacts with C–H bonds), rather than affinity for the hydrocarbon substrate [32]. Likewise, dicationic disolvento complexes can be generated; these would be expected to be much more electrophilic, and they *do* exhibit C–H activation, but only at benzylic or allylic positions (e.g., Eq. 2.8), not with simple alkanes; furthermore, the reactions are considerably slower than those of the analogous monocations of Scheme 2.9 [34]. It is clear that facile "displaceability" of a ligand is a crucial element of an efficient alkane functionalization system.

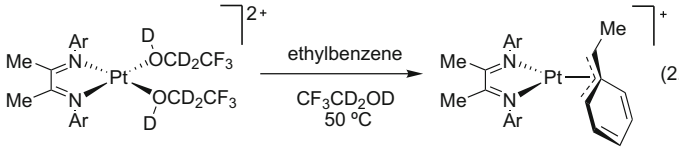

(2.8)

The question of the relative reactivity of different C–H bonds can also be addressed using these model systems. An anhydrous version of the system shown in Scheme 2.9 reacts readily with a variety of alkanes and cycloalkanes according to Eq. 2.9, with rapid β-hydrogen elimination following C–H activation; the rate constant for the various substrates (after correction for statistical factors) varies only slightly [35]. The same model complex was used to determine the relative reactivity of methane (using ^{13}C labeling) and methanol (Scheme 2.10), giving a ratio of rate constants k_2/k_1 around 1.3, [36] on the same order as that estimated for

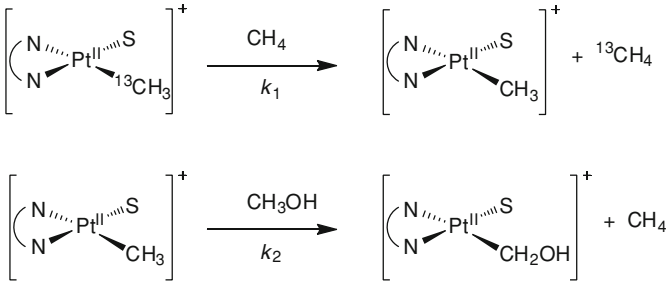

Scheme 2.10 Determination of relative reactivity of methane and methanol with model Pt(II) complex

the actual Shilov system (see above).

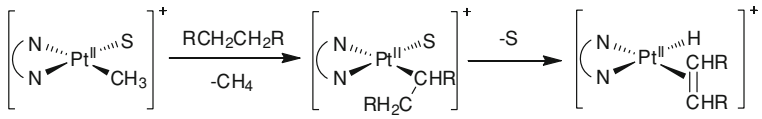

(2.9)

All these results, on both the actual Shilov system and models thereof, appear consistent with the C–H activation mechanism represented in Scheme 2.7 (reading bottom to top): rate-limiting associative formation of a σ complex, followed by fast oxidative cleavage of the C–H bond and deprotonation of the resulting alkyl(hydrido)Pt(IV) species. The rate-determining step is apparently *not* very sensitive to the nature of the coordinating species: primary and secondary C–H bonds as well as those adjacent to OH groups all react at about the same rate (after correcting for statistical factors), differing by no more than a factor of 3-5 or so. Only severe steric crowding—a tertiary C–H bond, or one adjacent to a quaternary center—and really strong electron withdrawing substitution (note that the C–H bonds of trifluoroethanol are not activated) appear to attenuate coordinating power sufficiently to inhibit reactivity. As indicated earlier, this situation carries both positive and negative implications. Selective alkane oxidation should be much more feasible here than with more traditional oxidants that follow radical pathways; on the other hand, functionalizing a substrate that presents more than one potential site of reaction with high selectivity to a single product will generally be difficult to achieve, in the absence of additional features such as directing substituents. We will see some examples of the latter in later sections.

2.2.2.2 Redox Step

Since attempts to independently generate the (alkyl)Pt(II) intermediate that would be formed by the C–H activation step result in virtually instantaneous protonolysis, conversion of that intermediate to (alkyl)Pt(IV) must be *extremely* fast in order to

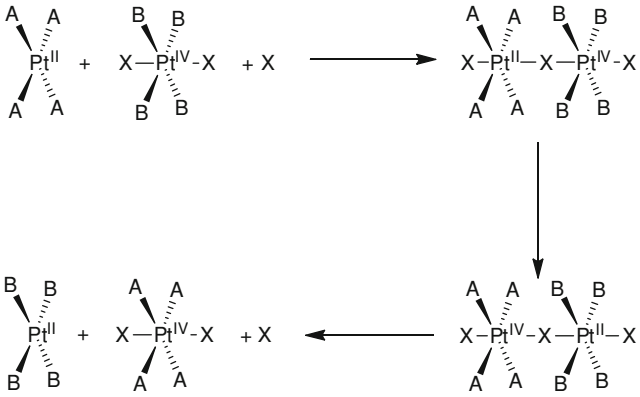

Scheme 2.11 Schematic representation of the inner-sphere mechanism for Pt(II)-Pt(IV) redox reactions

be able to compete under Shilov oxidation conditions. It is not at all obvious why it should be so fast. The "standard" mechanism for a redox reaction between Pt(II) and Pt(IV) is via a 2-electron, inner-sphere pathway, as in Scheme 2.11; the requirement for an additional X^- ligand in the symmetric bridged transition state is responsible for the commonly observed third-order kinetics [37]. Such a mechanism has been demonstrated for N-ligated complexes of the sort used for the model studies described in the previous section [38–40].

An example more closely relevant to the actual Shilov system, the self-exchange between $[PtCl_4]^{2-}$ and $[PtCl_6]^{2-}$, was examined by following the exchange of isotopically labeled Cl [41]; although rigorous quantitative comparison is not possible because of the complexity of the systems, the upper limit of that self-exchange rate would be far too slow (by at least several orders of magnitude) to compete with the lowest estimate of the rate of protonolysis. Of course, one *would* expect the reaction of $[PtCl_3R]^{2-}$ with $[PtCl_6]^{2-}$ to be faster (but how much faster?). First, there is a substantial driving force (absent in self-exchange) due to the replacement of Cl by R, which makes the Pt(II) complex more electron-rich and more susceptible to oxidation, as has been documented by both electrochemical data and reactivity trends in a model system [38]. Also, the greater *trans* effect of R should accelerate formation of the bridged species, a process that in effect amounts to nucleophilic attack on square planar Pt(II). Another possibility, however, is that the reaction involves *alkyl* transfer rather than electron transfer—although here too it is far from clear why that should be a fast process.

These two alternatives may be distinguished by labeling the respective Pt centers and determining which one the R group ends up on. For model systems, electron transfer is easily demonstrated by using different ligands on the Pt(II) and Pt(IV) reacting partners [38], but for the actual Shilov system, where RPt(II) is not readily available and all the other ligands are (freely exchanging) chloride and water, isotopically labeled Pt is required. The first such study took advantage of the observation that Zeise's salt, $[PtCl_3(C_2H_4)]^-$, is oxidized by $[PtCl_6]^{2-}$ to a

Scheme 2.12 Alternate pathways for oxidation of Zeise's salt to an (alkyl)Pt(IV) species

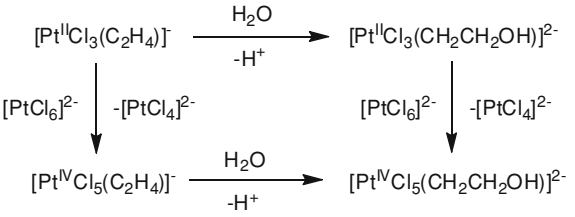

Scheme 2.13 Alternative S_N2 (top) and intramolecular reductive elimination (bottom) routes for liberation of RCl from RPt(IV)

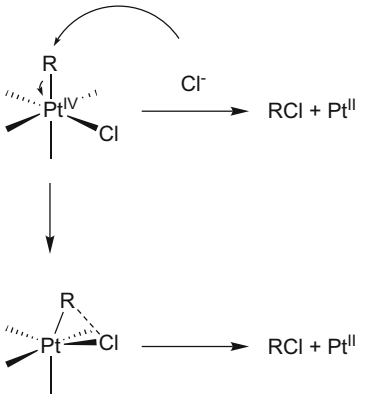

(2-hydroxyethyl)Pt(IV) species. There are two possible routes for that reaction: prior nucleophilic attack of water on the coordinated olefin to give (2-hydroxyethyl)Pt(II) which undergoes oxidation; or initial oxidation to a Pt(IV) ethylene complex that reacts with water (Scheme 2.12); only the former would be a true analog of the redox step of the Shilov system. Kinetics established that the former path is indeed followed, and use of enriched $[^{195}PtCl_6]^{2-}$ led to *no* enrichment in the (2-hydroxyethyl)Pt(IV) product, arguing for the electron transfer route [42]. Subsequently an analogous experiment, in which the insoluble $[PtCl_3R]^{2-}$ salt mentioned in the previous section was oxidized by $[^{195}PtCl_6]^{2-}$, led to the same conclusion [27].

2.2.2.3 C-X Bond Formation

Two issues pertain to the liberation of RX (X = OH, Cl) from (alkyl)Pt(IV). First, does the product form via intramolecular reductive elimination of RX, or by external nucleophilic attack of X at R, with Pt(II) as the leaving group (Scheme 2.13)? Second, does the reaction take place from the intact six-coordinate Pt(IV) complex, or from a five-coordinate intermediate species generated by prior ligand dissociation (as is common to many reductive elimination processes)? Since (as noted earlier) representative (alkyl)Pt(IV) complexes can be independently synthesized and are quite stable, this step has proven the most amenable to direct study.

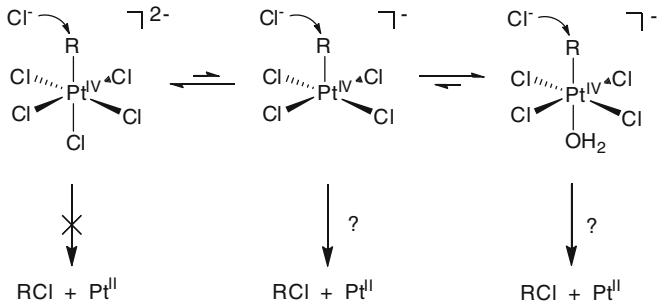

Scheme 2.14 Possible intermediates in liberation of RCl by nucleophilic attack; kinetics rules out the first, but does not distinguish between the other two

Scheme 2.15 Experiment demonstrating inversion of stereochemistry in formation of RCl from RPt(IV)

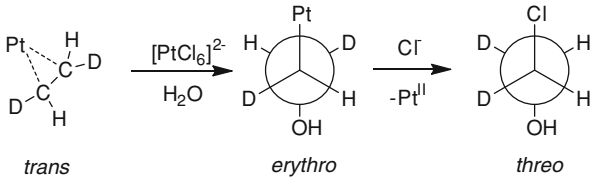

Early studies strongly supported nucleophilic attack; perhaps most telling was the observation that an external nucleophile, such as Br^-, is incorporated into RX *much faster* than it exchanges into a position *cis* to R in RPt(IV) [43]. The kinetics are also consistent with nucleophilic attack: the dependence of the rate of disappearance of RPt(IV) on chloride concentration takes the form shown in Eq. 2.10, while the proportion of RCl:ROH increases with $[Cl^-]$. The appearance of $[Cl^-]$ in the denominator suggests that the reaction proceeds via a five-coordinate intermediate; but in fact the kinetics are equally consistent with nucleophilic attack occurring at a six-coordinate complex with an aquo (but *not* a chloride) ligand *trans* to the R group (Scheme 2.14). While there is no way to distinguish between these two possibilities, the former seems clearly favored by the fact that it is the microscopic reverse of the first step of many examples of oxidative addition of methyl halide to square-planar, four-coordinate d^8 complexes [42].

$$\frac{-d[\mathrm{RPt^{IV}}]}{dt} = \frac{k_1[\mathrm{Cl^-}] + k_2[\mathrm{H_2O}]}{1 + K[\mathrm{Cl^-}]} \tag{2.10}$$

Conclusive evidence supporting the nucleophilic attack mechanism was obtained from a stereochemical study. A stereolabeled (alkyl)Pt(IV) complex was synthesized by the oxidation of Zeise's salt (as in Scheme 2.12) prepared from *trans*-1,2-dideuteroethylene; the resulting (mostly) *erythro* isomer of the (2-hydroxyethyl)Pt(IV) complex reacts with Cl^- to liberate *threo*-2-chloroethanol (Scheme 2.15), demonstrating inversion of configuration, as expected for S_N2 [42].

2.2.2.4 Global Mechanism Considerations

From the work summarized in the three preceding sections, we can say with confidence that the three-step sequence originally proposed for the Shilov system (Scheme 2.4) stands on very firm ground, and can fill in many of the finer mechanistic details for each of the three steps. How do they fit together to account for overall behavior? As already noted, the close similarity between Shilov oxidation and Pt(II)-catalyzed H/D exchange, in terms of both rates and selectivities for different C–H bonds, implies that the first step, C–H activation, is rate-determining for oxidation. That conclusion is consistent with *most* observations, but there are a couple of apparently discordant findings. Most notably, Shilov and coworkers reported that a solution used for oxidation of methane, after cooling, exhibited the NMR signal of $[PtCl_5(CH_3)]^{2-}$ [44]; if both steps 2 and 3 are significantly faster than step 1, one would not expect any significant buildup of that intermediate. (Indeed, a later examination under actual reaction conditions, using pressure-resistant NMR tubes, found no evidence of that NMR signal [45]).

Another is found in the kinetics for the oxidation of acetic acid to chloroacetic acid: the rate is independent of [Pt(IV)], as expected if step 1 is rate-limiting, but only up to 100 °C; at higher temperatures (and at low [Pt(IV)] levels) the rate law includes a term first-order in [Pt(IV)] [46]. The implication is that the activation energy for step 2 is lower than that for step 1, so that as the temperature is raised step 1 speeds up more and step 2 becomes rate-limiting. In the high-temperature regime the activation energy was measured to be around 9 kcal/mol [46], similar to the value of 7 kcal/mol determined for Pt(II)-Pt(IV) redox in a model system [38] and for the $[PtCl_4]^{2-}/[PtCl_6]^{2-}$ self-exchange reaction [38, 41].

As previously noted, the oxidation of RPt(II) (step 2) must be faster than protonolysis (reverse of step 1) for overall oxidation to succeed. The *relative* rates of those two processes have been estimated by two different procedures (both alluded to above). The (dimethyl)Pt(IV) complex shown in Scheme 2.6, besides undergoing C–C reductive elimination to give ethane, reacts in aqueous Cl^- at 95 °C to generate (transiently) the key (methyl)Pt(II) intermediate. If that reaction is carried out in the presence of varying concentrations of $[PtCl_6]^{2-}$ and H^+, the ratio of the rate constants for oxidation and protonolysis can be obtained straightforwardly from the relative amounts of (methyl)Pt(IV) (which is itself unstable to the reaction conditions, but the methyl chloride thus liberated can be measured) and methane produced [43]. A similar experiment can be carried out at lower temperature, by dissolving solid $[PtCl_3(CH_3)]^{2-}$ (part of the salt mixture obtained by reducing $[PtCl_5(CH_3)]^{2-}$ with cobaltocene) in aqueous $[PtCl_6]^{2-}/H^+$ [27]. The relative rate constants thus determined are (Scheme 2.16): $k_{ox}/k_{prot} \sim 20$ at 95 °C [43, 47] and near one at room temperature [27, 47]. By extrapolation, oxidation should be even more dominant around 120 °C, more typical of Shilov conditions.

The fact that the rate constant ratio increasingly favors oxidation as the temperature rises, along with the earlier report that oxidation becomes rate-limiting at higher temperatures, implies that the activation energies are in the order: C–H

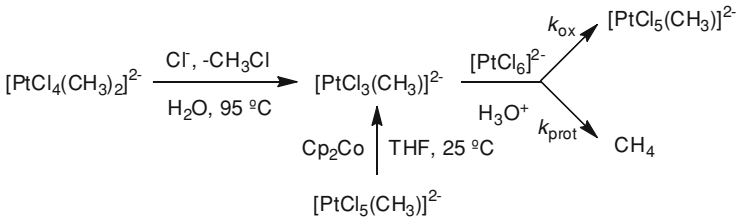

Scheme 2.16 Reactions used to determine relative rates of oxidation and protonolysis of an (alkyl)Pt(II) complex at elevated and room temperatures

activation (step 1) > oxidation (step 2) > protonolysis (reverse of step 1). That may not be unreasonable; one might expect protonolysis to have a low activation barrier. It should be noted, however, that these two studies were carried out in different media, water and aqueous acetic acid respectively. That could well have a significant impact on the oxidation step, since a reaction requiring two negatively charged species to get together should be facilitated by the more polar medium. This may account for a significant difference in behavior: whereas Shilov oxidation in acetic acid is accompanied by a substantial amount of H/D exchange [14–17], in water no H/D exchange takes place until after deposition of Pt metal has been observed [45, 48]. Thus, although protonolysis and oxidation may take place at comparable rates in acetic acid, in water protonolysis is always much slower than oxidation until the appearance of Pt metal, which may catalyze the exchange reaction itself and/or signal the point where the concentration of Pt(IV) has been reduced enough to allow protonolysis to compete.

This effect may also explain why the two media differ in the propensity to deposit Pt metal, which is much less pronounced in acetic acid than in water. Although Pt(II) can on its own disproportionate to Pt(IV) and Pt(0) under some conditions, it seems more likely that the appearance of Pt metal in the Shilov system results from oxidation of RPt(II) by inorganic Pt(II) (Eq. 2.11), which as discussed above should be thermodynamically more favorable than disproportionation. Since this redox reaction, like the previous one, involves two negatively charged participants, it could be much more important in water than in acetic acid. (The reaction of "purely" aqueous Pt(II) with hydrocarbons was examined by means of inverted micelles, as an alternative to the use of aqueous acetic acid; H/D exchange appears to behave more or less similarly, but formation of metallic Pt is observed [49].) An analog of the experiment portrayed in Scheme 2.16 indicated that $[PtCl_4]^{2-}$ is *not* capable of oxidizing $[PtCl_3(CH_3)]^{2-}$ competitively with protonolysis at room temperature [27], but if the same temperature trends hold here as for oxidation by $[PtCl_6]^{2-}$, at operating Shilov temperatures Eq. 2.11 could well be a competent mechanism for Pt metal formation.

$$\left[Pt^{II}Cl_3(CH_3)\right]^{2-} + \left[Pt^{II}Cl_4\right]^{2-} \longrightarrow \left[Pt^{IV}Cl_5(CH_3)\right]^{2-} + Pt^0 + 2Cl^- \qquad (2.11)$$

In the following sections we will examine potential applications, of both the original Shilov system and modifications thereof, within the context of this well-delineated mechanistic framework.

2.2.3 Potential Applications

Beyond the fundamental interest in Shilov oxidation as an unusual reaction, does it present any practical opportunities? If we are interested in large-scale applications, such as direct conversion of methane to methanol, we obviously need to replace Pt(IV) with something *much* cheaper—preferably O_2—as the stoichiometric oxidant. On the other hand, it is conceivable that the original Shilov system might be a useful tool in the laboratory-scale synthesis of complex products by functionalization at a saturated position, but only if sufficiently high selectivity can be achieved.

2.2.3.1 Alternate Oxidants

There are fairly severe constraints on possible choices for an alternate stoichiometric oxidant in a large-scale alkane functionalization process. First, it must be very cheap; for production of a fuel/commodity chemical such as methanol, it is most unlikely that anything but O_2 will be cheap enough. Unfortunately, unlike Pd (see below), it does not appear that any of the intermediate Pt species can be directly oxidized by O_2, so the oxidant will have to be regenerable by O_2 under reaction conditions. Second, while it has to oxidize the (alkyl)Pt(II) intermediate, it must not be strong enough to oxidize *inorganic* Pt(II), since the mechanism requires the latter for C–H activation. And finally, the rate of oxidation of (alkyl)Pt(II) must be extremely fast to compete with protonolysis. Given the particular mechanism of the Pt(II)-Pt(IV) redox process, it is not obvious what other oxidants could be equally fast.

In earlier work several oxidants were found to achieve some catalytic oxidation, although even the best results gave only a handful of turnovers. Some, such as chlorine [45] or peroxydisulfate [50], are clearly too expensive and *not* regenerable with O_2. Other systems use catalytic amounts of oxidants, such as $CuCl_2$ [51] or polyoxometalates [52, 53], which (at least in principle) *can* be reoxidized by dioxygen, making the latter the stoichiometric oxidant. Indeed, with Cu(II) under elevated O_2 pressures, ethanesulfonic acid (a water-soluble alkane surrogate) can be oxidized to 2-hydroxyethanesulfonic acid with a significant number (50 or more) of turnovers. Several other substrates, including methanesulfonic acid (which is somewhat less reactive, probably reflecting the effect of the fairly strong electron-withdrawing substituent), propanesulfonic acid, ethylphosphonic acid, and propionic acid, could be similarly oxidized to hydroxy compounds [54]. If this modified Shilov system could operate on methane, the overall reaction would

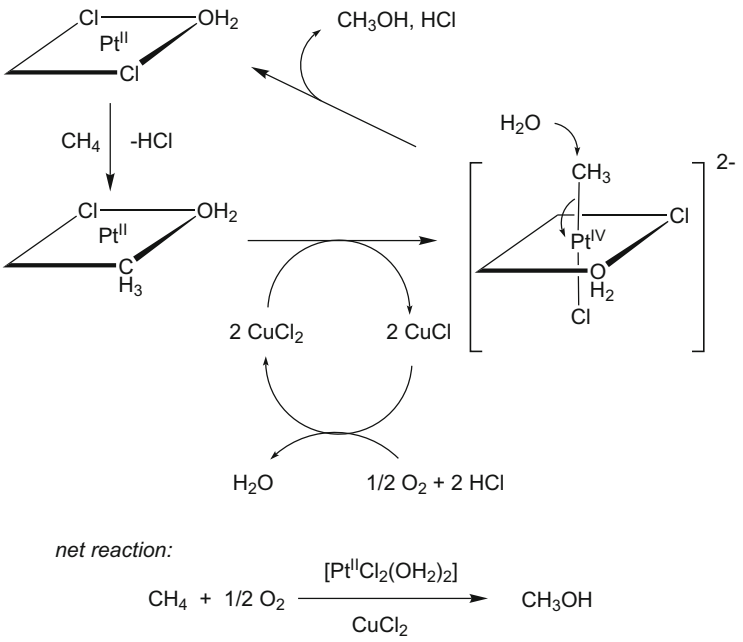

Scheme 2.17 Modified Shilov mechanism with Cu(II)/O_2

$$[PtCl_4]^{2-} + H_2O_2 + 2\,HCl \longrightarrow [PtCl_6]^{2-} + 2\,H_2O$$

$$[PtCl_6]^{2-} + 2\,H_2O_2 \longrightarrow [PtCl_4]^{2-} + O_2 + 2\,HCl$$

Scheme 2.18 Disproportionation of H_2O_2 accompanies its use as an oxidant in the Shilov system

amount to direct oxidation of methane to methanol by dioxygen (Scheme 2.17). Recently a Pt/Fe(III)/O_2 combination (discovered using a microfluidic screening device) showed some success for selective methane oxidation, giving up to 50 turnovers of a mixture of methanol and formic acid [55].

With most of these alternative oxidants (but not Cu(II)/O_2: see below) the catalyst dies in the same manner as the original Shilov system, by deposition of Pt metal, resulting in degradation of both activity and selectivity, since as noted earlier the latter is a good catalyst for alcohol oxidation. In one study, which used electrochemically regenerated polyoxometalate, the selectivity for oxidation of *p*-toluenesulfonic acid to the corresponding benzylic alcohol decreased steadily as the number of turnovers increased, accompanied by the appearance of Pt metal [56].

Hydrogen peroxide has also been shown to function as an alternative oxidant in the Shilov system, despite its being able to oxidize inorganic Pt(II), because it also functions as a reductant; the combination of steps in Scheme 2.18 maintains a

sufficient steady-state concentration of Pt(II) to allow C–H activation and functionalization to take place [57]. The downside, of course, is that large quantities of H_2O_2 are consumed; clearly this inefficiency would prevent any practical applications.

The ability of Cu(II) to function as an "appropriate" oxidant for Shilov chemistry was further tested by carrying out the competitive reactions of Scheme 2.16 using $CuCl_2$ instead of $[PtCl_6]^{2-}$. Somewhat surprisingly, the former turns out to be an even *faster* oxidant: at 95 °C, the ratio of the rate constant for oxidation to that for protonolysis of $[PtCl_3(CH_3)]^{2-}$ is around 200, an order of magnitude higher! Effective competitive oxidation was also observed for $FeCl_3$ and the polyoxometallate $[H_3PMo_9V_3O_{40}]^{3-}$, both of which exhibit reactivity approximately equal to that of $[PtCl_6]^{2-}$. Even more importantly, the competitive experiment can be performed using only a stoichiometric amount of Cu(II) under an O_2 atmosphere, and the same relative reactivity is observed, demonstrating that the recycle of Cu(I) to Cu(II) is fast compared to substrate oxidation [47].

Clearly fast oxidation is not a consequence of something special about the redox mechanism of Scheme 2.11. Indeed, Cu(II) seems much more likely to act as a *one*-electron oxidant, which would require a stepwise mechanism and a (presumably highly unstable) Pt(III) intermediate. Conceivably two-electron oxidation could be achieved via a pre-formed multimetallic complex involving two or more Cu(II) centers; however, fast oxidation is also observed using $[IrCl_6]^{2-}$ [47], and it seems extremely unlikely that this Ir(IV) species could function in anything other than a stepwise, one-electron mode (the oxidation of $[PtCl_4]^{2-}$ by $[IrCl_6]^{2-}$ has been shown to go by consecutive one-electron steps [58]). It thus appears that the (kinetically) facile oxidation of $[PtCl_3(CH_3)]^{2-}$ is not dependent upon any particular mechanism, and sufficient reactivity to compete with protonolysis can be achieved with a fairly wide range of (thermodynamically) competent oxidants.

Since Cu(II) is so effective an oxidant, and since when run under O_2 the effective concentration of oxidant should not decrease over time (until the O_2 is mostly consumed), one would think that this modification of the Shilov system should *not* deactivate by precipitation of metallic Pt. Indeed that appears to be the case—no appearance of Pt(0) was reported in the above-described study [54]—but nonetheless this catalytic system, comprised of Pt(II), Cu(II) and O_2, *does* deactivate. In later work (which found up to 100 turnovers for oxidation of the methyl group of *p*-toluenesulfonic acid) it was determined that the deactivation results from complete conversion of Pt(II) to Pt(IV) [59], a reaction also observed in the experiments measuring the relative rate of RPt(II) oxidation by Cu(II)/O_2 [47]. But Cu(II) by itself can't be capable of oxidizing inorganic Pt(II), since as discussed above that would preclude catalysis altogether; the reverse reaction, oxidation of CuCl by $[PtCl_6]^{2-}$, has been demonstrated and studied kinetically [60]. It must be the case, then, that the combination of Cu(II) and O_2 generates an oxidant that is thermodynamically stronger than Cu(II) alone and kinetically faster than O_2 alone, possibly a copper-peroxide complex. If not for this additional complication, the Pt(II)/Cu(II)/O_2 system could well comprise a practical catalyst for selective functionalization of certain C–H bonds.

2.2.3.2 Selective Transformations

While there remain major barriers to practical implementation of the Shilov system for functionalization of alkanes and related molecules, as discussed in preceding sections, it is certainly possible that useful applications might arise, given the right combination of desired target and available precursor. Almost certainly these would involve small-scale processes, where low catalytic efficiency and the cost of the oxidant need not be fatal flaws. Even then, we will normally want to functionalize at a particular position with high selectivity, and that will be attainable only in special cases: where potentially competing sites are deactivated by steric and/or electronic factors, or where a substituent on the substrate can lead to directed activation by coordinating to Pt. A few suggestive examples have been reported and are summarized here.

The formation of (some) ethylene glycol from ethanol was mentioned earlier; since the initial product of Shilov oxidation of ethane should be ethanol (along with ethyl chloride, depending on conditions), the direct conversion of ethane to ethylene glycol should be possible. That has been demonstrated, although no estimate of selectivity or yield was made [61]; but the earlier findings on ethanol oxidation show that there is little discrimination between C–H bonds, and coupled with the propensity for overoxidation—especially after Pt metal has begun to deposit—selectivities must be well below 50 %. Of course, one might *want* the "overoxidized" product: oxidation of ethane using a combination of Pt(II) and Pt(0) gave primarily acetic acid (along with some glycolic acid), although less than one equivalent was obtained [62]. While it is possible to deactivate C–H bonds by steric crowding or electronegative substitution, there is no obvious indication that particular bonds can be *activated*; for example the benzylic and terminal methyl C–H bonds in *p*-ethylbenzenesulfonic acid are about equally reactive [48].

As we move away from actual alkanes to more complex molecules, some degree of selectivity can be achieved by directed functionalization of potentially chelating substrates. Sen has shown that oxidation of alcohols, as well as carboxylic, sulfonic, and phosphonic acids, tend to give preferential reaction at sites that would lead to favorably sized rings upon C–H activation if the original functional group is also coordinated to Pt (Scheme 2.19). For carboxylic acids the typical selectivity order is α-CH $\ll$ β-CH $<$ γ-CH $\sim$ δ-CH [63].

In related chemistry, Sames has found that amino acids can be selectively hydroxylated by either the original or the Cu(II)-modified Shilov system. Thus valine is converted to hydroxyvaline (obtained as the lactone) in up to 50–60 % yield and 20 turnovers. Selectivity was proposed to arise via preferential attack at the γ position of valine coordinated through *both* O and N (Scheme 2.20). With other amino acids some pyrrolidine products were also obtained, via competing functionalization at the δ position followed by intramolecular S_N2 attack by N (either directly as shown in Scheme 2.21, or perhaps subsequent to formation of a chlorinated intermediate) [64].

The most elaborate example (we have gotten very far away from simple alkanes here!), from the same group, makes use of one of the Shilov models discussed

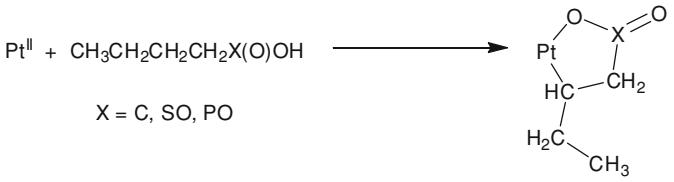

Scheme 2.19 Selective functionalization of organic acids via chelation

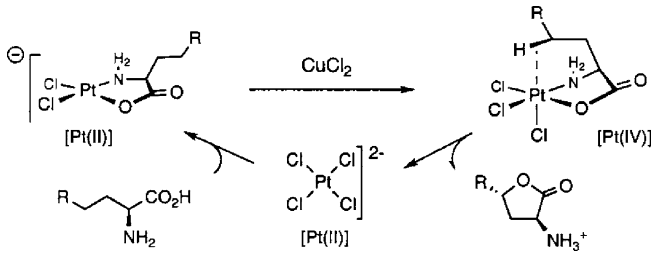

Scheme 2.20 Proposed mechanism for selective oxidation of valine. Reprinted from Ref. [64] with kind permission of © The American Chemical Society (2001)

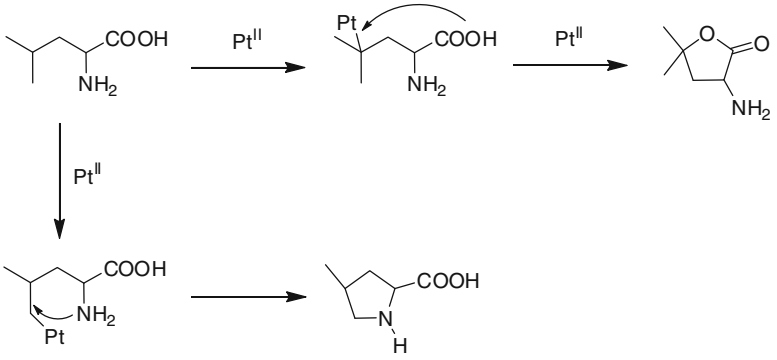

Scheme 2.21 Competing γ (top) and δ (bottom) functionalization of leucine

earlier: a substituted aniline containing the C–H group to be activated (the terminal end of an ethyl group) was incorporated into an imine ligand that could be coordinated to a $PtMe_2$ group. After protonolytic cleavage of one of the Pt-Me bonds, the resulting reactive Pt(II) center was in just the right position to selectively activate the target saturated C–H bond, resulting in an (alkyl)Pt(II) species. The latter spontaneously underwent β-hydride elimination, followed by detaching the resulting olefin—the desired product—from Pt (Scheme 2.22). This highly selective functionalization was a crucial step in the total synthesis of the antitumor agent rhazinilam [65].

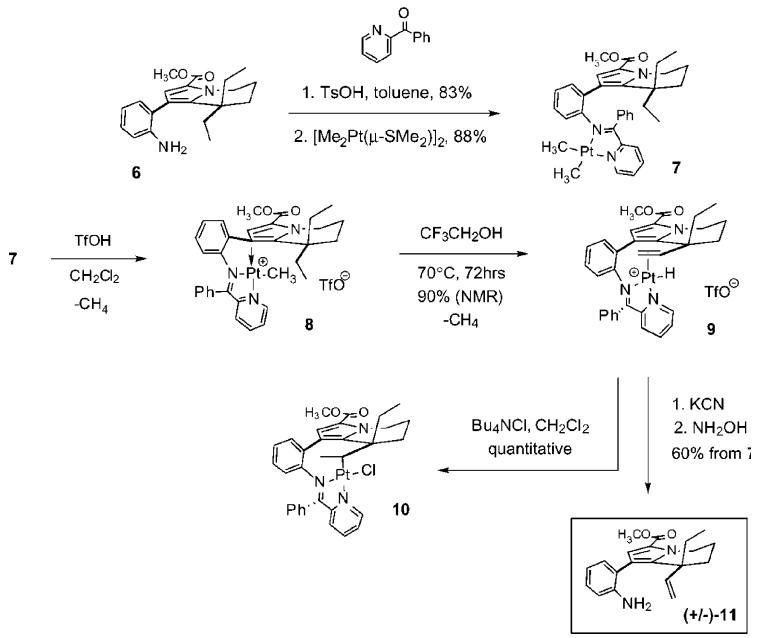

Scheme 2.22 Selective functionalization of a C–H bond by Pt(II) in the total synthesis of a complex natural product. Reprinted from Ref. [65] with kind permission of © The American Chemical Society (2002)

Electrophilic C–H activation has been increasingly used as a solution to complex organic synthesis problems, most commonly involving Pd; some examples (but by no means a comprehensive survey) will be presented in Sect. 2.4.1.2.

2.3 Other Platinum-Based Functionalizations

A *priori* there is no reason at all why the original Shilov system should be best suited for alkane functionalization, but few attempts at modification by introducing new ligands to the Pt coordination sphere have led to improvement—with one very notable exception.

2.3.1 Ligand-Substituted Complexes

As indicated earlier, there is a *very* large body of work on C–H activation by ligand-substituted Pt(II) complexes [23], but not so many examples of functionalization. Since C–H activation, the first step of the Shilov cycle, appears to

be rate-determining under most or all conditions, one should look first at the effect of ligands on that step. Early work by Shilov's group included substitution of various anions for chloride; the rate of H/D exchange correlates fairly well *inversely* with their *trans*-directing power: $CN^- < NO_2^- < I^- < Br^- < Cl^- < F^-$ [16, 17]. Since a variety of studies strongly indicate that displacement of water by the C–H bond of the alkane is rate-limiting for both H/D exchange and oxidation, that finding at first seems a bit surprising: a better *trans*-directing ligand might be expected to facilitate ligand substitution. DFT calculations suggest that such a simple correlation is not to be expected, as the predicted barriers depend strongly on solvation factors as well as the relative abundance of Pt(II) species and which ligand is replaced; for really strong *trans*-directing ligands such as cyanide or neutral amines and phosphines, the C–H activation barrier increases and becomes rate-limiting [66, 67]. Indeed, generally the addition of "good" ligands to the Shilov system completely inhibits C–H functionalization. Amino acids seem to be one exception: in addition to the intramolecular functionalizations discussed in the preceding section, substitution of $[Pt(glycinato)Cl_2]^-$ for $[PtCl_4]^{2-}$ in a standard Shilov reaction leads to (small) improvements in both activity and selectivity [68].

The inclusion of ligands in the Shilov system can be expected to affect the rates of all the steps differently; the effect upon the second and third steps, oxidation and C-X bond formation, can be particularly important if either one becomes rate-limiting for a particular catalytic reaction, as is certainly possible. (We will see an example in the following section.) One would expect that replacement of one or more electron-withdrawing chlorides by better-donating N- and P-centered ligands would facilitate oxidation, and that generally seems to be borne out. Of particular interest is the fact that some relevant Pt(II) complexes can be oxidized to Pt(IV) by O_2; examples include those shown in Eqs. 2.12 [69, 70] and 2.13 [71]. In the former the presence of *two* electron-releasing methyls along with the N–N ligand is required for the facile oxidation; in the latter, the availability of a "dangling" sulfonate group that can serve in chelate mode as the sixth ligand in the Pt(IV) product presumably provides the additional boost needed when the Pt(II) complex contains only one methyl group. No clearcut demonstration of a ligated system that sequentially effects both C–H activation and aerobic oxidation has been achieved, however. A possible example is the combination of $[Pt(Mebpym)Cl_2]^+$ (where Mebpym is derived from the bipyrimidine ligand discussed in the next section by methylation at one of the non-coordinated N centers) and the polyoxometalate $H_5PV_2Mo_{10}O_{40}$, supported on silica; that system was reported to catalyze oxidation of methane at 50 °C by O_2, giving some methanol and (mostly) acetaldehyde, with up to 30 turnovers [53]. The formation of acetaldehyde, a quite unexpected product, has not been completely explained.

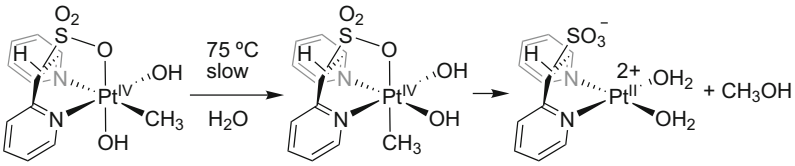

Scheme 2.23 Liberation of methanol from (methyl)Pt(IV) proceeds via isomerization to place a labile ligand *trans* to the methyl group

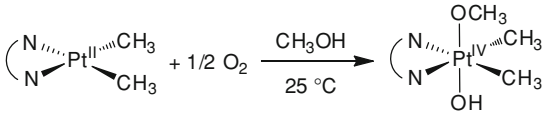

(2.12)

N-N = tmeda, bipy, phen

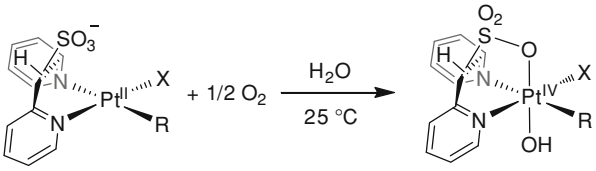

(2.13)

In contrast to the oxidation step, incorporation of strongly-binding ligands—especially chelators—may well be detrimental for the final C-X bond forming step. In most or all cases where the mechanism of that step has been elucidated, a vacant site *trans* to the Pt–C bond is required for nucleophilic attack by X at the R group, which will be more difficult or even impossible if that position is occupied by a good ligand. That situation is most clearly manifested by Vedernikov's Pt(IV) complex shown in Eq. 2.13 (where X = OH), which undergoes loss of methanol in water, but only at elevated temperature, and mechanistic examination shows that the net reductive elimination is preceded by geometrical isomerization, to get the methyl group *trans* to the labile sulfonate ligand (Scheme 2.23) [72]. Clearly there are a number of factors, including geometric ones, that will need to be considered in designing complexes for Shilov-like catalytic alkane functionalization.

2.3.2 The Catalytica System

There *is* one highly successful variant of Shilov chemistry based on ligand-substituted Pt(II): the 1998 report of Pt-catalyzed selective oxidation of methane to methyl bisulfate [73], an advance upon the earlier Hg-based system (Sect. 2.4.6), was and remains the most impressive achievement of high selectivity, conversion and yield in functionalization of a simple alkane. Whereas, as noted above, ligands generally are detrimental to the original Shilov system (which operates around 120 °C in water or aqueous acetic acid), that does not appear to

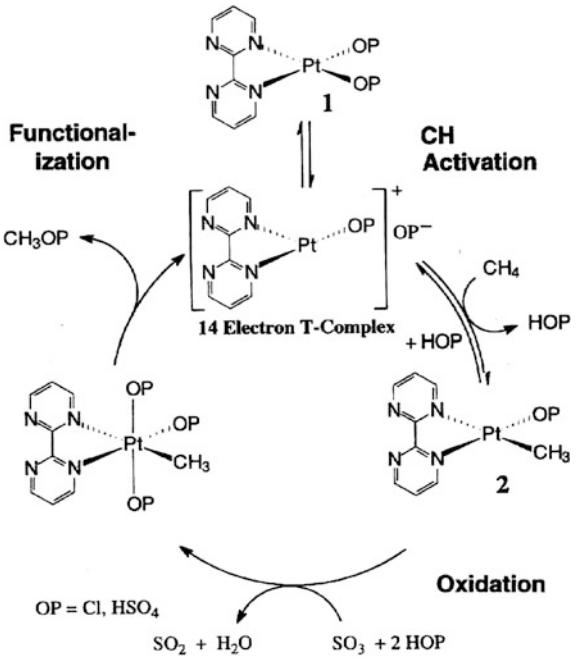

Scheme 2.24 Originally proposed mechanism for oxidation of methane by the Catalytica system. Reprinted from Ref. [73] with kind permission of © The American Association for the Advancement of Science (1998)

be the case under more extreme conditions: a number of bis(N-ligated)Pt(II) complexes—even the simplest example, $Pt(NH_3)_2Cl_2$—are moderately active for methane oxidation in concentrated sulfuric acid at 180 °C, oxidizing methane according to Eq. 2.14, with initial turnover rates on the order of 10^{-3}/s. While the simple ammine complex is only marginally stable to the reaction conditions, decomposing in less than an hour, the analogous bipyrimidine (bpym) complex (shown in Scheme 2.24) persists indefinitely. Indeed, it is not only kinetically inert but thermodynamically stable: it is readily generated by adding either $PtCl_2$ or Pt metal to a hot solution of bpym in concentrated H_2SO_4.

$$CH_4 + 2\ H_2SO_4 \longrightarrow CH_3OSO_3H + SO_2 + 2\ H_2O \qquad (2.14)$$

The mechanism originally proposed for this reaction (Scheme 2.24) is closely analogous to that of the Shilov system, with a couple of differences. First, as shown in the scheme, a dissociative route for activation of methane was suggested (without any specific experimental support), in contrast to the associative pathway established for several Shilov models. The question of which of the alternate paths the actual C–H bond cleavage follows (see Scheme 2.5 above) was left open. More importantly, in this system the rate-limiting step appears to be oxidation of Pt(II) to Pt(IV), rather than C–H activation, as indicated by the much greater extent of H/D exchange than in the Shilov system; indeed, the (bpym)Pt(II) complex can effect exchange without any oxidation at all by either going to a lower temperature (< 150 °C) or substituting non-oxidizing triflic acid as the reaction medium.

$$CH_4 + 2\,H_2SO_4 \longrightarrow CH_3OSO_3H + SO_2 + 2\,H_2O$$

$$CH_3OSO_3H + H_2O \longrightarrow CH_3OH + H_2SO_4$$

$$SO_2 + 0.5\,O_2 + H_2O \longrightarrow H_2SO_4$$

$$CH_2 + 0.5\,O_2 \longrightarrow CH_3OH$$

Scheme 2.25 Combined process for conversion of methane to methanol based on the Catalytica system

The Catalytica system achieves up to 90 % methane conversion with 81 % selectivity to methyl bisulfate, an overall yield of 72 %, far higher than any other reports. Based on considerations discussed above, such a result requires that the relative C–H bond reactivity of CH_4:CH_3OSO_3H be on the order of 100 :1, in contrast to the typically ~ 1:1 ratios observed for alkanes:alcohols in the Shilov system as well as models. (Unfortunately a direct comparison cannot be made using the models, as was done for methane and methanol, since methyl bisulfate will methylate model Pt(II) complexes instead of undergoing C–H activation.) Presumably this is a consequence of the strongly electron-withdrawing nature (and perhaps some steric contribution as well) of the sulfate substituent.

Although methyl bisulfate is not in itself a desirable product, it can be readily hydrolyzed to methanol; also the SO_2 byproduct can be reoxidized to H_2SO_4 by O_2. Hence this new reaction, coupled with two very old ones, comprises the net catalytic conversion of methane plus dioxygen to methanol (Scheme 2.25), with parameters of conversion and selectivity that appear potentially compatible with practical application. Unfortunately, more detailed analysis shows that the process will almost certainly *not* be close to competitive with the existing route from methane via syngas to methanol [74, 75], for several reasons. First, the rates are *far* too low: turnover frequencies on the order of 1/s are normally the minimum required for practical processes, and that is three orders of magnitude higher than the best results found here. Next, the chemistry only works in highly concentrated (fuming) sulfuric acid, and since water is a byproduct, the medium would need to be "regenerated" after a short time. Additionally, the complexity and cost of moving large quantities of sulfuric acid through a system consisting of three separate reactions is so high that it outweighs the advantages of high-yield, moderate temperature direct methane conversion. The bpym and related Pt complexes have been supported on solid polymers in an attempt to facilitate catalyst separation and recycling, which is one (but probably not the most important) of the process problems, with some success at reproducing the performance of the homogeneous system [76]. Furthermore, it seems very unlikely that this chemistry could be used for functionalizing anything *but* methane, as the products of more complex alkanes will almost certainly be unstable to the harsh reaction conditions.

Accordingly, most of the subsequent effort on this and related reactions has focused on better understanding of the mechanism and the factors controlling reactivity, which could lead to potentially more practical systems. Much of that work has been

computational, with the earliest work on the simpler ammine complex $Pt(NH_3)_2Cl_2$ suggesting that an H_2SO_4-solvated species, $[Pt(NH_3)_2(OSO_3H)(OSO_3H_2)]^+$, is a likely candidate for the C–H activating species via displacement of the sulfuric acid by methane; σ-CAM appeared to be more likely than oxidative addition for the actual C–H cleavage step [77]. A following study on the same system concluded that NH_3 displacement might be involved instead [78]. Subsequently several groups have focused on the "real" Catalytica catalyst, the (bpym)Pt complex, but their work has not yet converged on a single preferred mechanism, with differing conclusions about the coordination of the Pt(II) species responsible for C–H activation, the detailed mechanism of the latter, and the question of whether or not the distal (non-coordinated) nitrogens in the bpym ligand are protonated. The calculations do generally agree with some aspects of the originally proposed mechanism: that methane coordination rather than C–H bond cleavage is rate-determining for C–H activation, and that oxidation of Pt(II) to Pt(IV) by sulfuric acid (or, more probably, SO_3) is rate-determining for the overall catalytic oxidation. References to this work may be found in a very useful recent review of computational work on C–H activation in general [79].

Goddard has argued for the utility of computational "screening" to search for ways to overcome the limitations of catalytic systems that may be revealed by experimental and theoretical studies [80]. Applying this approach to methane oxidation, it was predicted that changing bpym to a monoanionic ligand such as picolinate should reduce the barrier to methane coordination, the rate-determining step for C–H activation, and experimental studies indeed showed such a complex was more active for H/D exchange in benzene than its bpym analog [81]. This counts only as a partial validation, so far, because the picolinate complex is not stable at temperatures (>100 °C) needed to activate methane (for either H/D exchange or oxidation). The problem of deactivation by water has also been addressed: experimentally it has been found that the addition of ionic liquids improves water tolerance, although at considerable cost in performance [82]; calculations do not establish exactly how the effect operates [83].

2.4 Functionalization by Other Metal (and Non-Metal) Centers

It may be useful first to review what the various Pt-based systems for electrophilic functionalization of C–H bonds have in common, and what differences might be expected when we switch to other metals. The chemical properties exhibited by complexes in the various oxidation states, as well as the ease of moving between oxidation states, play a central role. For Pt, oxidation states 0, +2 and +4 are all reasonably stable, with no great kinetic or thermodynamic barriers between them. We observe net electrophilic chemistry—the (reversible) reaction between Pt and RH to give RPt and H^+—in the +2 state, but the nucleophilic chemistry that accomplishes functionalization takes place only in the +4 state. Oxidation in effect thus amounts to an "umpolung" of the Pt–C bond, from $Pt(II)^{\delta+}$—$R^{\delta-}$ to $Pt(IV)^{\delta-}$—$R^{\delta+}$. Clearly it is

crucial that the interconversion between oxidation states be facile; more particularly, as discussed earlier, it must be substantially easier to oxidize RPt(II) than its inorganic precursor. All of this is accomplished by the Shilov and Catalytica systems. On the negative side, the Pt(0) state is easily accessible—indeed, for simple chloro-Pt species, the redox potentials for the $Pt^{0/II}$ and $Pt^{II/IV}$ couples are about equal—and Pt(0) once formed is hard to reoxidize, the most common cause of deactivation for the Shilov system. (The latter problem does not apply to the Catalytica system, but there are other limitations, as we have seen.)

For other metals, then, we need to consider how these requirements are satisfied: whether an oxidation state higher than the one responsible for the C–H activation is accessible; if not, whether both electrophilic activation and nucleophilic (or some other mode of) functionalization can be achieved at a single oxidation state; whether the catalyst can be too easily trapped in an inactive form. Other issues include substitutional lability—coordination of the C–H bond is often rate-determining—and, of course, cost, if practical applicability is the goal.

2.4.1 Palladium

Based on general periodic trends, oxidation of Pd(II) to Pd(IV) will be more difficult, for any given species, than the Pt analog. On the other hand, based on experience, it is generally easier to catch Pd(0) before it aggregates and reoxidize it to Pd(II) than to do the same for Pt(0). We might expect, then, that electrophilic functionalizations based on a $Pd^{0/II}$ cycle would prevail, in contrast to the $Pt^{II/IV}$ cycles discussed in the previous section. As we shall see, that mechanism does operate, but not in all cases: many functionalizations at sp^3 C–H bonds appear to involve Pd(IV) intermediates [84, 85]. Also direct oxidation by O_2 appears to be much more common for Pd than for Pt, a significant potential advantage [86].

2.4.1.1 Alkane Oxidation

While there is no good example of a palladium analog of the Shilov system (i.e., C–H activation by a Pd salt in aqueous solution), in strong acid solution Pd salts do activate alkanes, often at temperatures considerably lower than those required for Pt in the Catalytica system. The first clear demonstration was reported by Sen, who found that $Pd(OAc)_2$ reacts with adamantane or methane in trifluoroacetic acid (TFA) at 80 °C, to give the corresponding alkyl trifluoroacetate in better than 50 % yield (based on Pd), accompanied by deposition of Pd metal [87]. It should be noted, however, that there have been subsequent reports of difficulty in reproducing these yields, especially for methane.[4] One potential ambiguity is the

[4] See papers cited in references [5] and [6].

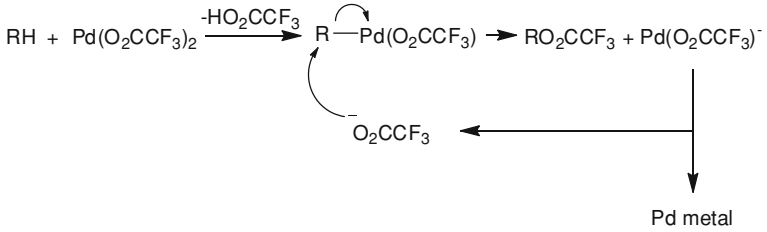

Scheme 2.26 Proposed mechanism for oxidation of alkanes by Pd(II) in TFA

use of acetate salts as precursors: methyl trifluoroacetate can be produced by the reaction of acetate with TFA, probably via a radical process, so any reaction that yields no more than two moles of product per $Pd(OAc)_2$ is open to some question, in the absence of labeling studies.

The proposed mechanism involves electrophilic activation of the C–H bond by Pd(II), followed by nucleophilic attack as in the Shilov mechanism (Scheme 2.26). (There is no real evidence that would exclude intramolecular reductive elimination as an alternate mechanism for the last step.) Sen observed no H/D exchange for adamantane, which seems rather surprising: that means that the (alkyl)Pd(II) intermediate must be more susceptible to nucleophilic cleavage (if that is what is happening) by trifluoroacetate (not the world's best nucleophile!) than to electrophilic cleavage by H^+. The latter is the reverse of the C–H activation step, which is more facile for Pd(II) than for Pt(II), and RPt(II) doesn't undergo nucleophilic attack at all. Why do we have such a dramatic reversal of trends? There do not appear to be any computational studies that might clarify this issue.

By analogy to the Wacker reaction, in which a Pd(II) salt oxidizes ethylene to acetaldehyde *stoichiometrically* (with Pd(0) deposition) or *catalytically*, in the absence or presence of an oxidant that can recycle Pd(0) to Pd(II) respectively, catalytic alkane oxidation under the above conditions ought to be possible. This has been achieved: addition of H_2O_2 as oxidant to a solution of $Pd(O_2CC_2H_5)_2$ (the propionate salt was used as precursor to avoid the ambiguity of acetate-derived product) in TFA at 90 °C gave $CH_3O_2CCF_3$ in up to 5 turnovers, based on Pd [88]. There is still some ambiguity, however: some $CH_3O_2CCF_3$ was observed even in the absence of any Pd salt, and it has been suggested that this chemistry does *not* involve electrophilic activation of a C–H bond at Pd(II), but rather oxidation by trifluoroperacetic acid formed in situ, possibly catalyzed by Pd(II). For example, the reported oxidation of cyclohexane by H_2O_2/TFA, catalyzed by Rh or Ru salts, has been shown to work equally well in the absence of any metal at all [89].

More recently this chemistry was reexamined with benzoquinone/O_2/$NaNO_2$ as a combined reoxidizing system, with up to 5 turnovers to $CH_3O_2CCF_3$ achieved; a labeling study was carried out to exclude the possibility that some of the product arose from the $Pd(OAc)_2$ precursor [90]. Somewhat surprisingly, a nearly 100 % yield of product based on Pd was reported in the absence of added oxidant, much better than the original report or any other reexamination. (It is not clear whether

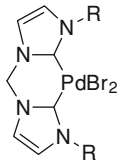

Fig. 2.2 Structure of methane-activating $Pd(NHC)_2$ complexes (R = Bu^t, Me)

the labeling study was done for the stoichiometric reaction.) These results seem reasonably unequivocal, but given the afore-mentioned problems of reproducibility, this apparently facile electrophilic activation of methane by Pd(II) in TFA at relatively mild temperatures may still be open to some question.

Sen has discovered an alternate alkane oxidation system involving palladium, but in this case *metallic* Pd. In combination with $CuCl_2$, light alkanes are oxidized by O_2 in the presence of CO, in aqueous TFA, at 90 °C [91, 92]. There is no indication that Pd(0) is oxidized during reaction; rather the proposed mechanism involves a Pd-catalyzed water gas shift reaction to generate H_2, which reacts with O_2 (again Pd-catalyzed) to form H_2O_2, which oxidizes alkane. Although there is unquestionably interesting chemistry going on, it probably does *not* involve electrophilic alkane activation, and will not be further discussed here.

A ligated Pd complex has also been found to effect this chemistry: the chelated bis(N-heterocyclic carbene) complex shown in Fig. 2.2 catalyzes the oxidation of methane to methyl trifluoroacetate by $K_2S_2O_8$, in TFA at 80–90 °C, with up to 30 turnovers achieved in 14 h [93]. The performance was significantly better than that of the simple $Pd(OAc)_2$ salt under the same conditions, indicating that the intact complex and not a decomposition product is the catalytically active species; indeed, the stability of the complex to the reaction conditions is notable, as the Pt analog decomposes immediately in TFA.

Under the more stringent Catalytica-like conditions, Pd(II) clearly does activate methane, but not exactly like Pt. Surprisingly, in addition to methyl bisulfate a significant amount of acetic acid (after hydrolysis), up to 3–4 turnovers per Pd, can be obtained [94]. Labeling studies showed that both carbon atoms come from methane, excluding the possible involvement of a contaminant. When labeled methanol was included in the reaction mixture, the label showed up *only* in the carboxylate end of the product (Scheme 2.27). The proposal was that the immediate precursors to acetic acid are methane and CO, the latter formed by oxidation of methanol; in agreement, some carboxylate-labeled acetic acid was obtained when the reaction was run under an atmosphere of labeled CO. Addition of CO also increased the selectivity to acetic acid *relative* to methyl bisulfate, but decreased the absolute yield (of both products), evidently because CO promotes reduction of catalyst to Pd(0) which deposits as Pd black.

These results may be explained by the "tandem" catalytic scheme shown in Scheme 2.28. Reaction begins with the electrophilic activation of methane by Pd(II) (upper left of the scheme), leading to (methyl)Pd(II) which can undergo competitive nucleophilic attack by bisulfate, giving methyl bisulfate (which becomes methanol

Scheme 2.27 Outcome of selective labeling experiments in the Pd-catalyzed oxidation of methane to acetic acid

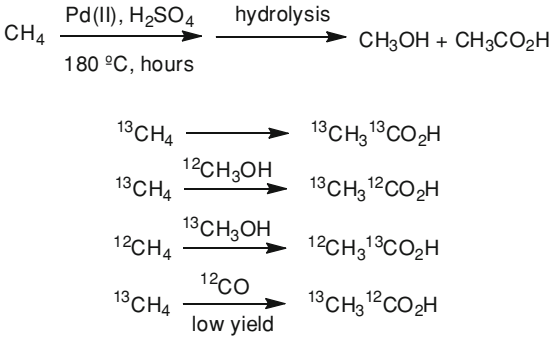

Scheme 2.28 Proposed mechanism for conversion of methane to acetic acid. Reprinted from Ref. [94] with kind permission of The American Association for the Advancement of Science (2003)

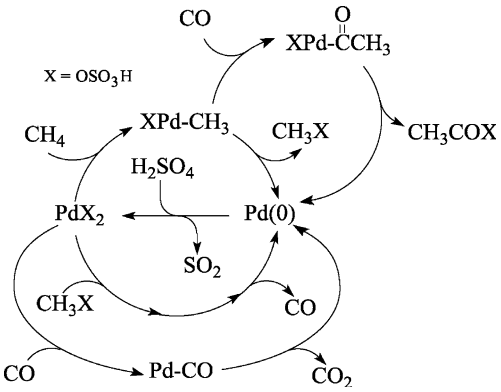

after hydrolysis) and Pd(0); or CO insertion, giving (acetyl)Pd(II), the precursor to acetic acid. The CO is formed in turn by Pd-catalyzed oxidation of methyl bisulfate or some other intermediate; besides inserting into the methyl-Pd bond, it can be oxidized to CO_2 along with Pd(0) formation. Pd(0) is reoxidized to Pd(II) by sulfuric acid; as in the Catalytica system that appears to be the rate-limiting step, and (unlike the Catalytica system) cannot keep up with reduction, so that the catalyst is deactivated over a few hours (faster with added CO) by Pd metal deposition.

Bell et al. subsequently reinvestigated this chemistry; while they were unable to reproduce the claimed yields under the original conditions, they found that carrying the reaction out under a methane-dioxygen atmosphere, with [95] or without added Cu(II), led to a significant increase in acetic acid yield—up to 14 turnovers per Pd—accompanied by (and surely due to) substantial inhibition of Pd metal formation [96]. This is consistent with the earlier conclusion that reoxidation by sulfuric acid is rate-limiting; indeed, these studies agreed in most regards with the previously proposed mechanism, with a couple of refinements. In particular, methyl bisulfate yields were dramatically higher in >100 % sulfuric acid, probably resulting from competing insertion of SO_3 into the methyl-Pd bond to give methanesulfonic acid, which has independently been shown to convert to methyl bisulfate under these conditions. An electrophilic mechanism was proposed in a

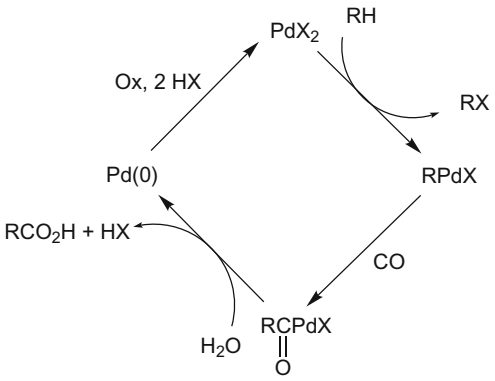

Scheme 2.29 Plausible mechanism for palladium-catalyzed oxidative carbonylation of alkanes. (HX = TFA; Ox = $K_2S_2O_8$, Cu(II), O_2)

recent report of oxidation of methane to methyl bisulfate over a *heterogeneous* catalyst, 5 % Pd/C [97]; however, as the reaction was carried out in oleum (50 % SO_3), it seems more likely that it proceeds via methanesulfonic acid, which can be formed under these (and even milder) conditions without any electrophilic activation at all (see Sect. 2.4.6)

While the preceding chemistry amounts to accidental oxidative carbonylation of methane, intentional oxidative carbonylation has also been pursued. Whereas direct carboxylation of an alkane with CO_2 (Eq. 2.15) is thermodynamically disfavored (as is simple carbonylation, Eq. 2.16), coupling carbonylation to oxidation (shown for a generic two-electron oxidant M^{2+} in Eq. 2.17) can make the overall process thermodynamically allowed. Following earlier work on oxidative carbonylation of arenes, Fujiwara showed that palladium salts can catalyze the conversion of methane and other light alkanes, as well as cyclohexane, to the corresponding carboxylic acids [98, 99]. Under the first conditions studied (TFA solution, 20-40 atm CO, 80 °C, $K_2S_2O_8$ as oxidant) up to 20 turnovers (based on Pd) of cyclohexanecarboxylic acid were obtained; later it was found that the addition of catalytic amounts of Cu(II) increased the yield to 200 turnovers (although the efficiency based on oxidant was less than 50 %) [100]. The mechanism, while not fully delineated, could involve the sequence of steps in Scheme 2.29 (which is quite similar to that of the top half of Scheme 2.28).

$$\mathrm{RH} + \mathrm{CO_2} \longrightarrow \mathrm{RCO_2H} \tag{2.15}$$

$$\mathrm{RH} + \mathrm{CO} \longrightarrow \mathrm{RCHO} \tag{2.16}$$

$$\mathrm{RH} + \mathrm{CO} + \mathrm{M^{2+}} + \mathrm{H_2O} \longrightarrow \mathrm{RCO_2H} + \mathrm{M} + 2\,\mathrm{H^+} \tag{2.17}$$

For methane, yields of acetic acid were significantly lower (up to 15 turnovers using $K_2S_2O_8$); it was found that O_2 could be substituted as oxidant, but with still lower yields [101]. Copper was required—indeed, for methane, copper alone worked as well as or better than reactions with palladium. This result and several others seem inconsistent with the assumption that electrophilic activation at Pd is responsible for this chemistry. It was found that CO_2 can be substituted for CO,

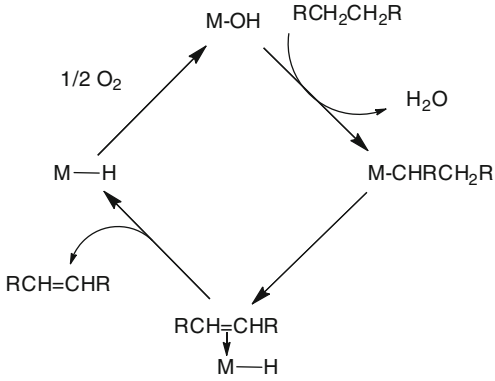

Scheme 2.30 Possible cycle for catalytic oxidative dehydrogenation of an alkane via electrophilic C–H activation

with comparable yields of acetic acid; it is far from clear how that finding could be accommodated in the proposed mechanism. Furthermore, $VO(acac)_2$ was found to be a much better catalyst for methane oxidative carbonylation; that almost certainly will *not* operate by an electrophilic mechanism, but rather by a radical pathway [102]. Certainly there could be more than one mechanism for this transformation, but the possibility that apparent electrophilic reactivity might actually be due, in whole or in part, to radical mechanisms (especially when reagents such as $K_2S_2O_8$ are involved) must always be kept in mind.

For alkanes other than methane, an alternative to oxygenation—perhaps a more likely one, especially in acidic media where alcohols will not be stable—is oxidative dehydrogenation. The chapter in this volume by Brookhart and Goldman covers the general topic of alkane dehydrogenation; most examples involve either thermal dehydrogenation, which is thermodynamically disfavored at temperatures accessible to homogeneous catalysts, or transfer dehydrogenation, for which a sacrificial—usually expensive—hydrogen acceptor is required. Oxidative dehydrogenation (Eq. 2.18) offers a means of overcoming both of those problems, both being thermodynamically favored and employing a cheap (even free, if air can be used) hydrogen acceptor. It has been studied extensively over traditional heterogeneous catalysts at elevated temperature, but CO_x is always a major byproduct; practically useful selectivities have not been achieved. Scheme 2.30 shows a plausible sequence, consisting of electrophilic activation, β-hydrogen elimination, and (in either order) dissociation of olefin and oxidation of M-H, that could lead to low-temperature, highly selective oxidative dehydrogenation.

$$RCH_2CH_2R + {}^1\!/_2\,O_2 \longrightarrow RCH{=}CHR + H_2O \qquad (2.18)$$

The oxidative aromatization of cyclohexanes, effected by $Pd(OAc)_2$ and $Na_2Cr_2O_7$, in TFA at 90 °C, was offered as an early example of electrophilic activation leading to oxidative dehydrogenation [103]. Cyclohexane itself did not react, but substituted cyclohexanes did, although yields were less than stoichiometric in Pd (up to 54 % for conversion of tetralin to naphthalene, the best case). Isotopic labeling experiments indicated that cleavage of a tertiary C–H bond was

the initial, rate-limiting step (for tetralin it would be a benzylic C–H bond), which might appear more consistent with homolytic C–H cleavage; on the other hand, the intermediacy of free cyclohexenes was ruled out, so organopalladium intermediates (however generated) must be involved.

Cyclohexene can be aromatized under considerably milder conditions (unsurprisingly). Disproportionation of cyclohexene to benzene plus cyclohexane—a transfer dehydrogenation—in the presence of palladium trifluoroacetate (Eq. 2.19) had been previously reported, but was proposed to involve Pd metal (deposited almost immediately) as a heterogeneous catalyst [104]. Under an atmosphere of O_2, in contrast, oxidative dehydrogenation is observed: at room temperature, cyclohexene is converted to benzene (plus water) by 5 mol % $Pd(O_2CCF_3)_2$ in acetone, in up to 25 % conversion and 100 % selectivity (Eq. 2.20). Several lines of evidence strongly indicated that this reaction is strictly homogeneous. Substituted cyclohexenes could be similarly aromatized, but neither cyclohexane nor tetralin underwent this reaction [105].

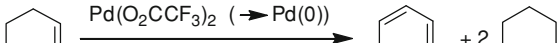

(2.19)

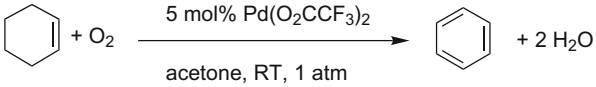

(2.20)

A similar result was obtained with a ligand-substituted Pd(II) catalyst: the hydroxy-bridged dimeric diimine complex shown in Scheme 2.31 catalyzes the oxidative dehydrogenation of cyclohexene at 60 °C in trifluoroethanol solution, again achieving up to 25 % conversion with 100 % selectivity. Mechanistic studies on the C–H activation of indene, which leads to a stable allylic Pd(II) complex (Scheme 2.31) rather than any catalysis, indicate that electrophilic C–H activation takes place at monomeric, monocationic Pd(II) centers produced via solvent-induced dissociation [106]. This may be contrasted to the Pt analog, for which activation of cyclohexene gives a stable cyclohexenyl complex, and the main active species is the dication, $[(\text{diimine})Pt(H_2O)_2]^{2+}$ [107]. It is not clear why different pathways are followed.

One might question whether reaction at an allylic C–H bond is truly representative of electrophilic activation: certainly there are many examples in the literature of interconversion between metal olefin complexes and metal allyls that do not look at all like electrophilic activation. Nonetheless, although these Pd (and Pt) complexes have not yet been shown to activate alkanes, closely related analogs (discussed earlier) do; it seems quite plausible that a more reactive version of these systems may be found to catalyze oxidative dehydrogenation of alkanes. Some oxidative dehydrogenation has been reported in Shilov chemistry, but except in cases where arenes (benzene, naphthalene) are generated, (alkene)Pt(II) complexes, in only small amounts, were obtained [16, 17].

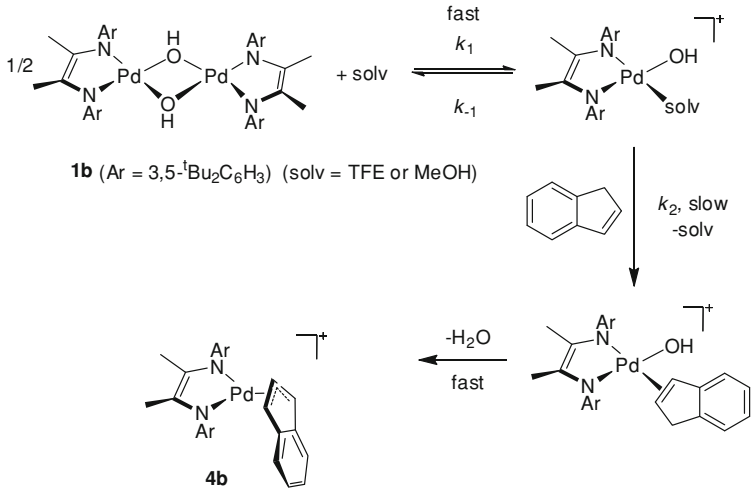

Scheme 2.31 Mechanism of electrophilic activation of an allylic C–H bond by a hydroxy-bridged dimeric Pd(II) complex

We will not consider Pd-catalyzed allylic oxidation of olefins, a topic that has received considerable attention of late [108], because there does not appear to be any likelihood of applying that chemistry to alkane functionalization (even though there are undoubtedly *some* mechanistic connections to the chemistry presented here).

2.4.1.2 Directed Functionalization

While cross-coupling reactions undoubtedly comprise the most important role of catalysis by palladium in organic synthesis, directed functionalization of C–H bonds, both aromatic and aliphatic, is becoming increasingly prominent. Obviously we are not dealing with simple alkanes here: these are reactions in which a molecule is coordinated to Pd, via a good ligating center (most often nitrogen), bringing the Pd center in proximity to the targeted C–H bond, which undergoes cyclometallation to give a C-Pd bond; the latter can then be functionalized by means of a variety of transformations. There are several good recent reviews devoted entirely [9] or in part [84, 85] to this topic, so only a few of the more informative points will be highlighted here.

Two generic mechanisms are shown in Scheme 2.32. In each case the reaction starts with C–H activation, presumed to be electrophilic in nature (computational studies have been reported only for aryl C–H bonds [109]). The top cycle proceeds via $Pd^{0/II}$ species, in which the functional group Y is attached to the carbon center that has undergone electrophilic activation at Pd(II) via reductive elimination; the resulting Pd(0) is reoxidized to complete the catalytic cycle. In the bottom one, the cyclometallated intermediate itself is oxidized to Pd(IV), which undergoes reductive elimination to give the functionalized product and regenerate Pd(II).

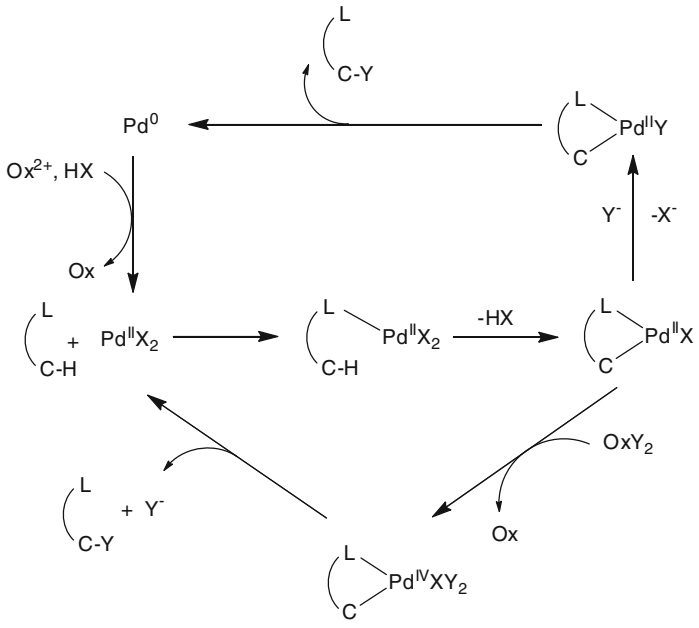

Scheme 2.32 Alternate mechanisms for directed oxidative functionalization of C–H bonds by Pd(II)

Other variants are also possible. As we shall see, whereas $Pd^{0/II}$ cycles appear to operate for most or all of the alkane oxidations discussed in the preceeding section, $Pd^{II/IV}$ or other routes involving oxidation of an organopalladium species predominate in this chemistry.

The "classic" example of Pd-catalyzed directed functionalization is the oxidation of phenylpyridine by $PhI(OAc)_2$ to the 2,6-diacetoxylated derivative (Eq. 2.21). In this case an aryl C–H bond is involved, but the reaction may be readily generalized to a wide variety of coordinating/directing ligating groups (various N-heterocycles, imines, oxime ethers, etc.) and, more relevant to our topic, to aliphatic sp^3 C–H bonds. Regioselectivity—the "directed" part of the descriptor—is established at the C–H activation stage, and appears to arise from two factors: a preference for reaction at primary C–H bonds (consistent with trends we have already seen for other cases of electrophilic activation), along with a preference for 5-membered rings in the cyclopalladated intermediates [9]. An illustrative example is shown in Scheme 2.33.

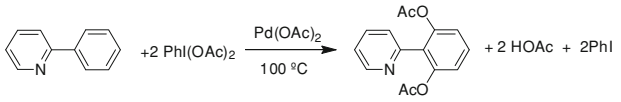

(2.21)

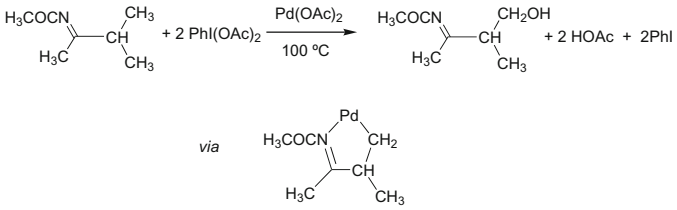

Scheme 2.33 Selectivity results from preference for primary C-H activation and a 5-membered palladacycle

Strong support for a $Pd^{II/IV}$ mechanism was obtained by starting with a preformed bis(phenylpyridyl) Pd(II) metallacycle, which is oxidized by $PhI(O_2CR)_2$ to give a *stable* (at room temperature) Pd(IV) derivative that decomposes smoothly to the phenylpyridyl ester and Pd(II) (Eq. 2.22) [110]. The mechanism for C–O bond formation appears to be intramolecular reductive elimination from a cationic 5-coordinate intermediate [111]. (Recall that *external* nucleophilic attack has been found to operate for Pt(IV) in the Shilov system, but this difference is perhaps not so surprising, as an aryl-M bond might reasonably be expected to be less susceptible to nucleophilic attack. Comparably detailed mechanistic understanding for alkyl activations is not yet available.) Recently, however, a related reaction was shown to proceed via a bimetallic Pd(III) intermediate [112], different from *both* of the alternatives shown in Scheme 2.32. It seems most likely that a number of detailed mechanisms are accessible; the one preferred will depend on a number of factors.

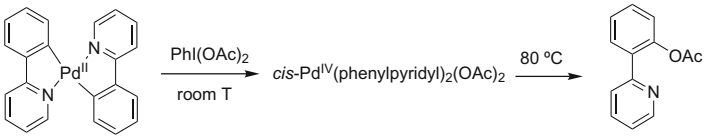

(2.22)

The acetoxy functionality may be installed at aliphatic C–H positions using other oxidants (by operating in acetic acid as solvent), including peroxides and even, for one particular class of substrate (8-methylquinolines), dioxygen. Similar reactions have been demonstrated for a wide variety of other functional groups: C–S bonds using $ArSO_2Cl$; C-X bonds using N-halosuccinimides, CuX_2, or XOAc; C–N and C–C bonds using various reagents. Directed dehydrogenation has also been reported [113]. The mechanism is not necessarily the same in all cases—some may well involve $Pd^{0/II}$ cycles—and few if any of the functionalizations are universally applicable—some are (so far) limited to sp^2 C–H bonds and/or intramolecular bond formation [9]. Nonetheless, the potential of this methodology for complex organic synthesis is clear; for example (Eq. 2.23) a C–C bond can be established between centers generated by C–H and C–Br activation at Pd [114]. The utility for functionalization of actual alkanes, though, remains to be demonstrated.

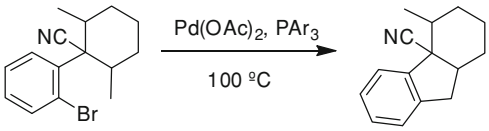

(2.23)

2.4.2 Iridium

The earliest well-defined reports of alkane activation involved iridium complexes; those were clearly *not* examples of electrophilic activation, but rather oxidative addition to Ir(I) [115, 116]. Somewhat later work, also from Bergman's group, does fit the definition used here: the Ir(III) complexes $Cp^*(PMe_3)IrMe(OTf)$ and $[Cp^*(PMe_3)IrMe(CH_2Cl_2)]^+$ activate a variety of C–H bonds, including those of alkanes, with loss of methane. The resulting alkyls exhibit interesting chemistry, such as β-hydride elimination to give stable (unfortunately so, precluding the possibility of catalytic alkane dehydrogenation) olefin hydride complexes, as in Eq. 2.24 [117, 118].

$$[Cp^*(PMe_3)Ir(CH_3)(CH_2Cl_2)]^+ + C_2H_6 \xrightarrow[\text{min}]{25\,^\circ C} [Cp^*(PMe_3)IrH(CH_2CH_2)]^+ + CH_4 \tag{2.24}$$

The reactions appear to proceed via an alkane complex of the 16-electron cationic intermediate $[Cp^*(PMe_3)IrMe]^+$. One might think that an oxidative addition/reductive elimination sequence would be less likely for an $Ir^{III/V}$ couple (and cationic, in addition) than for the previously studied $Ir^{I/III}$ couple (which involved a similar ligand set), preferring an alternative sigma-bond metathesis or σ-CAM route. On the other hand, oxidative addition/reductive elimination does operate in the Shilov system (or, at least, in models thereof; see above), which involves lower oxidation states ($Pt^{II/IV}$) but much less electron-donating ligands than the Cp^*/PMe_3 combination. In fact, a variety of experimental indications (none completely unequivocal) [119] along with computational studies [120, 121] support the oxidative addition/reductive elimination route.

The analogous hydrido complex, $[Cp^*(PMe_3)IrH(CH_2Cl_2)]^+$, was found to catalyze isotopic exchange between C_6D_6 and a wide variety of C–H bonds, including alkanes (methane, ethane, cyclohexane), which could be substantially deuterated in a few hours at −20 °C. Toluene undergoes exchange at both arene and benzylic positions; the *m*- and *p*- sites exchange rapidly even at −84 °C (the *o*-position is unreactive) while the methyl group requires −20 °C. Ferrocene and even decamethylferrocene are quite reactive as well; diethyl ether and THF, less so. Presumably the mechanism here as well involves oxidative addition/reductive elimination, as sketched out in Scheme 2.34 [122].

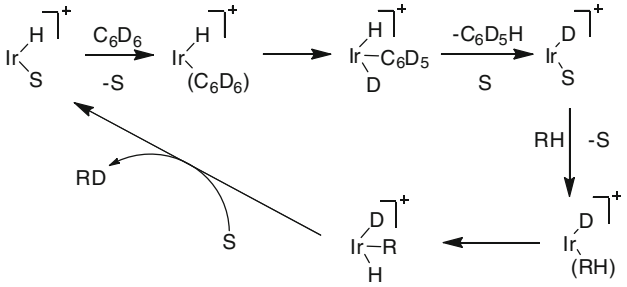

Scheme 2.34 Proposed mechanism for H/D exchange catalyzed by a cationic Ir(III) hydride complex

Alternatively, H/D exchange of C–H positions in water-soluble substrates can be achieved with D_2O, using Cp*(PMe_3)$IrCl_2$ as catalyst, although considerably more stringent conditions (hours at 135 °C) are required; a mechanism analogous to that for H/D exchange in the Shilov system was proposed [123]. The catalyst is not stable but disproportionates by ligand redistribution; studies on related complexes in which the phosphine ligand is covalently linked to the Cp ring did not succeed in the main goal of retarding decomposition, but did indicate that more electron-donating ligands accelerate reaction [124]. That would be consistent with the proposed mechanism, if C–H activation is rate-limiting. A related NHC complex catalyzes H/D exchange with CD_3OD or CD_3COCD_3 as deuterium source, but the scope is apparently more limited, as no simple alkanes were reported to react [125, 126].

Periana has studied C–H activation at a variety of Ir(III) centers. The earliest reports were on Ir(acac)$_3$, which catalyzes hydroarylation of olefins via an (aryl)Ir(III) intermediate generated by C–H bond activation. Computational studies implicate a mechanism described as "oxidative hydrogen migration," a sort of hybrid mechanism, wherein H is bonded strongly to the metal, as in oxidative addition, but also interacts weakly with both carbon centers, as in sigma bond metathesis, in the transition state [127]. This Ir complex has not been found to activate sp^3 C–H bonds; however, a closely related methyl compound does (Eq. 2.25), reacting with linear and cyclic alkanes as well as mesitylene (at the benzylic position) [128]. Detailed mechanistic studies were reported for activation of benzene, where the oxidative hydrogen migration mechanism seemed to be preferred again [129], but not for the alkane activations. The closely related bis(tropolonate) complex undergoes the same reactions with mesitylene and cyclohexane, but nearly an order of magnitude more rapidly than does (CH_3)-Ir(acac)$_2$(pyr) [130]. The methoxy complex (CH_3O)Ir(acac)$_2$(pyr) activates benzene to give the phenyl derivative, as well as catalyzing H/D exchange between benzene and water. Here the more "classical" sigma bond metathesis was calculated to be the lowest energy pathway; the favorable O–H interaction in the transition state (stronger than the C–H interaction in the transition state for activation by the methyl complex) and/or the disfavoring of Ir(V) by the more

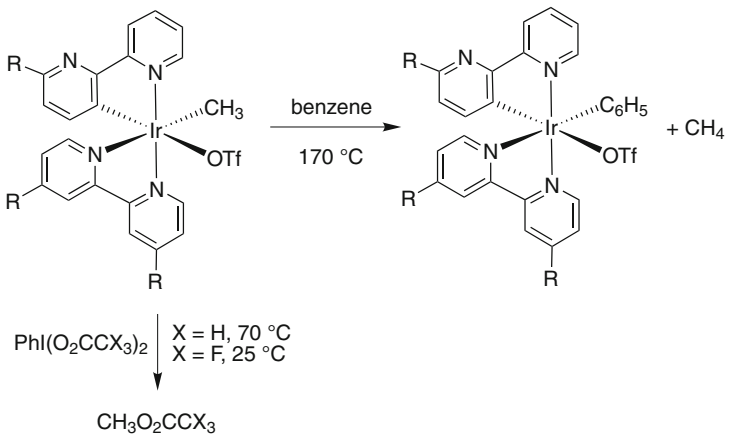

Scheme 2.35 C-H bond activation and C–O bond formation at an Ir(III) center

electronegative methoxy group were offered as possible reasons for the difference in C–H activation mechanism [131].

$$(CH_3)Ir(acac)_2(pyr) + RH \xrightarrow[3h]{130\,^{\circ}C} RIr(acac)_2(pyr) + CH_4 \qquad (2.25)$$

More recent studies have moved away from acac and other O-centered ligands to less electron-withdrawing N- and C-centered ligands. This reflects the possibility, noted earlier in work on Shilov models and also predicted by computational "screening"[80], that the most electrophilic metal center may well not make the optimal C–H functionalization catalyst, even if the C–H activation is electrophilic in nature, because displacement of water or other ligands by alkane may become the most difficult step in the cycle. The (N,N)-(N,C)-coordinated Ir(III) complex shown in Scheme 2.35 activates benzene (but not aliphatic C–H bonds) as well as catalyzing H/D exchange between benzene and acids; it also reacts with the strong oxidants $PhI(O_2CCX_3)$ (X = H, F) to cleave the Ir–C bond and form the corresponding methyl ester. The last reaction corresponds to the final step in a (hypothetical) catalytic methane oxidation; the detailed mechanism is not known [132].

The next-generation species suggested by computational screening, based on the (NNC)-ligand shown in Scheme 2.36, likewise catalyzes H/D exchange, but in this case will do so for methane and other alkanes as well as benzene. Calculations favor an electrophilic (or sigma bond metathesis) mechanism for the C–H activation step, with the H being removed by a departing trifluoroacetate; but the oxidative hydrogen migration route, in which the H moves to the phenyl group of the tridentate ligand, was not much higher in energy. Of greatest interest is the report that the complexes *catalyzes* methane oxidation by $NaIO_4$, giving up to 6 turnovers of methyl trifluoroacetate per Ir in 3 h at 180 °C [133]. This appears to be a nice validation of the computationally-informed design approach, but there is one caveat. The paper notes the presence of a "background" reaction between

Scheme 2.36 H/D exchange and methane oxidation catalyzed by a (NNC)-coordinated Ir(III) complex

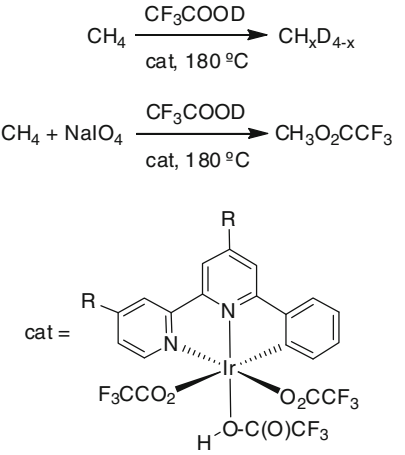

methane and periodate; the amount of product in the absence of Ir (given in the SI) is fully half of that obtained with Ir. Since there is no information on how the Ir-free reaction works (some sort of radical chemistry seems most likely), we must remain open to the possibility that the Ir "catalyst" is not actually effecting C–H activation by an electrophilic (or any other) route, but rather promoting the "background" mechanism in some fashion.

2.4.3 Rhodium

There is considerably less literature about rhodium than iridium, for reasons that are not clear. Only a few examples—none of them entirely unambiguous—of electrophilic activation have been reported. The earliest work involves a supported complex: methane reacts with a bis(allyl)Rh(III) center attached to silica at 100 °C, to give Rh hydride species along with C_3 and some C_4 hydrocarbons; labeling studies establish that the 4th carbon in the latter came from methane. The analogously supported (SiO)-RhHCl center reacts with methane to give methyl chloride and a (tentatively identified) (methyl)Rh(III)hydride; any of these supported species serves as a pre-catalyst for chlorination of methane at 100 °C. Electrophilic activation of methane at Rh(III) was proposed, even though the distribution of chlorinated methanes obtained was not substantially different from that expected for free-radical chlorination [134].

Sen found that $RhCl_3$ in a mixed $H_2O/C_3F_7CO_2H$ solvent catalyzes methane oxidation by O_2 at 80–85 °C; additional Cl^- and I^- in solution and CO in the gas phase are required as well. The main products are methanol (in part obtained as the perfluorobutyrate ester) and acetic acid; overall rates on the order of 3 turnovers/h could be obtained. The only byproduct observed was formic acid. (It is not clear whether an attempt was made to detect formation of CO_x from methane, which

would require labeling.) The obvious possibility that acetic acid arises via Monsanto-like carbonylation of intermediate methanol (with the aid of iodide) was ruled out by labeling, implicating a mechanism wherein a (methyl)Rh(III) intermediate undergoes competitive nucleophilic attack (by water or perfluorobutyrate) and CO insertion [135]. Calculations suggest that the (methyl)Rh(III) species is generated by oxidative addition to a Rh(I) complex, $[RhI_2(CO)_2]^-$, which could certainly be generated under reaction conditions [136]. Reactions of ethane and higher alkanes do not seem entirely in accord with this proposal, however: they also undergo oxidation, but substantial amounts of C–C cleavage products are obtained, especially for butane and above. Also, surprisingly, propane showed a 5:1 preference (statistically corrected) for reaction at the secondary C–H bond (giving isopropyl esters and acetone) than at the primary position, the opposite of the predominant trend for electrophilic activations. The role of CO was also unclear: obviously it is needed for the carbonylation products, but no simple oxidation takes place in the absence of CO; it was suggested that the combination of CO and water leads to H_2O_2 as in the metallic Pd system discussed earlier.

Russian workers (simultaneously and subsequently) examined this system in greater detail. In H_2O/TFA higher rates are obtained, with maximum turnovers to methanol (and methyl trifluoroacetate), acetic acid, and formic acid at 95 °C around 12, 6 and 9 per hour respectively; substantial CO_2 formation was also measured, but shown to arise entirely from CO oxidation. *No* H/D exchange with solvent was detected, a possible argument against *any* (methyl)Rh intermediate, although no such strong conclusion was drawn; on the other hand, several lines of evidence implicated the important participation of a good oxidant, H_2O_2 or HOI [137]. ^{18}O-labelling studies proved particularly telling: in the presence of $H_2^{18}O$ (which rapidly exchanges into TFA), there is much less $CF_3C^{16}O^{18}OCH_3$ and $CF_3C^{18}O_2CH_3$ than the amount of label in the TFA, ruling out a mechanism involving nucleophilic attack by trifluoroacetate (or water) on a (methyl)Rh intermediate. In contrast, label from $^{18}O_2$ showed up in the product in about the same proportion as in the reagent, implying that the C–O bond is formed from O_2 or a derivative (such as H_2O_2) thereof. The authors were not ready to completely rule out a mechanism involving C–H activation at Rh, offering possible schemes that might account for the observations, but suggested that activation at an O-centered species, such as a (peroxo)Rh complex, seems most likely [138]. Inclusion of this chemistry as an example of electrophilic alkane functionalization must thus be considered at best equivocal.

Rhodium(III) porphyrin complexes such as Rh(ttp)Cl (ttp = tri-*p*-tolylporphyrin) react with cyclic and linear alkanes at 120 °C or higher to give the corresponding alkyls, Rh(ttp)R; with linear alkanes, only primary alkyl products are obtained. The hydride Rh(ttp)H was found to be a viable intermediate, and mechanisms involving electrophilic activation by that species (the reaction is accelerated for porphyrins bearing electron-withdrawing substituents), following either an oxidative addition/reductive elimination sequence or sigma bond metathesis, were proposed. However, the Rh(II) dimer $(Rh(ttp))_2$ was also found as an intermediate, so the two-center one-electron oxidative addition mechanism

established by Wayland (Eq. 2.26) [139] was offered as a parallel path [140]. It seems more likely that *only* the latter is followed, since reaction of a solution of cyclohexane in benzene gives the cyclohexyl but no phenyl product. One would expect benzene to be at least as reactive as an alkane in either of the routes suggested for electrophilic activation (and certainly the phenyl product should be stable if formed), whereas aryl C–H bonds are known to be unreactive by Wayland's mechanism.

$$\left(\mathrm{Rh^{II}(porph)}\right)_2 + \mathrm{R-H} \rightarrow \mathrm{Rh^{III}(porph)R} + \mathrm{Rh^{III}(porph)H} \qquad (2.26)$$

The hydroxo-bridged dimer $[(\mathrm{COD})\mathrm{Rh^{I}}(\mu\text{-}\mathrm{OH})]_2$ was investigated for comparison to the (dicationic) diimine-Pd and –Pt analogs discussed above, with the idea that displacement of solvent by a C–H bond would be more facile for this uncharged system. The latter *does* appear to be the case, but increased reactivity does not result; rather there is a switch of rate-determining step, from coordination of substrate for Pd and Pt, to C–H bond cleavage for Rh. As a consequence only the highly reactive C–H bond of indene can be activated (Eq. 2.27), and the reaction is *slower*, not faster, than the corresponding Pd case [141]. The exact nature of the C–H activation process is not clear.

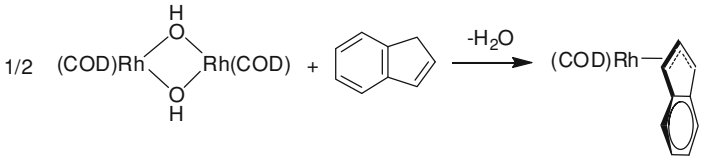

(2.27)

2.4.4 Gold

While there are a number of example of C–H activation and functionalization involving gold complexes, most are limited to arenes and other unsaturated centers [142]. The clearest example of electrophilic functionalization of an alkane by gold is Periana's demonstration that Au(III) exhibits reactivity akin to the Catalytica system. In strong acid (sulfuric, triflic), at 180 °C, methane is stoichiometrically oxidized to the corresponding methyl ester, with deposition of metallic gold; H_2SO_4 (or SO_3) is not able to keep gold in solution by reoxidation. However, the addition of selenic acid (which is known to oxidize gold) effects catalytic oxidation, with turnover frequencies around 10^{-3}/s and up to 30 total turnovers. (Again, it should be noted that there is a significant background reaction: selenic acid in sulfuric acid oxidizes methane in the absence of gold, at a rate about 1/5 of the gold-catalyzed process.) While little experimental evidence bearing on mechanism is available, computational studies suggested functionalization takes place by nucleophilic attack on (methyl)Au(III), and found that several different mechanisms for reaching the

latter—activation at Au(III); activation at Au(I) by either electrophilic substitution or oxidative addition/reductive elimination, followed by oxidation of (methyl)Au(I) to (methyl)Au(III)—all appear to be energetically feasible [143]. Comparing the three metallic systems for oxidation of methane in sulfuric acid—the (bpym)Pt(II) complex (see above), Hg(II) (see below), and Au—shows that they all operate with similar rates ($\sim$3 turnovers per hour at 180 °C for Hg and Au; $\sim$10 at 200 °C for Pt) and achieve similar maximal product concentrations ($\sim$0.5–1.5 *M*), corresponding to only tens of total turnovers [144].

There is an intriguing report of gold-dependent biological oxidation of methane to methanol by the microorganism *Micrococcus luteus*; electrophilic activation at Au(III) was proposed as a possible mechanism, but there is no supporting evidence [145]. Both Au(I) and Au(III) complexes have been reported to catalyze alkane oxygenation by H_2O_2; at 75 °C in acetonitrile, cyclooctane was oxidized to a mixture of the hydroperoxide, alcohol and ketone, with a total of 520 turnovers after 144 h. Both the appearance of the hydroperoxide as a product and the selectivities observed with linear alkanes (oxidation at tertiary > secondary > primary positions) strongly implicate a radical mechanism, rather than anything to do with electrophilic activation [146].

2.4.5 Copper

Electrophilic arene activation by Cu is fairly common, although detailed mechanistic understanding is quite limited [147], but there do not appear to be any well-substantiated examples of alkane activation. As noted in the section on Pd, there are a number of combined Pd/Cu oxidation catalysts, some of which work nearly as well (or even better) with Cu alone. That *could* be taken as an indication that both operate by similar mechanisms, but it could also suggest that electrophilic activation is not involved for *either* Cu *or* Pd. An example is the aminomethylation of alkanes by trimethylamine *N*-oxide, in which a mixture of alkyldimethylamine and alkyl trifluoroacetate is obtained (Eq. 2.28). Cu alone gives the highest absolute yield of amine, but the combined catalyst gives the highest ratio of amine to ester [148]. Although an alkylcopper intermediate was proposed, a radical mechanism seems more probable (which does not necessarily rule out an alkylcopper intermediate), since a radical scavenger substantially inhibited product formation; also the preferential oxidation of the secondary C–H position is more consistent with radical than electrophilic activation. (Methane could not be oxidatively aminomethylated, although some oxidation to methyl trifluoroacetate was observed.) The oxidation of alkanes by H_2O_2, catalyzed by a tetranuclear Cu(II) cluster complex, is almost certainly radical in nature [149].

$$\begin{aligned} &CH_3CH_2CH_3 + (CH_3)_3NO \xrightarrow[TFA,150\,^\circ C]{Cu(OAc)_2} (CH_3)_2CHCH_2N(CH_3)_2 \\ &\quad + (CH_3)_2CHO_2CCF_3 \end{aligned} \tag{2.28}$$

2.4.6 Mercury

The Pt-based Catalytica system (Sect. 2.3.2 above) was discovered as a follow-on to an earlier report from the same group, that mercuric salts catalyze oxidation of methane to methyl bisulfate in concentrated sulfuric acid at 180 °C [150]. (Closely related chemistry, at higher temperature, had been reported previously in the patent literature [151]). A similar mechanism was proposed, involving electrophilic activation of methane by Hg(II). The presumed next step, nucleophilic C–Hg bond cleavage by bisulfate, would generate Hg(0), which was never observed; but its reoxidation by sulfuric acid and/or comproportionation with Hg(II) to give Hg(I) should both be rapid; the corresponding reaction in (non-oxidizing) triflic acid gives a stoichiometric amount of methyl triflate along with mercurous triflate. Independently-synthesized $CH_3Hg(OSO_3H)$ reacts at 180 °C in sulfuric acid to give both methyl bisulfate (at a rate consistent with the overall catalytic process) and methane (the reverse of electrophilic activation), all supporting the proposed mechanism. The best methane yields obtained, around 43 %, are not so high as those obtained with Pt, but still impressive.

An alternate view of this chemistry was offered by Sen, who examined the reaction of methane in sulfuric acid with Hg(II) as well as other $1e^-$ ($K_2S_2O_8$, Ce(IV)) and $2e^-$ (Pd(II)) oxidants and found that they *all* gave CH_3OSO_3H, although the yield exceeded stoichiometry with respect to oxidant only with Hg(II). Sen postulated that all these systems follow the same mechanism, which surely could not involve electrophilic activation in all cases, and therefore must consist of generation of methyl radicals, via H-atom abstraction and/or stepwise electron transfer followed by loss of proton. The methyl radical would be the precursor to product, possibly by further oxidation to the carbocation which is trapped by bisulfate. The fact that methyl bisulfate also appeared as the major product obtained from ethane oxidation, via C–C cleavage, was taken to support the electron transfer mechanism [21].

Several additional observations also bear upon the mechanistic issues. Although formation of some $CH_3Hg(OSO_3H)$ was observed at lower temperatures, the inability to synthesize that species by reaction of methyl bisulfate and either Hg(I) or Hg(II) was taken as evidence that it does *not* form via electrophilic activation of methane at Hg(II), but rather via coupling of $CH_3\bullet$ and Hg(I). Methanesulfonic acid (CH_3SO_3H, MSA) was a minor product in some reactions, but control experiments were reported to demonstrate that it does not convert further to CH_3OSO_3H under reaction conditions. (As noted earlier, and discussed below, that conclusion was not correct.) Sen acknowledged that the high selectivity to the latter product requires that the C–H bond in methane be considerably more reactive than that of CH_3OSO_3H, which is not obviously consistent with a radical mechanism, but argued that it could be so, as a consequence of the electronegativity of the sulfonate group [21].

In a subsequent paper, however, Sen found that MSA is the main product at 90 °C with either Hg(II) or $K_2S_2O_8$ as promoter; furthermore, MSA *is* oxidized to methyl bisulfate at 160 °C in fuming sulfuric acid, even without any other oxidant present [152]. Subsequently Bell extended this chemistry to other promoters [153],

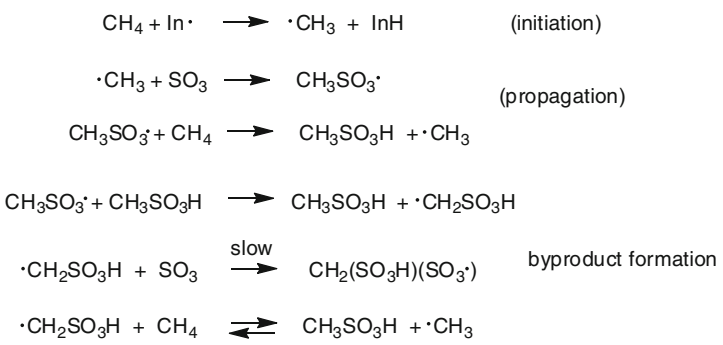

Scheme 2.37 Radical mechanism for oxidation of methane to MSA

including catalyzed oxidations by O_2 [154]. These observations clearly indicate that a radical-based route for oxidizing methane to methyl bisulfate via MSA is viable, perhaps as in Scheme 2.37. It is possible to account for the good selectivity without arguing that the C–H bond in MSA is much less reactive than that of methane (as Sen does); instead it could be that $\bullet CH_2SO_3H$ *is* generated, but it does not readily couple with SO_3 (some $CH_2(SO_3H)_2$ is observed as a byproduct under many conditions [153]), so most of it is quenched by reaction with methane.

Nonetheless, it seems very likely that the catalytic electrophilic mechanism does operate as well for Hg(II) (and others, particularly Pd(II)), since considerably higher production of methyl bisulfate relative to additive are obtained than with radical initiators. The failure to generate the (methyl)Hg(II) species by alkylation of Hg(I) or Hg(II) does not really prove anything; indeed, if C–O bond formation results from nucleophilic attack of bisulfate on (methyl)Hg(II), the *correct* attempt at its preparation (the microscopic reverse) would be the reaction of a methylating agent with Hg(0).

This chemistry has been incorporated into a heterogeneous catalyst: a mixture of methane and O_2 was passed over a bed of $BaSO_4$ nanotubes impregnated with metal (Pt(II), Hg(II), Ce(IV) or Pb(IV)) sulfate salts and concentrated sulfuric acid at 170–230 °C. Up to 50 % methane conversion was achieved, with up to 60–70 % selectivity to methanol (it was not clear whether the product stream underwent hydrolysis before analysis). All four different metals behaved approximately the same, which seems more consistent with a radical than an electrophilic activation mechanism [155].

2.4.7 Miscellaneous

Among the promoters for methane oxidation in oleum, iodine (which can be added in various chemical forms) has been found to be unexpectedly effective [156, 157]. It is not clear whether this is electrophilic or radical chemistry; a gas-phase experiment implicates electrophilic activation at I^+ as the most probable route [158], but the chemistry in sulfuric acid could certainly be quite different.

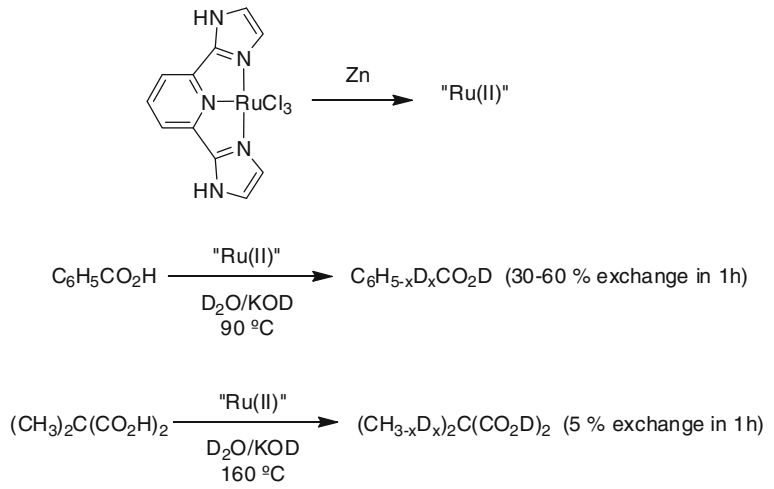

Scheme 2.38 Ru(II)-catalyzed H/D exchange via "nucleophilic" activation

Periana and Goddard have attempted to instantiate their prediction of possible "nucleophilic" activation [1] with ruthenium: the (NNN)-ligated Ru(III) complex shown in Scheme 2.38 can be reduced to a (presumed) Ru(II) species that catalyzes H/D exchange of aromatic C–H bonds, as well as certain aliphatic ones (more slowly), in the presence of strong base [159]. The proposed mechanism includes a C–H bond cleavage step that closely resembles sigma bond metathesis; although termed nucleophilic by the authors, it fits (stoichiometrically) the definition of electrophilic activation employed here. No alkane activation or any functionalization was reported.

An uncharacterized product obtained from the reaction of nickelocene with $LiAlH_4$ was reported to react with methane at 70 °C, giving H/D exchange with D_2; alcoholysis of the resulting (also uncharacterized) solid with EtOD gave CH_3OD [160]. An unspecified C–H activation at a Ni center was proposed, but no followup work has appeared.

Lastly, one might consider Basset's supported organometallic chemistry as electrophilic functionalization: Zr(IV), Ta(V) and W(VI) alkyl and/or hydride species, attached to silica, alumina, or other oxide surfaces via M–O bonds, react with alkanes via sigma bond metathesis, leading to transformations such as alkane hydrogenolysis and alkane metathesis [161]. Strictly speaking these are not functionalizations, as no functional groups are introduced, but they do represent rare examples of productive (if not yet practical) alkane transformations at early transition metal centers.

2.5 Conclusions and Prospects

We have seen that electrophilic activation by a number of late transition metal species can serve as the basis for functionalization of saturated C–H bonds. These reactions can be quite facile, some taking place even below room temperature,

although in other cases severe conditions are required. Most of the well-defined chemistry involves Pt, Pd or Ir centers; there are a number of examples with other metals that *may* proceed by this route, but the evidence is at least somewhat inconclusive: alternate mechanisms, most probably radical in character, could also account for some or all of the observations. Indeed, for at least some reactions there is good reason to believe that two (or more?!) parallel mechanisms might operate simultaneously; the Hg-catalyzed oxidation of methane in sulfuric acid may be such a case.

Up to now the best examples of utility are in the realm of directed functionalization of C–H bonds that are part of a more complex molecule—i.e., not for simple alkanes. For the latter, the only transformations with really useful conversions and selectivities are those of methane in strong acids, but as discussed earlier, even these are not practical, and it is not obvious whether the difficulties are surmountable; furthermore, they are almost certainly unsuited to higher alkanes. There have been a few interesting examples involving the latter, such as the Shilov oxidation of ethane to ethylene glycol, but the selectivities are not as good, and (like the Catalytica methane oxidation) rates are far too slow. Oxidative dehydrogenation looks like an attractive opportunity for selective alkane functionalization, but as yet it has not been demonstrated for an actual alkane.

Despite these (so far) limited accomplishments, the prospects for this approach to alkane functionalization are quite encouraging. We understand a lot (though by no means all that we would like) about the mechanisms, and factors controlling reactivity, for a number of prototypical reactions. With the range of metals and ligands available, and the powerful experimental and computational tools that have been developed, a practical application of electrophilic functionalization of alkanes may well appear in the not too distant future.

Acknowledgments I am grateful to the many students and posdocs, and specially to my Caltech colleague John Bercaw, with whom I have worked on this topic; their names are listed in the references to our work in this chapter. My collaboration and discussion with them have contributed greatly to any understanding and insight I have managed to convey.

References

1. Ess DH, Nielsen RJ, Goddard WA, Periana RA (2009) J Am Chem Soc 131:11686
2. Thompson ME, Baxter SM, Bulls AR, Burger BJ, Nolan MC, Santarsiero BD, Schaeffer WP, Bercaw JE (1987) J Am Chem Soc 109:203
3. Perutz RN, Sabo-Étienne S (2007) Angew Chem Int Ed 46:2578
4. Labinger JA, Bercaw JE (2002) Nature 417:507
5. Stahl SS, Labinger JA, Bercaw JE (1998) Angew Chem Int Ed 37:2180
6. Fekl U, Goldberg KI (2003) Adv Inorg Chem 54:259
7. Chepaikin EG (2004) Kinet Catal 45:307
8. Dick AR, Sanford MS (2006) Tetrahedron 62:2439
9. Lyons TW, Sanford M (2010) Chem Rev 110:1147
10. Garnett JL, Hodges RJ (1967) J Am Chem Soc 89:4546

11. Hodges RJ, Webster DE, Wells PB (1971) J Chem Soc (A) 3230
12. Gol'dshleger NF, Tyabin MB, Shilov AE, Shteinman AA (1969) Zh Fiz Khim 43:2174
13. Gol'dshleger NF, Eskova VV, Shilov AE, Shteinman AA (1972) Zh Fiz Khim 46:1353
14. Shilov AE, Shul'pin GB (1987) Russ Chem Rev 56:442
15. Shilov AE, Shul'pin GB (1997) Chem Rev 97:2879
16. Shilov AE (1984) Activation of saturated hydrocarbons by transition metal complexes. Reidel, Dordrecht
17. Shilov AE, Shul'pin GB (2000) Activation and catalytic reactions of saturated hydrocarbons in the presence of metal complexes. Kluwer, Dordrecht
18. Labinger JA (2004) J Mol Catal 220:27
19. Labinger JA, Herring AM, Bercaw JE (1990) J Am Chem Soc 112:5628
20. Labinger JA (2001) in Natural Gas Conversion VI: Proceedings of the Sixth International Gas Conversion Symposium, June 18-21, 2001, Alaska. Iglesia E, Spivey JJ, Fleisch TH (eds.), Elsevier, Amsterdam, 325
21. Sen A, Benvenuto MA, Lin M, Hutson AC, Basickes N (1994) J Am Chem Soc 116:998
22. Sen A, Lin M, Kao L-C, Hutson AC (1992) J Am Chem Soc 114:6385
23. Lersch M, Tilset M (2005) Chem Rev 105:2471
24. Zamashchikov VV, Popov VG, Rudakov ES, Mitchenko SA (1993) Dokl Akad Nauk SSSR 333:34
25. Siegbahn PEM, Crabtree RH (1996) J Am Chem Soc 118:4442
26. Zhu H, Ziegler T (2006) J Organomet Chem 691:4486
27. Wang L, Stahl SS, Labinger JA, Bercaw JE (1997) J Mol Cat A 116:269
28. Stahl SS, Labinger JA, Bercaw JE (1996) J Am Chem Soc 118:5961
29. Holtcamp MW, Labinger JA, Bercaw JE (1997) J Am Chem Soc 119:848
30. Johansson L, Ryan OB, Tilset M (1999) J Am Chem Soc 121:1974
31. Wick DD, Goldberg KI (1997) J Am Chem Soc 119:10235
32. Zhong HA, Labinger JA, Bercaw JE (2002) J Am Chem Soc 124:1378
33. Wik BJ, Lersch M, Tilset M (2002) J Am Chem Soc 124:12116
34. Driver TG, Williams TJ, Labinger JA, Bercaw JE (2007) Organometallics 26:294
35. Chen GS, Labinger JA, Bercaw JE (2007) Proc Natl Acad Sci 104:6915
36. Owen JS, Labinger JA, Bercaw JE (2006) J Am Chem Soc 128:2005
37. Mason WR (1972) Coord Chem Rev 7:241
38. Scollard JD, Day M, Labinger JA, Bercaw JE (2001) Helv Chim Acta 84:3247
39. Peloso A (1987) Gazz Chim Ital 117:51
40. Peloso A (1991) Polyhedron 10:2191
41. Rich RL, Taube H (1954) J Am Chem Soc 76:2608
42. Luinstra GA, Wang L, Stahl SS, Labinger JA, Bercaw JE (1995) J Organomet Chem 504:75
43. Zamashchikov VV, Litvenenko SL, Uzhik ON, Galat VF (1986) Zh Obshch Khim 56:2417
44. Kushch LA, Lavrushko VV, Misharin YuS, Moravsky AP, Shilov AE (1983) Nouv J Chem 7:729
45. Horváth IT, Cook RA, Millar JM, Kiss G (1993) Organometallics 12:8
46. Lavrushko VV, Shilov AE, Shteinman AA (1975) Kinet Katal 16:1479
47. Weinberg DR, Labinger JA, Bercaw JE (2007) Organometallics 26:167
48. Labinger JA, Herring AM, Lyon DK, Luinstra GA, Bercaw JE, Horváth IT, Eller K (1993) Organometallics 12:895
49. Gaemers S, Keune K, Kluwer AM, Elsevier CJ (2000) Eur J Inorg Chem 1139
50. Basickes N, Hogan TE, Sen A (1996) J Am Chem Soc 118:13111
51. Gol'dshleger NF, Lavrushko VV, Khrushch AP, Shteinman AA (1976) Izv. Akad. Nauk SSSR Ser Khim 2174
52. Geletii YV, Shilov AE (1983) Kinet Katal 24:486
53. Bar–Nahum I, Khenkin AM, Neumann R (2004) J Am Chem Soc 126:10236
54. Lin M, Shen C, Garcia–Zayas EA, Sen A (1000) J Am Chem Soc 2001:123
55. Kreutz JE, Shukhaev A, Du W, Druskin S, Daugolis O, Ismagilov RF (2010) J Am Chem Soc 132:3128

56. Freund MS, Labinger JA, Lewis NS, Bercaw JE (2001) J Mol Catal 87:L11
57. Devries N, Roe DC, Thorn DL (1997) J Mol Catal A 189:17
58. Halpern J, Pribanic M (1968) J Am Chem Soc 90:5942
59. Baker RT, Brown GH, Carpenter J, Davis ME, Labinger JA, Bercaw JE, unpublished results
60. Moodley KG, Nicol MJ (1977) J Chem Soc Dalton Trans 239
61. Hutson AC, Lin M, Basickes N, Sen A (1995) J Organomet Chem 504:69
62. Sen A, Lin M, Kao L-C, Hutson AC (1992) J Am Chem Soc 114:6385
63. Basickes N, Sen A (1995) Polyhedron 14:197
64. Dangel BD, Johnson JA, Sames D (2001) J Am Chem Soc 123:8149
65. Johnson JA, Li N, Sames D (2002) J Am Chem Soc 124:6900
66. Zhu H, Ziegler T (2008) Organometallics 27:1743
67. Zhu H, Ziegler T (2009) Organometallics 28:2773
68. Chen GS, Labinger JA, Bercaw JE (2009) Organometallics 28:4899
69. Rostovtsev VV, Labinger JA, Bercaw JE, Lasseter TL, Goldberg KI (1998) Organometallics 17:4530
70. Rostovtsev VV, Henling LM, Labinger JA, Bercaw JE (2002) Inorg Chem 41:3608
71. Vedernikov AN (2009) Chem Commun 4781
72. Khusnutdinova JR, Zavalij PY, Vedernikov AN (2007) Organometallics 26:3466
73. Periana RA, Taube DJ, Gamble S, Taube H, Satoh T, Fujii H (1998) Science 280:560
74. Lange J-P, Tijm PJA (1996) Chem Engin Sci 51:2379
75. Conley BL, Tenn WJ, Young KJH, Ganesh SK, Meier SK, Ziatdinov VR, Mironov O, Oxgaard J, Gonzales J, Goddard WA, Periana RA (2006) J Mol Catal A 251:8
76. Palkovits R, Antonietti M, Kuhn P, Thomas A, Schüth F (2009) Angew Chem Int Ed 48:6909
77. Mylvaganam K, Bacskay GB, Hush NS (1999) J Am Chem Soc 121:4633
78. Mylvaganam K, Bacskay GB, Hush NS (2000) J Am Chem Soc 122:2041
79. Balcells D, Clot E, Eisenstein O (2010) Chem Rev 110:749
80. Muller RP, Philipp DM, Goddard WA (2003) Top Catal 23:81
81. Ziatdinov VR, Oxgaard J, Mironov OA, Young KJH, Goddard WA, Periana RA (1997) J Am Chem Soc 128:7404
82. Cheng JH, Li ZW, Haught M, Tang YC (2006) Chem Commun 4617
83. Xu Z, Oxgaard J, Goddard WA (2008) Organometallics 29:257
84. Muñiz K (2009) Angew Chem Int Ed 48:9412
85. Sehnal P, Taylor RJK, Fairlamb IJS (2010) Chem Rev 110:824
86. Stahl SS (2004) Angew Chem Int Ed 43:3400
87. Gretz E, Oliver TF, Sen A (1987) J Am Chem Soc 109:8109
88. Kao L-C, Hutson AC, Sen A (1991) J Am Chem Soc 113:700
89. Moody CJ, O'Connell JL (2000) Chem Commun 1311
90. An Z, Pan X, Liu X, Han X, Bao X (2006) J Am Chem Soc 128:16028
91. Lin M, Hogan T, Sen A (1997) J Am Chem Soc 119:6048
92. Shen C, Garcia-Zayas EA, Sen A (2000) J Am Chem Soc 122:4029
93. Muehlhofer M, Strassner T, Herrmann WA (2002) Angew Chem Int Ed 41:1745
94. Periana RA, Mironov O, Taube DJ, Bhalla G, Jones CJ (2003) Science 301:814
95. Zerella M, Mukhopadhyay S, Bell AT (2004) Chem Commun 1948
96. Zerella M, Kahros A, Bell AT (2006) J Catal. 237:111
97. We X, Ye LM, Zhu MX, Yuan YZ (2008) Chin J Catal 29:720
98. Fukiwara Y, Jintoku T, Uchida Y (1989) New J Chem 13:649
99. Nakata K, Yanaoka Y, Miyata T, Taniguchi Y, Takaki K, Fujiwara Y (1994) J Organomet Chem 473:329
100. Nakata K, Watanabe J, Takaki K, Fujiwara Y (1991) Chem Lett 1437
101. Nakata K, Jintoku T, Taniguchi Y, Takaki K, Fujiwara Y (1995) Chem Lett 244
102. Taniguchi Y, Hayashida T, Shibasaki H, Piao D, Kitamura T, Yamaji T, Fujiwara Y (1999) Org Lett 1:557
103. Kao L-C, Sen A (1991) New J Chem 15:575

104. Trost BM, Metzner PJ (1980) J Am Chem Soc 102:3572
105. Bercaw JE, Hazari N, Labinger JA (2008) J Org Chem 73:8654
106. Bercaw JE, Hazari N, Labinger JA, Oblad PF (2008) Angew Chem Int Ed 47:9941
107. Williams TJ, Caffyn AJM, Hazari N, Oblad PF, Labinger JA, Bercaw JE (2008) J Am Chem Soc 130:2418
108. For leading references see Campbell AN, White PB, Guzei IA, Stahl SS (2010) J Am Chem Soc 132:15116
109. Ke Z, Cundari TR (2010) Organometallics 29:821, and references cited therein
110. Dick AR, Kampf JW, Sanford MS (2005) J Am Chem Soc 127:12790
111. Racowski JM, Dick AR, Sanford MS (2009) J Am Chem Soc 131:10974
112. Powers DC, Ritter T (2009) Nat Chem 1:302
113. Giri R, Maugel N, Foxman BM, Yu J-Q (2008) Organometallics 27:1667
114. Hitce J, Retailleau P, Baudoin O (2007) Chem Eur J 13:792
115. Janowicz AH, Bergman RG (1982) J Am Chem Soc 104:352
116. Hoyano JK, Graham WAG (1982) J Am Chem Soc 104:3723
117. Burger P, Bergman RG (1993) J Am Chem Soc 115:10462
118. Arndtsen BA, Bergman RG (1970) Science 1995:270
119. Klei SR, Golden JT, Burger P, Bergman RG (2002) J Mol Catal A 189:79
120. Stour DL, Zaric S, Niu SQ, Hall MB (1996) J Am Chem Soc 118:6068
121. Su MD, Chu SY (1997) J Am Chem Soc 119:276
122. Golden JT, Andersen RA, Bergman RG (2001) J Am Chem Soc 123:5837
123. Klei SR, Golden JT, Tilley TD, Bergman RG (2002) J Am Chem Soc 124:2092
124. Klei SR, Tilley TD, Bergman RG (2002) Organometallics 21:4905
125. Corberán R, Sanaú M, Peris E (2006) J Am Chem Soc 128:3974
126. Feng Y, Jiang B, Boyle PA, Ison EA (2010) Organometallics 29:2857
127. Oxgaard J, Muller RP, Goddard WA, Periana RA (2004) J Am Chem Soc 126:352 (and references cited therein)
128. Wong-Foy AG, Bhalla G, Liu XY, Periana RA (2003) J Am Chem Soc 125:14292
129. Bhalla G, Liu XY, Oxgaard J, Goddard WA, Periana RA (2005) J Am Chem Soc 127:11372
130. Bhalla G, Periana RA (2005) Angew Chem Int Ed 44:1540
131. Tenn WJ, Young KJH, Bhalla G, Oxgaard J, Goddard WA, Periana RA (2005) J Am Chem Soc 127:14172
132. Young KJH, Mironov OA, Periana RA (2007) Organometallics 26:2137
133. Young KJH, Oxgaard J, Ess DH, Meier SK, Stewart T, Goddard WA, Periana RA (2009) Chem Commun 3270
134. Kitajima N, Schwartz J (1984) J Am Chem Soc 106:2220
135. Lin M, Hogan TE, Sen A (1996) J Am Chem Soc 118:4574
136. Hristov JH, Ziegler T (2003) Organometallics 22:3513
137. Chepaikin EG, Bezruchenko AP, Leshcheva AA, Boyko GN, Kuzmenkov IV, Grigoryan EH, Shilov AE (2001) J Mol Catal A 169:89
138. Chepaikin EG, Bezruchenko AP, Boiko GN, Gekhman AE, Moiseev II (2006) Kinet Catal 47:12
139. Wayland BB, Ba S, Sherry AE (1991) J Am Chem Soc 113:5305
140. Chan YW, Chan KS (2008) Organometallics 27:4625
141. Bercaw JE, Hazari N, Labinger JA (2009) Organometallics 28:5489
142. Skouta R, Li C-J (2008) Tetrahedron 64:4917
143. Jones CJ, Taube D, Ziatdinov VR, Periana RA, Nielsen RJ, Oxgaard J, Goddard WA (2004) Angew Chem Int Ed 43:4626
144. De Vos DE, Sels BF (2005) Angew Chem Int Ed 44:30
145. Levchenko LA, Sadkov AP, Lariontseva NV, Koldasheva EM, Shilova AK, Shilov AE (2002) J Inorg Biochem 88:251
146. Shul'pin GB, Shilov AE, Süss-Fink G (2001) Tetrahedron Lett 42:7253
147. King AE, Huffman LM, Casitas A, Costas M, Ribas X, Stahl SS (2010) J Am Chem Soc 132:12068

148. Taniguchi Y, Horie S, Takaki K, Fujiwara Y (1995) J Organomet Chem 504:137
149. Kirillova MV, Kirillov AM, Mandelli D, Carvalho WA, Pombeiro AJL, Shul'pin GB (2010) J Catal 272:9
150. Periana RA, Taube DJ, Evitt ER, Löffler DG, Wentrcek PR, Voss G, Masuda T (1993) Science 259:340
151. Snyder JC, Grosse AV. 1950, U. S. Patent 2493038 (cited in ref. 144)
152. Basickes N, Hogan TE, Sen A (1996) J Am Chem Soc 118:13111
153. Mukhopadhyay S, Zerella M, Bell AT (2005) Adv Synth Catal 347:1203
154. Mukhopadhyay S, Bell AT (2004) Adv Synth Catal 346:913
155. Li F, Yuan G (2005) Chem Commun 2238
156. Periana RA, Mirinov O, Taube DJ, Gamble S (2002) Chem Commun 2376
157. Gang X, Zhu YM, Birch H, Hjuler HA, Bjerrum NJ (2004) Appl Catal A 261:91
158. Davico GE (1997) J Phys Chem A 109:3433
159. Hashiguchi BG, Young KJH, Yousufuddin M, Goddard WA, Periana RA (2010) J Am Chem Soc 132:12542
160. Rubtsova TB, Kirjakov NV, Soloveichik GL, Shilov AE (1993) Mendeleev Commun 89
161. Basset J-M, Copéret C, Soulivong D, Taoufik M, Cazat JT (2010) Acc Chem Res 43:323 (and references cited therein)

Chapter 3
Catalytic Carbon–Boron Bond Formation via Activation of Alkane C–H Bonds

Chulsung Bae

Abstract Alkanes are extremely unreactive toward nucleophiles and electrophiles because they are composed of nonpolar, strong, saturated C–H and C–C bonds. Thus, although they are abundant natural resources, alkanes are notoriously underutilized in chemical synthesis, and the selective functionalization of alkane to produce useful organic products is a major challenge in organic chemistry. Among different C–H functionalization methods of alkanes, transition metal-catalyzed functionalization has the selectivity advantage (tertiary C–H < secondary C–H < primary C–H bonds) and can afford more desirable terminally functionalized alkanes. Direct functionalization of the C–H bonds of alkanes to C–B bonds is a particularly attractive method because the boron moiety of alkane can be converted to a variety of functional groups using the rich chemistry of organoboron compounds. This chapter describes the development of direct borylation of alkane C–H bonds catalyzed by transitional metal complexes since 1995. The scope of the reaction, mechanistic understanding via computational studies and kinetic experiments, and challenges for broader applications in practical organic synthesis are discussed.

C. Bae (✉)
Department of Chemistry, University of Nevada Las Vegas,
4505 Maryland Parkway, 454003, Las Vegas, NV 89154-4003, USA
e-mail: chulsung.bae@unlv.edu

Present Address:
C. Bae
Department of Chemistry and Chemical Biology, Rensselaer Polytechnic Institute,
110 8th Street, Troy, NY 12180, USA

P. J. Pérez (ed.), *Alkane C–H Activation by Single-Site Metal Catalysis*,
Catalysis by Metal Complexes 38, DOI: 10.1007/978-90-481-3698-8_3,
© Springer Science+Business Media Dordrecht 2012

3.1 Introduction

The development of efficient alkane functionalizations has been one of the most challenging topics in chemistry. Alkanes, or saturated hydrocarbons, are inert because their C–H bonds have high bond dissociation energy (typically 90–100 kcal/mol) and very low acidity (estimated $pK_a = 50–60$) and basicity. So although they are abundant in nature—alkanes are major components of natural gas and petroleum—converting them directly to more valuable products is difficult. Currently, most alkanes are either burned as a fuel in combustion processes, which generate economically unattractive by-products carbon dioxide and water, or converted to alkenes using a thermal cracking process. Although the latter generates more useful products that can be further converted to synthetically useful organic molecules such as alcohols and carbonyl compounds, the industrial thermal dehydrogenation reaction is an inefficient process that requires high temperatures (typically 800–1000 °C). Thus, efficient and selective functionalization of alkane C–H bonds could shorten the multi-step synthetic process currently used for alkane conversion and, as a result, offer enormous economic benefits.

The C–H bonds of alkanes can be cleaved using strong acids (superacids) and free radicals [1, 2] Unfortunately, when these highly reactive species interact with alkanes, they do not generate products selectively but instead yield a mixture of products that result from the functionalization of various C–H bonds. Selectivity among different C–H bonds in these reactions depends on the strength of the bonds (for free radical processes) and the stability of the resulting carbocations (in superacidic processes). Therefore, the order of relative reactivity is tertiary C–H > secondary C–H > primary C–H bonds. In reality, however, terminally functionalized linear alkanes, which are derived from the functionalization of primary C–H bonds, are often the most desirable products.

In contrast to the selectivity of the C–H bond cleavage in free radical or electrophilic pathways, transition metal complexes preferentially attack at the least hindered terminal C–H bonds and make the least substituted positions more reactive in the C–H bond activation step [3, 4]. Thus, the C–H activation of alkanes via organometallic pathways can afford potentially more useful terminally functionalized linear alkane products. Since the 1980s, many transition metal complexes that can cleave alkane C–H bonds by oxidative addition have been developed [5]. Unfortunately, most of them require stoichiometric amounts of metal complexes to break the C–H bonds of alkanes, which is impractical in large-scale syntheses because the metal complexes used in the process are generally more expensive than the functionalized alkane products.

Rhodium-catalyzed photochemical carbonylation of linear alkanes can give terminal aldehydes with high selectivity, but it also produces secondary photo-products [6–8]. Dehydrogenation of linear alkanes is a thermodynamically uphill process, as such, it has traditionally required the presence of a sacrificial hydrogen acceptor for the reaction to proceed [9]. Although homogeneous alkane dehydrogenations based on thermally stable iridium–pincer complexes—even without a

hydrogen acceptor—were developed during the last decade, the initially formed terminal alkenes tend to isomerize to give a mixture of terminal and internal alkene products in high conversion [10–14].

Organoboron compounds are an important class of synthetic intermediates in organic synthesis. Thanks to the rich chemistry pioneered by Brown and co-workers, organoboron moieties in a molecule can be converted to a variety of important functional groups including alcohols, amines, halides, aldehydes, and others [15, 16]. During the past fifteen years, direct functionalization of C–H bonds via transition metal–boryl complexes has offered a new pathway for the preparation of organoboron molecules from unreactive alkanes and arenes [17, 18]. In principle, the direct borylation of C–H bonds offers economic and environmental benefits because alkanes are abundant raw materials, and organoboron compounds have traditionally been prepared via multi-step synthetic routes.

The borylation of alkane C–H bonds with a diboron or a borane reagent to form a linear alkylborane is an exothermic reaction (Eq. 3.1). Computational studies of the bond dissociation energies of closely related boron compounds have revealed that the thermodynamics of the alkane borylation are favorable, which serve as the driving force of the chemical process [19, 20]. The sum of the bond dissociation energies of the first-stage products of Eq. 3.1 is 21 kcal/mol larger than that of the reactants: B–B (104 kcal/mol) and C–H (98 kcal/mol) versus B–C (112 kcal/mol) and B–H (111 kcal/mol). The second stage of the reaction is also slightly exothermic by 7 kcal/mol: C–H (98 kcal/mol) and B–H (111 kcal/mol) versus B–C (112 kcal/mol) and H–H (104 kcal/mol). Overall, the combination of the synthetic versatility of organoboron compounds, robust selectivity for terminal C–H bonds, and favorable thermodynamics makes the borylation of alkane C–H bonds an extraordinarily attractive approach to practical alkane functionalization.

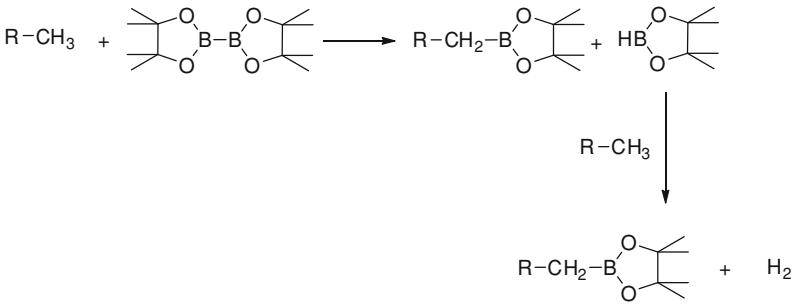

(3.1)

3.2 C–B Bond Formation via Alkane C–H Activation

3.2.1 Stoichiometric C–B Bond Formation

Inspired by a report of the successful functionalization of arene C–H bonds with $CpFe(CO)_2Bcat$ (Bcat = $BO_2C_6H_4$, catecholboryl) [21], Hartwig and co-worker prepared various transition metal–boryl complexes of Fe, Ru, and W and examined

their photochemical reactivity with C–H bonds of *n*-pentane (Table 3.1).Additionally, the same authors prepared [22, 23]. Although $CpFe(CO)_2Bcat$ functionalized the C–H bonds of arenes and alkenes under photochemical conditions, it did not react with the C–H bonds of alkanes, possibly because of the reaction of the metal boryl complex with the sp^2-hybridized C–H bonds of the catecholate (cat) or cyclopentadienyl (Cp) groups. To avoid this reaction, they prepared sterically hindered derivatives of the complex **1a** and **1b** in which they replaced Cp with pentamethylcyclopentadienyl (Cp*) and blocked the aromatic C–H bonds with dialkyl substituents at the ortho positions. When **1a** and **1b** were tested with pentane, both iron–boryl complexes afforded pentylboronate ester in 15 and 20 % yields, respectively (Table 3.2, entries 2 and 3). When sp^2-hydridized positions of only one of the cat and Cp groups were blocked in the iron–boryl complexes, the resulting complexes (i.e., **1c** and **1d**) were unreactive toward alkanes, demonstrating the importance of blocking all aromatic C–H bonds in the metal complexes in reactions with alkanes (Table 3.2, entries 4 and 5). Compared to iron complex **1b**, the second-row ruthenium complex **2** and the third-row analog tungsten complex **3a** produced the alkylboronate product in higher yields (Table 3.2, entries 6 and 7). Similar to the results seen with substitutions in the iron–boryl complex system, replacement of the dimethylcatecholboryl group of **3a** with unsubstituted cat in **3b** reduced reactivity toward alkanes and resulted in low yields of the borylated product (Table 3.2, entry 8).

Additionally, the same authors prepared ruthenium–boryl complexes containing boryl ligands with different electron-donating abilities to investigate the electronic effect of boryl ligands on reactivity in the functionalization of alkane C–H bonds (Table 3.3). The CO stretching frequencies of the ruthenium–boryl complexes in IR spectra indicated that the electron-donating effect of the boryl groups in the complexes was ordered dialkylboryl (BR_2, R = alkyl) > pinacolboryl (Bpin) > dithioboryl [$B(SR)_2$] > Bcat [23]. Although the yield for the alkylboronate product was significantly greater with ruthenium complex **5** than with **2**, presumably because Bpin is a stronger electron-donating group than Bcat (Table 3.3, entries 1 and 2), the reactivities of the other boryl groups did not follow the order of electron-donating strength. For example, metal complexes with dialkylboryl groups (i.e., **8a** with BBN, where BBN = 9-borabicyclo[3.3.1]nonyl; **8b** with BCy_2, where Cy = cyclohexyl; **8c** with BMe_2, where Me = methyl)— the strongest electron-donating groups found among the boryl complexes—were much less reactive toward alkane C–H bonds than were ruthenium–Bpin complex **5** (Table 3.3, entries 2 and 5–7). In addition, complex **9** with a dithioboryl group (BS_2Tol = B−1,2-S_2C_6H-4-Me)—a stronger electron donor than Bcat—did not form the product at all (Table 3.3, entry 8). The fact that **9** reacts with C–H bonds of benzene in moderate yields but does not react with those of pentane under identical photochemical conditions suggests that the ruthenium dithioboryl intermediate has lower reactivity toward alkane C–H bonds than toward arene C–H bonds. Based on these contradictory trends, the authors concluded that the electronic properties of the boryl group had an insignificant influence on the formation of the proposed 16-electron intermediate but affected the reactivity of the intermediate toward alkane C–H bonds, nevertheless.

Table 3.1 Transition metal–boryl complexes examined for photochemical functionalization of *n*-pentane

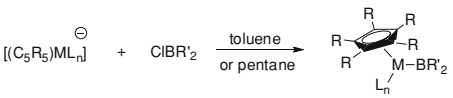

Entry	Chloroborane	Complex	M	L_n	R
1	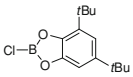	**1a**	Fe	$(CO)_2$	Me
2	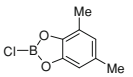	**1b**	Fe	$(CO)_2$	Me
3	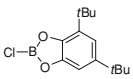	**1c**	Fe	$(CO)_2$	H
4		**1d**	Fe	$(CO)_2$	Me
5	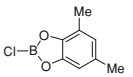	**2**	Ru	$(CO)_2$	Me
6	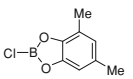	**3a**	W	$(CO)_3$	Me
7		**3b**	W	$(CO)_3$	Me
8	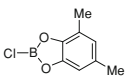	**4**	Mo	$(CO)_3$	Me
9	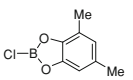	**10a**	W	$(CO)_2PXy_3$	Me
10	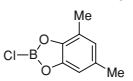	**10b**	W	$(CO)_2PMe_3$	Me
11		**5**	Ru	$(CO)_2$	–
12		**6**	W	$(CO)_3$	–
13		**7**	Fe	$(CO)_2$	Me
14		**8a**	Ru	$(CO)_2$	Me
15		**8b**	Ru	$(CO)_2$	Me
16		**8c**	Ru	$(CO)_2$	Me
17	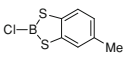	**9**	Ru	$(CO)_2$	Me

Table 3.2 Steric effect of cyclopentadienyl and boryl ligands on photochemical reactions with *n*-pentane

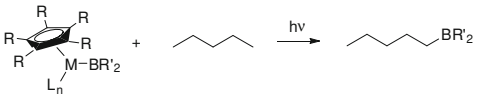

Entry	Compound		Yield
1		$CpFe(CO)_2(Bcat)$	<1
2	**1a**	$Cp^*Fe(CO)_2[Bcat(t Bu)_2]$	15
3	**1b**	$Cp^*Fe(CO)_2[Bcat(Me)_2]$	20
4	**1c**	$CpFe(CO)_2[Bcat(t Bu)_2]$	<1
5	**1d**	$Cp^*Fe(CO)_2[Bcat]$	<1
6	**2**	$Cp^*Ru(CO)_2[Bcat(Me)_2]$	40
7	**3a**	$Cp^*W(CO)_3[Bcat(Me)_2]$	85
8	**3b**	$Cp^*W(CO)_3[Bcat]$	20

Table 3.3 Electronic effect of boryl ligands on photochemical reactions with *n*-pentane

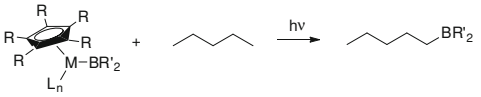

Entry	Compound		Yield
1	**2**	$Cp^*Ru(CO)_2[Bcat(Me)_2]$	40
2	**5**	$Cp^*Ru(CO)_2[Bpin]$	78
3	**6**	$Cp^*W(CO)_3[Bpin]$	72
4	**7**	$Cp^*Fe(CO)_2[BBN]$	20
5	**8a**	$Cp^*Ru(CO)_2[BBN]$	8
6	**8b**	$Cp^*Ru(CO)_2[BCy_2]$	<1
7	**8c**	$Cp^*Ru(CO)_2[BMe_2]$	<1
8	**9**	$Cp^*Ru(CO)_2[BS_2Tol]$	<1

The effect of dative ligands in tungsten–boryl complexes was investigated by comparing functionalization yields and selectivity toward the C–H bonds of alkane using tricarbonyl and phosphine carbonyl complexes (**3a**, **10a**, and **10b**). Tungsten–boryl complexes that contain a phosphine ligand (**10a** and **10b**) reacted with the C–H bonds of alkanes but with lower yields than the tricarbonyl complex **3a**. Between two phosphine complexes, **10a** with a bulkier trixylylphosphine ligand produced pentylboronate ester in higher yield (59 %) compared to complex **10b** (32 %), which has a smaller and more basic trimethylphosphine ligand (Table 3.4).

When **3a**, **10a**, and **10b** react with alkane C–H bonds, a reactive 16-electron intermediate will be formed from the dissociation of phosphine or CO ligands, and depending on which ligand dissociates different intermediates are expected. If the reaction of **10a** and **10b** involves dissociation of a phosphine ligand, it would generate 16-electron intermediate $Cp^*W(CO)_2[Bcat(Me)_2]$, an intermediate identical to that formed in the reaction of complex **3a**. In this case, the three tungsten complexes should give similar yields and regioselectivities in reactions with

Table 3.4 Effect of dative ligands on the reactivity of photochemical reactions with *n*-pentane

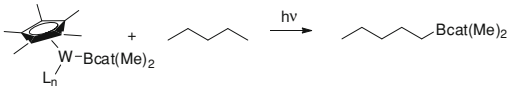

Entry	Compound		Yield
1	**3a**	$Cp^*W(CO)_3[Bcat(Me)_2]$	85
2	**10a**	$Cp^*W(CO)_2[Bcat(Me)_2](PXy_3)$	59
3	**10b**	$Cp^*W(CO)_2[Bcat(Me)_2](PMe_3)$	32

hydrocarbons, and the addition of extra phosphine would inhibit the formation of borylated alkyl products. Alternatively, if reaction with C–H bonds occurs through the dissociation of CO ligands, **3a**, **10a**, and **10b** would produce three different 16-electron intermediates with the general formula $Cp^*W(CO)[Bcat(Me)_2](L)$, where L = CO, PXy_3, and PMe_3. In this case, the three complexes would have different reaction yields and regioselectivities when they react with hydrocarbons, and the addition of extra phosphine to **10b** would form bisphosphine complex $Cp^*W(CO)[Bcat(Me)_2](PMe_3)_2$ in competition with the formation of alkylboronate products.

When **10a** and **10b** reacted with isopentane and toluene, they formed mixtures of products with almost identical isomer ratios (Table 3.5, entries 2 and 3 vs. entries 5 and 6). In addition, the three complexes—**3a**, **10a**, and **10b**—showed identical isotope effects when photolyzed with an equimolar mixture of *n*-pentane and *n*-pentane-d_{12} (Table 3.6, entries 3–5). Furthermore, addition of extra PMe_3 to the photochemical reaction of **10b** and *n*-pentane failed to yield the bisphosphine complex but resulted in lower product yields instead. These experimental results examining regioselectivity, isotope effects, and added phosphine effect (see Tables 3.5 and 3.6) strongly suggested that **3a**, **10a**, and **10b** primarily underwent the common intermediate $Cp^*W(CO)_2[Bcat(Me)_2]$ via the dissociation of CO, PXy_3, and PMe_3, respectively, when they reacted with the C–H bonds of hydrocarbon substrates. The difference in borylated product yields among the three complexes also suggested, however, that **10a** and **10b** dissociated not only phosphine ligand but also CO, generating two intermediates—reactive $Cp^*W(CO)_2[Bcat(Me)_2]$ and unreactive $Cp^*W(CO)[Bcat(Me)_2](PR_3)$ (where R = Xy for **10a** and Me for **10b**)—simultaneously. The authors theorized that **10a** and **10b** generated lower amounts of the reactive 16-electron intermediate and afforded lower product yields than those of **3a** because the latter 16-electron intermediate is unreactive toward alkane C–H bonds. Because the reactive 16-electron intermediate can be generated from all three complexes, however, their regioselectivities and isotope effects were likely to be unaffected. This postulate has been confirmed by comparison experiments of the photochemical reactions of **3a** and **10b** with C_6D_6. Tricarbonyl complex **3a** produced higher yield (84 %) of C_6D_5-$Bcat(Me)_2$ than that produced by monophosphine dicarbonyl complex **10b** (54 %). Furthermore, whereas **3a** gave a similar yield with both an alkane and an arene (85 % with *n*-pentane and 84 % with C_6D_6), **10b** produced much higher yield with the arene than with the alkane (54 % with C_6D_6 and 32 % with *n*-pentane).

Table 3.5 Comparison of photochemical reactions of $Cp^*W(CO)_2[Bcat(Me)_2](L)$ with alkanes and arenes

Entry	Complex	Ligand	Hydrocarbon	Yield (%) or isomer ratio
1	**10a**	PXy_3 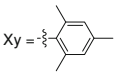		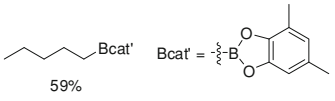 59%
2	**10a**	PXy_3		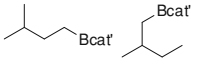 10 : 1
3	**10a**	PXy_3		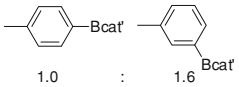 1.0 : 1.6
4	**10b**	PMe_3		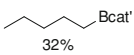 32%
5	**10b**	PMe_3		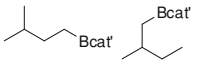 11 : 1
6	**10b**	PMe_3		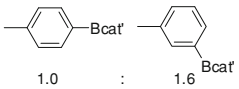 1.0 : 1.6

Table 3.6 Kinetic isotope effects of photochemical reactions of metal–boryl complexes with *n*-pentane/*n*-pentane-d_{12}

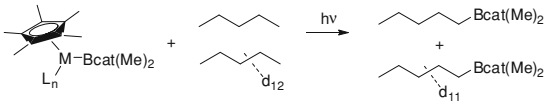

Entry	Compound		k_H/k_D
1	**1b**	$Cp^*Fe(CO)_2[Bcat(Me)_2]$	1.9
2	**2**	$Cp^*Ru(CO)_2[Bcat(Me)_2]$	2.2
3	**3a**	$Cp^*W(CO)_3[Bcat(Me)_2]$	5.1
4	**10a**	$Cp^*W(CO)_2[Bcat(Me)_2](PXy_3)$	4.9
5	**10b**	$Cp^*W(CO)_2[Bcat(Me)_2](PMe_3)$	5.1

These observations were rationalized as follows: The reactive $Cp^*W(CO)_2[Bcat(Me)_2]$ intermediate, which can be formed via CO dissociation of **3a** or phosphine dissociation of 1**0b**, has a similar reactivity toward the C–H bonds of alkanes and arenes; however, the unreactive $Cp^*W(CO)[Bcat(Me)_2](PMe_3)$ intermediate, which can only be formed via CO dissociation of **10b**, has significantly higher reactivity toward arene C–H bonds than alkane C–H bonds. Because **10b** generates two 16-electron intermediates and one of them is much less reactive toward alkane C–H bonds, it gives a lower yield of borylated alkane products than for borylated arene products.

The kinetic isotope effects of iron, ruthenium, and tungsten complexes that contain dicarbonyl and $Bcat(Me)_2$ ligands (i.e., **1b**, **2**, and **3a**) in reactions with equimolar mixtures of *n*-pentane and perdeuterated *n*-pentane were compared to

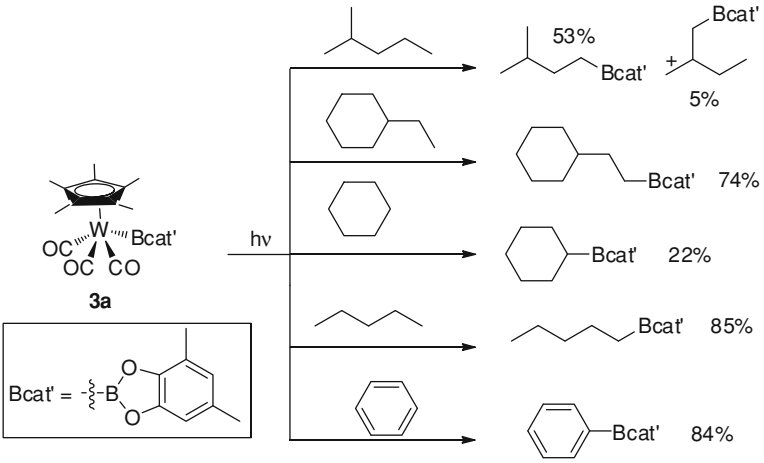

Scheme 3.1 Regioselectivity of tungsten–boryl complex **3a** with various hydrocarbon C–H bonds

gain additional mechanistic insight (Table 3.6, entries 1–3). The authors hypothesized that if alkanes produced the corresponding borylated products through a pathway involving a [Bcat(Me)$_2$] free radical, the three complexes would have the same isotope effect because the reactivity of the boryl radical would be identical regardless of the origin of the radical precursor. The study of isotope effect revealed that the three complexes have different isotope effect values, excluding the possibility of a boryl radical pathway for the alkane borylation (Table 3.6, entries 1–3).

As shown in Scheme 3.1, the reaction of **3a** with different nonlinear alkanes occurred preferentially at the terminal C–H bonds. Functionalization of 2-methylbutane occurred more readily at less hindered terminal primary C–H bonds. The ratio of the two borylated isomers was approximately 11:1 (53 % vs. 5 %). Ethylcyclohexane contains primary, secondary, and tertiary C–H bonds in a ratio of 3:12:1. The reaction of ethylcyclohexane with **3a** afforded a borylated alkane product functionalized only at the primary C–H bonds of the ethyl group in 74 % yield. When primary C–H bonds were unavailable, **3a** indeed reacted with secondary C–H bonds but in significantly lower yield (22 % for cyclohexane vs. 85 % for *n*-pentane). Thus, regioselective preference of **3a** for alkane C–H bonds is determined by the steric environment around C–H bonds and differs distinctly from the regioselectivity of typical free radical–mediated alkane functionalization (tertiary C–H > secondary C–H > primary C–H). This marked difference in regioselectivity also supports the conclusion drawn from kinetic isotope effects, the nonradical pathway of C–H borylation.

Based on experimental results from the additions of CO and PMe_3 to **3a** and their effects on reactions with *n*-pentane, Hartwig and co-worker proposed a plausible mechanism (shown in Scheme 3.2). Photochemical dissociation of CO

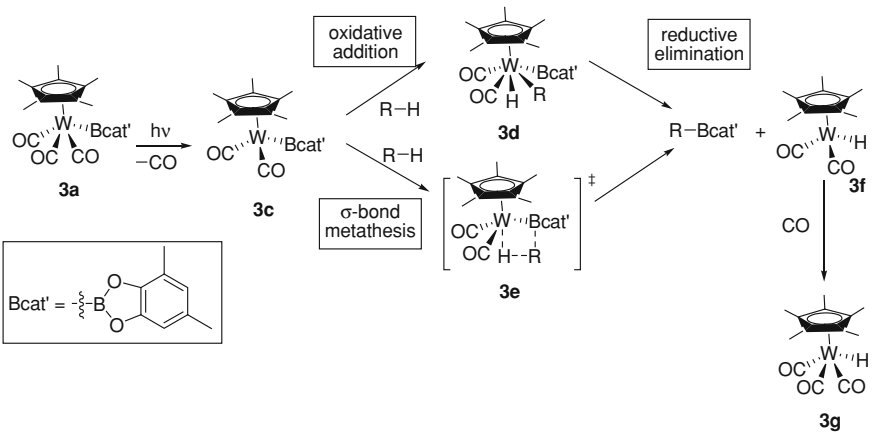

Scheme 3.2 Proposed mechanism of C–H borylation of alkane with transition metal–boryl complex

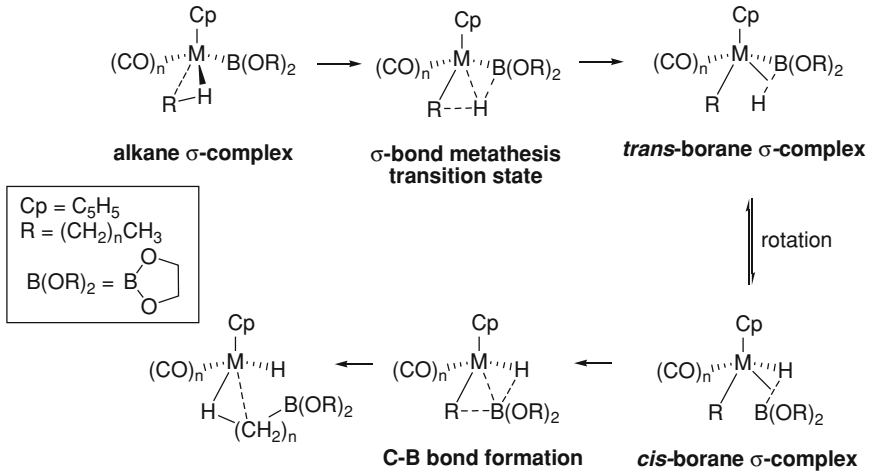

Scheme 3.3 Computationally proposed lowest-energy pathway for the reaction of transition metal–boryl complexes with alkanes

from **3a** produces the reactive 16-electron intermediate Cp*W(CO)$_2$Bcat′ (**3c**), which reacts with alkane C–H bonds through oxidative addition to form Cp*W(CO)$_2$(H)(R)Bcat′ (**3d**) and releases an alkylboronate product via reductive elimination. The resulting metal complex, Cp*W(CO)$_3$H (**3f**), recombines with CO and forms Cp*W(CO)$_3$H (**3g**), which can be observed experimentally using ^{1}H NMR spectroscopy. An alternative pathway via σ-bond metathesis with structure **3e** has also been suggested as a possible route.

Because distinguishing these two pathways is experimentally difficult, a combination of computational and experimental studies was performed to elucidate the pathways further [24]. The computed lowest-energy pathway favors the σ-bond metathesis route shown in Scheme 3.3. In the proposed pathway, the 16-electron intermediate first reacts with the C–H bonds of the alkane to form an alkane σ-complex, which then converts to a borane σ-complex via a single-step transition state. In the borane σ-complex, the boryl ligand and the alkyl moiety are positioned trans to each other. Thus they undergo rotation to form *cis*-borane σ-complex, which then forms a C–B bond in the next step and dissociates the alkylboronate product. Although the oxidative addition of C–H bonds was calculated to have a higher energy than that of σ-bond metathesis (4 and 11 kcal/mol for the tungsten–boryl complex and the iron–boryl complex, respectively), a related calculation study conducted by Lin and co-worker proposed pathways based on oxidative addition of C–H bonds via a one-step mechanism for iron–boryl complex and a two-step mechanism for tungsten–boryl complex [25].

3.2.2 Catalytic C–B Bond Formation of Alkanes Using Transition Metal Complexes

3.2.2.1 Rhenium-Catalyzed Photochemical Borylation of Alkanes

The monoboryl–tungsten complexes reported by Hartwig and co-worker [22, 23] reacted with alkane C–H bonds only stoichiometrically because the regeneration of the boryl complex from these complexes required additional steps and reagents. The Hartwig research group later reported the first regioselective catalytic functionalization of terminal C–H bonds of linear alkanes using rhenium catalysts under photochemical conditions [26]. They initially conducted stoichiometric photochemical reactions of $Cp'M(CO)_3$ (**11**: $Cp' = C_5H_4Me$, M = Mn; **12**: $Cp' = C_5H_5$, M = Re; **13**: $Cp' = C_5Me_5$ (Cp*), M = Re) with bis(pinacolato) diboron (B_2pin_2) in neat pentane using a 450 watt medium-pressure Hanovia mercury arc lamp (Scheme 3.4). Although complexes **11** and **12** generated 1-pentylboronate ester selectively, the yields were low (35 % and 50 %, respectively). Rhenium complex **13** afforded terminal functionalized alkane product quantitatively, but regeneration of the complex was unsuccessful, presumably because of the formation of inactive bridging carbonyl dimers [27] $(\eta\text{-}C_5Me_5)_2Re(_2\mu\text{-}CO)(CO)_4$ and $(\eta\text{-}C_5Me_5)_2Re_2(\mu\text{-}CO)_3$ after the completion of the catalytic cycle. To achieve a catalytic functionalization of the reaction, the authors conducted the same reaction with additional CO (2 atm) and a catalytic amount of **13** (2.4 mol %), which produced the alkylboronate product in 95 % yield (Table 3.7, entry 1). Without additional CO, the catalytic reaction produced the borylated alkane product in low yield (22 %) in spite of the fact that the catalyst was entirely consumed. In the presence of a catalytic amount of **13**

Table 3.7 Rhenium-catalyzed photochemical, regioselective C–H borylation of alkanes.[a]

Entry	Substrate	Catalyst Loading (mol %/time h)	Product(s)	Yield (%) of R-Bpin
1		2.4/56	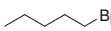	95
2		3.4/55		83[b] (65/18)
3		5.0/60	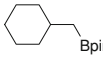	75
4	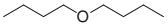	5.0/45	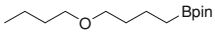	100
5		4.9/46	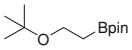	82
6[c]		2.5/56	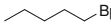	97

[a] A mixture of 2.4–5.0 mol % of Cp*Re(CO)$_3$, dodecahydrotriphenylene (internal standard), bis(pinacolato)diboron (B_2pin_2), CO (2 atm), and alkane was irradiated with a 450 watt medium-pressure Hanovia mercury arc lamp. Yields were determined by GC or 1H NMR spectroscopy, and yields of isolated products were determined after purification by column chromatography using silica gel

[b] The two terminal regioisomers were obtained in a ratio of 3.6:1

[c] 2.5 mol % of *trans*-[Cp*Re(CO)$_2$(Bpin)$_2$] was used as catalyst

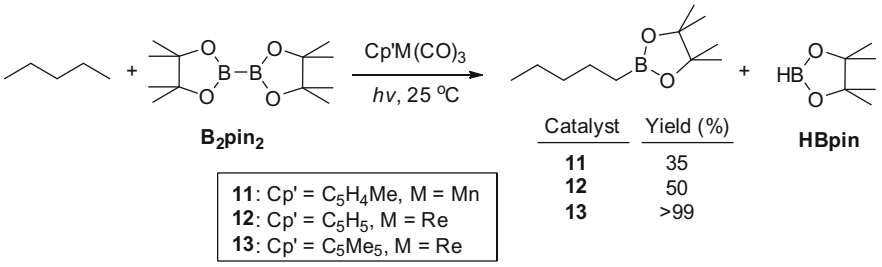

Scheme 3.4 Stoichiometric photochemical C–H borylation of pentane using B_2pin_2 and Cp′M(CO)$_3$

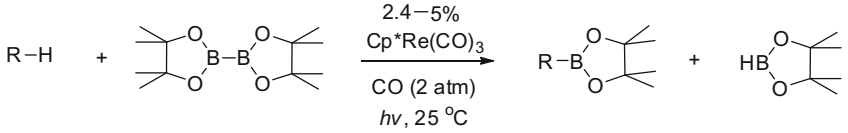

Scheme 3.5 Rhenium-catalyzed photochemical functionalization of alkanes

(2.4–5.0 mol %) alkanes and alkyl ethers were converted to their corresponding alkylboronate esters in good to excellent yields with high regioselectivity (Scheme 3.5 and Table 3.7). Interestingly, pinacolborane (HBpin), which is generated as a by-product in the catalytic cycle and can induce additional borylation at C–H bonds in thermal catalytic conditions (see Sect. 3.2.2.2) [28], did not afford borylation products under photochemical conditions.

The rhenium-catalyzed photochemical borylation showed a strong dependence on the steric hindrance around C–H bonds and an exceptionally high regioselectivity toward primary C–H bonds over secondary or tertiary C–H bonds in alkane functionalization. The reaction of *n*-pentane generated 1-pentylboronate ester as the sole functionalized product. None of internal borylated pentanes, which could be produced through activation of secondary C–H bonds, were observed. The borylation of 2-methylbutane, which has two types of methyl groups, also produced only terminal-functionalized alkane products—3-methyl-1-butylboronate ester and 2-methyl-1-butylboronate ester—in a ratio of 3.6:1 (Table 3.7, entry 2). This result indicated that functionalization occurred more readily at the less hindered methyl group. Methylcyclohexane reacted to give 1-cyclohexyl-1-methylboronate ester in 75 % yield, suggesting that the rhenium catalyst was more reactive toward primary C–H bonds than secondary or tertiary C–H bonds (Table 3.7, entry 3). Because of low reactivity with secondary C–H bonds, cyclohexane did not produce any borylated cyclohexane products under the reaction conditions. An addition of 2-butylboronate ester to the reaction of *n*-pentane and B_2pin_2 was undertaken to investigate whether these observed terminal borylated alkanes resulted from the isomerization of the products that were formed from the initial borylation of secondary C–H bonds. The branched alkylboronate ester remained unchanged during the formation of linear alkylboronate ester, suggesting that no isomerization occurred and the selective functionalization was a result of a regioselective reaction of the rhenium catalyst with primary C–H bonds.

The rhenium-catalyzed photochemical borylation tolerates ether functionality. Basic heteroatoms in ether apparently do not interfere with the catalytic process of the reaction. For example, di-*n*-butyl ether reacted with B_2pin_2 and produced 4-butoxy-1-butylboronate ester quantitatively (Table 3.7, entry 4). No product from the borylation of the C–H bond next to oxygen in the ether was detected. Similarly, reaction of *tert*-butyl ethyl ether afforded a product with boronate ester at the terminal position of the ethyl group (Table 3.7, entry 5). The higher yield from di-*n*-butyl ether compared to that of *tert*-butyl ethyl ether also reflects the sensitivity of the functionalization to the steric environment around the methyl group.

To investigate potential mechanism of the C–H functionalization reaction, the Hartwig group prepared *trans*-[Cp*Re$(CO)_2$(Bpin$)_2$] from the reaction of Cp*Re$(CO)_3$ and B_2pin_2 in cyclohexane solvent. Its cis isomer was observed early in the reaction. Both cis and trans isomers of [Cp*Re$(CO)_2$(Bpin$)_2$] reacted quantitatively with *n*-pentane to form *n*-pentylboronate ester under photochemical conditions (Table 3.7, entry 6), strongly suggesting that the bisboryl–rhenium complexes are potential intermediates in the catalytic cycle of the reaction. Based on these results, they proposed the mechanism shown in Scheme 3.6. The borylation of alkane starts with photochemical dissociation of a carbonyl group from Cp*Re$(CO)_3$ and oxidative addition of B_2pin_2 to form *cis*- and *trans*-[Cp*Re$(CO)_2$(Bpin$)_2$]. The bisboryl intermediates undergo dissociation of CO, and the resulting unsaturated bisboryl complex reacts with alkane C–H bonds via either oxidative addition generating a Re^{V} intermediate or σ-bond metathesis process involving Re^{III}. Finally, reductive elimination of alkylboronate ester and association of CO regenerates the catalyst precursor Cp*Re$(CO)_3$.

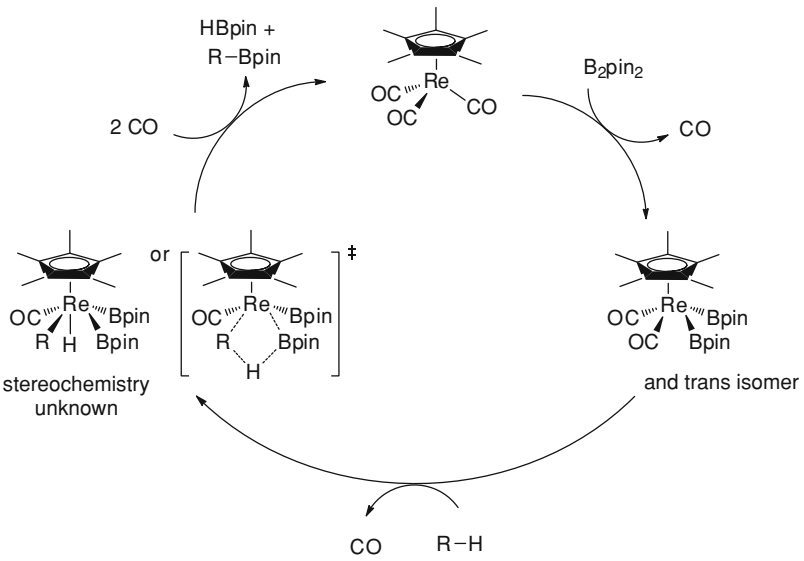

Scheme 3.6 Proposed mechanism for rhenium-catalyzed photochemical C–H borylation of alkanes

3.2.2.2 Iridium- and Rhodium-Catalyzed Thermal Borylation of Alkanes

The thermal catalytic borylation of C–H bonds of alkanes, a more practical alkane functionalization process, was reported by Hartwig and co-workers in 2000 [28]. Encouraged by promising results of stoichiometric functionalization with $Cp^*W(CO)_3Bcat'$ ($Cp^* = C_5Me_5$, $cat' = 1,2\text{-}O_2C_6H_2\text{-}3,5\text{-}Me_2$) [22, 23], and catalytic photochemical borylation with $Cp^*Re(CO)_3$ [26], they synthesized a series of Cp*ML complexes that can react with diboron or borane compounds to form transition metal–boryl complexes via oxidative addition. Because dative ligands such as polyhydrides, alkenes, and η^4-arenes are expected to generate reactive unsaturated boryl complexes more readily than CO ligands do via thermally induced ligand dissociation, they prepared Cp^*IrH_4 (**14**) [29], $Cp^*Ir(\eta^2\text{-}C_2H_4)$ (**15**) [30], $Cp^*Rh(\eta^2\text{-}C_2H_4)_2$ (**16**) [30], $Cp^*Rh(C_2H_3SiMe_3)_2$ (**17**) [31], $Cp^*Rh(H)_2(SiEt_3)_2$ (**18**) [32], and $Cp^*Rh(\eta^4\text{-}C_6Me_6)$ (**19**) [33] and tested them as catalyst precursors for borylation of *n*-octane with B_2pin_2 (Scheme 3.7).

The iridium complexes indeed catalyzed the reaction, but their activity was too slow: with 10 mol % loading of **14** or **15**, the complete conversion of HBpin—generated from the first phase of the reaction of *n*-octane and B_2pin_2—took 10 days at 200 °C. Although this low reactivity is ineffective for catalytic reactions, it helps in the preparation and isolation of iridium (V) hydrido boryl complexes, which are assumed to be potential intermediates in the catalytic process [34].

Switching the catalyst precursor to rhodium complex **16**, the second-row analog of **15**, induced more reactive borylation of *n*-octane at 150 °C, completely converting B_2pin_2 to HBpin in 1 h. The HBpin generated in situ was consumed within

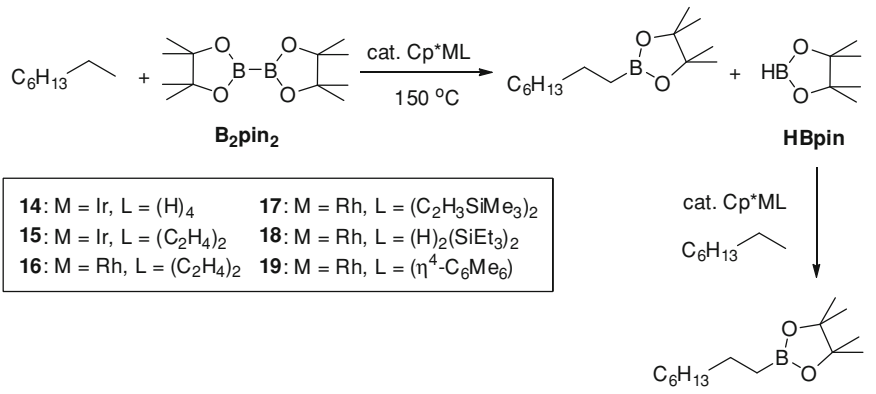

Scheme 3.7 Thermal, catalytic borylation of *n*-octane

5 h, and *n*-octylpinacolboronate ester (*n*-octylBpin) was obtained as the sole product in 84 % overall yield. Similar to the previous results of alkane functionalization with transition metal–boryl complexes [22, 23, 26], only terminal-functionalized alkane product was obtained with the rhodium catalyst precursors. Although no other regioisomers of borylated octane were detected, a small percentage of side products were obtained from the borylation of the ethylene ligands, including $C_2H_5(Bpin)$, $C_2H_4(Bpin)_2$, $C_2H_3(Bpin)_3$, and $C_2H_2(Bpin)_4$.

To avoid side reaction with the alkene ligands, Hartwig and co-workers prepared and tested rhodium complexes containing more labile vinylsilane (complex **17**), silyl (complex **18**), and chloride ($[Cp^*RhCl_2]_2$) ligands in the borylation, but found these to be less reactive than **16**. The reaction catalyzed by complex **19**, which would release unreactive hexamethylbenzene ligand in the borylation, gave the highest yield of *n*-octylBpin without forming any ligand borylation products (Table 3.8, entry 3). Hexamethylbenzene rhodium complex **19** was more reactive than vinylsilane complex **17**, silyl complex **18**, and $[Cp^*RhCl_2]_2$. Although **19** was less reactive than **16** initially, the former had much better long-term activity, allowing higher conversion to the product with low catalyst loading and prolonged reaction time.

The molar amount of the borylated alkane product was higher than that of B_2pin_2, suggesting that the HBpin by-product also reacted with *n*-octane in the presence of the rhodium catalyst to form additional product

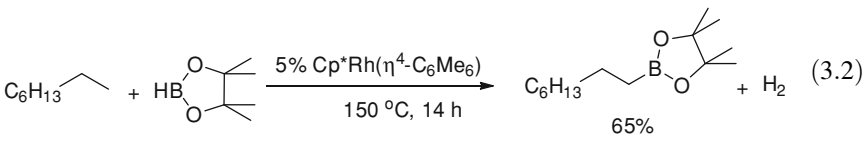

(3.2)

(see Scheme 3.7, second reaction). In contrast to the rhenium-catalyzed photochemical borylation of alkane [26], in which HBpin was unreactive, *n*-octane

Table 3.8 Thermal, regioselective C–H borylation of alkanes catalyzed by rhodium complexes[a]

Entry	Alkane	Catalyst/time (h)	Product(s)	Yield (%)[b]
1		**16** (5 mol %)/5	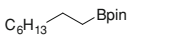	84
2		**16** (1 mol %)/110	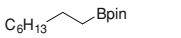	64
3		**19** (5 mol %)/25	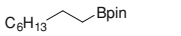	88
4		**19** (1 mol %)/80	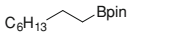	72
5	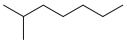	**16** (2.5 mol %)/30	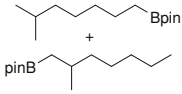	73 (61+12)
6	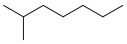	**19** (1 mol %)/60	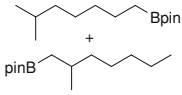	61 (50+11)
7		**19** (6 mol %)/80	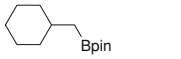	49
8	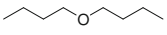	**19** (4 mol %)/80	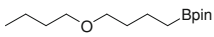	64

[a] A solution of rhodium catalyst, alkane, and B_2pin_2 was heated at 150 °C
[b] GC yields based on the overall reaction in Scheme 3.7

reacted with HBpin cleanly in a separate rhodium-catalyzed thermal borylation and formed *n*-octylBpin and dihydrogen (Eq. 3.2). Thus, the reported yields in Table 3.8 are based on the overall reaction in Scheme 3.7.

As shown in Table 3.8, the borylation of alkanes generates products in which the C–H bonds of less sterically hindered methyl group are selectively functionalized. For example, 2-methylheptane has two types of terminal CH_3 groups, and its reaction produced a mixture of 6-methyl-1-heptylboronate ester and 2-methyl-1-heptylboronate ester in a ratio of 5:1; less hindered CH_3 group was preferentially functionalized (Table 3.8, entries 5 and 6). Methylcyclohexane had a slow reaction rate and lower product yield because of its lower concentration and steric hindrance around the CH_3 group (Table 3.8, entry 7). Di-*n*-butyl ether reacted rapidly with B_2pin_2 but not with the HBpin generated in situ. As a result, even with higher catalyst loading, the yield of borylation product was lower than that of *n*-octane (Table 3.8, entry 8). Rhodium complex **19** was more active in the borylation of arene C–H bonds than in that of alkane C–H bonds: benzene was functionalized to give phenylBpin in 82 % yield with 0.5 mol % of **19**. The high reactivity of **19** toward arene C–H bonds but low reactivity toward methylene C–H bonds allowed for the development of a catalytic borylation of various arenes in the presence of cyclohexane solvent [35].

3.2.2.3 Rhodium-Catalyzed Borylation of Alkanes Containing Heteroatoms

Rhodium-catalyzed thermal borylation selectively functionalizes terminal methyl groups of linear and branched alkanes even in the presence of heteroatom moieties, significantly enhancing synthetic practicability [36]. tert-Butyl-protected alcohol,

Table 3.9 Substrate scope of rhodium-catalyzed borylation of terminal C–H bonds[a]

Reactant	Reactant:B_2pin_2	Cp*Rh(η^4-C_6Me_6) (mol %)	Product	Yield (%)[b]
	10:1	5	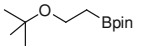	91
	1:1	10		48[c]
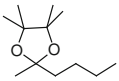	10:1	5	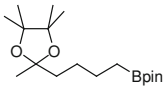	74
	1:2	17		70
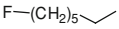	10:1	5	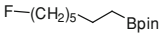	83[d]
	1:2	10		46
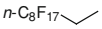	10:1	5	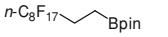	90
	1:2	10		84
	10:1	5	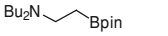	75[e]
	1:1	10		33
	10:1	5	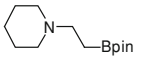	55[e]
	1:2	10		67

[a] Reaction condition: Cp*Rh(η^4-C_6Me_6) and B_2pin_2 150 °C, 24 h. B_2pin_2 = bis(pinacolato)diboron; Bpin = pinacolboryl; HBpin = pinacolborane

[b] GC yields based on the reaction R-H + B_2pin_2 →R-Bpin + HBpin

[c] In cyclohexane solvent (3 equiv)

[d] 140 °C, 12 h

[e] GC yields based on the reaction R-H + B_2pin_2 → R-Bpin + H_2

pinacol acetal of ketone, partially fluorinated alkanes, and tertiary amines reacted with B_2pin_2 in the presence of Cp*Rh(η^4-C_6Me_6) precatalyst to produce the corresponding pinacolboronate esters in moderate to good yields (Table 3.9). HBpin generated in situ in these reactions reacted with the alkane substrates only in the case of tertiary amines. Thus the yields of the tertiary amine substrates reported in Table 3.9 are based on conversion to dihydrogen, whereas those of other substrates are based on conversion to their corresponding alkylboronate esters.

Heteroatom substrates containing different types of alkane C–H bonds also generated borylated products that contain the Bpin group exclusively at the terminal position: no borylation occurred at the C–H bonds next to heteroatom (N, O, F) moieties. Studies of the electronic effects of heteroatoms in the borylation have shown that functionalization occurs preferentially at the methyl group closer to the electron-withdrawing heteroatom. For example, the reaction of ethyl butyl ether produced a mixture of ethyl-Bpin and butyl-Bpin in a ratio of 1:4 (Scheme 3.8, a). Comparison of this result with the borylation product ratio of *N*,*N*-diethyl-3-aminopentane (Scheme 3.8, b) showed that the electronic effect of nitrogen was less pronounced than that of oxygen, possibly because of the more coordinating nature of basic nitrogen atoms. The borylation result from a 1:1 mixture of ethyl butyl ether and *n*-dibutyl ether indicated that the methyl in the ethyl group was more reactive than those of the butyl groups, and all three butyl groups had similar reactivity (Scheme 3.8, c). Consistent with the borylation results of N- or O-containing alkanes, an equal mixture of (perfluoro-*n*-octyl)ethane and *n*-octane generated a reaction mixture composed of 96 % fluoroalkylboronate ester and 4 % octylboronate ester, suggesting that a methyl group near an electron-withdrawing group is more reactive (Scheme 3.8, d).

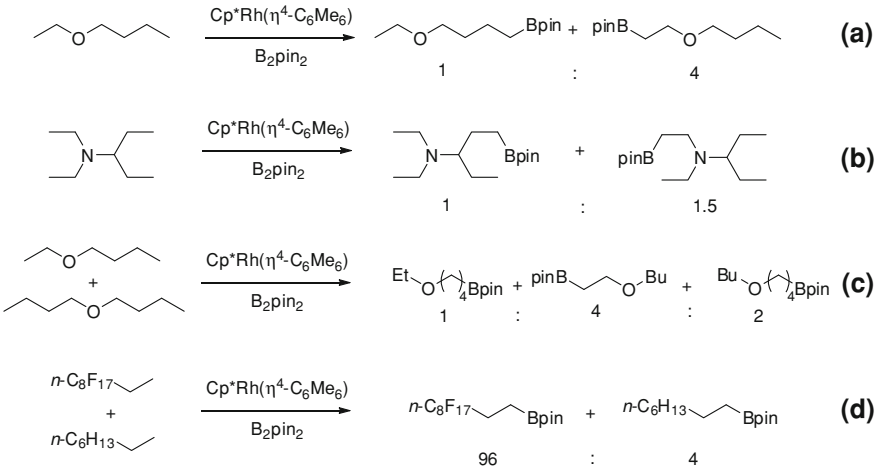

Scheme 3.8 Electronic effects in rhodium-catalyzed borylation of alkane C–H bonds

Alkanes containing hetroatom functionality are more valuable substrates than unfunctionalized alkanes in organic synthesis. Accordingly, it is desirable to use these reagents as limiting agents in a synthetic process involving rhodium-catalyzed C–H borylation. Because the hydrogens in methylene groups are unreactive with rhodium catalysts—a phenomenon demonstrated in the borylation of methylcyclohexane [28]—unfunctionalized cycloalkanes such as cyclohexane and cyclooctane can serve as inert solvents in the catalytic reaction. In general, when organic substrates are used under neat conditions (i.e., present in excess), their yields are higher than when they are used as limiting reagents in cyclohexane solvents. This observation has been rationalized by the results of competing reactions of an unsaturated rhodium–boryl intermediate with in situ generated HBpin by-product and alkane substrates. In a separate experiment, increasing concentration of HBpin in rhodium-catalyzed alkane C–H borylation was found to induce slower rates [37]. Thus, when alkane substrates are used as limiting reagents, the reaction system has a relatively higher concentration of HBpin and its reaction with alkane substrates occurs more slowly and in lower yields.

3.2.2.4 Borylation of Alkanes Catalyzed by Boratabenzene–Rhodium Complexes

Boratabenzene is a six-membered aromatic ring containing a substituted boron. When it is used as a ligand in transition metal complexes, the electronic density of its metal center can be tuned by selection of an appropriate substituent attached to the boron in the ring. For example, a dialkylamino group is a strong donor, whereas a phenyl group is a weak donor. Both of these boratabenzenes are weaker donors than the isoelectronic Cp or Cp* ligands.

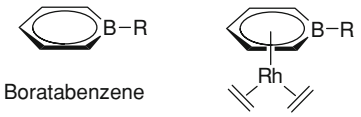

20: R = Ph
21: R = NMe_2

Bazan and co-workers synthesized rhodium complexes of boratabenzene (**20** and **21**) and investigated their catalytic activity in alkane C–H borylation (Eq. 3.3) [38]. The activities of the boratabenzene rhodium complexes were compared with that of **19** using ^{11}B NMR spectroscopy and GC–MS to monitor product formation. When these rhodium complexes catalyzed the C–H borylation of *n*-octane at 50 °C, the order of reactivity was **20** > **21** > **19**. The product yield from **20** was about 20 %, whereas that from **19** was only 7 % after 500 h. Although **20** and **21**

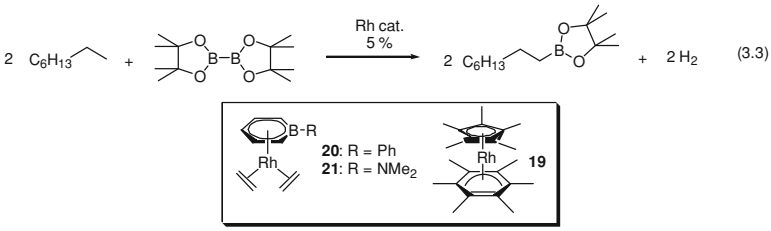

(3.3)

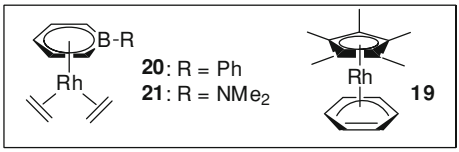

were more active precatalysts than **19** in reactions at 50 °C, they were less stable and became inactive at higher temperatures. Thus, the conversion catalyzed by **19** improved to 50 % over 150 h at 95 °C, whereas **20** and **21** degraded after 24 h and afforded only 15 % conversion at that temperature.

3.2.2.5 Ruthenium-Catalyzed Borylation of Alkanes

Although several transition metal complexes have been reported to catalyze the functionalization of arene and benzylic C–H bonds, rhodium complexes are the most advanced catalysts reported to date for thermal functionalization of unactivated alkane C–H bonds. Encouraged by the fact that $[Cp^*RhCl_2]_2$ catalyzed the functionalization of *n*-octane [36], Hartwig and co-workers tested its ruthenium analog $[Cp^*RuCl_2]_2$ (**22**) and a series of ruthenium complexes in functionalizations of terminal C–H bonds of *n*-octane by reacting them with B_2pin_2

Table 3.10 Ruthenium-catalyzed C–H borylation of *n*-octane

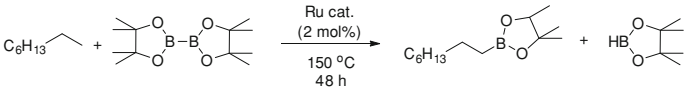

Entry	Ru catalyst	Conversion (%)[a]	Yield (%)[a]
1	$[Cp^*RuCl_2]_2$ (**22**)	99	98 [75][b]
2	$[Cp^*RuCl]_4$ (**23**)[c]	99	65
3	Cp*Ru(H)(COD) (**24**)	80	58
4	Cp*Ru(Cl)(TMEDA) (**25**)	98	95
5	$[Cp^*Ru(OMe)]_2$ (**26**)	65	7
6	Ru(COD)(η^3-2-methylallyl)$_2$ (**27**)	59	7
7	$Ru(acac)_3$ (**28**)	76	4

[a] Determined using GC. Bpin = pinacolboryl; COD = 1,5-cyclooctadiene
[b] Isolated yield in brackets
[c] 5 mol % of Ru used

Table 3.11 Ruthenium-catalyzed C–H borylation of heteroatom-containing substrates

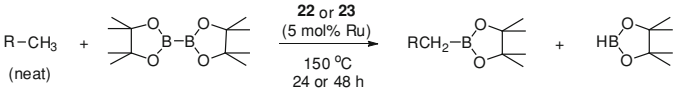

Entry	Product	Catalyst/loading (mol %)	Time (h)	Yield (%)[a]
1	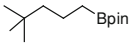	**22**/2.5	48	94
2	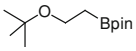	**22**/2.5	48	70
3	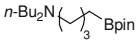	**23**/1.25	24	80
4	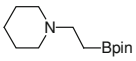	**22**/2.5	48	80
5		**22**/2.5	48	>90

[a] Yields determined using GC

(Table 3.10) [39]. Among the ruthenium complexes screened, **22** was most active and converted *n*-octane and B_2pin_2 to *n*-octylBpin and HBpin quantitatively after 48 h at 150 °C (Table 3.10, entry 1). Unlike the reaction catalyzed by rhodium complexes [28], however, **22** was an inactive precatalyst in the reaction of *n*-octane with HBpin. Not only linear and branched alkanes but also dialkyl ethers, linear and cyclic tertiary amines, and partially fluorinated alkanes were catalyzed by ruthenium complexes **22** and **23** to give borylated products in which functionalization occurred at terminal methyl groups (Table 3.11).

Similar to the regioselectivity of rhodium-catalyzed borylation [28, 36], the sterically less hindered methyl groups were more reactive than more hindered ones in the ruthenium-catalyzed functionalization of branched alkanes (Scheme 3.9, a). The electronic effects of heteroatoms were also observed in the reaction of unsymmetrical dialkyl ethers. The terminal methyl group closer to oxygen atom was more reactive than distant group (Scheme 3.9, b). The similarity in

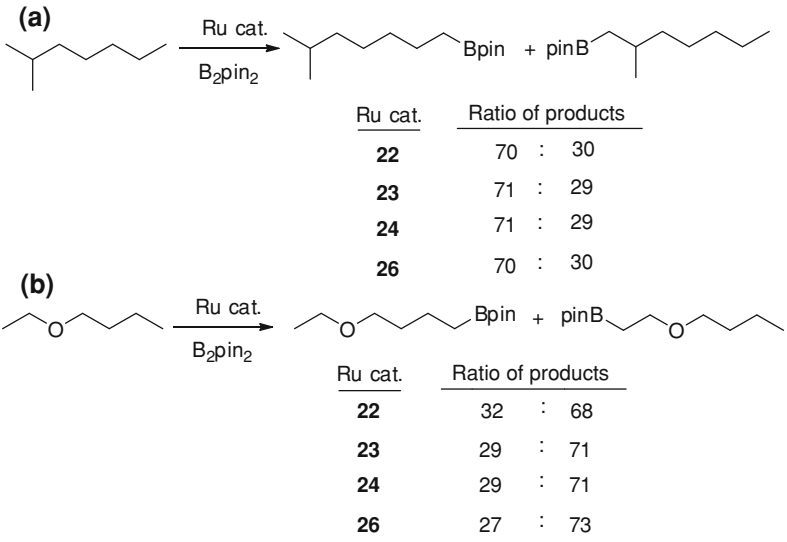

Scheme 3.9 Steric and electronic effects of ruthenium-catalyzed C–H borylation of alkanes

regioselectivity observed for the ruthenium complexes in Scheme 3.9 suggested that they all proceeded through a common active catalyst intermediate.

In contrast to the relative reactivity of rhodium-catalyzed borylation [28], the functionalization at alkane C–H bonds occurred more readily than that of arenes in the ruthenium-catalyzed borylation. Whereas alkane was quantitatively converted to its borylated product in the presence of **22** after 48 h at 150 °C, phenylBpin was obtained in only 20 % yield when benzene was used as a substrate. Surprisingly, further studies revealed that the presence of arene inhibited the catalytic borylation of alkane. When a 35:1 mixture of *n*-octane and benzene was heated for 24 h at 150 °C in the presence of B_2pin_2 and 2.5 mol % of **22**, the yield of *n*-octylBpin decreased to 4 % and phenylBpin was obtained in 25 % yield. Although the exact reason for the inhibition is unknown, the authors speculated that the active ruthenium intermediate was poisoned by forming catalytically inactive $[Cp^*Ru(\eta^6\text{-}C_6H_6)]^+$ from the reaction with benzene [40].

To gain insight into the mechanism of ruthenium-catalyzed borylation, Hartwig and co-workers attempted to prepare a pinacolboryl complex with ruthenium without success. Instead, when they reacted **24** with diaminoboranes, they obtained symmetrically bridging ruthenium–boryl complexes **29a** and **29b** (Eq. 3.4).

Although **29a** and **29b** could not be the exact intermediates in the ruthenium-catalyzed borylation of alkanes with B_2pin_2, they most certainly served as

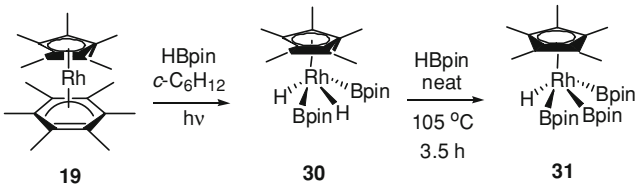

Scheme 3.10 Synthesis of bisboryl– and trisboryl–rhodium complexes

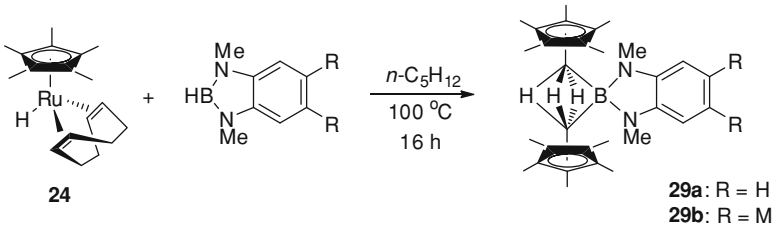

(3.4)

precatalysts in the reaction: 2 mol % of **29b** afforded *n*-octylBpin in 20 % yield after 48 h at 150 °C. Considering that HBpin reagents are, in general, more reactive than aminoborane reagents, the more reactive pinacolboryl analogs of **29a** and **29b** are likely active intermediates in a catalytic cycle.

3.2.3 Mechanistic/Theoretical Studies of Rhodium-Catalyzed C–H Borylation of Alkane

Hartwig, Hall, and co-workers conducted a combination of experimental and theoretical studies on possible rhodium–boryl intermediates and proposed a mechanism for the thermal, catalyzed borylation of alkanes [37]. Photochemical dissociation of labile ligand from Cp*Ru(η^4-C_6Me_6) (**19**) in the presence of excess of HBpin and cyclohexane solvent generated bisboryl–rhodium complex **30** in 95 % yield based on NMR spectroscopic analysis (Scheme 3.10). Removal of C_6Me_6 via sublimation and recrystallization from pentane afforded pure **30** in 86 % yield. Heating bisboryl complex **30** with neat HBpin at 105 °C generated a mixture of trisboryl complex **31** and starting boryl complex **30** in a ratio of 5:1. Evaporation of the remaining HBpin yielded pure **31** in 51 % yield after recrystallization from pentane. Interestingly, the conversion of **30** and HBpin to **31** and dihydrogen, shown in Scheme 3.10, was found to be a reversible process: heating **31** and dihydrogen in cyclohexane solvent for 36 h at 40 °C produced HBpin and a mixture of **30** and **31** in a ratio of 9:1.

Solution NMR and X-ray diffraction data indicated that the two boryl ligands of **30** are positioned in a trans arrangement. These data also suggested that a weak B–H bonding interaction exists in complexes **30** and **31**, which leads to the conclusion that both complexes adopt a four-legged piano stool geometry in which the hydride ligand is positioned closer to one of the boryl groups than the other. Theoretical studies using density functional theory (DFT) calculations supported the conclusions of these experimental results. Because of a partial H–B bonding interaction, when **30** and **31** dissociate ligands under thermal conditions, HBpin is more rapidly extruded than dihydrogen and B_2pin_2 from **30** and **31**, respectively. The dissociation of HBpin generates a 16-electron intermediate that reacts with alkane C–H bonds via either oxidative addition or σ-bond metathesis. The dissociation rate of HBpin from **31** was faster than that of **30**, which translates into the faster reaction rate of **31** compared to **30** with alkane C–H bonds.

DFT calculations were also performed to obtain information on the pathway of the reaction of methane and model rhodium–boryl complexes (**30′** and **31′**), where Cp* was replaced with Cp and pinacolboryl ligand with glycolboryl groups. The studies suggested that the cleaving of alkane C–H bonds by rhodium–boryl complexes and the C–B bond formation in the product occurs through σ-bond metathesis, as shown in Scheme 3.11. Once borane dissociates from bisboryl complex **30′** to give the 16-electron monoboryl hydride complex **32′**, it coordinates to the methane C–H bond to generate intermediate **34′**. Then, **34′** undergoes simultaneous C–H bond cleavage and B–H bond formation with a single transition state structure, **35′-TS**, to give coordinated borane complex **36′**. Complex **36′** forms C–B bond through multicentered transition state **37′-TS** and generates **38′**, which finally dissociates the borylated methane product to give dihydride complex **39′**. Trisboryl complex **31′** likely follows a pathway similar to that of bisboryl complex **30′** (see Scheme 3.11).

Miyamoto and co-workers reported a related theoretical study on the mechanism of alkane C–H borylation catalyzed by rhodium complexes [41]. Based on a model borylation reaction of methane and borane catalyzed by monoboryl trihydride–rhodium complex **45**, the authors proposed a catalytic cycle that involves extrusion of dihydrogen from **45** to form a 16-electron monoboryl hydride complex **46**, which subsequently reacts with methane via an oxidative addition and releases CH_3BH_2 via reductive elimination (Scheme 3.12).

The difference in proposed mechanisms between σ-bond metathesis [37] and oxidative addition/reductive elimination [41] might stem from simplifications made in the computational studies by Miyamoto and co-workers. In their studies, monoboryl trihydride complex **45** is the precursor rhodium complex, which dissociates dihydrogen to generate 16-electron monoboryl complex **46**. This assumption differs from the experimental observations in a related study by Hartwig, Hall, and co-workers: bisboryl dihydride and trisboryl hydride complexes, not monoboryl trihydride complex, were observed in the catalytic borylation of alkane [37]. In both bisboryl– and trisboryl–rhodium complexes, the dissociation of borane, which resulted in 16-electron rhodium intermediates, was much faster than that of dihydrogen. Furthermore, instead of using an alkoxy boryl ligand, such as that experimentally derived from the reaction of HBpin or B_2pin_2, Miyamoto and co-workers used BH_2 as the boryl ligand,

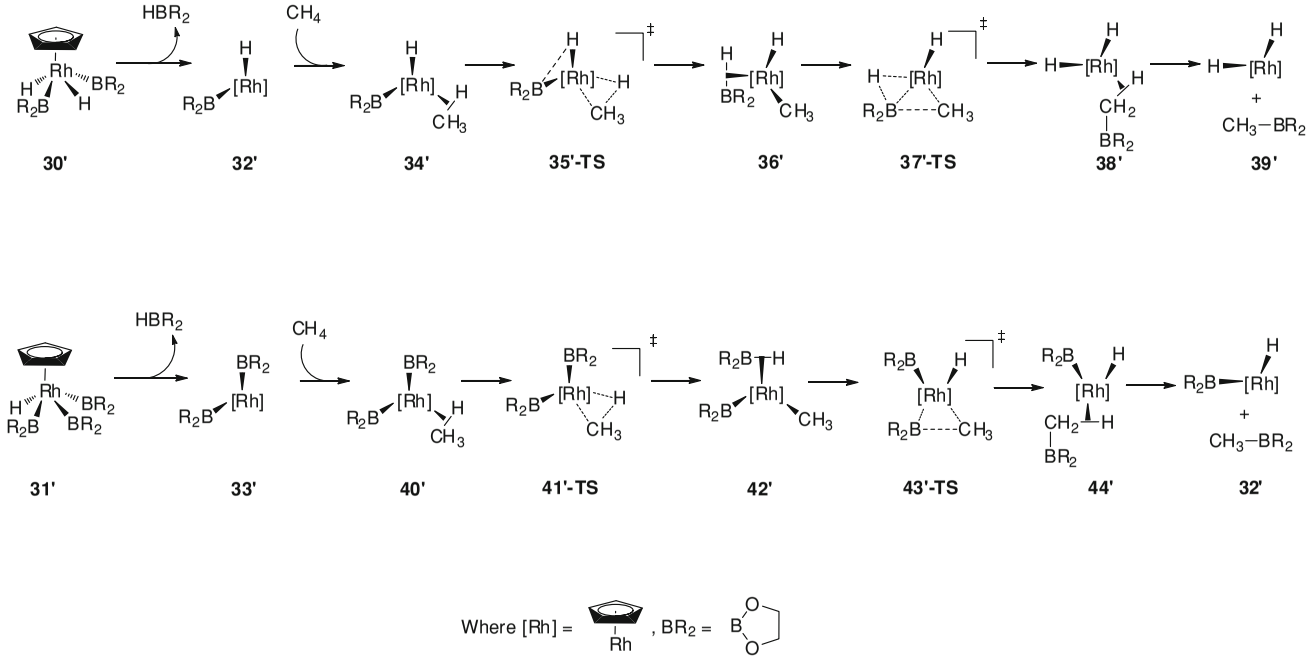

Scheme 3.11 Proposed mechanism of C–H bond cleavage and C–B bond formation studied by DFT calculations

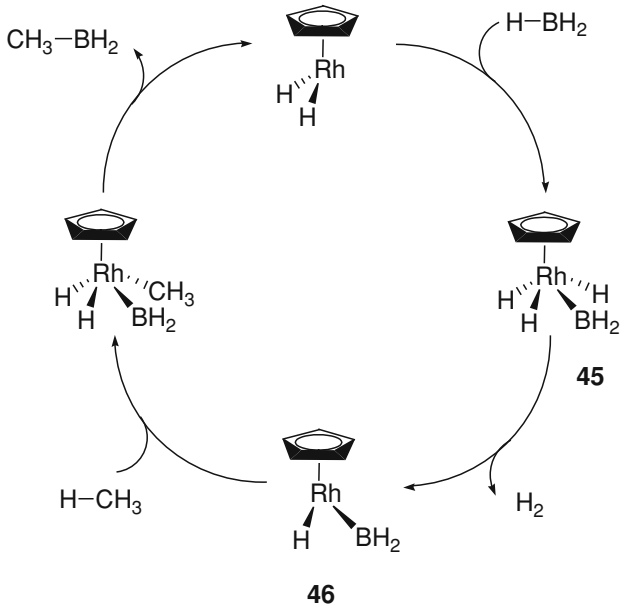

Scheme 3.12 Proposed mechanism of rhodium-catalyzed alkane borylation by Miyamoto and co-workers

which induces much stronger B–H interactions in a hydridoborate complex in the computational model study. From an experimental and theoretical study by Hartwig, Hall, and co-workers [37] the alkoxy groups on the boryl ligand appear to play important roles, modulating the strength of B–H interactions and thus allowing the formation of borylated alkane products through σ-bond metathesis.

The difference in proposed mechanisms between σ-bond metathesis [37] and oxidative addition/reductive elimination [41] might stem from simplifications made in the computational studies by Miyamoto and co-workers. In their studies, monoboryl trihydride complex **45** is the precursor rhodium complex, which dissociates dihydrogen to generate 16-electron monoboryl complex **46**. This assumption differs from the experimental observations in a related study by Hartwig, Hall, and co-workers: bisboryl dihydride and trisboryl hydride complexes, not monoboryl trihydride complex, were observed in the catalytic borylation of alkane [37]. In both bisboryl– and trisboryl–rhodium complexes, the dissociation of borane, which resulted in 16-electron rhodium intermediates, was much faster than that of dihydrogen. Furthermore, instead of using an alkoxy boryl ligand, such as that experimentally derived from the reaction of HBpin or B_2pin_2, Miyamoto and co-workers used BH_2 as the boryl ligand, which induces much stronger B–H interactions in a hydridoborate complex in the computational model study. From an experimental and theoretical study by Hartwig, Hall, and co-workers [37] the alkoxy groups on the boryl ligand appear to play important

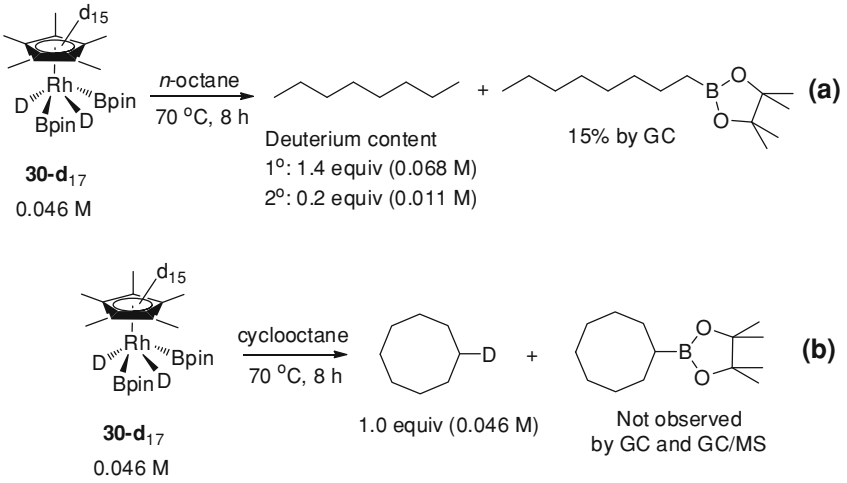

Scheme 3.13 Comparison of reactions of perdeuterated bisboryl–rhodium complex with (a) *n*-octane, and (b) cyclooctane

roles, modulating the strength of B–H interactions and thus allowing the formation of borylated alkane products through σ-bond metathesis.

Experimental and computational studies were conducted to elucidate the potential origin of the exclusive selectivity of rhodium-catalyzed borylation for primary C–H bonds [42]. A hydrogen/deuterium exchange reaction between perdeuterated bisboryl dihydride–rhodium complex **30-d$_{17}$** and *n*-octane suggested that the cleavage of C–H bonds by the 16-electron complex is a reversible process, as evidenced by the incorporation of deuterium from **30-d$_{17}$** into the primary and secondary C–H bonds of *n*-octane. The also revealed that the exchange rate of primary C–H bonds is faster than that of secondary C–H bonds (Scheme 3.13, a). The same exchange reaction with cyclooctane induced the transfer of an appreciable amount of deuterium from **30-d$_{17}$** to secondary C–H bonds, but in contrast to the results of *n*-octane, borylated cyclooctane product was not formed (Scheme 3.13, b). The incorporation of the isotope into the C–H bonds of cyclooctane without formation of cycloalkylboronate ester suggests that although the cleavage of secondary C–H bonds can occur, C–B bond formation from secondary alkyl intermediates is much slower than that from appropriate primary alkyl intermediates. DFT studies support the outcome of this experimental observation: because the transition state for C–B bond formation from secondary alkylboryl intermediate is 7.9 kcal/mol higher than that of C–H bond cleavage, the formation of cycloalkylboronate ester product cannot occur readily.

Based on the results of isotope exchange studies, qualitative kinetic data, and DFT calculations of the reaction between model bisboryl–rhodium complex Cp*Rh(H)$_2$(BO$_2$C$_2$H$_4$) and primary and secondary C–H bonds of propane, Hartwig, Hall, and co-workers concluded that the origin of exclusive selectivity of rhodium-catalyzed borylation for primary C–H bonds results from the cumulative

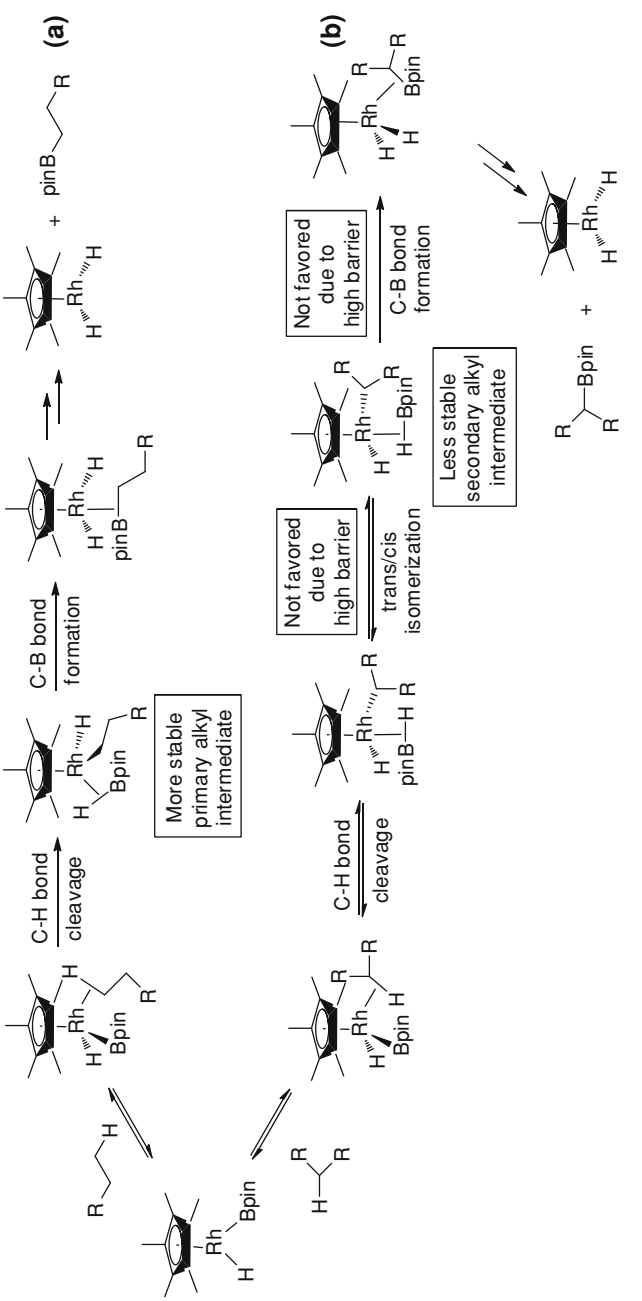

Scheme 3.14 Origin of selectivity in rhodium-catalyzed borylation of (a) primary, and (b) secondary C–H bonds

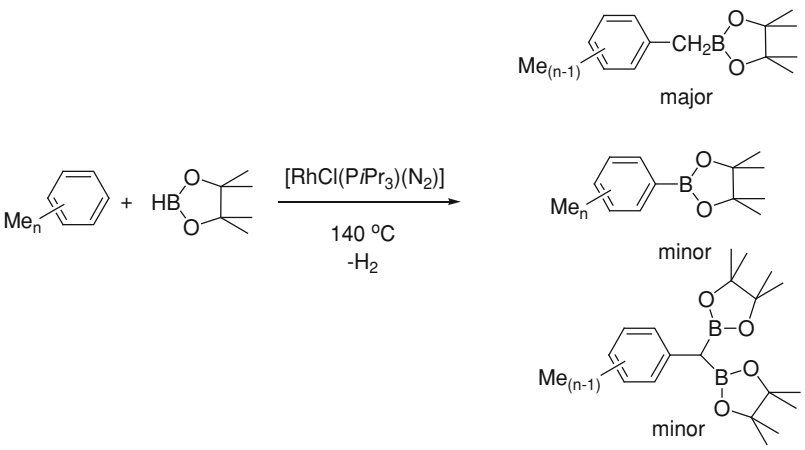

Scheme 3.15 Rhodium-catalyzed benzylic C–H borylation of alkylbenzenes

Table 3.12 Rhodium-catalyzed benzylic C–H borylation of alkylbenzenes with pinacolborane.[a]

Entry	Arene	Time (h)	Additive	Total yield[b]	Product ratio[c]
1	Toluene	14	–	40 (3)	85:3:9:3
2	Toluene	58	–	64 (5)	82:3:11:4
3	Toluene	80	–	69 (7)	81:3:12:4
4	Toluene	14	BHT[d] (50 %)	34 (2)	86:2:9:3
5[e]	Toluene	14	–	48 (4)	83:3:10:4
6	*p*-Xylene	80	–	41[f]	98:2[g]
7	Mesitylene	80	–	17[h]	

[a] Yields and product ratios were determined by GC and based on HBpin in the reaction in Scheme 3.15

[b] Includes $PhCH(Bpin)_2$ for which the yield is shown separately in parenthesis

[c] Product ratio of $PhCH_2Bpin$ to 2-MeC_6H_4Bpin to 3-MeC_6H_4Bpin to 4-MeC_6H_4Bpin determined by GC

[d] 2,6-Di-*tert*-butyl-4-methylphenol (BHT), 50 mol % based on HBpin

[e] 1 Mol % of $[Rh(Cl)(H)(Bpin)(PiPr_3)_2]$ was used as a catalyst

[f] Yield of 4-$MeC_6H_4CH_2Bpin$

[g] Ratio of monoborylated products. The minor isomer (probably 2,5-$Me_2C_6H_3Bpin$) was characterized by GC–MS. Two bisborylated compounds (4:1 by GC) were also observed. The GC ratio of monoborylated to bisborylated products = 95:5

[h] Yield of 3,5-$Me_2C_6H_3CH_2Bpin$. No other isomer was detected. Two bisborylated products and one trisborylated product were also detected by GC–MS

contributions of selective, reversible cleavage of primary C–H bond over secondary C–H bond by the 16-electron intermediate to form a more stable alkyl intermediate and more favorable, irreversible C–B bond formation with the primary alkyl intermediate than the secondary alkyl intermediates (Scheme 3.14).

3.2.4 Catalytic Borylation of Benzylic C–H Bonds

Marder and co-workers reported C–H borylation of alkylbenzenes with an unusual selectivity toward benzylic C–H bonds [43]. When [RhCl(P*i*Pr$_3$)(N$_2$)] was used as a catalyst precursor for the borylation of alkylbenzens and HBpin, the main products were derived from benzylic C–H activation rather than from aromatic C–H activation (Scheme 3.15 and Table 3.12). In the case of the reaction of toluene, bisborylated benzyl product was formed in yields up to 7 % (Scheme 3.15), suggesting that the Bpin group in the benzylic position activated the remaining benzylic C–H bonds for second borylation. The fact that the addition of a radical inhibitor, such as 2,6-di-*tert*-butyl-4-methylphenol, reduced the reactivity or selectivity insignificantly excludes a radical mechanism pathway (Table 3.12, entry 4).

Compared to the thermal borylation catalyzed by the "Cp*Rh" system [28], this new rhodium-catalyzed C–H borylation process works in a different way in terms of selectivity and reactivity. For example, when [{Cp*RhCl$_2$}$_2$] was the precursor catalyst in the borylation of toluene and HBpin to generate the "Cp*Rh" system, the major products were MeC$_6$H$_4$Bpin in an ortho:meta:para ratio of 5:65:30. The benzyl borylated product (PhCH$_2$Bpin) was formed in only trace amounts (<0.5 % based on GC–MS analysis). In addition, although [RhCl(P*i*Pr$_3$)(N$_2$)] catalyzed the borylation of aromatic C–H bonds of benzene and HBpin, its reaction with B$_2$pin$_2$ resulted in no borylated arene products. As well, the borylation reaction of alkane and HBpin did not occur when [RhCl(P*i*Pr$_3$)(N$_2$)] was used as a catalyst precursor.

By reacting the precursor catalyst with 2 equiv of HBpin in the presence of benzene, the same authors isolated a potential intermediate, [Rh(Cl)(H)(Bpin)(P*i*Pr$_3$)(N$_2$)] (**47**), in the catalytic reaction. Rhodium–boryl complex **47** catalyzed the borylation of toluene and HBpin with the same product ratio and a slightly improved yield compared with the precursor catalyst (Table 3.12, entry 5). Based on the results of NMR studies of the isolated rhodium–boryl complex with benzene and toluene [43] and theoretical studies using DFT calculations [44], they proposed a potential reaction mechanism that starts with 14-electron rhodium complex **48** derived from reductive elimination of Cl–Bpin from **47**. Benzylic C–H bond activation to form an η^3-benzyl complex **49** via oxidative addition of toluene and subsequent reductive coupling of two rhodium-hydride bonds gives η^2-dihydrogen complex **50** (Scheme 3.16). Substitution of the dihydrogen ligand with HBpin produces η^2-H–Bpin complex **51**. Oxidative addition of B–H bond of **51** to form η^3-benzyl intermediate **52** and subsequent reductive coupling of B–C bond provide complex **53**. Finally, release of the benzyl borylated product from **53** via reductive elimination regenerates the 14-electron complex **48**, completing the catalytic cycle.

Miyaura and co-workers tested various commercial transition metal catalysts for the borylation of toluene. Although NiCl$_2$, PtCl$_2$(COD), RhCl$_3$, IrCl$_3$, and RuCl$_3$ were inactive, a palladium precursor catalyst with 3 mol % Pd(OAc)$_2$ or PdCl$_2$ and B$_2$pin$_2$ catalyzed borylation at the benzylic C–H bonds of toluene in low yields at 100 °C [11 % yield from Pd(OAc)$_2$ and 33 % yield from PdCl$_2$] [45]. Inspired by

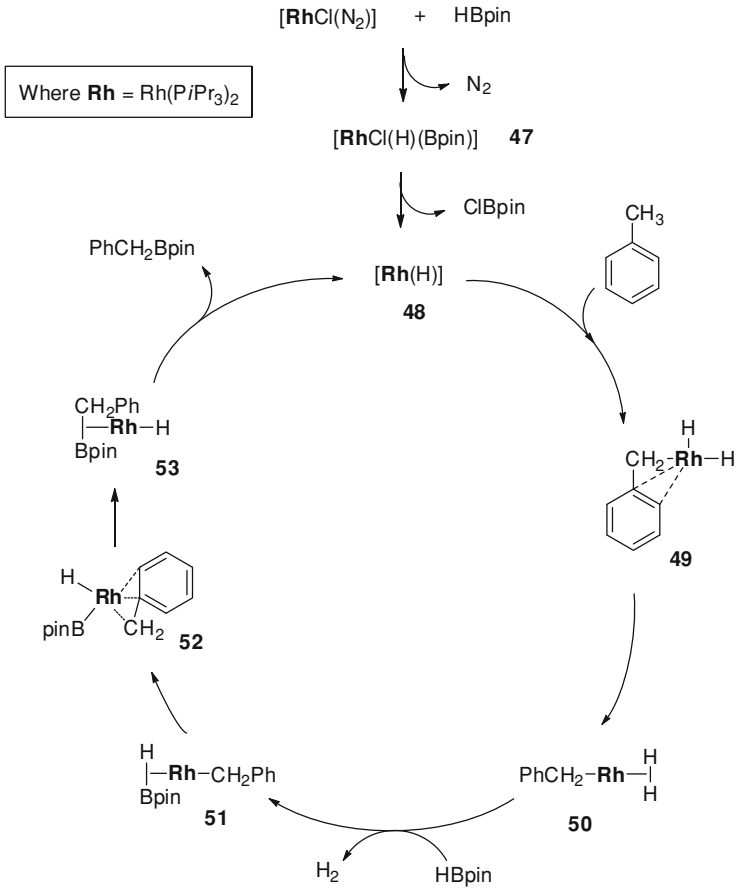

Scheme 3.16 Proposed mechanism of rhodium-catalyzed benzylic C–H borylation

this result, they attempted to improve yields of the palladium-catalyzed borylation reaction by adding phosphine ligands in hopes of preventing the formation of palladium black that was observed during the early stages of the reaction. The addition of the ligand had a negative effect on the reaction rate, however.

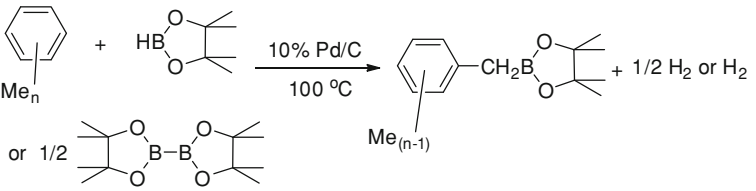

(3.5)

Table 3.13 Palladium-catalyzed benzylic C–H borylation of alkylbenzenes with B_2 pin_2 or HBpin

Entry	Reactant	Product	Yield from B_2pin_2[a] (%)	Yield from HBpin[a] (%)
1		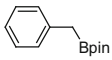	74	52
2		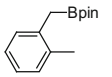	77	–
3		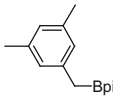	79	–
4	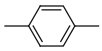	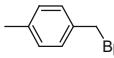	72	51
5		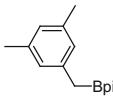	64	45
6[b]		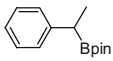	39 15	15 6
7[b]		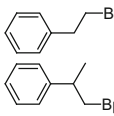	38	13
8[b]	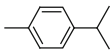	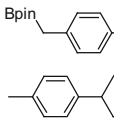	39 9	42 5

[a] Yields were determined by GC based on boron atom in B_2pin_2 or HBpin in Eq. 3.5
[b] 6 mol % catalyst was used

They finally achieved efficient borylation of benzylic alkylbenzene C–H bonds with a palladium on carbon catalyst (10 % Pd/C; 3–6 mol % catalyst loading) that yielded benzyl pinacolborylated products in high yields (Eq. 3.5 and Table 3.13).

Reaction rate studies of toluene and B_2pin_2 at 100 °C revealed that the borylation reaction is a two-step process in which the reaction of toluene with B_2pin_2 is fast and quantitative and the subsequent reaction of toluene with the HBpin formed in situ is slow. Both toluene and polymethylated benzenes were smoothly borylated to give monoborylated products selectively (Table 3.13, entries 1–5). Ethylbenzene yields a mixture of benzylborylated and homobenzyl derivative products (in an approximate 3:1 ratio), in which the latter is presumably formed through isomerization of the benzylpalladium intermediate to a homobenzylpalladium specie via a β-hydride elimination–insertion process (Table 3.13, entry 6). As alkyl substituents become larger, such as isopropyl groups, the borylation gives the homobenzyl derivative product more selectively owing to larger steric hindrance at the benzylic carbon (Table 3.13, entry 7). Although the borylation of

4-isopropytoluene occurs more selectively at the methyl position, it is also accompanied by a small amount of homobenzyl derivative product (Table 3.13, entry 8). Unfortunately, this palladium-catalyzed benzylic C–H borylation does not tolerate the presence of heteroatoms in the alkylbenzenes and affords only low yields even with higher catalyst loading and extended reaction time.

Beller and co-workers investigated the borylation of *o*-xylene with HBpin using various commercially available iridium and rhodium catalyst precursors and P- and N-donor ligands. They discovered that a combination of $[Rh(COD)Cl]_2$, [Rh(COD)acac], or $Rh_2(OAc)_4$ with bipyridyl catalyzed borylation of benzylic C–H bonds selectively (Eq. 3.6) [46].

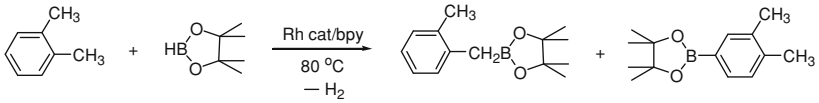

Precursor catalyst	Yield (%) Benzylboryl : Arylboryl
$[Rh(COD)Cl]_2$/2bpy	59 : 4
[Rh(COD)acac]	67 : 3
$Rh_2(OAc)_4$	39 : 3

(3.6)

(3.6)

3.3 Synthetic Applications of Catalytic C–B Bond Formation and Polyolefin Functionalization

Because boronic ester can serve as a useful intermediate in organic synthesis, a sequence reaction of rhodium-catalyzed borylation of alkane C–H bonds and conversion of the boronic ester to other functional groups has been developed (Table 3.14) [36]. Suzuki–Miyaura reactions of crude alkylboronic esters prepared from C–H borylation with 1-bromo-4-*tert*-butylbenzene in the presence of $Pd(dba)_2$ (dba = dibenzylideneacetone), 1,1′-bis(diisopropylphosphino) ferrocene [$Fc(PiPr_2)_2$], and base produced cross-coupled products (Table 3.14, entries 1–3). Oxidation of alkylBpin using basic aqueous hydrogen peroxide gave the corresponding alcohol product in good yield (Table 3.14, entry 4). Alkylboronic esters can be converted to the corresponding alkyl trifluoroborates by reacting with KHF_2 (Table 3.14, entries 5 and 6).

Another synthetic application of alkane C–H borylation is selective and controlled functionalization of polyolefins. Owing to their excellent processability, good chemical stability, and low production cost, polyolefins are the most widely used commercial polymers in the world [47, 48]. Despite those favorable properties, however, the low surface energy of polyolefins caused by a lack of polar

Table 3.14 Sequential conversions of alkane C–H bonds to pinacolboronate ester and other functional groups

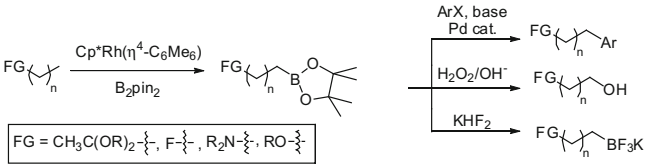

Entry	Reactant	Condition[a]	Product	Yield (%)
1		A,B	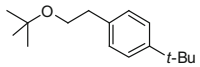	87[b]
2	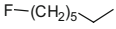	A,C	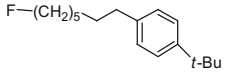	29[b]
3	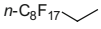	A,B	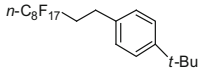	64[b]
4	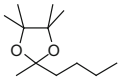	A,D	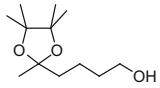	68[c]
5[e]		A,E	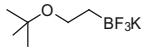	86[c]
6[b]		A,E	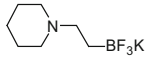	69[c,d]

[a] Conditions: (A) B_2pin_2, 5 mol % Cp*Rh(η^4-C_6Me_6), neat, 150 °C; (B) 1-Bromo-4-*tert*-butylbenzene (2 equiv), CsOH (4 equiv), $Pd(dba)_2$ (10 mol %), and $Fc(PiPr_2)_2$ (10 mol %) in toluene, 100 °C; (C) Same as B but CsF and dimethylformamide were used in place of CsOH and toluene; (D) H_2O_2 and KOH in THF and H_2O; (E) KHF_2 in CH_3OH

[b] Yields calculated by GC

[c] Yields calculated by ^1H NMR

[d] Yields based on the reaction of B_2pin_2 with R–H to form R–Bpin and H_2

functionality has prevented broader application of these materials in applications where compatibility with polar material is critical.

Two approaches to prepare functionalized polyolefins have been pursued: copolymerization with functionalized olefin monomers and postfunctionalization of pre-formed polymers. In the former approach [49–53], the functionalized olefin comonomer usually displays greatly reduced reactivity in polymerization when catalyzed by transition metal complexes. Poisoning of the polymerization catalyst by heteroatom moieties (e.g., nitrogen and oxygen) in the comonomer results in functionalized polyolefins with low molecular weights and a low concentration of functionality. In the latter approach [54, 55], free radical–mediated polymer modification has been dominantly used because of a lack of reactive sites in polyolefins. The free radical pathway, however, is accompanied by side reactions that can cleave and couple polymer chains and, as a result, change the mechanical properties of the functionalized polymer materials.

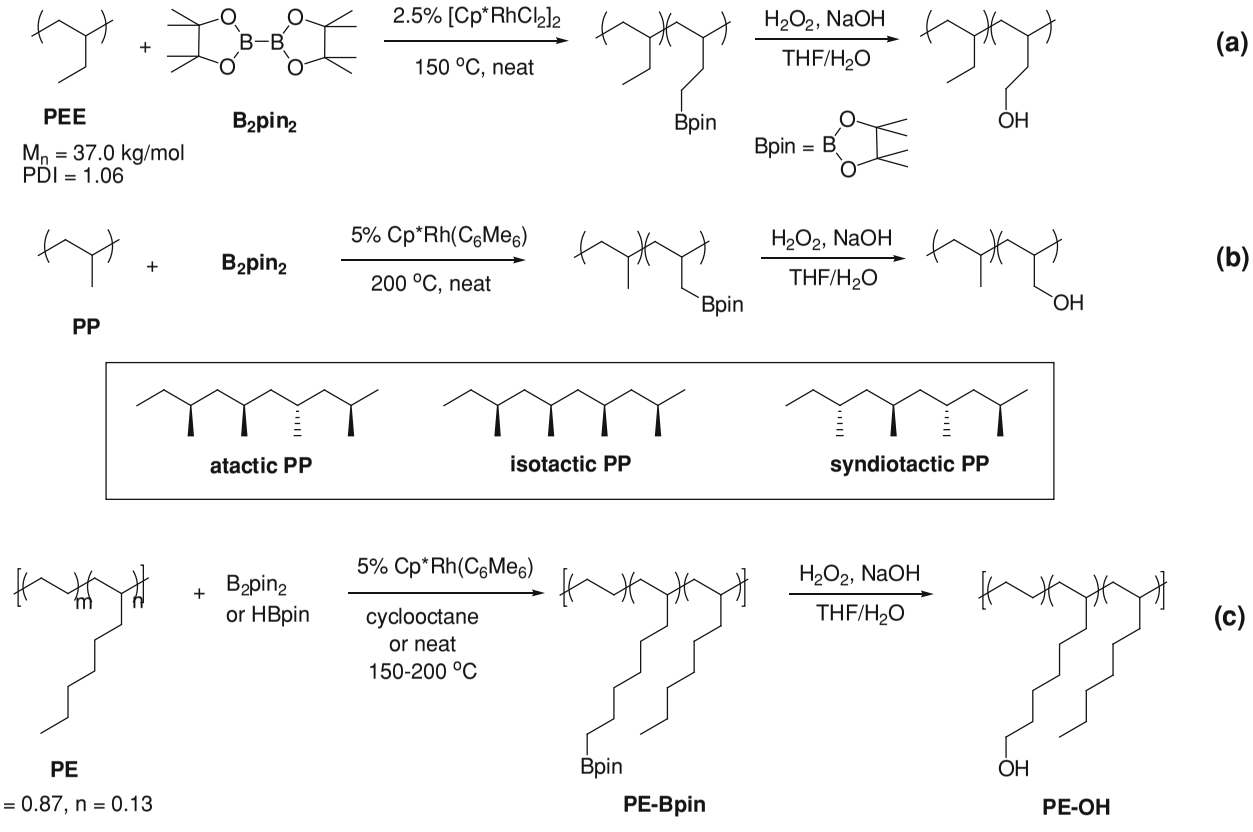

Scheme 3.17 Regiospecific functionalization of polyolefins using rhodium-catalyzed borylation of alkane C–H bonds

Table 3.15 Regioselective C–H functionalization of isotactic poly(1-butene) with bis(pinacolato)diboron.[a]

Entry	Ratio[b]	**PB-Bpin** $M_n x10^{-3}$ (PDI)[c]	**PB-OH** $M_n x10^{-3}$ (PDI)[c]	**PB-OH** OH mol %[d]	**PB-OH** Contact angle
1	0.02	51.5 (5.6)	55.0 (5.0)	1.8	104.4°
2	0.03	53.9 (5.1)	61.9 (5.6)	2.7	102.7°
3	0.05	58.7 (4.7)	61.6 (5.3)	3.5	102.0°
4	0.07	64.9 (5.9)	63.1 (5.4)	4.6	100.5°
5	0.15	70.2 (5.9)	69.0 (5.6)	7.7	100.4°
6	0.30	68.9 (5.3)	68.9 (5.6)	11.0	93.9°
7	0.45	73.0 (4.6)	74.4 (5.9)	15.3	92.2°
8	0.60	75.4 (3.7)	77.6 (5.9)	18.6	90.9°

[a] Starting material: isotactic poly(1-butene) (PB) (M_n = 51.6 kg/mol, PDI = 4.9)
[b] Initial ratio of bis(pinacolato)diboron/polymer repeating unit
[c] M_n in kg/mol and polydispersity index (PDI) measured using size exclusion chromatography at 40 °C relative to polystyrene standards. THF was used as eluent
[d] Mol % of $–CH_2OH$ relative to the terminal methyl group of the side chains of PB-OH
[e] Contact angles of other polymers: PB (105.6°), 6.4 % *t*-butylacrylate-grafted PB-*g*-PtBA (100.7°), 6 % acrylic acid-grafted PB-*g*-PAA (96.8°)

Hartwig, Hillmyer, and co-workers reported the first regioselective functionalization of a model polyolefin, polyethylethylene (PEE), using the rhodium-catalyzed thermal borylation of alkane C–H bonds (Scheme 3.17a) [56]. Only the terminal C–H bonds of the ethyl side chain were borylated under the reaction conditions without affecting the internal C–H bonds of the polymer chain. Later, they successfully applied the new polymer functionalization method to crystalline commercial polyolefins, polypropylene (PP) and low-density linear polyethylene (PE) (Scheme 3.17b–c) [57, 58]. Compared to the functionalization of PEE, the C–H borylation of PP produced a much lower concentration (max. 1.5 mol %) of the functionalized side chain because of greater steric hindrance around the methyl side group. The same authors used 1 % hydroxy-functionalized isotactic PP as a macroinitiator for ring-opening polymerization of ε-caprolactone and prepared graft copolymers of isotactic PP and polycaprolactone. The graft copolymers acted as an effective compatibilizer for composites of isotactic PP and polycaprolactone and reduced phase separation of the two immiscible polymers. Major advantages of polyolefin functionalization based on rhodium-catalyzed C–H borylation over conventional free radical–mediated methods are that (a) the functionalization site is highly regioselective in the polymer chain, occurring only at the primary C–H bonds of alkyl side chains, and (b) it does not induce deleterious side reactions that can negatively affect polymer chain length, maintaining average molecular weights and molecular weight distributions of the precursor polymer.

Recently, Bae and co-workers synthesized hydrophilic graft copolymers of polyolefins using a combination of rhodium-catalyzed C–H borylation and controlled radical polymerization of polar vinyl monomers (Scheme 3.18) [59, 60]. The catalytic C–H borylation of isotactic poly(1-butene) (PB) with B_2pin_2

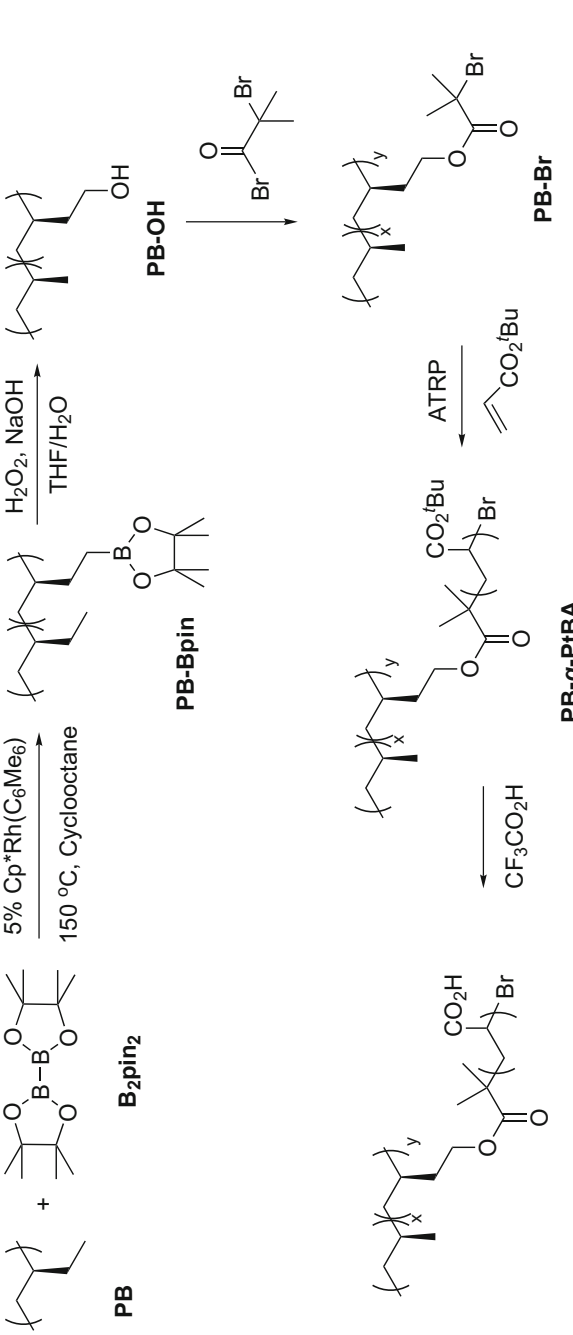

Scheme 3.18 Synthesis of graft copolymers of isotactic poly(1-butene)

produced up to 19 mol % of functionalized side chains without causing significant deleterious side reactions (Table 3.15). The polarity of the functionalized PBs was studied using water contact angle measurements. As more hydroxy group was incorporated, the contact angle systematically decreased, indicating an increase in polymer hydrophilicity. The 1.8 mol % hydroxy-functionalized polymer (PB-OH; see Scheme 3.18) was further reacted with 2-bromoisobutyl bromide to generate a macroinitiator (PB-Br). An amphiphilic graft copolymer (PB-*g*-PAA) was synthesized via controlled atom radical polymerization of *t*-butylacrylate from the macroinitiator and subsequent deprotection of the *t*-butyl group with trifluoroacetic acid.

3.4 Conclusion and Challenges

During the last 15 years significant progress has been made in the transformation of alkane C–H bonds to C–B bonds using transition metal complexes. Among the metal complexes reported, Cp*Rh complexes are the most advanced catalysts in direct thermal borylation of alkane C–H bonds. Through computational studies using DFT calculation and kinetic experiment results, researchers have gained considerable mechanistic insight into these reactions. The preferred pathway involves cleavage of terminal alkane C–H bonds by a reactive 16-electron intermediate via σ-bond metathesis. The abundance of alkane reagents, the high regioselectivity toward sterically less hindered primary C–H bonds, and the versatility of organoboron compounds in organic synthesis are attractive features of the catalytic C–B bond formation reaction. The current processes of alkane C–H bond borylation, however, still need significant improvement in substrate scope, reaction conditions, and catalyst activity before they can be adopted as practical organic synthetic methods. Broad tolerance of functional groups and mild reaction conditions would allow many types of functionalized alkanes to be used as substrates and be converted to more valuable products in fewer synthetic steps. Nevertheless, considering the rapid development of catalytic C–B bond formation directly from alkane C–H bonds in a short period of time, further progress in this field will eventually lead to more effective and economic uses of alkanes as raw materials.

Acknowledgments The author acknowledges financial support from National Science Foundation and Nevada Renewable Energy Consortium.

References

1. Olah GA, Prakash GKS, Sommer J (1985) Superacids. Wiley, New York
2. Olah GA, Molnar A (1995) Hydrocarbon Chemistry. Wiley, New York
3. Labinger JA, Bercaw JE (2002) Nature 417:507–514
4. Crabtree RH (2001) J Chem Soc Dalton Trans 2437–2450

5. Arndtsen BA, Bergman RG, Mobley TA, Peterson TH (1995) Acc Chem Res 28:154–162
6. Sakakura T, Tanaka M (1987) J Chem Soc Chem Commun 758–759
7. Sakakura T, Sodeyama T, Sasaki K, Wada K, Tanaka MJ (1990) J Am Chem Soc 112: 7221–7229
8. Rosini GP, Zhu K, Goldman AS (1995) J Organomet Chem 504:115–121
9. Crabtree RH, Mihelcic JM, Quirk JM (1979) J Am Chem Soc. 101:7738–7740
10. Jensen CM (1999) Chem Commun 2443–2449
11. Xu WW, Rosini GP, Gupta M, Jensen CM, Kaska WC, Krogh-Jespersen K, Goldman AS (1997) Chem Commun 2273–2274
12. Liu F, Goldman AS (1999) Chem Commun 655–656
13. Liu F, Pak EB, Singh B, Jensen CM, Goldman AS (1999) J Am Chem Soc 121:4086–4087
14. Haenel MW, Oevers S, Angermund K, Kaska WC, Fan HJ, Hall MB (2001) Angew Chem Int Ed 40:3596–3600
15. Ramachandran PV, Brown HC (eds) (2001) Organoboranes for syntheses American Chemical Society, Washington, vol. 783
16. Pelter A, Smith K, Brown HC (1988) Borane reagents. Academic, London
17. Ishiyama T, Miyaura N (2003) J Organomet Chem 680:3–11
18. Mkhalid IAI, Barnard JH, Marder TB, Murphy JM, Hartwig JF (2010) Chem Rev 110: 890–931
19. Rablen PR, Hartwig JF (1996) J Am Chem Soc 118:4648–4653
20. Sasaki S, Kikuno T (1997) Inorg Chem 36:226–229
21. Waltz KM, He X, Muhoro C, Hartwig JF (1995) J Am Chem Soc 117:11357–11358
22. Waltz KM, Hartwig JF (1997) Science 277:211–213
23. Waltz KM, Hartwig JF (2000) J Am Chem Soc 122:11358–11369
24. Webster CE, Fan Y, Hall MB, Kunz D, Hartwig JF (2003) J Am Chem Soc 125:858–859
25. Lam WH, Lin Z (2003) Organometallics 22:473–480
26. Chen H, Hartwig JF (1999) Angew Chem Int Ed 38:3391–3393
27. Hoyano J, Graham W (1982) J Chem Soc Chem Commun 27–28
28. Chen H, Schlecht S, Semple TC, Hartwig JF (2000) Science 287:1995–1997
29. Gibert TM, Hollander FJ, Bergman RG (1985) J Am Chem Soc 107:3508–3516
30. Maitlis PM, Moseley K, Kang JW (1970) J Chem Soc A 2875–2883
31. Lenges CP, White PS, Brookhart M (1999) J Am Chem Soc 121:4385–4396
32. Ruiz J, Mann BE, Spencer CM, Taylor BF, Maitlis PM (1987) J Chem Soc Dalton Trans 1963–1966
33. Bowyer WJ, Merkert JW, Geiger WE, Rheingod AL (1989) Organometallics 8:191–198
34. Kawamura K, Hartwig JF (2001) J Am Chem Soc 123:8422–8423
35. Tse MK, Cho JY, Smith MR III (2001) Org Lett 3:2831–2833
36. Lawrence JD, Takahashi M, Bae C, Hartwig JF (2004) J Am Chem Soc 126:15334–15335
37. Hartwig JF, Cook KS, Hapke M, Incarvito CD, Fan Y, Webster CE, Hall MB (2005) J Am Chem Soc 127:2538–2552
38. Woodmansee DH, Bu X, Bazan GC (2001) Chem Commun 619–620
39. Murphy JM, Lawrence JD, Kawamura K, Incarvito C, Hartwig JF (2006) J Am Chem Soc 128:13684–13685
40. Suzuki H, Omori H, Lee DH, Yoshida Y, Fukushima M, Tanaka M, Moro-oka Y (1994) Organometallics 13:1129–1146
41. Wan X, Wang X, Luo Y, Takami S, Kubo M, Miyamoto A (2002) Organometallics 21: 3703–3708
42. Wei C, Jiménez-Hoyos CA, Videa MF, Hartwig JF, Hall MB (2010) J Am Chem Soc 132:3078–3091
43. Shimada S, Batsanov AS, Howard JAK, Marder TB (2001) Angew Chem Int Ed 40: 2168–2171
44. Lam WH, Lam KC, Lin Z, Shimada S, Perutz R, Marder TB (2004) J Chem Soc Dalton Trans 1556–1562
45. Ishiyama T, Ishida K, Takagi J, Miyaura N (2001) Chem Lett 1082–1083

46. Mertins K, Zapf A, Beller M (2004) J Mol Catal A Chem 207:21–25
47. Coates GW (2000) Chem Rev 100:1223–1252
48. Imanishi Y, Naga N (2001) Prog Polym Sci 26:1147–1198
49. Berkefeld A, Mecking S (2008) Angew Chem Int Ed 47:2538–2542
50. Ittel SD, Johnson LK, Brookhart M (2000) Chem Rev 100:1169–1203
51. Boffa LS, Novak BM (2000) Chem Rev 100:1479–1493
52. Chung TC (2002) Prog Polym Sci 27:39–85
53. Yashuda H, Ihara E (1997) Adv Polym Sci 133:53–101
54. Moad G (1999) Prog Polym Sci 24:81–142
55. Boaen NK, Hillmyer MA (2005) Chem Soc Rev 34:267–275
56. Kondo Y, Garcia-Cuadrado D, Hartwig JF, Boaen NK, Wagner NL, Hillmyer MA (2002) J Am Chem Soc 124:1164–1165
57. Bae C, Hartwig JF, Boaen Harris NK, Long RO, Anderson KS, Hillmyer MA (2005a) J Am Chem Soc 127:767–776
58. Bae C, Hartwig JF, Chung H, Harris NK, Switek KA, Hillmyer MA (2005b) Angew Chem Int Ed 44:6410–6413
59. Shin J, Chang AY, Brownell LV, Racoma IO, Ozawa CH, Chung H–Y, Peng S, Bae C (2008) J Polym Sci Part A Polym Chem 46:3533–3545
60. Jo TS, Yang M, Brownell LV, Bae C (2009) J Polym Sci Part A Polym Chem 47:4519–4531

Chapter 4
Alkane Dehydrogenation

Michael Findlater, Jongwook Choi, Alan S. Goldman and Maurice Brookhart

Abstract The dizzying array of disparate applications of alkenes has established them as perhaps the most important class of feedstocks in the chemical industry. The dehydrogenation of alkanes, the most abundant and inexpensive hydrocarbons, is a simple and attractive route for producing alkenes. This chapter addresses the challenges presented by the activation of strong C–H bonds present in alkanes and the ongoing need for the development of efficient and selective methods of dehydrogenation. In particular, the use of homogeneous dehydrogenation as an alternative to high temperature heterogeneous processes is discussed. A major focus of this review is on the deployment of so called 'pincer-ligand' based catalyst systems for use in transfer dehydrogenations. The development and use of supported pincer catalysts is considered.

4.1 Introduction

Alkenes are versatile feedstocks which are readily transformed into an array of value-added fine chemicals and pharmaceutical intermediates, polymers, detergents, lubricants and fuels. Alkanes are the most abundant and inexpensive

M. Findlater · M. Brookhart (✉)
Department of Chemistry, University of North Carolina at Chapel Hill,
Chapel Hill, NC 27599, USA
e-mail: mbrookhart@unc.edu

J. Choi · A. S. Goldman (✉)
Department of Chemistry and Chemical Biology,
Rutgers, The State University of New Jersey,
New Brunswick, NJ 08903, USA
e-mail: alan.goldman@rutgers.edu

P. J. Pérez (ed.), *Alkane C–H Activation by Single-Site Metal Catalysis*,
Catalysis by Metal Complexes 38, DOI: 10.1007/978-90-481-3698-8_4,
© Springer Science+Business Media Dordrecht 2012

hydrocarbons available and thus one of the most attractive routes for producing alkenes is through dehydrogenation. However, this conceptually simple process poses difficulties since it requires the activation of strong carbon-hydrogen bonds. As alkanes often possess numerous carbon-hydrogen bonds, *selective* dehydrogenation adds a further level of challenge.

Heterogeneous dehydrogenation catalysts are used on large scales in industrial processes [1]. For example, styrene is produced from ethyl benzene, and ethylene and propylene are produced from low molecular weight alkanes. These processes are run at very high temperatures (500–900 °C) where the favorable entropy for loss of hydrogen offsets the unfavorable enthalpy of dehydrogenation (typically ca. 28–30 kcal/mol). Carbon–carbon bond cleavage (cracking) and olefin isomerization occur during such processes and selectivities are poor. Thus these processes are normally confined to simple systems such as ethyl benzene.

This chapter is focused on homogeneous alkane dehydrogenations which operate at temperatures far below those used in heterogeneous processes. Low temperature processes are achieved, for the most part, by using a transfer dehydrogenation scheme generally illustrated in Eq. 4.1. These reactions are normally close to thermoneutral and with the proper selection of acceptor they can be exothermic and equilibria can lie significantly to the right as will be discussed later in detail.

$$R\text{-}CH_2\text{-}CH_2\text{-}R' + A \rightleftharpoons RHC{=}CHR' + AH_2 \qquad (4.1)$$

The potential for good selectivity and the low energy requirements are attractive features of these homogeneous reactions. A major disadvantage is the requirement for an acceptor molecule. Of course, the challenge of activating strong carbon-hydrogen bonds under mild conditions is significantly greater than at the high temperatures used in heterogeneous systems. Based on advances in C–H activation reactions, as described in many chapters in this book, options for designing and developing new dehydrogenation catalysts continue to expand.

Reviews covering aspects of alkane dehydrogenation have appeared [2–6].

4.2 Early Work

Crabtree et al. [7] first reported stoichiometric alkane dehydrogenation in 1979, using the cationic Ir(III) complex, $(IrH_2(acetone)_2L_2)^+$, **1**, (L = PPh_3). Dehydrogenation of hydrocarbons was established through the reaction of **1** with several cyclic monoene complexes. For example, reaction of cyclohexene with **1** yields (1,3-cyclohexadiene)IrL_2^+ (Eq. 4.2). More significantly, Crabtree observed that saturated cycloalkanes react with **1** in the presence of t-butylethylene (TBE) as a hydrogen acceptor to yield unsaturated complexes. Cyclopentane yields the cyclopentadienyl hydride complex (Eq. 4.3), and cyclooctane yields a 1,5-cyclooctadiene complex (Eq. 4.4).

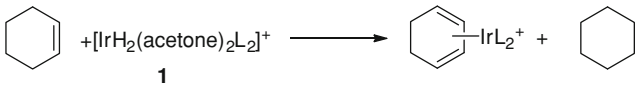

(4.2)

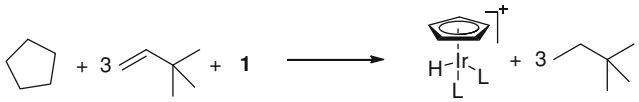

(4.3)

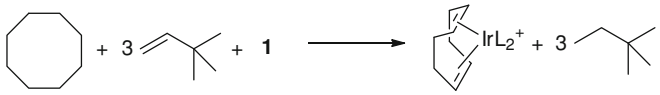

(4.4)

Crabtree noted that TBE was "indispensible" as a hydrogen acceptor in these systems. Less bulky olefins such as ethylene or styrene formed stable iridium complexes which were unreactive with alkanes. TBE was to become widely used as an acceptor. It is sufficiently bulky that it does not deactivate catalysts through strong coordination, it lacks allylic hydrogens so no allyl complexes can irreversibly form and no isomers can be generated via hydrogen migrations. Crabtree ruled out operation of this catalysis through a heterogeneous process. Similar stoichiometric transformations of cycloalkanes were subsequently reported by Felkin and coworkers [8, 9] using $ReH_7(PPh_3)_2$.

The first systems for catalytic homogeneous dehydrogenations of alkanes were discovered independently by the Felkin [10–12] and Crabtree groups [13, 14]. Felkin showed that the previously studied systems, $(PAr_3)_2ReH_7$, catalyzed the transfer dehydrogenation of cyclic alkanes using TBE as acceptor. The [P(*p*-$FC_6H_4)_3$]-based catalyst (**2**) proved most reactive. Remarkably, dehydrogenation occurs at temperatures as low as 30 °C, albeit with low turnover numbers (1.6 TOs in 10 min). The turnover number increases to nine when reactions are run at 80 °C under the same conditions (Eq. 4.5) [10]. Dehydrogenation of methylcyclohexane yielded three of the possible four monoenes, with none of the thermodynamically stable isomer, 1-methylcyclohexene. The isomer ratios were dependent on the phosphine used. These results ruled out both the involvement of Re colloids and of radicals.

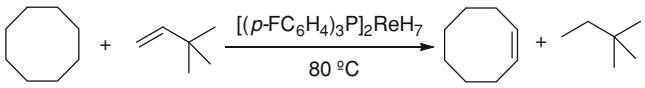

TON = 9

(4.5)

In a follow-up study Felkin et al. [11] reported a series of iridium and ruthenium hydrides which were more productive than the rhenium pentahydride system. In the transfer dehydrogenation of cyclooctane with TBE at 150 °C, the [(*p*-$FC_6H_4)_3P]_3RuH_4$ catalyst afforded 50 TOs, the [(*p*-$FC_6H_4)_3P]_2IrH_5$ system 35 TOs and the ($^i Pr_3P)_2IrH_5$ (**3**) system 70 TOs (Eq. 4.6).

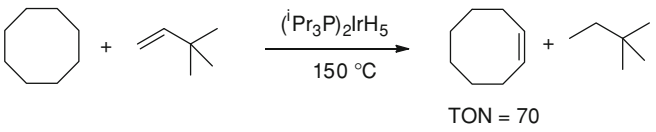

(4.6)

Subsequent catalytic studies by Crabtree et al. [14, 15] employed neutral Ir(III) carboxylate complexes, $IrH_2(\eta^2\text{-}O_2CCF_3)(PR_3)_2$ (R = *p*-FC_6H_4 and cyclohexyl (Cy)). Both thermal and photochemical procedures were reported. In the case of the $(p\text{-}FC_6H_4)_3P$-substituted catalyst 30 TOs were achieved thermally using the cyclooctane/TBE system at 150 °C. Analysis of the solution of the deactivated catalyst revealed formation of 1 equivalent of C_6H_5F indicating that catalyst decay occurred via P–C bond cleavage. Photolysis-driven dehydrogenations of cyclic and linear alkanes could be carried out at 25 °C. While turnovers were greater in the presence of TBE as acceptor, Crabtree noted that dehydrogenation could be effected with no added acceptor and that the energy of photolysis provides the driving force to overcome the unfavorable reaction energy. For example, photolysis of $IrH_2(\eta^2\text{-}O_2CCF_3)(PCy_3)_2$ (**4**) in the presence of cyclooctane yields cyclooctene (7 TOs, Eq. 4.7)

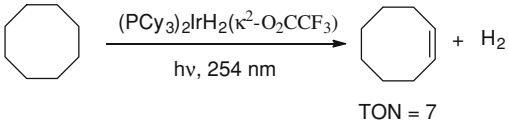

(4.7)

The thermal and photochemical mechanisms proposed [14, 15] for these systems are shown in Scheme 4.1. Transfer of hydrogen from $IrH_2(\eta^2\text{-}O_2CCF_3)L_2$ is presumed to occur via η^2 to η^1 conversion of the carboxylate ligand followed by coordination of TBE. Insertion followed by reductive elimination and loss of 2,2-dimethylbutane results in generation of the unsaturated $IrL_2(O_2CCF_3)$ complex which is capable of activating alkanes via C–H insertion (the microscopic reverse of the previous reductive elimination reaction). Photochemical activation is assumed to induce loss of hydrogen and lead directly to the unsaturated complex $IrL_2(O_2CCF_3)$.

These early studies of Crabtree and Felkin established the cyclooctane/TBE system as the benchmark system used to screen catalysts for transfer dehydrogenation (Eq. 4.8). As noted earlier TBE is bulky, coordinates weakly to transition metal centers, and lacks reactive allylic hydrogens. Furthermore the transfer reaction has a substantial negative enthalpy (ca. −7 kcal/mol) due to the low enthalpy of dehydrogenation of cyclooctane (+22.4 kcal/mol) related to strain in the 8-membered ring. The equilibrium of Eq. 4.8 therefore lies far to the right, eliminating concerns about reversibility.

In the late 1980s, following reports of photochemical alkane carbonylation $RhCl(CO)(PMe_3)_2$ (**5**) [16, 17], the groups of Tanaka [18], Saito [19], and Goldman [20] independently reported that photolysis of **5** in the presence of alkanes resulted

Scheme 4.1 Mechanistic proposal for the alkane dehydrogenation reaction catalyzed by complexes 3–4

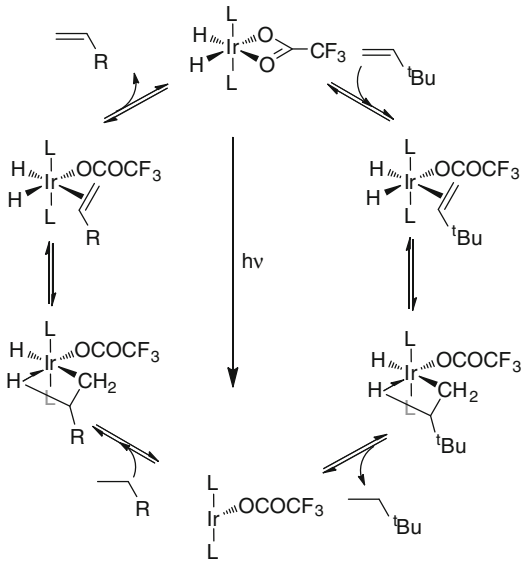

in catalytic formation of alkenes and hydrogen in the absence of acceptor. Linear as well as cyclic alkanes were viable substrates. Relatively low temperatures were employed

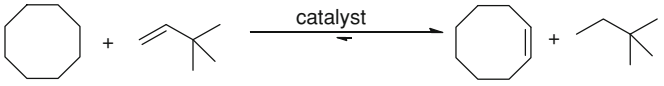

(4.8)

ranging from 25 to 90 °C. Turnover numbers were 1–2 orders of magnitude higher than those observed with earlier studies of iridium and rhenium catalysts. For example, it was observed that irradiation of a 0.4 mM solution of **5** in cyclooctane with a 500-W Hg-arc lamp yielded cyclooctene at a turnover rate of 300/h. Total turnovers up to 5,000 were achieved [20, 21].

A detailed mechanistic investigation of this photocatalytic reaction revealed several unique features. Two possible mechanisms were proposed, differing in the order of loss of cyclooctene and hydrogen from the 18-electron cyclooctene dihydride Rh(III) intermediate (**A**) (the mechanistic scheme in which cyclooctene first dissociates is shown in Scheme 4.2). The key feature of either variant is that the only photochemical step is loss of CO from **5**, and that this step is part of the catalytic cycle and does not merely serve to generate an unsaturated metal complex to provide an entry into the cycle. The energy needed to drive the highly endothermic dehydrogenation is derived from re-formation of the photochemically cleaved Rh-CO bond, which serves to displace H_2 as shown in Scheme 4.2 (in the alternative pathway, CO displaces cyclooctene after H_2 is dissociated from **A**) [20, 21].

In later studies it was shown [22, 23] that the key 14-electron intermediate of the photolysis reaction (Scheme 4.2), $RhCl(PMe_3)_2$, could be generated thermochemically

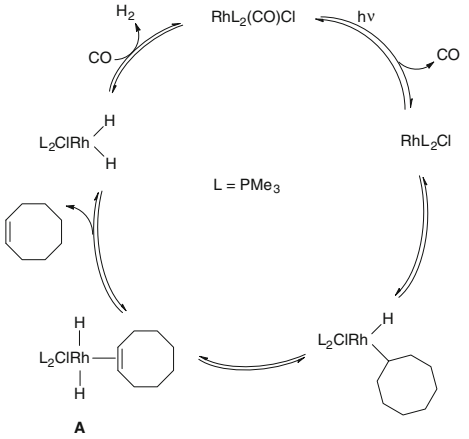

Scheme 4.2 Mechanistic proposal for the photochemically induced alkane dehydrogenation reaction catalyzed by complex $Rh(PMe_3)_2Cl(CO)$ **(5)**

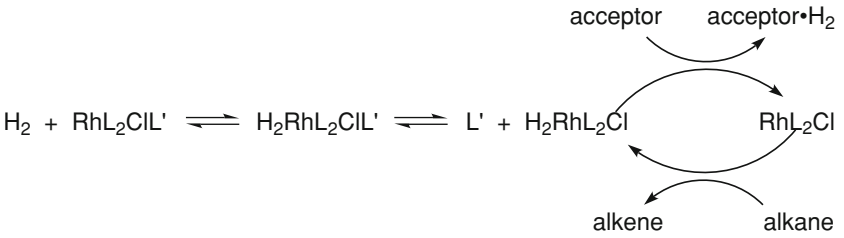

Scheme 4.3 Mechanistic proposal for the thermal alkane dehydrogenation reaction catalyzed by complex $Rh(PR_3)_2Cl(CO)$ (5)

rather than photochemically by the reaction of dihydrogen with $RhCl(CO)(PMe_3)_2$ in the presence of acceptor olefin. Initially the dihydride $H_2RhCl(PMe_3)_2$ is generated. Hydrogenation of the acceptor olefin then yields $RhCl(PMe_3)_2$. Thus, the sequence shown in Scheme 4.3 can be used to carry out transfer dehydrogenation; remarkably, rates are greatly accelerated under high hydrogen pressure. For example, a solution of 0.20 mM **5** and 3.8 M norbornene (as acceptor) in cyclooctane (100 °C) under 1,000 psi hydrogen produces 0.19 M cyclooctene product (950 TOs) in 15 min [22].

Species containing ligands more labile than CO, $RhCl(L)(PMe_3)_2$ ($L = P^iPr_3$, PCy_3), and the dimer $[ClRh(PMe_3)_2]_2$ are even more reactive [23]. In experiments conducted at 50 °C in cyclooctane using $RhCl(P^iPr_3)(PMe_3)_2$ and norbornene as acceptor, 60 turnovers/h are observed. These experiments at low temperatures point to the high reactivity of the $RhCl(PMe_3)_2$ monomer (which is not present in observable concentration) [22, 23]. The major disadvantage of this method is that a

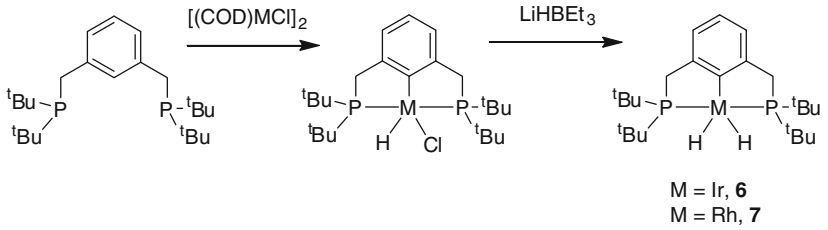

Scheme 4.4 Synthesis of catalysts precursors

high fraction of the acceptor is sacrificed to hydrogenation. In related chemistry, Belli and Jensen [24] reported that the isolable $H_2IrCl(P^iPr_3)_2$ showed very low activity for cyclooctane/TBE transfer dehydrogenation (4 TOs, 150 °C).

In 1990 Saito [25] reported that acceptorless dehydrogenation could be achieved using catalysts of the type $RhCl(PAr_3)_3$ in cyclooctane at 151 °C. Vigorous refluxing was required to remove hydrogen and drive the endothermic reaction toward alkene. Modest turnovers were achieved (ca. 12–14 after 50 h) and the turnover frequency leveled off over time, possibly due to buildup of olefin in solution which could capture hydrogen and drive the reaction back toward alkane. Aoki and Crabtree [26] reported a similar procedure for acceptorless dehydrogenation of cyclooctane with the added twist of sometimes employing an inert perfluoroalkane co-solvent or purging with argon. Iridium catalysts of the general type $IrH_2(O_2CR)(PCy_3)_2$ as well as a tungsten catalyst, $(triphos)WH_6$, were employed. As in the Saito system [25], turnovers were modest (maximum observed = 36).

4.3 The Pincer Era

In 1996 Jensen, Kaska and coworkers [27, 28] reported the use of pincer-ligated iridium complexes as hydrogen transfer catalysts. Reduction of the pincer hydrido chloride complexes (^{tBu4}PCP)IrHCl and (^{tBu4}PCP)RhHCl reported by Moulton and Shaw [29] gave the corresponding dihydrides. The synthetic routes to these complexes, (^{tBu4}PCP)$IrH_{2,\ 6}$, and (^{tBu4}PCP)RhH_2 (**7**) are shown in Scheme 4.4.

Employing the benchmark COA/TBE system, Jensen and Kaska demonstrated that the Ir complex **6** is quite active, exhibiting ca. 82 TO/h at 150 °C. Even more remarkably, the TOF increased to 12/min at 200 °C, with no catalyst decomposition observed over 7 days. Catalysis is inhibited by nitrogen (no doubt through formation of stable dinitrogen complexes [30, 31]) and by excess t-butylethylene (see mechanistic discussion below). In contrast to the Ir system, the Rh analog, **7**, shows low activity at 150 °C. These observations using the t-butyl-substituted PCP pincer-ligated system represented a major advance in alkane dehydrogenation chemistry and have stimulated numerous groups to explore synthetic and mechanistic aspects of dehydrogenation chemistry using a wide range of pincer-derived iridium

complexes. The remainder of this chapter will focus on the most significant experimental advances employing pincer iridium complexes.

Following initial catalysis employing **6** and the COA/TBE system, Kaska, Jensen and coworkers [28] reported efficient dehydrogenation of other cyclic alkanes including cyclohexane, methylcyclohexane and decalin. In the case of cyclohexane, dehydrogenation to benzene could be achieved using excess acceptor olefin (Eq. 4.9).

The exceptional stability of the Ir pincer complexes provided a means to achieve acceptorless dehydrogenation. Refluxing cyclodecane (bp = 201 °C) with either t-butyl-substituted Ir pincer, **6**, or the sterically less-crowded, (^{iPr4}PCP)IrH$_4$, **8**,

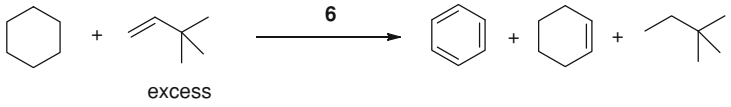

(4.9)

yields cyclodecene as gaseous hydrogen is lost from the system [32, 33]. (The tetrahydrides rapidly lose H_2 at elevated temperatures so tetrahydride and dihydride catalyst precursors yield identical results). The i-Pr derivative **8** proved more effective than t-Bu derivative **6**; 1000 TO could be achieved in dehydrogenation of cyclodecane (Eq. 4.10). Moreover, this catalyst was used to effect the first acceptorless dehydrogenation of a linear alkane, *n*-undecane to undecene isomers [33]. Computational studies [34] suggested that electron-donating substituents in the para-position of the pincer aryl group should favor oxidative addition of C–H bonds to the unsaturated 14-electron intermediate, a key reaction in the transfer dehydrogenation cycle(see below). Employing para-methoxy derivatives (*p*-MeO-^{tBu4}PCP)IrH$_2$ (**9**) and (*p*-MeO-^{iPr4}PCP)IrH$_2$) (**10**) gave substantial increases in turnover numbers

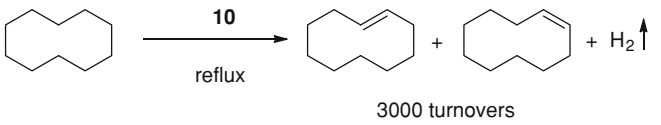

(4.10)

for the acceptorless dehydrogenation of cyclodecane [35]. For example, using (*p*-MeO-^{iPr4}PCP)IrH$_2$), **10**, over 3,000 turnovers were obtained in 24 h at reflux. However, the para-methoxy derivatives did not yield increased productivity in transfer dehydrogenations of either cyclic or linear alkanes employing TBE as acceptor.

Conversion of linear alkanes to value-added α-olefins through acceptorless dehydrogenation is economically quite attractive. However, the current method has drawbacks which need to be addressed. With time, turnover frequencies diminish which may be due to either (or both) thermodynamically favorable back reaction as product olefin builds up or inhibition of dehydrogenation by product olefin through formation of Ir(I) olefin complexes. Furthermore, even though α-olefins have been shown to be the kinetic product of acceptorless dehydrogenation, subsequent

isomerization degrades this product to a thermodynamic mixture of olefins which is comprised primarily of the more stable internal alkenes. Since (PCP)IrH_2 species are key intermediates in dehydrogenation (see below), it was initially assumed [36] that olefin isomerization occurred predominantly through the classical hydride addition/elimination mechanism for isomerization [37, 38]. For example, for an α-olefin this involves 2,1-insertion into the Ir–H bond to form the secondary alkyl complex followed by β-elimination with the opposite regiochemistry to 2-alkenes (Eq. 4.11). More recent studies have shown that this assumption was incorrect and that isomerization occurs largely through a π-allyl hydride

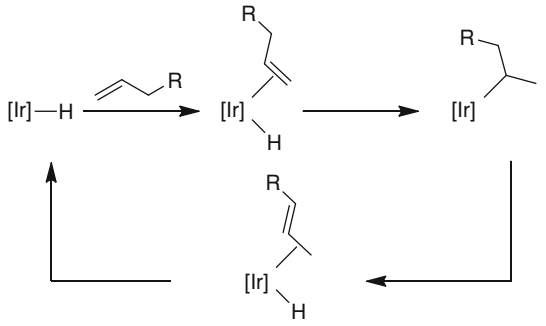

(4.11)

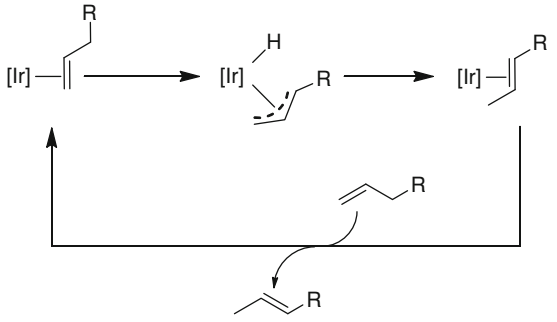

(4.12)

intermediate formed from a (PCP)Ir(olefin) complex [39]. Equation 4.12 illustrates isomerization of a 1-alkene to a 2-alkene via this mechanism.

The mechanism of transfer dehydrogenation of cyclooctane using TBE as acceptor has received close scrutiny [40, 41]. The overall catalytic cycle is shown in Scheme 4.5. Beginning with the 16-electron iridium dihydride, **6**, insertion of TBE yields the alkyl hydride complex, **11**. Reductive elimination yields alkane (2,2-dimethylbutane) and the 14-electron Ir(I) complex, **12**. This species can undergo an unproductive oxidative addition with TBE to form vinyl hydride **13** or, to close the cycle, oxidative addition of cyclooctane to cyclooctyl hydride, **14**, followed by β-elimination to reform dihydride, **6**, and cyclooctene product. In addition to examining the working catalytic system, individual components of the cycle were studied independently. For example, using deuterium labeling, the hydrogenation of

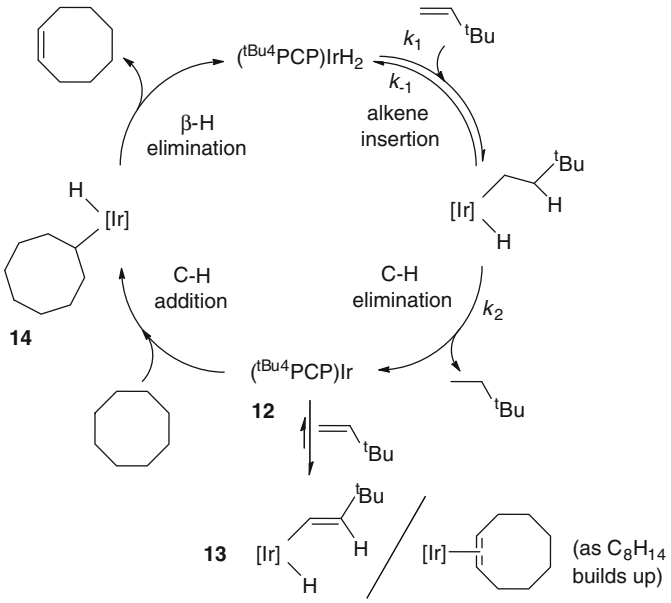

Scheme 4.5 Mechanism of transfer dehydrogenation of cyclooctane using TBE as acceptor

TBE by dihydride, **6**, was shown to be partially reversible with the back reaction (k_{-1}, β -elimination) competitive with reductive elimination of alkane, $CH_3CH_2C(CH_3)_3$ (k_2) [40]. The Ir(I) 14-electron species, (^{tBu4}PCP)Ir, **12**, is in rapid equilibrium (relative to the catalytic turnover frequency) with the Ir(III) vinyl hydride species (^{tBu4}PCP)Ir(H)(CH = CH^{t}Bu), **13**, as established by dynamic low temperature NMR studies [41]. The kinetic dependence of the turnover frequency (TOF) on acceptor TBE is a function of its concentration. At low TBE, the catalyst resting state is the dihydride, **6**, and the TOF is first-order in TBE. At high concentration, the catalyst resting state is the vinyl hydride, **13**, and the TOF is first-order in cyclooctane and inversely dependent on TBE. In a catalytic run, kinetics will be complex as TBE concentration decreases from high values to low values.

In the dehydrogenation of *n*-alkanes, the catalyst resting state is the (^{tBu4}PCP)Ir(1-alkene) complex; thus the product olefin, 1-alkene, inhibits catalysis as it builds up. Such strong binding by 1-alkene accounts for the more rapid dehydrogenation of cyclooctane—in spite of the intrinsically greater reactivity of (^{tBu4}PCP)Ir toward *n*-alkane than cyclooctane—since the product olefin, cyclooctene, binds much more weakly to the Ir(I) center than to 1-alkene [39, 42, 43].

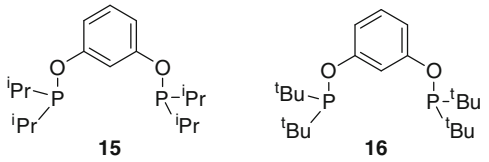

A large number of variations on iridium PCP pincer complexes have been reported. Among the most extensively studied are the bis-phosphinite pincer complexes in which the methylene bridges of the PCP pincer ligand have been replaced by oxygen. Early reports of bis-phosphinite systems include (^{iPr4}POCOP)IrH$_2$ **15**, prepared by Jensen and coworkers [44] and (^{tBu4}POCOP)IrH$_2$, **16**, prepared by Brookhart and coworkers [45, 46]. The pincer ligands are readily prepared from resorcinol and the iridium hydrochloride complex (**17**) is prepared in a standard procedure by reaction of the pincer ligand with the dimer, [(COD)IrCl]$_2$ (COD = 1,5-cyclooctadiene). Brookhart and coworkers showed that treatment of the hydrochloride, (^{tBu4}POCOP)IrHCl (**17**), with NaO^{t}Bu results in dehydrochlorination and, in the presence of trapping ligands, L, formation of (^{tBu4}POCOP)IrL. This procedure provides a convenient route to both the dihydride, **18**, and the ethylene complex, (^{tBu4}POCOP)Ir(C_2H_4), **19**, as shown in Eq. 4.13. Both complexes serve as convenient initiators of hydrogen transfer reactions.

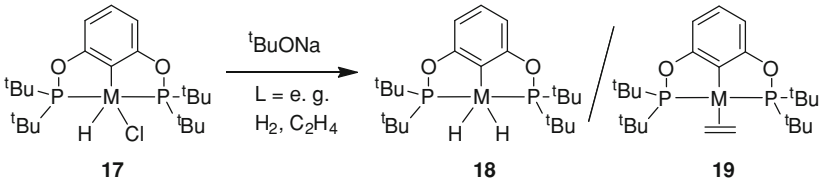

(4.13)

(^{tBu4}POCOP)IrHCl, **17**, together with both various *para*-substituted derivatives and dihydride **18** [45, 46] have been employed for hydrogen transfer reactions in the COA/TBE system. In addition to production of cyclooctene, cyclooctadiene was observed at high conversions. These systems show high catalytic activities and indeed **17** and derivatives exhibit nearly an order of magnitude greater reactivity for COA/TBE transfer dehydrogenation than the PCP analog, **6**. On the other hand, this system shows significantly lower activity for transfer dehydrogenation of linear alkanes relative to **6** [43, 47]. Use of excess TBE acceptor and long reaction times resulted in conversion of COA to ethyl benzene and ortho-xylene via a process likely involving formation of cycloctatriene, electrocyclic ring closure to bicycle[4.2.0]octadiene, ring cleavage and hydrogenation of the strained cyclobutane moiety and further dehydrogenation to the aromatic products [46].

Mechanistic studies of the (^{tBu4}POCOP)Ir system have been carried out and conclusions are summarized in Scheme 4.6 [45, 46]. The overall cycle is similar to that of the PCP system (Scheme 4.5); however there are subtle but significant differences. TBE binds to the iridium center in a π fashion, not via formation of a vinyl hydride complex. Importantly, the resting state at all TBE concentrations is initially the TBE complex, **20**. Competition studies show that COE binds more strongly to the Ir center than TBE so that as hydrogen transfer proceeds, the resting state shifts from TBE complex **20** to the COE π-complex **21**. The rate of hydrogenation of TBE by ^{tBu4}POCOP dihydride **18** is far faster than the comparable rate with ^{tBu4}PCP dihydride, **6** [43, 47].

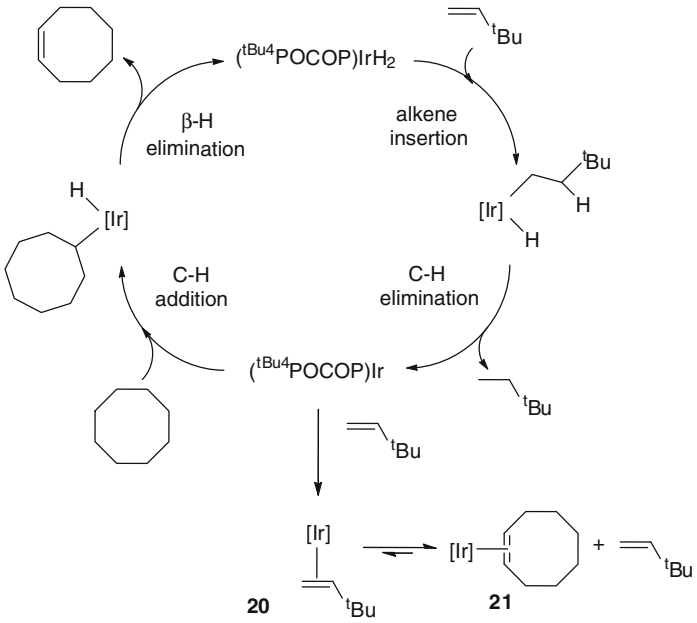

Scheme 4.6 The (POCOP)Ir-based mechanism

DFT calculations suggest that differences in the reactivities and binding affinities of the (PCP)Ir and (POCOP)Ir systems can largely be attributed to steric factors [39, 43, 47]. The shorter P–O and C–O bonds in the POCOP system versus the P–C and C–C bonds in the PCP system result in a more acute P–Ir-P angle in the POCOP system and thus a more open fourth coordination site. For example, the P–Ir-P angle in (^{tBu4}POCOP)Ir(CO) is 157.5° while in (^{tBu4}PCP)Ir(CO) it is 164.5° [48]. The more open coordination site in (^{tBu4}POCOP)Ir species serves to rationalize the observation that TBE binds in a π fashion to (^{tBu4}POCOP)Ir whereas the less sterically demanding vinyl hydride bonding mode is favored for the ^{tBu4}PCP system. Similarly, (^{tBu4}POCOP)Ir binds α-olefins much more strongly than does (^{tBu4}PCP)Ir, which appears to result in the reduced activity for dehydrogenation of linear alkanes by (^{tBu4}POCOP)Ir relative to (^{tBu4}PCP)Ir as noted earlier.

In addition to *t*-butyl- and *i*-propyl- substituted (PCP)Ir and (POCOP)Ir systems discussed above, a number of other closely related iridium pincer complexes have been prepared and examined for use in hydrogen transfer reactions. A selection of these complexes is shown in Fig. 4.1. The anthraphos-supported pincer system, **22**, has been reported by Haenel, Kaska, Hall and coworkers [49]. These complexes appear to be particularly robust and exhibit thermal stability at temperatures as high as 250 °C. The activity of the t-butyl-substituted anthraphos systems in COA/TBE hydrogen transfer experiments was shown to be less than that of the ^{tBu4}PCP analog; the authors suggest that increased steric crowding around the metal center may be responsible for reduced activity. The adamantyl-substituted system,

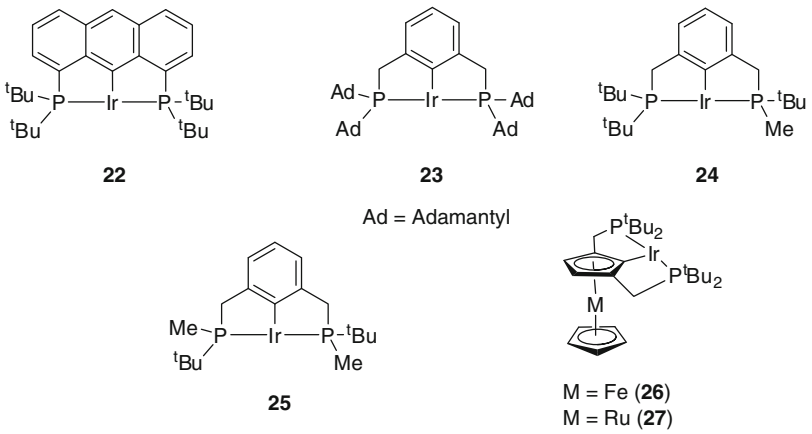

Fig. 4.1 Recently developed iridium pincer complexes used in hydrogen transfer reactions

(^{Ad4}PCP)Ir, **23**, has been synthesized and its catalytic activity studied [50]. It was proposed that the steric and electronic properties of the adamantyl group should be quite similar to those of the t-butyl group but the adamantyl groups may be more resistant to P–C bond cleavage or cyclometallation relative to the *t*-butyl groups, thus imparting higher thermal stability relative to the *t*-butyl derivatives. Indeed, increased stability was observed for the adamantyl systems which show considerable catalyst lifetimes at 250 °C. High thermal stability is particularly important in acceptorless dehydrogenations where high temperatures are needed to drive this exothermic reaction and promote loss of dihydrogen. Use of **23** in acceptorless dehydrogenation of cyclodecane under reflux conditions led to higher overall turnover numbers relative to the (^{tBu4}PCP)Ir and (^{iPr4}PCP)Ir systems.

The higher turnover frequencies and productivities of (^{iPr4}PCP)Ir systems relative to (^{tBu4}PCP)Ir systems demonstrate that steric factors play a significant role in influencing reactivity. In an effort to further probe steric effects and identify even more reactive catalysts, complexes generated by replacing t-butyl groups with methyl groups in PCP systems have been explored, both computationally and experimentally [51]. The catalytic reactivity of the monomethyl-substituted complex, **24**, is found to be substantially greater than either (^{iPr4}PCP)Ir, **8**, or (^{tBu4}PCP)Ir, **6**, in both transfer dehydrogenation and acceptorless dehydrogenation. Transfer dehydrogenation of *n*-octane using **24** gave 980 turnovers in 5 h at 150 °C relative to 96 and 208 turnovers for **8** and **6**, respectively, under the same conditions. DFT analysis of the monomethyl tri-*t*-butyl substituted system showed that the transition state energy for *β*-hydride elimination from the intermediate alkyl hydride complex is significantly lower than for the tetra-*t*-butyl substituted system. This step is calculated to be rate-determining in the dehydrogenation cycle; thus the computations are consistent with the experimental observations. Use of **25** in which a second methyl group has been replaced results in no additional increase in activity; in fact, somewhat lower reactivity is observed.

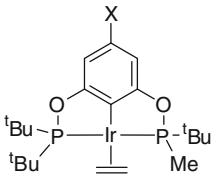

M = -O$^-$K$^+$ (**28**)
M = -OMe (**29**)
M = -OP(^{t}Bu)$_2$ (**30**)

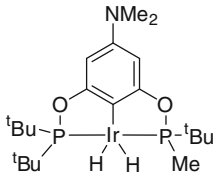

31

Fig. 4.2 Pincer complexes capable of being anchored to solid-phase supports

Computational analysis indicates that a second methyl-for-t-butyl substitution [to give species (^{tBu2Me2}PCP)Ir] results in relatively little additional lowering of the β-hydride elimination barrier, and this is largely compensated for by an increase in olefin binding affinity. The reduced dehydrogenation activity of **25** compared to **24** could be a result of such an increase in olefin binding energy and/or it may result from formation of inactive dimeric species (again due to decreased steric bulk) during catalysis [51].

Unusual iron and ruthenium metallocene-based iridium pincer complexes, **26** and **27**, have been described by Koridze and coworkers [52]. These complexes show excellent activity in COA/TBE transfer dehydrogenations. For example, the iron complex **26** shows a turnover number of 3,300 in 8 h at 180 °C relative to 1,840 turnovers for (^{tBu4}PCP)Ir, **6**, under similar conditions. The authors propose steric effects are likely responsible for increased activities of **26** and **27**. The P–Ir-P angle in the in the carbonyl derivative of **26** is 157.8°, more acute than the corresponding PCP angle in (^{tBu4}PCP)Ir(CO) of 164.5° [48]. Accordingly, the fourth coordination site is sterically less restricted, and more comparable to the POCOP systems. The authors also suggest that the interaction of the remote Cp ring with the t-butyl substituents on phosphorus may contribute to the increased activity.

Most studies concerning the use of pincer iridium catalysts for dehydrogenation have focused on homogeneous systems. For many applications, however, supported systems are desirable due to their potential for recycling and the ease of separation of catalyst from product. In addition, supported catalysts often exhibit higher thermal stabilities than homogeneous systems. Scott, Brookhart, Goldman and coworkers [53] have reported several methods for supporting iridium PCP and POCOP pincer complexes for use in alkane dehydrogenation. Functional groups were introduced into the para position of the aryl ring of the pincer ligand so that the iridium complex could be covalently attached to silica and to Merrifield resins. In each case these systems exhibited only moderate activity in COA/TBE hydrogen transfer reactions.

By far the best method found to immobilize these catalysts involved adsorbing catalysts containing basic functionalities at the para position onto γ-alumina through a Lewis acid–base interaction [53]. Figure 4.2 shows complexes used in these experiments. Complex **28**, which contains an oxide functionality, was demonstrated to be strongly bound to the alumina surface through ICP-MS analysis.

Essentially no leaching (ca. 0.02 % Ir) occurs upon washing the supported catalyst three times with cyclooctane at 200 °C. Applying this system to COA/TBE hydrogen transfer (3,000 equiv COA and TBE) resulted in 1,990 turnovers in 40 h (200 °C), and also formation of 810 equivalents of 2,3-dimethyl-2-butene and 200 equivalents of 2,3-dimethyl-1-butene (Eq. 4.14).

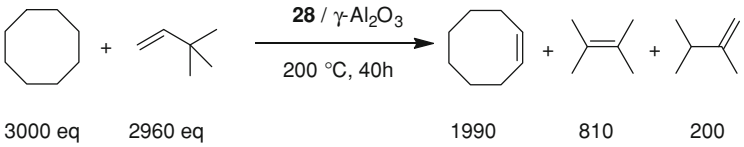

(4.14)

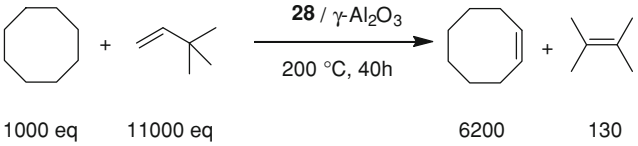

(4.15)

These olefins are formed from acid-catalyzed isomerization of TBE and do not function as hydrogen acceptors. Good recyclability was observed; however each recycle produced increasing amounts of the isomerized olefins. Acid-catalyzed isomerization of TBE could be greatly retarded by adsorbing **28** on basic alumina specially prepared by calcining γ-alumina pretreated with sodium hydroxide. Using **28** adsorbed on this basic alumina, together with 11,000 equivalents of TBE and COA, 6200 turnovers were obtained in 15 h at 240 °C accompanied by only 130 equivalents of rearranged olefin (Eq. 4.15).

The solid state [31] P MAS NMR spectrum of **28** adsorbed on γ-alumina shows a single resonance at δ 177 ppm which is close to the solution value of δ 170 ppm and indicates the pincer complex is intact with no significant change in structure. Exposing this sample to COA/TBE at 200 °C over sufficient time to achieve 1,090 turnovers and reanalysis by [31] P MAS NMR spectroscopy shows little catalyst decomposition [53].

The adsorbed phosphinite complex, **30**, behaves quite differently. Analysis of the [31] P MAS NMR spectrum shows little change in the [31] P signals of the coordinated phosphorus nuclei but a dramatic shift in the signal for the para-phosphinite from δ151 ppm in solution to δ 78 ppm. Adsorption of a species chosen to model the para-derivatized pincer aryl group, phenyl di-t-butylphosphinite, shows a similar [31] P MAS shift; extraction of the alumina with THF shows that the species responsible for this upfield signal is adsorbed di-t-butylphosphine oxide [54]. A mechanism for this surface reaction has been proposed and involves attack of a surface hydroxyl on the phosphinite group and release of phenoxide. Attack of phenoxide ion on the resulting $AlO(H)P(t\text{-}Bu)_2$ group releases the phosphine oxide and results in covalent binding of the aryloxy group to the alumina surface (Scheme 4.7).

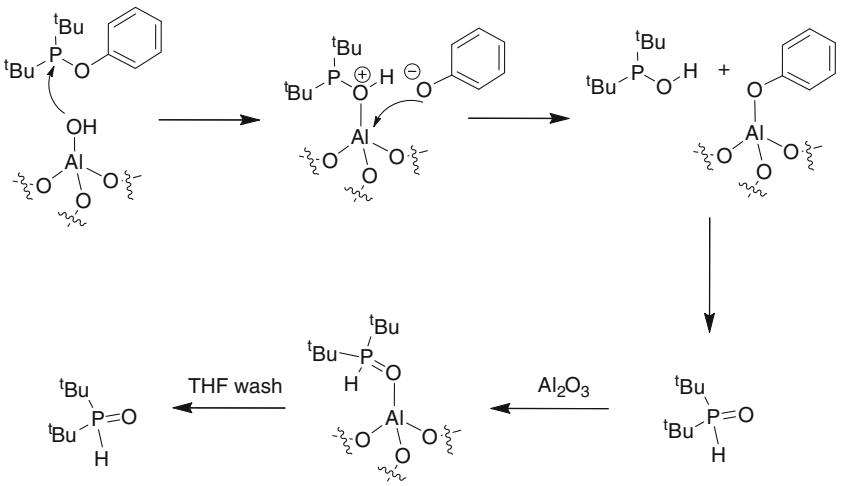

Scheme 4.7 Explanation of the observation of release of phosphine oxide

Consistent with this proposal is the complete absence of leaching of catalyst from alumina under conditions previously described. Indeed, catalyst anchoring using this methodology has provided exceptionally stable supported catalysts for use in heterogeneous catalytic alkane metathesis reactions (see below).

4.4 Alkane Metathesis

As noted earlier, the obvious potential utility of alkane dehydrogenation catalysis is in producing value-added olefins from abundant alkane feedstocks. A less obvious application of alkane dehydrogenation is for alkane metathesis (sometimes referred to as molecular redistribution or disproportionation) [55, 56]. Alkane metathesis converts alkanes to alkanes of lower and higher molecular weights. The strategy for achieving such chain redistribution was first put forth by Burnett and Hughes, involving a dual catalyst system as shown in Scheme 4.8 and illustrated for metathesis of hexane [55]. *n*-Hexane is dehydrogenated by catalyst (M) to form MH_2 and 1-hexene (for simplicity, selectivity for forming an α-olefin is assumed, see below). The 1-hexene then undergoes olefin metathesis to form ethylene and 5-decene. These olefins are hydrogenated by MH_2 to form ethane and decane. The overall conversion is nearly thermo-neutral so that, clearly, complete conversion to C_2 and C_{10} products will not occur. An attractive feature of this dual catalyst system is that *no sacrificial acceptor is required*.

Assuming selectivity in dehydrogenation to form α-olefins, the expected products of the metathesis of any linear C_nH_{2n+2} alkane will be ethane and $C_{2n-2}H_{4n-2}$ (Eq. 4.16). Complications resulting in formation of alkanes with carbon numbers other than those shown in Eq. 4.16, however, could include olefin isomerization prior

Scheme 4.8 The dual catalyst strategy for Alkane Metathesis

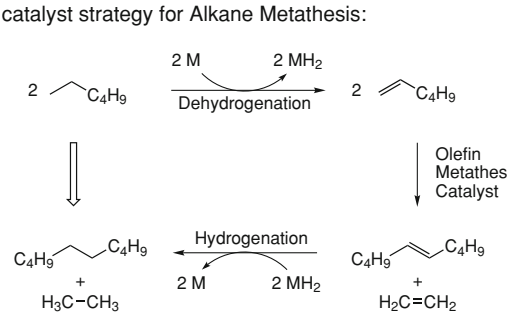

to olefin metathesis and non-selective dehydrogenations to produce internal olefins. Furthermore, as longer chain product alkanes build up, these can undergo

$$C_nH_{2n+2} \longrightarrow C_2H_6 + C_{2n-2}H_{4n-2} \tag{4.16}$$

metathesis to produce alkanes with chain lengths exceeding 2n − 2. These issues will be discussed in more detail below.

One major potential application of alkane metathesis is in upgrading lower molecular weight linear alkanes to linear alkanes which are valuable as diesel fuel (C_9–C_{19}). As petroleum stocks dwindle, the world will increasingly rely on the Fischer–Tropsch (FT) process as a source of alkanes for use as transportation fuel [57–60]. The FT process converts syn gas (CO plus H_2, derived from natural gas, coal or, potentially, other carbon sources including oil shale or biomass), to linear hydrocarbons. This is a chain-growth process which yield a broad Schultz-Flory distribution of linear alkanes, C_1 to $>C_{100}$. High molecular weight alkanes (typically, $C_{n\ >\ 19}$) can be hydrocracked to yield a distribution of lower molecular weight alkanes. While C_1–C_3 alkanes are useful for heating gas, the C_4–C_8 linear alkanes are not in high demand as either heating or transportation fuel. Low-MW n-alkanes (a major component of so-called natural gas liquids or condensates) also constitute a very substantial and growing fraction of world hydrocarbon production [61–63]. The upgrading of these alkanes to higher molecular weights thus represents an important potential source of diesel fuel. It is also worth noting that diesel engines are ca. 30 % more efficient than gasoline engines and that linear alkanes have a much higher cetane rating than branched alkanes while burning more cleanly (to give less particulate matter) than conventional diesel fuel. Accordingly, worldwide demand for diesel, and FT diesel in particular, is increasing more rapidly than demand for gasoline [64].

Burnett and Hughes in 1973 [55] were the first to report alkane metathesis using a combination of two heterogeneous catalysts, a platinum on alumina catalyst for dehydrogenation/hydrogenation and tungsten oxide on silica for olefin metathesis. Butane was passed over these supported catalysts at 400 °C, resulting in formation of a mixture of C_1–C_8 hydrocarbons (Eq. 4.17). The formation of methane and small amounts of branched hydrocarbons indicates that C–C bond cleavage occurs by secondary routes in addition to the alkane metathesis mechanism shown in Scheme 4.8.

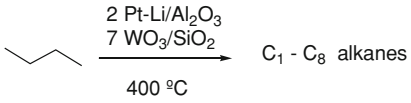

(4.17)

Following the work of Burnett and Hughes, Bassett, Coperet et al. [65–67] published an impressive series on papers describing heterogeneous single-site catalysts which achieve alkane metathesis at much lower temperatures, 150 °C. Both a tantalum hydride on silica and a tungsten hydride on alumina were examined as initiating catalysts. These supported hydrides were fully characterized by a variety of sophisticated spectroscopic techniques including solid-state NMR and ESR, EXAFS, and TEM. The primary substrate examined was propane. Turnover numbers were low with between 60 and 120 turnovers achieved over 120 h. The major metathesis products included ethane and *n*-butane, *n*-pentane and *n*-hexane, but methane and branched C_5 and C_6 hydrocarbons were also formed (Eq. 4.18). These surface species presumably are able to activate alkanes to form surface bound alkylidenes which then allows operation of the metathesis mechanism in Scheme 4.8. Methane and branched hydrocarbons form by other processes involving surface-mediated C–C bond-cleavage and bond-forming reactions. No higher hydrocarbons were examined.

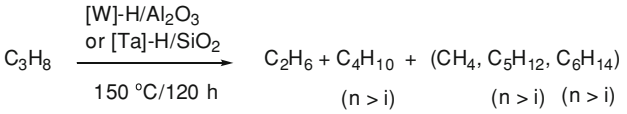

(4.18)

The first homogeneous alkane metathesis catalytic system was reported by Goldman, Brookhart and coworkers in 2006 [68]. Iridium pincer complexes (^{tBu4}PCP)IrH_2, **6**, and (^{tBu4}POCOP)IrH_2, **18**, were used as the dehydrogenation/hydrogenation catalysts and the standard molybdenum-based Schrock catalyst, **32** [69], was used to effect olefin metathesis.

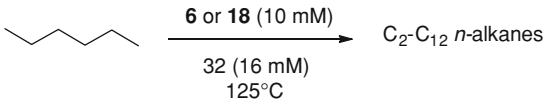

(4.19)

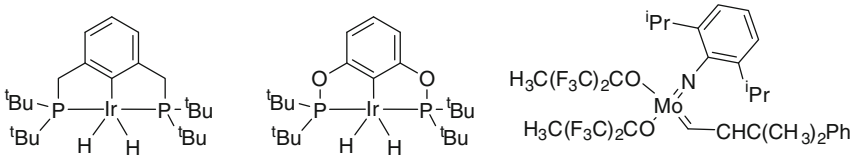

6 **18** **32**

This dual catalyst system was used to metathesize *n*-hexane at 125 °C (Eq. 4.19). Since the equilibrium, alkane + M ↔ olefin + MH_2, lies far to the left, two

equivalents of olefin were added initially to ensure the presence of a sufficient steady-state concentration of olefin in the system to affect olefin metathesis.

Typical results obtained for these two catalytic systems are summarized in Table 4.1. Moderate efficiencies are observed. (^{tBu4}POCOP)IrH_2 (10 mM) or (^{tBu4}PCP)IrH_2 (10 mM) in combination with Mo catalyst **32** (16 mM) converts hexane (7.5 M) to 2.05 M and 1.25 M alkane metathesis products, respectively. Turnover frequencies are low and catalytic activities fall to near zero after ca. 48 h. Addition of a second charge of Schrock catalyst to the solutions results in the resumption of catalytic activity at rates comparable to the initial rates. These observations imply that the iridium catalysts are stable under these conditions (consistent with thermal stabilities of these systems discussed earlier in this chapter), while the molybdenum catalyst decays at 125 °C. The limited stability of **32** is in accord with earlier studies by Schrock and coworkers [70]; a bimolecular decay mechanism involving a molybdenum methylene intermediate likely operates.

The distribution of alkane products for these metathesis reactions is shown in Table 4.1. As noted earlier, ideally only ethane and decane would be observed initially. However, as seen in Table 4.1, primary products range from C_2 to C_{10}. (Alkanes $C_{n>10}$ arise from secondary metathesis of primary alkane products with carbon numbers between 7 and 10). Moderate selectivity for C_2/C_{10} products is seen with the (^{tBu4}PCP)IrH_2 catalyst which gives a $C_{10}/(C_7–C_{10})$ molar product ratio of 0.49, where $C_7–C_{10}$ alkanes represent all of the possible primary "heavy" products from metathesis of *n*-hexane.

There are two plausible mechanisms responsible for lack of selectivity and it is likely that both can play an important role. First, as noted earlier in this chapter, pincer iridium complexes catalyze isomerization of olefins through a π-allyl mechanism. Thus, as shown in Scheme 4.9 olefin isomerization coupled with olefin metathesis produces alkanes of carbon numbers ranging from C_3 to C_9. Metathesis of internal olefins is most likely to occur with ethylene as the partner and thus higher initial production of C_5 and C_7 olefins (and thus C_5 and C_7 alkanes) compared to $C_{3–4}$ and $C_{8–9}$ products may be expected. This trend is somewhat reflected in the data in Table 4.1.

A second cause for lack of selectivity may arise from the initial lack of selectivity in the dehydrogenation reaction. High selectivity for formation of α-olefins has been established for the (^{tBu4}PCP)Ir system [36], but recent results indicate a lack of selectivity with significant quantities of internal olefins produced upon dehydrogenation of linear alkanes by the (^{tBu4}POCOP)Ir system [43, 47]. A significant challenge is presented in untangling dehydrogenation selectivities, olefin isomerization rates relative to olefin metathesis rates and secondary metathesis of product alkanes to model product distributions as a function of time, knowing all the while that the metathesis catalyst is decaying!

NMR spectroscopic investigations of working catalyst systems have revealed the resting state(s) of the iridium catalysts [68]. In the case of the (^{tBu4}PCP)Ir system, the resting state is the dihydride complex, **6**. Since the steady state concentration of olefin during catalysis is quite low, this observation is consistent with the fact that the dihydride complex is the resting state in the COA/TBE transfer

Table 4.1 Metathesis of *n*-hexane (7.6 M) by 19, 18 or 6 (10 mM) and 32 (16 mM): distribution of C_2–C_{15} *n*-alkane products

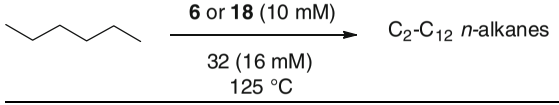

Entry	[Ir]	[TBE] (mM)	Temp (°C)	T (h)	Product concentration (mM)												Total product (M)
					$C_2 + C_3$	C_4	C_5	C_7	C_8	C_9	C_{10}	C_{11}	C_{12}	C_{13}	C_{14}	$C_{\geq 15}$	
1	**19**	0	125	24	233	191	319	234	133	122	81	22	9	5	2	1	1.35
				48	261	215	362	265	147	138	89	25	11	6	3	1	1.52
				96	264	218	372	276	154	146	95	26	12	6	3	1	1.57
Added additional 32 (8 mM)																	
				120	502	436	721	420	239	223	153	56	30	18	10	5	2.81
2	**18**	20	125	24	458	345	547	258	151	139	95	29	13	6	3	2	2.05
3	**6**	20	125	23	131	176	127	306	155	37	49	232	18	4	4	10	2	1.25

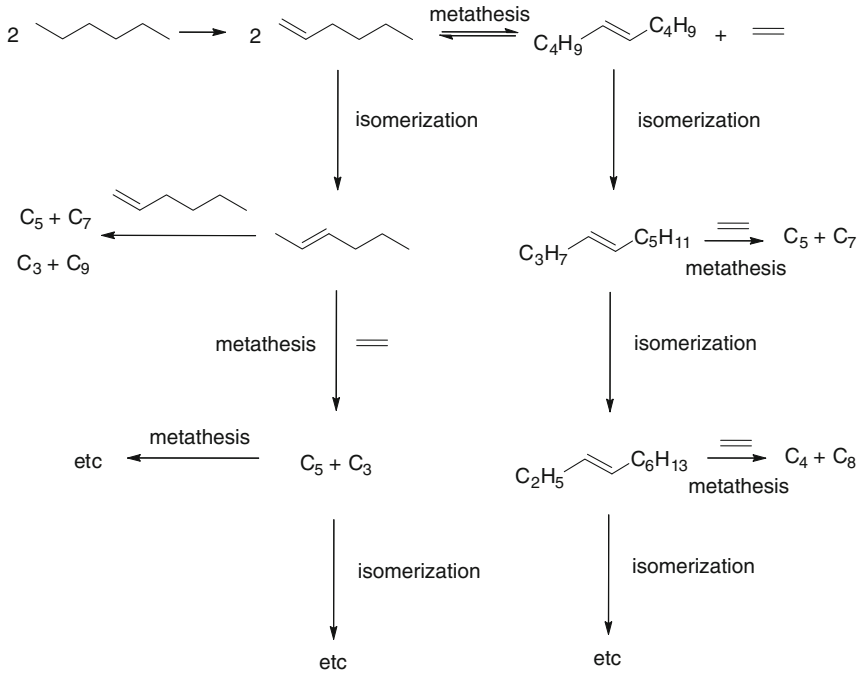

Scheme 4.9 Olefin isomerization can account for poor selectivity

hydrogenation system when the TBE concentration is low (see earlier discussion in this chapter). Thus the turnover-limiting step in this system involves hydrogenation of olefins by **6**, more specifically, hydrogenation of internal olefins since internal olefins are hydrogenated much more slowly by **6** than ethylene or α-olefins. In the case of the (^{tBu4}POCOP)Ir system, the catalyst resting states are (^{tBu4}POCOP)Ir(olefin) complexes. Again, this is consistent with observations in the COA/TBE hydrogen transfer system, where the TBE π-complex is the resting state in the initial stages of hydrogen transfer. Initially, the dominant resting state is the ethylene complex (^{tBu4}POCOP)Ir(ethylene), with minor concentrations of α-olefin complexes observable. As catalysis proceeds, the olefin metathesis catalysis decays so that ultimately ethylene is not produced. Any remaining ethylene (or α-olefins) present serve now as hydrogen acceptors and hexane is converted to hexene. This results in conversion of the mix of initial iridium resting states to a single species, the 1-hexene complex, (^{tBu4}POCOP)Ir(1-hexene).

While initial studies of homogeneous alkane metathesis systems focused on tetra-t-butyl-substituted (PCP)Ir and (POCOP)Ir complexes in combination with the Schrock Mo complex, **32**, later investigations were expanded by screening iridium catalysts bearing other substituents on phosphorus and a range of molybdenum and tungsten imido alkylidene catalysts. Sterically less-hindered pincer complexes,

(^{iPr4}PCP)IrH$_2$, (^{tBu3Me}PCP)IrH$_2$, and (^{tBu2Me2}PCP)IrH$_2$ in combination with Mo catalyst **32** were shown to provide increased productivities but lower selectivity for formation of C_2/C_{10} products from metathesis of hexane [71]. The most productive catalyst was (^{tBu3Me}PCP)IrH$_2$ which was ca. 2.5 times more productive than the benchmark catalyst (^{tBu4}PCP)IrH$_2$. The least hindered catalyst, (^{tBu2Me2}PCP)IrH$_2$, showed very high initial activity but rapid decomposition leading to overall lower productivity. Schrock and coworkers [72] screened over forty tungsten and molybdenum alkylidene imido catalysts in combination with pincer iridium catalysts. In general, the tungsten catalysts proved more effective than the molybdenum catalysts due to their higher thermal stabilities. The most effective catalyst was W(NAr)(CHR)(OSiPh$_3$)$_2$ (Ar = 2,6-diisopropylphenyl, R = CMe$_2$Ph); productivity exceeded that of the standard catalyst, **32**, by a factor of ca. 2.

The heterogeneous metathesis catalyst, Re_2O_7 supported on alumina is considerably more stable than homogeneous Schrock-type catalysts and thus was examined in combination with iridium pincer catalysts for metathesis of decane at 175 °C [68]. Use of (^{tBu4}POCOP)IrH$_2$ (9 mM) and Re_2O_7/Al_2O_3 (16 mM effective Re_2O_7 concentration) in decane (5.1 M) gave 3.6 M alkane products after 11 days. No selectivity was seen for formation of C_2/C_{18} products; alkanes ranged from C_2 to C_{28}. An even more productive co-catalyst was the *p*-methoxy derivative of (^{tBu4}PCP)IrH$_4$ which produced 4.4 M product under the same conditions (again unselectively) after 9 days; at that point, the molar quantity of the starting alkane, n-decane, only slightly exceeded that of the C_9 and C_{11} alkanes.

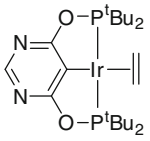

33

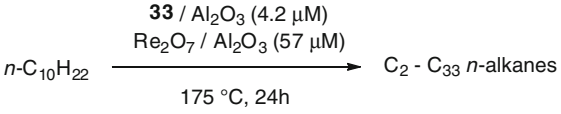

(4.20)

A fully heterogeneous system was developed based on combining Re_2O_7/Al_2O_3 with supported iridium pincer complexes [73]. As discussed earlier in this chapter, iridium complexes were supported by installing basic groups on the aryl backbone of the pincer complex and adsorbing these on alumina. High turnover numbers, normally in the range of 2,000, could be achieved in the metathesis of decane with these systems. For example, employing **33** (4.2 μM) on Al_2O_3 with Re_2O_7 (57 μM) on Al_2O_3 afforded 1910 turnovers after 24 h at 175 °C (Eq. 4.20). Again selectivities are poor and a range of alkanes, C_2–C_{33}, can be observed.

Since the Re_2O_7/Al_2O_3 catalyst functions best at lower temperatures, while the iridium catalysts are most active at high temperatures, a "two pot" reactor was designed to separate the catalysts so each operated at the optimal temperature [73]. The supported iridium catalyst on alumina operates at high temperatures (220 °C) in one pot; dehydrogenation products distill to the second pot maintained at 50 °C containing the Re_2O_7/Al_2O_3 where olefin metathesis occurs, then metathesized olefins return to the first pot where they are hydrogenated. Using **28** (*p*-OK) on

Al_2O_3 and metathesizing *n*-octane, 3,900 turnovers were obtained after 52 h. Moderate recyclability is observed; a total of ca. 6,900 turnovers were achieved after three cycles. These are the highest turnovers yet achieved in alkane metathesis. Secondary products ($C_{n>14}$) are minimal as these higher hydrocarbons do not distill from the first pot.

Alkane metathesis has also been extended to cyclic hydrocarbons cyclooctane and cyclodecane [74]. The (^{tBu4}POCOP)Ir and (^{tBu3Me}PCP)Ir systems in combination with the molybdenum catalyst yield cyclic oligomers in decreasing quantities with increasing carbon number. Cyclooctane yields $C_{16}H_{32}$, $C_{24}H_{48}$, $C_{32}H_{64}$ and $C_{40}H_{80}$ in ratios of 14:9.4:4.6:2.2, respectively, at 125 °C over 12 h with the (^{tBu3Me}PCP)Ir catalyst. The general mechanism for formation of these oligomers is shown in Scheme 4.10. With the more hindered catalyst (^{tBu4}PCP)IrH_2, polyethylene was observed along with low yields of cyclic oligomers. Polyethylene presumably forms from ring-opening polymerization of cyclooctene, followed by transfer hydrogenation of the unsaturated polymer.

4.5 Dehydroaromatization of *n*-Alkanes

In the course of investigating the catalytic activity of (MeO–^{iPr}PCP)IrH_4, Zhu et al. [35] found that the use of a high concentration of hydrogen acceptor (4.6 M NBE, as compared with typical acceptor concentrations of ca. 0.3 M) resulted in formation of benzene, albeit in low yields, from the dehydroaromatization of *n*-hexane (Eq. 4.21).

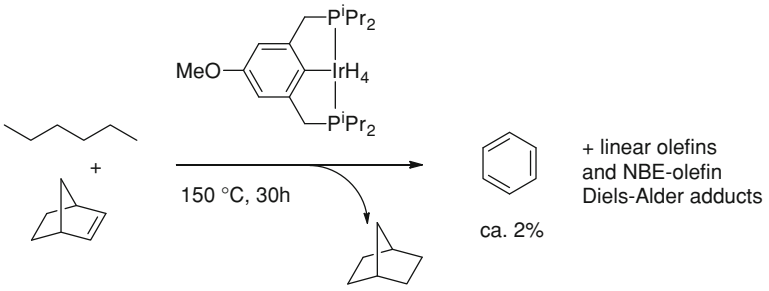

(4.21)

This scope of this reaction was recently explored in much more depth, using other bis(iso-propylphosphino)-substituted pincer complexes, including (^{iPr4}PCP)IrH_4 (**8**), the hybrid phosphine/phosphinite-pincer catalyst, **34**, and the anthraphos derivative, **35** [75].

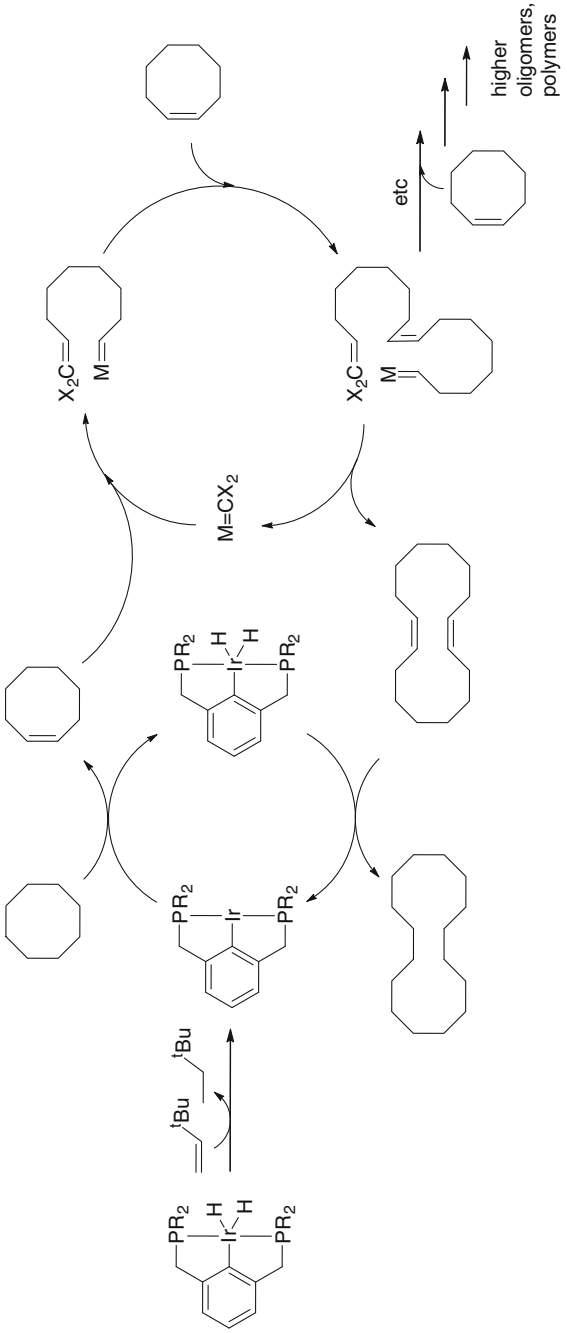

Scheme 4.10 Alkane metathesis with cyclic hydrocarbons

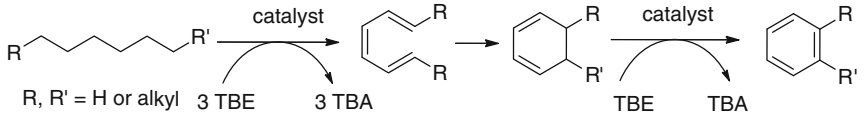

Scheme 4.11 Mechanism of the arene dehydroaromatizations

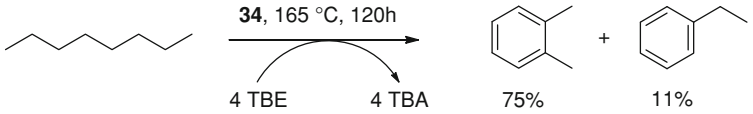

(4.22)

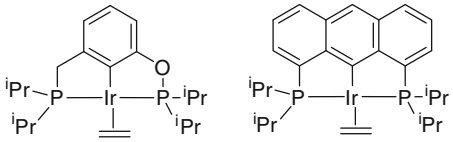

34 **35**

As required by the stoichiometry of *n*-alkane dehydroaromatization, four equivalents of acceptor per mol *n*-alkane were used, and longer reaction times and higher temperatures were employed, resulting in substantially higher yields of benzene. Catalyst **34** showed the highest productivity, e.g. 44 % yield of benzene (670 mM) after heating a solution of 6.13 M TBE with 1.53 M n-hexane for 120 h at 165 °C. Even higher dehydroaromatization yields were obtained with higher *n*-alkane substrates and with four equiv TBE, e.g. 86 % yield of total aromatics, primarily *o*-xylene with some ethylbenzene, from *n*-octane (Eq. 4.22) [75].

Propene was successfully used as a potentially more economical acceptor in place of TBE, although the resulting yield of aromatics was lower (38 %). Ideally the dehydroaromatization would be conducted without the use of any acceptor; this has not been reported.

The proposed mechanism of dehydroaromatization is shown in Scheme 4.11. Extensive dehydrogenation and double-bond isomerization generates conjugated trienes which are well known to undergo electrocyclization to give cyclohexadienes. Dehydrogenation of the cyclohexadiene (perhaps preceded by double-bond isomerization) gives the aromatic product.

Aromatization of *n*-alkanes by heterogeneous catalysts is well known to occur at high temperatures (typically 500–700 °C). Such processes are unselective and tend to give aromatics with only methyl substituents on the ring (e.g. toluene or xylene) due to cleavage of the relatively weak benzylic bonds under such conditions [76–78]. Thus it is noteworthy that the carbon number of the *n*-alkane substrate was generally conserved in the pincer-iridium catalyzed reactions, e.g. *n*-decane gave mainly C10 aromatic products (Eq. 4.23).

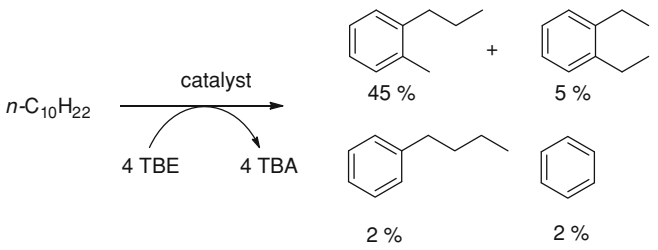

(4.23)

The side-chains of the reaction products are exclusively non-branched as would be expected based on the mechanism of Scheme 4.11. This contrasts with the structure of alkylarenes that are produced by industrial routes, typically by Friedel–Crafts alkylation of arenes with linear olefins [79–81]. Such methods gives almost exclusively products with branched alkyl side chains. Arenes with linear side chains and their derivatives offer potentially different physical properties from branched species, such as increased thermal stability, but there are no established catalytic routes to synthesize them from hydrocarbon reagents. Thus, compared with conventional routes to alkylarenes, pincer-iridium catalysts potentially offer products otherwise inaccessible on the commodity chemical scale, in addition to the advantage of using low-cost *n*-alkane feedstock.

Curiously, *n*-dodecane and higher *n*-alkanes gave significant yields of benzene (Eq. 4.24), particularly at early reaction times. The initial rates of benzene production were no greater in runs in which aromatic or aliphatic cyclics were added prior to the reaction.

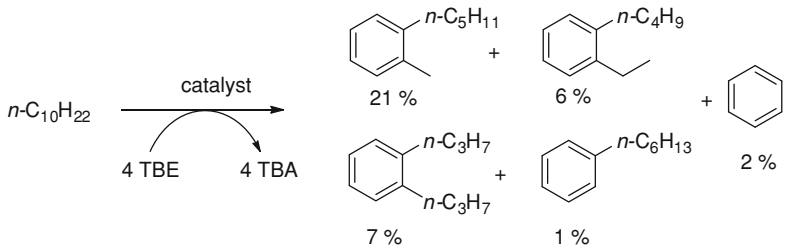

(4.24)

Thus benzene did *not* appear to be derived from a secondary reaction subsequent to aromatization of the *n*-alkane; the actual mechanism of benzene formation has yet to be determined [75].

4.6 Looking Ahead

Significant progress has been made in developing alkane dehydrogenation catalysts. The development of iridium pincer complexes has given rise to catalytic systems which exhibit high turnover numbers in both transfer dehydrogenations employing

acceptor olefins and in acceptorless modes, and convenient protocols have been devised to generate efficient supported iridium pincer catalyst systems. Pincer iridium catalysts have been coupled with olefin metathesis catalysts to generate a dual catalyst system for alkane metathesis which does not require a sacrificial acceptor. Multiple dehydrogenations of linear alkanes have been shown to result in conjugated trienes which, following electrocyclic ring closure and further dehydrogenation, produce valuable aromatic products.

Despite these advances many challenges remain including:

1. Development of inexpensive first-row transition metal catalyst systems.
2. Discovery of catalysts operating at lower temperatures which exhibit high selectivity for formation of alpha-olefins and no subsequent olefin isomerization activity.
3. Development of inexpensive acceptors. Oxygen would be ideal as an acceptor, requiring air stable complexes, probably non-phosphine based supporting ligands.
4. Development of functional group tolerant catalyst systems so that dehydrogenation may be used to selectively introduce unsaturation into complex molecules.

Opportunities also exist for incorporating alkane dehydrogenation into other dual catalyst systems as has been demonstrated for alkane metathesis.

Acknowledgments We gratefully acknowledge the National Science Foundation (Grant CHE-0719307) for supporting J.C., and the National Science Foundation Center for Enabling New Technologies through Catalysis (CENTC) for funding 165 aspects of the work discussed in this review, and for supporting M.F. and (in part) A.S.G and M.B.

References

1. Dean JA (ed) (1985) Lange's handbook of chemistry, 13th edn. McGraw-Hill, New York
2. Crabtree RH (1985) Chem Rev 85:245
3. Goldman AS, Ghosh R (2005) In: Dyker G (ed) Handbook of C–H transformations—applications in organic synthesis. Wiley-VCH, New York, p 616
4. Morales-Morales D (2009) Iridium complexes in organic synthesis. Wiley-VCH, Weinheim, p 325
5. Dobereiner GE, Crabtree RH (2010) Chem Rev 110:681
6. Choi J, MacArthur AHR, Brookhart M, Goldman AS (2011) Chem Rev 111:1761
7. Crabtree RH, Mihelcic JM, Quirk JM (1979) J Am Chem Soc 101:7738
8. Baudry D, Ephritikhine M, Felkin H (1980) J Chem Soc Chem Commun 24:1243
9. Baudry D, Ephritikhine M, Felkin H (1982) J Chem Soc Chem Commun 14:606
10. Baudry D, Ephritikhine M, Felkin H, Holmes-Smith R (1983) J Chem Soc Chem Commun 14:788
11. Felkin H, Fillebeen-Khan T, Gault Y, Holmes-Smith R, Zakrzewski J (1984) Tetrahedron Lett 25:1279
12. Felkin H, Fillebeen-Khan T, Holmes-Smith R, Lin Y (1985) Tetrahedron Lett 26:1999
13. Burk MJ, Crabtree RH, Parnell CP, Uriarte RJ (1984) Organometallics 3:816
14. Burk MJ, Crabtree RH, McGrath DV (1985) J Chem Soc Chem Commun 24:1829
15. Burk MJ, Crabtree RH (1987) J Am Chem Soc 109:8025

16. Sakakura T, Tanaka M (1987) J Chem Soc Chem Commun 10:758
17. Sakakura T, Tanaka M (1987) Chem Lett 16:1113
18. Sakakura T, Sodeyama T, Tokunaga Y, Tanaka M (1988) Chem Lett 17:263
19. Nomura K, Saito Y (1988) J Chem Soc Chem Commun 3:161
20. Maguire JA, Boese WT, Goldman AS (1989) J Am Chem Soc 111:7088
21. Maguire JA, Boese WT, Goldman ME, Goldman AS (1990) Coord Chem Rev 97:179
22. Maguire JA, Goldman AS (1991) J Am Chem Soc 113:6706
23. Maguire JA, Petrillo A, Goldman AS (1992) J Am Chem Soc 114:9492
24. Belli J, Jensen CM (1996) Organometallics 15:1532
25. Fujii T, Saito Y (1990) J Chem Soc Chem Commun 10:757
26. Aoki T, Crabtree RH (1993) Organometallics 12:294
27. Gupta M, Kaska WC, Jensen CM (1997) Chem Commun:461
28. Gupta M, Hagen C, Kaska WC, Cramer RE, Jensen CM (1997) J Am Chem Soc 119:840
29. Moulton CJ, Shaw BL (1976) J Chem Soc Dalton Trans 11:1020
30. Lee DW, Kaska WC, Jensen CM (1998) Organometallics 17:1
31. Ghosh R, Kanzelberger M, Emge TJ, Hall GS, Goldman AS (2006) Organometallics 25:5668
32. Xu W, Rosini GP, Gupta M, Jensen CM, Kaska WC, Krogh-Jespersen K, Goldman AS (1997) Chem Commun 23:2273
33. Liu F, Goldman AS (1999) Chem Commun 7:655
34. Krogh-Jespersen K, Czerw M, Zhu K, Singh B, Kanzelberger M, Darji N, Achord PD, Renkema KB, Goldman AS (2002) J Am Chem Soc 124:10797
35. Zhu K, Achord PD, Zhang X, Krogh-Jespersen K, Goldman AS (2004) J Am Chem Soc 126:13044
36. Liu F, Pak EB, Singh B, Jensen CM, Goldman AS (1999) J Am Chem Soc 121:4086
37. Herrmann WA, Prinz M (2002) In: Cornils B, Herrmann WA (eds) Applied homogeneous catalysis with organometallic compounds, vol 3, 2nd edn. Wiley-VCH, Weinheim, p 1119
38. van Leeuwen PWNM (2004) In homogeneous catalysis: understanding the art. Kluwer Academic Publishers, Dordrecht, p 101
39. Biswas S, Brookhart M, Choliy Y, Goldman A, Huang Z, Krogh-Jespersen K (2010) Abstracts of papers, 239th ACS national meeting, San Francisco, CA, United States, 21–25 March 2010, INOR
40. Renkema KB, Kissin YV, Goldman AS (2003) J Am Chem Soc 125:7770
41. Kanzelberger M, Singh B, Czerw M, Krogh-Jespersen K, Goldman AS (2000) J Am Chem Soc 122:11017
42. Goldman AS, Renkema KB, Czerw M, Krogh-Jespersen K (2004) In: Goldberg KI, Goldman AS (eds) Activation and functionalization of C–H bonds, ACS Symposium Series 885, Washington, DC, p 198
43. Biswas S, Choliy Y, Krogh-Jespersen K, Brookhart M, Goldman AS (2009) Abstracts of papers, 238th ACS national meeting, Washington, DC, United States, 16–20 Aug 2009, INOR
44. Morales-Morales D, Redon R, Yung C, Jensen CM (2004) Inorg Chim Acta 357:2953
45. Göttker-Schnetmann I, Brookhart M (2004) J Am Chem Soc 126:9330
46. Göttker-Schnetmann I, White P, Brookhart M (2004) J Am Chem Soc 126:1804
47. Biswas S, Ahuja R, Ray A, Choliy Y, Krogh-Jespersen K, Brookhart M, Goldman AS (2008) Abstracts of papers, 236th ACS national meeting, Philadelphia, PA, United States, 17–21 Aug 2008, INOR
48. Morales-Morales D, Redon R, Wang Z, Lee DW, Yung C, Magnuson K, Jensen CM (2001) Can J Chem 79:823
49. Haenel MW, Oevers S, Angermund K, Kaska WC, Hua-Jun Fan; Hall MB (2001) Angew Chem Intl Ed 40:3596
50. Punji B, Emge TJ, Goldman AS (2010) Organometallics 29:2702
51. Kundu S, Choliy Y, Zhuo G, Ahuja R, Emge TJ, Warmuth R, Brookhart M, Krogh-Jespersen K, Goldman AS (2009) Organometallics 28:5432

52. Kuklin SA, Sheloumov AM, Dolgushin FM, Ezernitskaya MG, Peregudov AS, Petrovskii PV, Koridze AA (2006) Organometallics 25:5466
53. Huang Z, Brookhart M, Goldman AS, Kundu S, Ray A, Scott SL, Vicente BC (2009) Adv Synth Catal 351:188
54. Vicente BC, Huang Z, Brookhart M, Goldman AS, Scott SL (2011) Dalton Trans 41:752
55. Burnett RL, Hughes TRJ (1973) Catalysis 31:55
56. Chen C-Y, O'Rear DJ (2008) Collect Czech Chem Commun 73:1105
57. Dry ME (2002) Catal Today 71:227<Query ID="Q6 Text="Reference [57] has been splitted into Refs. [57–60] and subsequent references are renumbered. Please check." –>
58. Leckel D (2009) Energy Fuels 23:2342
59. Kamara BI, Coetzee J (2009) Energy Fuels 23:2242
60. Hildebrandt D, Glasser D, Hausberger B, Patel B, Glasser BJ (2009) Science 323:1680
61. International Energy Agency (IAE) World Energy Outlook 2008, pp 250–261
62. Aleklett K, Hook M, Jakobsson K, Lardelli M, Snowden S, Soderbergh B (2010) Energy Policy 38:1398
63. Ayala LF, Kouassi JP (2007) Energy Fuels 21:1592
64. Stockle M, Knight T (2010) Hydrocarb Process 89:55
65. Vidal V, Theolier A, Thivolle-Cazat J, Basset J-M (1997) Science 276:99
66. Basset JM, Coperet C, Lefort L, Maunders BM, Maury O, Le Roux E, Saggio G, Soignier S, Soulivong D, Sunley GJ, Taoufik M, Thivolle-Cazat J (2005) J Am Chem Soc 127:8604
67. Roux EL, Taoufik M, Copéret C, Mallmann Ad, Jean Thivolle-Cazat Basset J-M, Maunders BM, Sunley GJ (2005) Angew Chem 44:6755
68. Goldman AS, Roy AH, Huang Z, Ahuja R, Schinski W, Brookhart M (2006) Science 312:257
69. Schrock RR, Murdzek JS, Bazan GC, Robbins J, DiMare M, O'Regan M (1990) J Am Chem Soc 112:3875
70. Schrock RR (2005) Chem Commun 22:2773
71. Nawara-Hultzsch AJ, Supplee C, Kundu S, Hackenberg J, Punji B, Goldman AS, Bailey BC, Schrock RR (2009) Abstract of papers, 238th ACS national meeting, Washington, DC, United States, 16–20 Aug 2009, INOR
72. Bailey BC, Schrock RR, Kundu S, Goldman AS, Huang Z, Brookhart M (2009) Organometallics 28:355
73. Huang Z, Rolfe E, Carson EC, Brookhart M, Goldman AS, El-Khalafy SH, MacArthur AHR (2010) Adv Synth Catal 352:125
74. Ahuja R, Kundu S, Goldman AS, Brookhart M, Vicente BC, Scott SL (2008) Chem Commun 2:253
75. Ahuja R, Punji B, Findlater M, Supplee C, Schinski W, Brookhart M, Goldman AS (2011) Nat Chem 3:167
76. Smiešková A, Rojasová E, Hudec P, Šabo L (2004) Appl Catal A 268:235
77. Davis R (1994) J Heterog Chem Rev 1:41
78. Komarewsky VI, Riesz CH (1939) J Am Chem Soc 61:2524
79. Rueping M, Nachtsheim BJ (2010) Beilstein J Org Chem 6(6):1
80. Olah GA, Reddy VP, Prakash GKS (2005) Kirk-Othmer Encycl Chem Technol 12(5th edn.):159
81. Perego C, Ingallina P (2002) Catal Today 73:3

Chapter 5
Alkane C–H Oxygenation Catalyzed by Transition Metal Complexes

Anna Company, Julio Lloret, Laura Gómez and Miquel Costas

Abstract Alkane oxidation reactions are of fundamental importance in bulk and fine chemistry, but the inert character of alkyl C–H bonds poses formidable challenges to the design of reagents that could enable their selective oxidation. Highly reactive-oxidizing reagents are needed, and this factor poses major problems in terms of chemo and regioselectivity. Despite all these conditionings, because of its technological and biological significance and implications, and because of the fundamental scientific challenge that selective oxidation of sp^3 C–H bonds represents, research in the field is rich, and major breakthroughs have appeared over the last years. Collected and discussed in the following pages are metal-based systems that mediate the catalytic oxidation of alkane C–H bonds leading to C–O bond formation under homogeneous conditions, and where organometallic interactions do not participate in the C–H bond breakage. The chapter has been focused in systems that have specific synthetic and or biological relevance, and/or cases where well-defined transition metal catalysts have been studied.

5.1 Introduction and Scope

The functionalization of hydrocarbons in general, and alkanes in particular, which come from natural gas and crude oil is of great technological interest because their abundance in nature makes them convenient chemical feedstocks [1–4]. On this

A. Company · J. Lloret · L. Gómez · M. Costas (✉)
Department de Química, Universitat de Girona, Campus de Montilivi,
17071 Girona, Spain
e-mail: miquel.costas@udg.edu

P. J. Pérez (ed.), *Alkane C–H Activation by Single-Site Metal Catalysis*,
Catalysis by Metal Complexes 38, DOI: 10.1007/978-90-481-3698-8_5,
© Springer Science+Business Media Dordrecht 2012

regard, selective and catalytic oxidation of raw materials is an important area for the chemical industry because of the need to produce oxygen-containing chemicals from fossil hydrocarbons.

On the other hand, oxidized alkane frameworks are ubiquitous constituents of organic molecules with biological relevance. The construction of these molecules is at the fundamental interest of modern synthetic organic chemistry. Because of their low reactivity, alkyl C–H bonds are not usually seen as functional groups, and their functionalization is commonly disregarded in organic synthesis. One-step selective transformation of ubiquitous alkyl C–H bonds of organic compounds into C–O bonds, a process that often needs several steps, will minimize functional group manipulations, thus enabling the rapid build-up of molecular complexity from inert functionalities, unlocking opportunities for markedly different synthetic strategies. Methodologies for selective oxidation of alkane C–H bonds can therefore offer the possibility to redesign synthetic organic chemistry [5–7].

The direct conversion of alkyl C–H into C–O bonds is a thermodynamically highly favorable transformation, but it faces very fundamental challenging problems related with the kinetically inert nature of C–H bonds [8]. Their general lack of reactivity arises from the fact that C and H atoms are held together by strong, non-polarized and localized bonds. Neither low-energy empty orbitals, nor high-energy filled orbitals that could facilitate a chemical reaction are available [5]. The lack of low barrier energy paths constitutes a substantial difference with regard to sp^2 and sp C–H bonds, which most commonly translates into a characteristically distinct reluctantly inert nature of the alkyl sp^3 C–H bond. In order to overcome this lack of reactivity problem, highly reactive-oxidizing reagents are needed, and this factor very much conditions the chemistry.

For bulk chemistry, a major challenge is to design sustainable processes. That requires design of chemical transformations with efficient atom economy, and that work under mild conditions.

For synthetic organic chemistry, the highly reactive nature of C–H oxidizing reagents poses major problems in terms of chemo and regioselectivity [6]. In terms of chemoselectivity, the first challenge is to direct oxidation towards C–H bonds when other functional groups, which are commonly more reactive, are present in substrate molecules. A second major challenge is the ability to stop functionalization at the required oxidation state, as the over-oxidation of functionalized products is often highly thermodynamically downhill, and kinetically more favorable in comparison with C–H bonds. In third place, regioselective C–H oxidation is a tremendous challenge. Most organic molecules contain many different types of C–H bonds, and usually there is very little difference in the electronic and structural characteristics among the various C–H bonds in alkanes. Therefore, developing transformations that regioselectively functionalize a C–H bond within a complex structure constitutes a challenge.

Despite all these conditionings, because of its technological and biological significance and implications, and because of the fundamental scientific challenge that selective oxidation of sp^3 C–H bonds represents, research in the field is rich, and major breakthroughs have appeared over the last years. Collected and

discussed in the following pages are different metal-based systems that have proven competent for mediating the catalytic oxidation of alkane C–H bonds under homogeneous conditions.

The purpose of this chapter is to review alkane oxidation systems, leading to C–O bond formation, where organometallic interactions do not participate in the C–H bond breakage [5]. Two very basic reactions are considered in this chapter, depending on the reagent that attacks the C–H bond;

a) Reactions where the C–H bond is attacked by a metal-oxo or metal-peroxo species
b) Reactions where the C–H bond is attacked by an organic radical, generally an oxygen atom centered type of radical (hydroxyl or alkoxyl radicals). This radical has been previously generated by reaction of the catalyst with the oxidant.

The former are the most interesting reactions because the metal can confer specific reactivity characteristic of the oxidizing species, which, in turn, can translate in selectivity properties.

In both cases, with very little exceptions, the reaction of the oxidizing species with the alkyl C–H bond leads to its homolytic cleavage, generating a carbon centered radical. The lifetime of this radical also defines the chemistry. When the radical has a relative long lifetime that permits escape from the solvent cage, it becomes a free-diffusing radical. Free diffusing radicals undergo stereoscrambling, and can be trapped by external O_2. That is the case for reactions initiated by hydroxyl or alkoxyl radicals. It is also the case for most metal centered reactions, where the C–H breakage reaction is executed by a transition metal complex (generally containing a metal-oxo unit). Differentiation between radical initiated or transition metal complex initiated C–H bond oxidations can be done on the basis of C–H regioselectivity considerations, because the selectivity of free radicals (generally hydroxyl and alkoxyl radicals) is known [9].

In some specific and most interesting cases, following C–H bond breakage, the C–O bond formation event is very fast, and the radical has a short lifetime that does not allow it to escape from the solvent cage, the reaction is stereospecific, and external O_2 is not incorporated into products.

There are also a few examples where C–H oxidations are proposed to occur via oxo-group insertion into a C–H bond. Such reaction is well established for dioxiranes [10], but a clear cut example for a transition metal complex is to the best of our knowledge, still lacking. That is in sharp contrast with the chemistry of metal-nitrene and metal-carbene units, for which ligand insertion into C–H bonds is well documented [11].

Because of the extensive literature, some selection has had to be made. Porphyrin systems have not been included in the chapter. The topic of C–H oxidation at metalloporphyrins by itself would suffice and justify a book, and excellent reviews and chapters can be found in the literature [12–14]. The so called Gif systems have not been reviewed either. These systems have been excellently reviewed [15–17], and further developments have not been accomplished since then.

We have decided also to focus on catalytic systems and not to include reagents that work only under stoichiometric conditions. In addition, we have chosen to specially focus the chapter in systems that can have specific synthetic and or biological relevance, and/or cases where well-defined transition metal catalysts are studied. We apology if the reader feels that some important contribution has passed unadverted to us. We have also chosen to organize the systems depending on the catalyst metal. Because iron complexes are the most extensively studied and because some mechanistic considerations arising from this chemistry can be translated into catalytic oxidations mediated by other transition metal ions, they will be first described.

5.2 Alkane C–H Oxidation Catalyzed by Iron Complexes

Based on environmental, sustainability and cost considerations, the development of iron-based catalytic oxidation technologies is considered a very attractive strategy [18–20], and it has become nowadays a very active field [18, 19]. The C–H oxidation chemistry taking place at non-heme iron dependent oxygenases has inspired the design of alkane oxidation catalysts [21–23]. Unfortunately, Fe-based oxidation reactions have traditionally been performed in conditions of large excess of substrate, because of overoxidation problems, which very much hampered their potential as tools in organic synthesis. On the other hand, the rich red-ox chemistry of iron complexes, the inherent challenges in the spectroscopic characterization of iron species, posed by their most common paramagnetic nature, and the presence of very subtle sensitive reaction landscapes traditionally have severely conditioned our understanding of the chemistry. Despite of these difficulties, the progress in the field during the last decade has been spectacular, and it has changed from free-diffusing radical transformations, with poor selectivity and synthetic value, to exquisitely site selective stereospecific C–H hydroxylations of complex organic molecules with synthetically useful yields. Relevant work in the field is discussed in the following pages. The number of papers in the iron catalyzed alkane C–H oxidation topic makes impossible to describe a full account of the published contributions. We have had then to make a somewhat subjective selection of relevant contributions. We apologize if the reader finds that in the selection process, some important work has passed unadverted to us.

5.2.1 Fenton Chemistry

The oxidation of tartaric acid by reaction between iron(II) salts and hydrogen peroxide under acidic aqueous solutions was originally reported by Fenton more than one century ago [24]. The species that originate from this combination, known as the “Fenton reagent”, are powerful and effective oxidants for a number

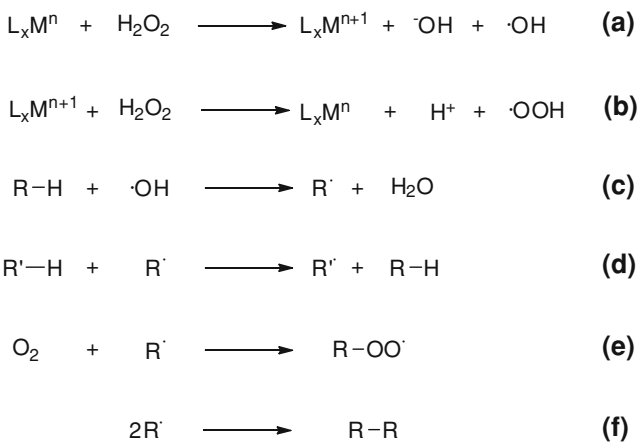

Scheme 5.1 Fenton reaction, and selected radical chain reactions that follow

of organic compounds, including alkanes. The definition of Fenton systems has been subsequently extended to the combination of red-ox active transition metal ions, and peroxides [25]. In a broad sense, the Fenton reaction bears tremendous relevance in biology [26], medicine [27, 28], environmental sciences [29–31], and in the field of oxidation chemistry [22, 32–34].

Haber and Weiss suggested that the mechanism of the Fenton reaction involves formation of highly reactive hydroxyl radicals (Scheme 5.1, reaction a) [35]. Hydrogen peroxide can also act as a reducing agent (reaction b), and in this reaction the metal ion recovers the initial reduced state.

The hydroxyl radical is a very powerful oxidant that reacts with alkanes generating a carbon centered alkyl radical (reaction c), that diffuses in solution. This alkyl radical is highly reactive and has a number of possible reactions. Some of these (d–f), but not all, are shown in Scheme 5.1. In general, the same set of reactions applies when alkyl peroxides react with transition metal ions, although alkoxyl radicals are less reactive than hydroxyl radicals, and thus they exhibit a higher degree of C–H selectivity than hydroxyl radicals [33].

Reaction of O_2 with alkyl radicals occurs at diffusion controlled rate [9]. Therefore, in the presence of O_2, reaction (e) most commonly dominates the chemistry, and the fate of the ROO· species determines the pattern of products that result from the reaction. In the particular case of alkylperoxyl radicals generated in the oxidation of methylene groups, bimolecular reaction of two radicals results in the formation of equimolar amounts of alcohol and ketone, by a Russell-type termination (Eq. 5.1) [36].

$$2\ \mathrm{RR'CHOO\cdot} \rightarrow [\mathrm{RR'CHOOOOCHRR'}] \rightarrow \mathrm{RR'CHOH} + \mathrm{O_2} + \mathrm{O} = \mathrm{CRR'} \quad (5.1)$$

Cycloalkanes are very commonly used as substrate tests in oxidation catalysis studies. The observation of nearly equimolar amounts of the corresponding alcohol and ketone constitutes a first strong indication that reactions take place via free-diffusing alkyl radicals [22].

Despite the fact that free-radical interpretation of the Fenton chemistry offers a solid frame to understand the experimental observations, the mechanism of the Fenton reaction is still a focus of debate [32, 37, 38], between authors that understand that reaction as a free-diffusing radical process [9, 25, 39], and those that defense a metal-centered interpretation [40, 41].

In the present chapter, the free-radical interpretation of the mechanism of this reaction becomes especially important since a good part of the catalytic systems described herein involve the reaction of red-ox active transition metal complexes with peroxides. Reaction patterns arising from some of these reactions are indicative of free-radical processes. However, as it will be obvious along this chapter, the use of the term "Fenton chemistry" as a general free-radical mechanistic frame to account for the reaction between red-ox active transition metals and peroxides is simply incorrect. Careful control of the catalyst structure and red-ox properties, type of peroxide, as well as reactions conditions permit the design of catalytic systems where the interaction between the peroxide and the catalyst results in the formation of metal centered reagents, with specific chemical properties. That is a very important consequence because the specific chemical properties of the metal centered reagent should determine its selectivity against chemically and stereochemically distinct C–H bonds, and thus it lays at the basis of selective C–H oxidation transformations.

5.2.2 Alkane Oxidation by Simple Iron Salts

Bolm et al. described a very simple system that employs $FeCl_3$ (2 mol %) in combination with TBHP (3 equiv.) as oxidant in pyridine at 82 °C to selectively oxidize benzylic C–H bonds. The method affords carbonyl compounds in modest (15 %) to excellent (>99 %) yields (Scheme 5.2) [42].

Alkylarenes and cycloalkanes can also be oxidized to the corresponding ketones in modest yields (35–50 %) with H_2O_2 (5 equiv.) in acetonitrile at room temperature, using $Fe(ClO_4)_2{\cdot}6H_2O$ (10 mol %) as catalyst and acetic acid (20 mol %) as additive (Scheme 5.3) [43].

In two recent reports, simple iron salts such as $Fe(ClO_4)_2$, $Fe(BF_4)_2$, $Fe(ClO_4)_3$, and $FeCl_3$, in combination with H_2O_2 were described to catalyze cyclohexane oxidation to a mixture of cyclohexanol and cyclohexanone with excellent yields (Table 5.1). The system is particularly remarkable because it works under rather simple and mild experimental conditions. It only requires 1 mol % catalyst loading, employs 1.5 equiv. H_2O_2 as oxidant, and reactions proceed at 50 °C under argon atmosphere for 2–23 h [44, 45]. The addition of a tridentate ligand dapb, or a pentadentate dapab (Scheme 5.4) improves the selectivity of the reactions (Table 5.1). In the latter case, the oxidation of the more challenging 1-heptane substrate was accomplished in 65 % yield to a mixture of alcohols and ketones (82 % substrate conversion).

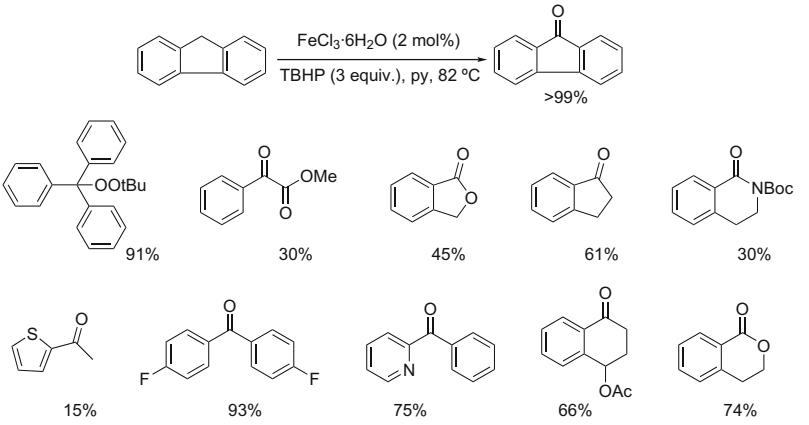

Scheme 5.2 Catalytic oxidation of alkylarenes with $FeCl_3$ salts and TBHP. Reaction scope along with yields is shown in the bottom

Scheme 5.3 Catalytic oxidation of cycloalkanes and alkylarenes with Fe^{II} salts and H_2O_2/AcOH. Reaction scope along with yields is shown in the bottom

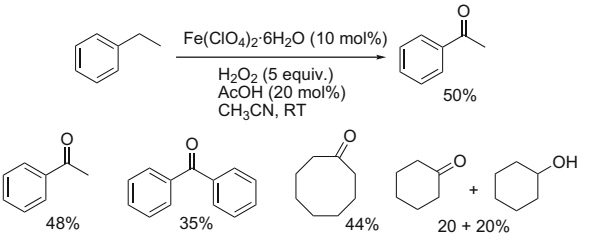

From a mechanistic point of view, several aspects of the system strongly suggest that reactions proceed via implication of freely diffusing radicals. In first place, no reaction occurs in acetone, and yields are also substantially diminished in the presence of DMSO. Both acetone and DMSO are well-known scavengers of free hydroxyl radicals. In addition, the alcohol/ketone ratio obtained in the oxidation of cyclohexane is close to 1, indicative of a Russell-type termination. Finally substantial amounts of cyclohexyl hydroperoxide (4–42 %) are detected in the reactions run under air. However, the exact nature of the species responsible for C–H bond breakage in such an efficient and selective manner is intriguing. The combination of H_2O_2 and simple iron salts can be seen as a simple Fenton process, where highly reactive hydroxyl radicals are generated. However, the simple implication of hydroxyl radicals is inconsistent with the nearly quantitative efficient consumption of the oxidant in the conversion of cyclohexane into alcohol and ketone products. Peroxide disproportionation processes arising from reaction of hydroxyl radicals with H_2O_2 are thus somewhat suppressed in this system. Substrate mass balance also discards substantial formation of cycloalkane overoxidized products, typical from Fenton-type of reactions. Therefore, the reported data is most consistent with the generation of a selective C–H oxidation reagent, which reacts with the substrate to form a carbon-centered diffusing radical.

Table 5.1 Catalytic Oxidation of cyclohexane with different iron catalysts and H_2O_2

Catalyst	Conversion	Products A/K/P[a](%)	A/K	Σ Product yields(%)	Byproducts (%)
$Fe(BF_4)_2$ + dapab	100	52.5/47.5	1.11	100	0
$Fe(BF_4)_2$ + dapb	100	32/42/6	0.77	81	19
$Fe(BF_4)_2$	100	29/19/34	1.55	81	19
$Fe(ClO_4)_2$ + dapb	100	37/54/-	0.68	91	9
$Fe(ClO_4)_2$	100	27/60/-	0.46	87	13
$FeCl_3$ + dapb	93	35/58/-	0.61	93	<1
$FeCl_3$	99	25/55/-	0.45	79	20

1 mol % catalyst/1.5 equiv. H_2O_2/50°C in acetonitrile under air
[a] Cyclohexanol/Cyclohexanone/Cyclohexyl peroxide

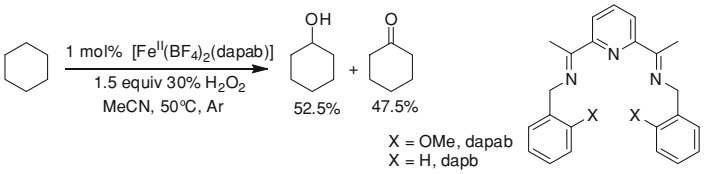

Scheme 5.4 Cyclohexane oxidation catalyzed by $[Fe^{II}(L)](BF_4)_2$

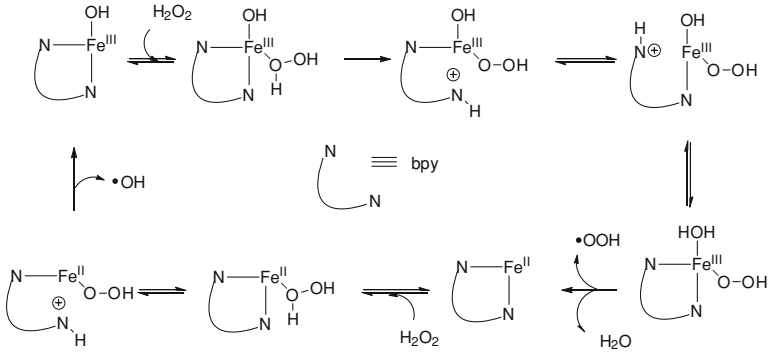

Scheme 5.5 Schematic proposal of the effect of bpy in Fe-catalyzed oxidations

Shul'pin et al. have described that 2,2′-bipyridine accelerates $FeCl_3$ catalyzed H_2O_2 oxidation of alkanes in acetonitrile solution at 60 °C [46]. Cyclohexyl hydroperoxide is initially formed, and then it is transformed in the course of the reaction into cyclohexanol and cyclohexanone. Oxidations are characterized by low C–H selectivity parameters reminiscent of those determined for hydroxyl-radical generating systems, and stereoscrambring is observed in the oxidation of *cis*-1,2-dimethylcyclohexane. The authors proposed that the bipyridine ligand facilitates proton-abstraction from a H_2O_2 molecule coordinated to the iron ion (Scheme 5.5).

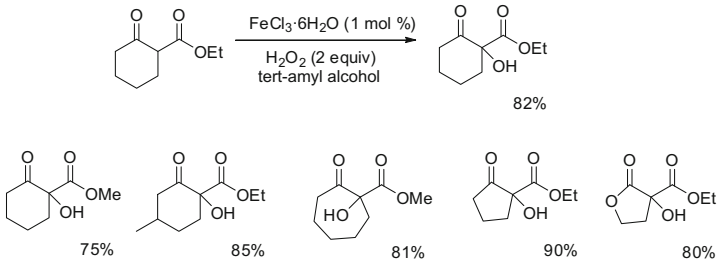

Scheme 5.6 Selective oxidation of β-ketoesters catalyzed by $FeCl_3{\cdot}6H_2O$

Beller et al. [47], recently described that $FeCl_3{\cdot}6H_2O$ in combination with H_2O_2 (2–6 equiv.) selectively hydroxylates β-ketoesters. Cyclic β-ketoesters are hydroxylated in excellent yields (75–90 %) by using 1 mol % catalyst and 2 equiv. of 30 wt % H_2O_2 in tert-amyl alcohol (Scheme 5.6). When a large loading of $FeCl_3{\cdot}6H_2O$ is employed, chlorination instead of hydroxylation takes place (Eq. 5.2).

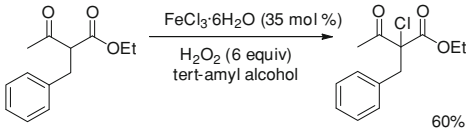

(5.2)

5.2.3 Alkane Oxidation by Polynuclear Fe^{III} Complexes

5.2.3.1 Prototypical Examples

Oxo and/or carboxylate bridged diiron complexes can be seen as simple structural models of the active site of hydroxylases such as soluble methane monooxygenase, or alkane monooxygenases [48–50], which mediate the hydroxylation of substrates with strong C–H bonds. Because of that, and because of the rather simple synthetic accessibility to such type of compounds, they have been widely studied as alkane oxidation catalysts [22]. Prototypical structures of alkane oxidation catalysts studied are shown in Scheme 5.7.

From the point of view of product yields, substrate conversion into products attained by these catalysts is modest or moderate. In most of the cases, reactions are performed under conditions of large excess of substrate. 10–100-fold excess of substrate is commonly employed. In addition, substrate scope is scarce and often limited to cycloalkanes. These reactions bear then very little synthetic utility, but instead they were mostly studied with the aim of providing functional and structural models of non-heme iron-dependent oxygenases, and in some cases to study mechanistic details of the reactions [22].

From the perspective of product yields, two examples appear particularly remarkable; the dinuclear $[Fe^{III}_2(\mu\text{-}O)(NO_3)_2(BBP)_2(CH_3OH)_2](NO_3)_2$, (Scheme 5.8)

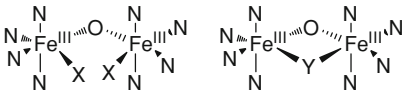

Scheme 5.7 General schematic diagram of oxo-bridged diiron complexes studied in alkane oxidation reactions. N atoms stand for N-based ligands, generally of bidentate or tetradentate nature

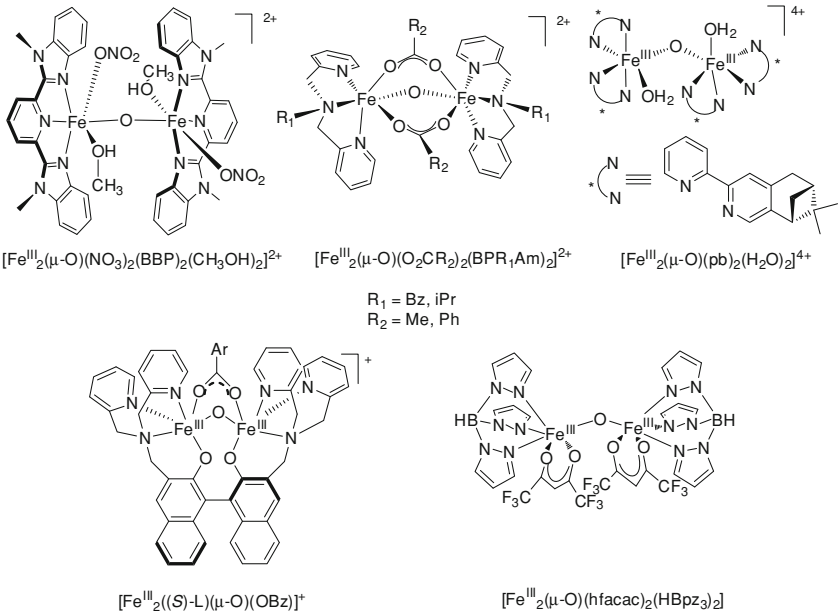

Scheme 5.8 Selected oxo-bridged diferric complexes employed in oxidation catalysis

catalyzes the oxidation of cyclohexane with 51 % substrate conversion into an equimolar mixture of cyclohexanol and cyclohexanone (A/K = 1.2), when using TBHP as oxidant [51]. On the other hand, the hexanuclear iron carboxylate $[Fe^{III}_6(\mu_3\text{-O})_3(\mu\text{-OH})(p\text{-}NO_2C_6H_4CO_2)_{11}(DMF)_4]$, which contains a very unusual $[Fe^{III}_6(\mu_3\text{-O})_3(\mu\text{-OH})]^{11+}$ core catalyzes cyclohexane oxidation using H_2O_2 as oxidant, affording mixtures of cyclohexanol and cyclohexanone in up to 29.7 % yield based on substrate [52]. In both cases, reaction patterns are indicative of reactions that involve formation of free-diffusing carbon-centered radicals.

Indeed, from the point of view of reaction mechanisms, free-radical paths generally dominate the chemistry. Reaction of the complexes with peroxides show product selectivity patterns indicative of the generation of hydroxyl or alkoxyl radicals, that are finally responsible for a H-abstraction of the substrate, thus

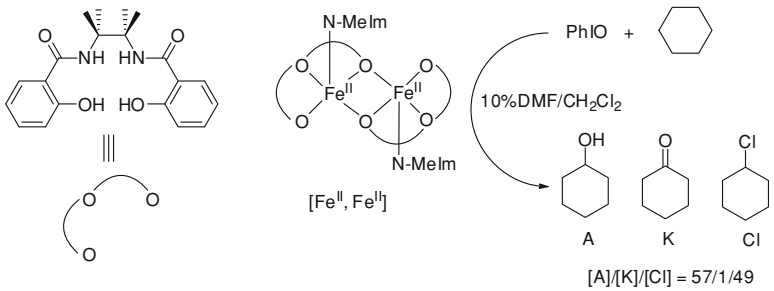

Scheme 5.9 Schematic diagram of the diferrous complex described by Caradonna, and its catalytic oxidation of cyclohexane

initiating free-diffusion radical paths [22, 51–54]. Cyclohexane is oxidized to a roughly 1:1 mixture of cyclohexanol and cyclohexanone, indicative of a Russell-type termination [36]. Yields are very sensitive to the presence of O_2, which is incorporated into products, and finally stereoscrambling in oxidized substrates is observed.

Nevertheless, selected μ-oxo bridged diferric catalysts, under special reaction conditions provide selectivity patterns in their reactions that suggest the involvement of a metal centered hydroxylation reaction [55, 56].

$[Fe^{III}_2(\mu\text{-O})(O_2CR_2)_2(BPR_1Am)_2]^{2+}$ and $[Fe^{III}_2((S)\text{-L})(\mu\text{-O})(OBz)](ClO_4)$ (Scheme 5.8), catalyze the oxidation of cyclohexane with MCPBA, affording high A/K ([alcohol]/[ketone]) ratios and high normalized $3^\circ/2^\circ$ C–H selectivity values in the oxidation of adamantane [55, 57]. It is interesting to notice that the reaction patterns associated to $[Fe^{III}_2((S)\text{-L})(\mu\text{-O})(OBz)](ClO_4)$ catalyzed oxidations employing H_2O_2 or TBHP as oxidant are more consistent with free-diffusing radical type of transformations. Therefore, both the oxidant and the nature of the catalyst appear to be crucial in defining reaction mechanisms.

$[Fe^{III}_2(\mu\text{-O})(L)_4(H_2O)_2]^{4+}$ (L = Phen, bpy and derivatives) in combination with H_2O_2 catalyze the oxidation of *trans*-1,4-dimethylcyclohexane with partial retention of the configuration, and only partial cyclopropane ring opening in the oxidation of the radical clock *trans*-1-methyl-2-phenyl-cyclopropane [58].

The $[Fe^{III}_2(\mu\text{-O})(hfacac)_2(HBpz_3)_2]$ complex (Scheme 5.8) uses a combination of O_2/Zn/HOAc to oxidize alkanes with very unusual C–H selectivity parameters. A high A/K = 23 is obtained in the oxidation of cylohexane, and the normalized selectivity for the tertiary C–H bond of adamantane is 82 [59].

Caradonna and co-workers have described that the diiron(II) compound shown in Scheme 5.9 catalyzes the hydroxylation of cyclohexane with PhIO as oxidant with high turnover numbers (>100) and very high selectivity for forming cyclohexanol vs cyclohexanone (A/K = 57) [60]. Large amounts of chlorocyclohexane are also formed presumably by reaction of carbon-centered radicals with CH_2Cl_2 solvent. A remarkable aspect of this complex is that catalytic efficiency depends critically in the oxidation state of the two iron atoms; high product yields are obtained for the $[Fe^{II}, Fe^{II}]$ complex, but both the $[Fe^{II}, Fe^{III}]$ and the $[Fe^{III}, Fe^{III}]$ proved to be practically inactive in cyclohexane and toluene oxidation reactions.

Scheme 5.10 Asymmetric oxidations performed by chiral diferric complexes

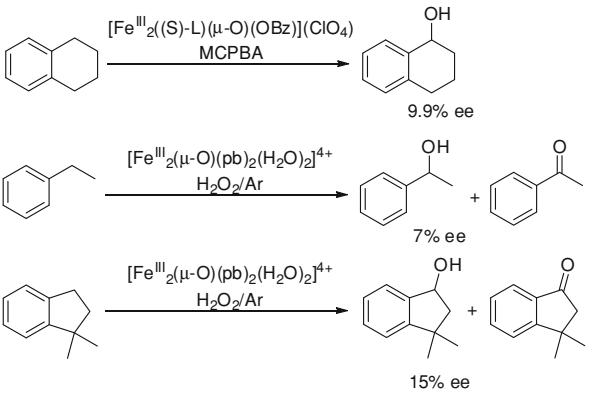

Mechanistic studies indicate that reaction of the [Fe^{II}, Fe^{II}] complex with $2e^-$ oxidants cause the formation of highly reactive, short-lived [Fe^{II}, $Fe^{IV}O$] mixed-valence intermediates that are responsible for the C–H oxidation activity. In the absence of substrates, the mixed valence species collapse via reorganization to a catalytically inactive Fe^{III}-O-Fe^{III} dimer [61–63].

5.2.3.2 Chiral Complexes in C–H Oxidation Reactions

Diferric oxo-bridged chiral complexes (Schemes 5.8 and 5.10) have been studied with the aim of developing asymmetric C–H oxidation catalysts, but little success has been obtained so far. The binaphthol based complex [Fe^{III}_2((*S*)-L)(μ-O)(OBz)](ClO_4) catalyzes the oxidation of tetralin with MCPBA, affording the corresponding ketone with a very modest 9.9 % ee [57]. On the other hand, the pineno-bipyridine based diferric complex [$Fe^{III}_2(\mu\text{-O})(pb)_2(H_2O)_2]^{4+}$ catalyzes the oxidation of ethylbenzene with H_2O_2 to a mixture of acetophenone and sec-phenethyl alcohol (2.9 TN), the latter with 7 % ee. Hydroxylation of dimethylindane affords the corresponding alcohol (1.8 TN, 15 % ee) and ketone (1.5 TN) [64].

5.2.3.3 Methane Oxidation at Oxo-Bridged Polynuclear Iron Complexes

Selected examples of polynuclear iron complexes have been reported to be capable of mediating the challenging oxidation of methane. Sorokin et al., described the catalytic oxidation of methane with H_2O_2 at mild temperatures (25–60 °C) by using a μ-nitrido diiron phthalocyanine catalyst (Fe^{III} $Pc^tBu_4)_2N$ (Scheme 5.11). In acetonitrile solution, methane oxidation afforded formic acid as the main product. Conclusive evidence that products arise from methane instead of acetonitrile oxidation was obtained by isotopic labeling experiments, and by supporting the catalyst over silica, and performing reactions in water. In water solvent, methane was oxidized to a mixture of methanol, formaldehyde and formic acid, with total TN over 400.

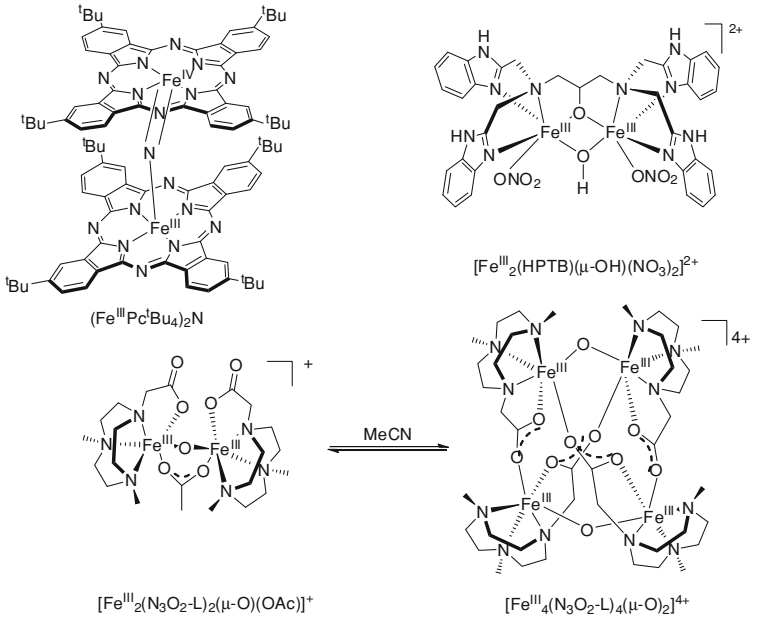

Scheme 5.11 Structural diagram of diiron complexes that catalyze methane oxidation. The bottom part of the diagram also show the equilibrium between $[Fe_2(N_3O_2\text{-}L)_2(\mu\text{-}O)(OAc)]^+$ and $[Fe_4(N_3O_2\text{-}L)_4(\mu\text{-}O)_2]^{4+}$

Furthermore, isotopic labeling experiments demonstrated that formic acid was derived from methane oxidation. GC–MS of the formic acid formed from the oxidation of isotopically labeled CH_4 (47 % $^{13}CH_4$ and 53 % $^{12}CH_4$) indicated it to be 44 % $H^{13}COOH$, within experimental error agreement with the isotopic composition of the substrate. The authors propose that a formally described nitride bridged species Fe^{IV}-N-Fe^{V}(O), formed via H_2O_2 2e$^-$ oxidation of the Fe^{IV}-N-Fe^{III} resting state of the catalyst is directly responsible for the oxidation of methane [65].

Süss-Fink and co-workers have reported that the tetranuclear complex $[Fe^{III}_4(N_3O_2\text{-}L)_4(\mu\text{-}O)_2]^{4+}$ (Scheme 5.11) catalyzes the oxidation of methane with H_2O_2 in water to afford methanol, attaining up to 24 catalytic cycles in 4 h. In acetonitrile, the complex is in equilibrium with the dimeric $[Fe^{III}_2(N_3O_2\text{-}L)_2(\mu\text{-}O)(OAc)]^+$ form [54]. Higher linear alkanes and cycloalkanes are also oxidized by both the dinuclear and the tetranuclear complexes in acetonitrile solution, with up to 43 TN. Cyclohexane is initially oxidized to cyclohexylhydroperoxide, which then evolves into cyclohexanol and cyclohexanone. Stereoscrambled tertiary alcohols are formed in the oxidation of substrates containing tertiary C–H bonds such as *cis*-1,2-dimethylcyclohexane. These reaction patterns are indicative of the implication of free-diffusing radicals. However, on the basis of C–H site selectivity patterns, the authors conclude that a selective oxidant rather than hydroxyl radicals are the species that initiate C–H oxidation.

Shul'pin et al. have described that $[Fe^{III}_2(HPTB)(\mu\text{-}OH)(NO_3)_2](NO_3)_2$ (Scheme 5.11) in combination with certain aminoacids (pyrazine-2-carboxylic acid, pyrazine-2,3-dicarboxylic acid and picolinic acid), catalyzes the oxidation of light alkanes such as ethane (21 TN) and methane (4 TN) with H_2O_2. Ethane was transformed into ethyl hydroperoxide, acetaldehyde and trace amounts of acetic acid. Methyl hydroperoxide and formaldehyde were obtained from the oxidation of methane. Reactions proceed with low C–H bond site selectivites, and stereo-scrambling is observed in the oxidation of decalines. On these bases, the authors propose that hydroxyl radicals are responsible for the chemistry [66].

5.2.4 Alkane Oxidation by Mononuclear Iron Complexes with N-based Ligands

Mononuclear iron(II) complexes containing N-based ligands have been very extensively pursued during the last decade [22, 23, 67]. A particularly relevant aspect of the use of N-based ligands is that it led to the discovery of very selective iron catalysts that perform the stereospecific hydroxylation of alkanes (Eq. 5.3). Synthetically useful synthetic methodologies have also emerged from the use of these complexes. A very challenging aspect of this chemistry is that catalytic activity of a complex is dramatically dependent on ligand structure. Accurate design of the ligand is necessary and not obvious.

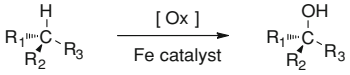

(5.3)

5.2.4.1 Iron Complexes with Tridentate and Pentadentate Ligands

Representative examples of iron complexes containing tridentate [68, 69], and pentadentate [70–73], ligands explored in oxidation catalysis are shown in Schemes 5.12 and 5.13 and results on catalysis are collected in Table 5.2. Tridentate iron(II) complexes shown in Scheme 5.12 react with H_2O_2 to afford small amounts of cyclohexane oxidation products (1.4–17.5 % with respect to H_2O_2, < 1 % with respect to substrate). The identification of cyclohexyl hydroperoxide as a reaction product, the low A/K ratio (1–3) and the low efficiency of the reactions suggest that the role of the iron complexes is the initiation of Fenton-type processes.

Complexes with pentadentate ligands are shown in Scheme 5.13. Those incorporating amido binding groups were first explored as structural and functional models of Fe-Bleomycin [70, 71]. Fe-Bleomycin is a member of a family of

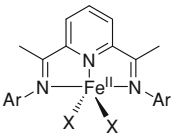

X = Cl, CF_3SO_3

Ar = 2,6-iPr_2-C_6H_3
2,6-Me_2-C_6H_3

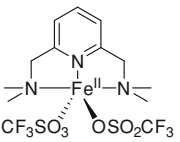

$[Fe^{II}(OTf)_2(Py(NMe_2)_2)]$

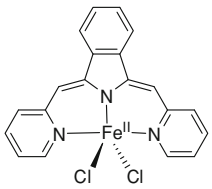

$[Fe^{II}(Cl)_2(Ind)]$

$[Fe^{II}Cl_2(Py(Im^{iPr2}Ph)_2)]$, X = Cl, Ar = 2,6-$iPr_2$-$C_6H_3$
$[Fe^{II}(OTf)_2(Py(Im^{iPr2}Ph)_2)]$, X = Cl, Ar = 2,6-$iPr_2$-$C_6H_3$
$[Fe^{II}Cl_2(Py(Im^{Me2}Ph)_2)]$, X = Cl, Ar = 2,6-$Me_2$-$C_6H_3$
$[Fe^{II}(OTf)_2(Py(Im^{Me2}Ph)_2)]$, X = Cl, Ar = 2,6-$Me_2$-$C_6H_3$

Scheme 5.12 Iron catalysts with tridentate N-based ligands. OTf stands for CF_3SO_3 anion

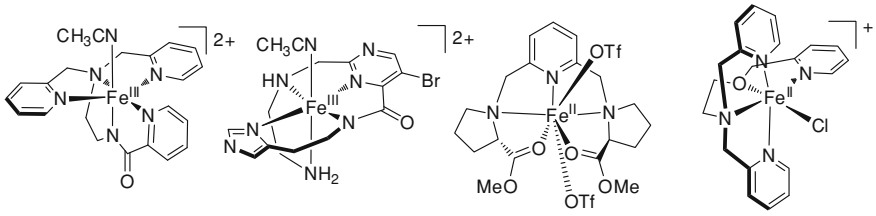

$[Fe^{III}(PaPy_3)(CH_3CN)]^{2+}$ $[Fe^{III}(PMA)(CH_3CN)]^{2+}$ $[Fe^{II}(CF_3SO_3)_2(Py(ProMe)_2)]$ $[Fe^{II}(tpoen)(Cl)]^{+}$

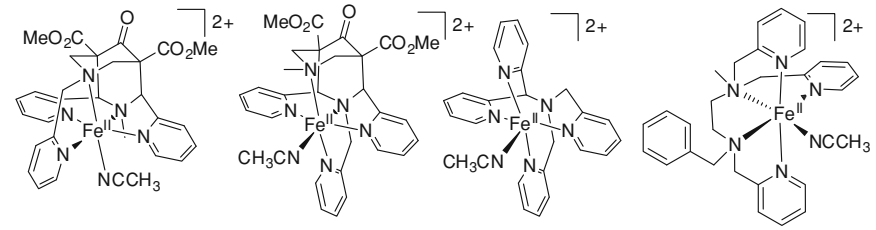

$[Fe^{II}(BpdL_2)(CH_3CN)]^{2+}$ $[Fe^{II}(BpdL_3)(CH_3CN)]^{2+}$ $[Fe^{II}(N4Py)(CH_3CN)]^{2+}$ $[Fe^{II}(BnTPEN)(CH_3CN)]^{2+}$

Scheme 5.13 Iron catalysts with pentadentate ligands

antitumor antibiotics, which mediates very fast double-strand DNA cleavage [74]. Activated Bleomycin, responsible for oxidative DNA cleavage has been spectroscopically characterized as a ferric hydroperoxide species [70, 71]. The complexes $[Fe^{III}(PaPy_3)(CH_3CN)]^{2+}$ and $[Fe^{III}(PMA)(CH_3CN)]^{2+}$ were designed as synthetic models of Bleomycin, and were also studied in the oxidation of alkanes using TBHP and H_2O_2 as oxidants. Oxidation of cyclohexane was accomplished with moderate yields with respect to the oxidant, to a nearly equimolar mixture of cyclohexanol and cyclohexanone. ^{t}Butyl cyclohexylperoxide was also obtained as oxidation product when TBHP was used as oxidant, especially when reactions

Table 5.2 Oxidation of alkanes with H_2O_2 catalyzed by Fe^{II} complexes containing tridentate and pentadentate ligands

Catalyst	Oxidant Cat/Ox/Subs[a]	Cyclohexane Efficiency[b] (%)	A/K[c]	KIE[d]	Adamantane 3°/2°[e]	Ref
Tridentate Ligands						
$[Fe^{II}Cl_2(PyIm^{IPr2}Ph_2)]$	H_2O_2 1:10:1000(Air)	1.4	1.3			[68]
$[Fe^{II}(OTf)_2(PyIm^{IPr2}Ph_2)]$	H_2O_2 1:10:1000(Air)	5.2	1.0			[68]
	H_2O_2 1:100:1000(Air)	1.4	1.8			[68]
$[Fe^{II}Cl_2(PyIm^{Me2}Ph_2)]$	H_2O_2 1:100:1000(Air)	1.9	2.1			[68]
$[Fe^{II}(OTf)_2(PyIm^{Me2}Ph_2)]$	H_2O_2 1:10:1000(Air)	4.9	1.5			[68]
	H_2O_2 1:10:1000(Air)	2.0	3.1			[68]
$[Fe^{II}(OTf)_2(Py(N^{Me2})_2)]$	H_2O_2 1:10:1000(Air)	3.9	1.3			[68]
$[Fe^{II}Cl_2(Ind)]$	H_2O_2 1:10:1000(Air)	17.5	0.7			[69]
Pentadentate Ligands						
$[Fe^{III}(PaPy_3)(CH_3CN)]^{2+}$	H_2O_2 1:150:200(Air)	18	1.0	–	–	[71]
	TBHP 1:150:200(Air)	13	0.7	–	–	[71]
$[Fe^{III}(PMA)(CH_3CN)]^{2+}$	TBHP 1:100:350(N_2)	62 [f]	1.0	6.5	6.2	[70]
	$H_2O_2$1:100:350(N_2)	15	0.9	–	–	[70]
$[Fe^{II}Cl(tpoen)]^{+}$	$H_2O_2$1:200:1000(N_2)	12.2	2.4		3.2	[75]
	MCPBA1:200:1000(N_2)	24.9	3.2		18.5	[75]
$[Fe^{II}(N4Py)(CH_3CN)]^{2+}$	MCPBA 1:100:1000(N_2)	38	5.6	4.5	18	[76]
	PAA 1:100:1000(N_2)	9	4.6	4.9	9	[76]
	H_2O_2 1:100:1000(N_2)	43	1.4	1.5	3.1	[77]
$[Fe^{II}(BpdL_2)(CH_3CN)]^{2+}$	$H_2O_2$1:100:1000(Ar)	32	2.1	2.2	3.6	[79]
$[Fe^{II}(BpdL_3)(CH_3CN)]^{2+}$	$H_2O_2$1:100:1000(Ar)	30	1.0	3.8	5.0	[79]
$[Fe^{II}(OTf)_2(Py(ProMe)_2)]$	TBHP 1:10:500(Air)	42 [g]	0.6		12.6	[72]

[a] Catalyst:Oxidant:Substrate ratio, in acetonitrile
[b] With respect to Oxidant,
[c] A = cyclohexanol, K = cyclohexanone. A/K = (mols A/mols K)
[d] Measured in cyclohexanol formation from competitive oxidation of equimolar amounts of c-C_6H_{12} and c-C_6D_{12}
[e] 3°/2° = 3x(1-adamantanol)/(2-adamantanol + 2-adamantanone)
[f] 5.3 % Cyclohexyl-tertbutylperoxide was also obtained
[g] Yield = 10 x([alcohol] + [ketone])/[TBHP]

were run under N_2. Overall, the product pattern is consistent with oxidations being performed by ^{t}butoxyl radicals generated via a Fenton-type process.

More recently, $[Fe^{II}(N4Py)(CH_3CN)]^{2+}$, $[Fe^{II}Cl(tpoen)]^{+}$ and bispidine-based $[Fe^{II}(BpdL_2)(CH_3CN)]^{2+}$ and $[Fe^{II}(BpdL_3)(CH_3CN)]^{2+}$ complexes were also studied as alkane oxidation catalysts [75, 76, 78, 79]. Using H_2O_2 as oxidant, and under conditions of large excess of substrate, moderate to good yields were obtained in the oxidation of cyclohexane. Under inert atmospheres, the four complexes afford analogous low A/K ratios (1.0–2.4) in the oxidation of cyclohexane, KIE values $\sim$1.5–3.8, relative small 3°/2° ratios in adamantane oxidation (3.1–5), and large incorporation of O_2 into oxidation products when reactions are run under O_2. The sum of these observations strongly supports the implication of

hydroxyl radicals in these transformations, presumably formed via Fenton-type reactions between Fe^{II} complexes and H_2O_2.

On the other hand, the use of peracids (MCPBA and peracetic acid (PAA)) in combination with $[Fe^{II}(N4Py)(CH_3CN)]^{2+}$ and $[Fe^{II}(Cl)(tpoen)]^{+}$ results in strikingly different reaction patterns that strongly suggest the implication of a more selective oxidant [75, 76]. Oxidation of cyclohexane by $[Fe^{II}(N4Py)(CH_3CN)]^{2+}$ exhibits a large KIE ($4.5 > KIE > 4.9$) and a large cyclohexanol/cyclohexanone ratio ($4.3 > A/K > 7.2$). With both catalysts, the tertiary C–H bond of adamantane is oxidized with high selectivity ($18.5 > 3°/2° > 9$). In the case of $[Fe^{II}(N4Py)(CH_3CN)]^{2+}$, the authors propose that a $Fe^{IV} = O$ species, which is spectroscopically detected under catalytic conditions, is responsible for the selective C–H oxidation reactions.

An iron complex with a pentadentate ligand $[Fe^{II}(Bntpen)]^{2+}$ has been recently studied in the generation of $[Fe^{IV}(O)(Bntpen)]^{2+}$ by using cerium(IV)ammonium nitrate (CAN) as oxidant and H_2O as oxygen source [73]. The $Fe^{IV} = O$ species species is competent for performing the stoichiometric oxidation of an alkyl arene. On these bases, catalytic oxidation of ethylbenze to acetophenone (9 TN) and 1-phenylethanol (1 TN) was accomplished by using $[Fe^{II}(Bntpen)]^{2+}$ (0.02 mM) as catalyst and CAN (10 mM) as oxidant. ^{18}O-labelling studies in the oxidation of thioanisole indicated that water is the oxygen source in the oxidation reactions.

Departing from N-only based systems, Gebbink et al. have described an interesting diastereopure seven-coordinate iron(II) complex $[Fe^{II}(OTf)_2(Py(ProMe)_2)]$ that adopts an unusual pentagonal bipyramidal coordination geometry [72]. Under conditions of large excess of substrate (500 equiv.), this proline-based complex catalyzes ethylbenzene oxidation with TBHP (10 equiv.), to afford acetophenone (5.4 TN) and 1-phenylethanol (4 TN) with a modest 6.5 % ee. This constitutes a unique report where stereoselective (albeit very modest) C–H bond oxidation with a mononuclear iron catalyst has been accomplished.

5.2.4.2 Iron Complexes with Tetradentate Ligands

Representative examples of these ligands are shown in Scheme 5.14. Two main families of complexes bearing tetradentate ligands have been most studied in the oxidation of alkanes: tpa (tripodal) and mep (linear) families [80–84]. Mononuclear iron(II) complexes $[Fe(mep)(CH_3CN)_2]^{2+}$ and $[Fe(tpa)(CH_3CN)_2]^{2+}$ are specially efficient catalysts in terms of H_2O_2 oxidant converted into products, but most interestingly, the mechanistic probes clearly point towards the mediation of metal-based oxidants (Table 5.3) [81]. Oxidation of cyclohexane affords mainly cyclohexanol, and minor amounts of cyclohexanone. Oxidation of *cis*-1,2-dimethylcyclohexane occurs at the tertiary C–H stereospecifically. Adamantane is oxidized with a high 3°/2° selectivity, and kinetic isotope effects evaluated in the competitive oxidation of cyclohexane vs cyclohexane-d_{12} are relatively high (3–4.3), indicative that the breakage of the C–H bond is involved in the rate-determining step of the reactions. More recently, a new family of tetradentate

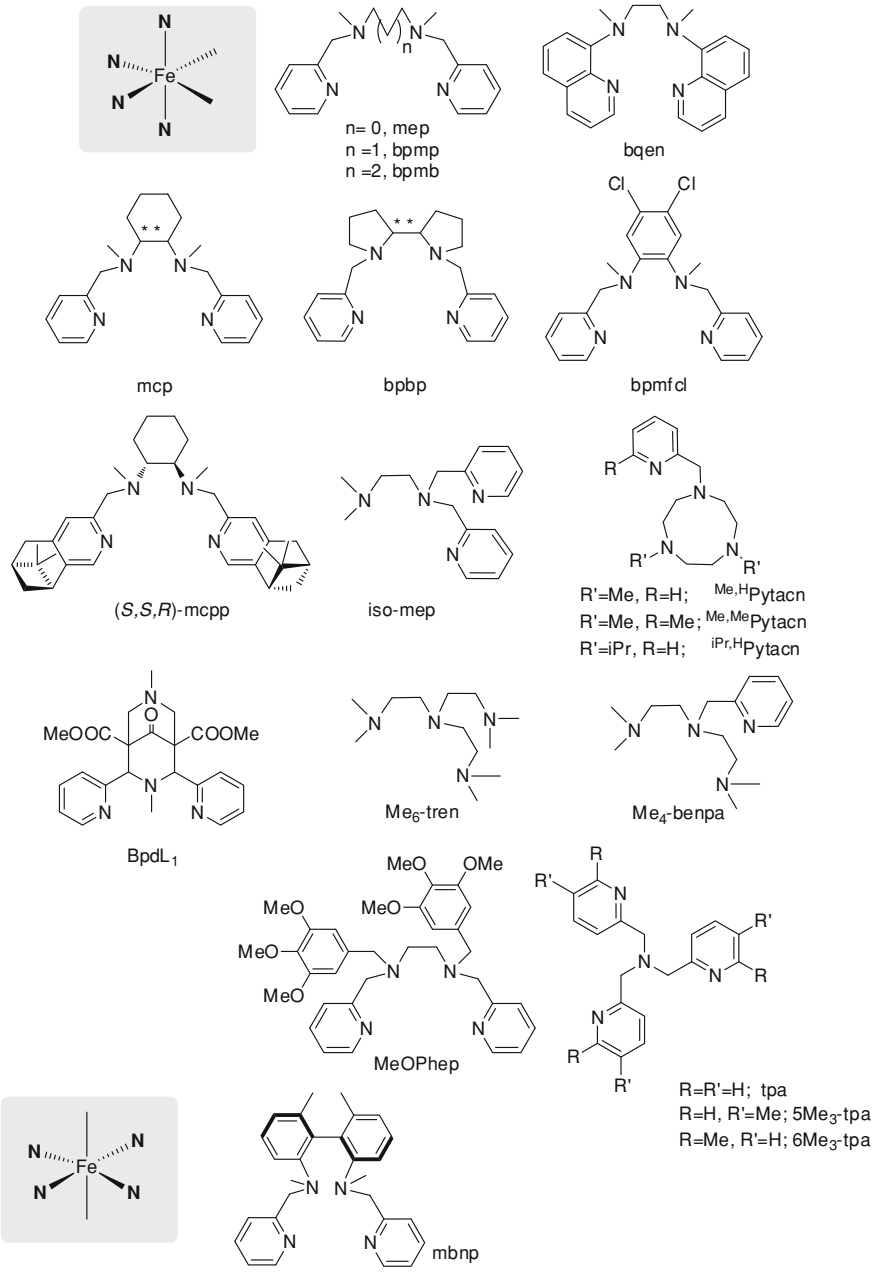

Scheme 5.14 Schematic representation of relevant tetradentate ligands used to prepare mononuclear iron(II) complexes to perform alkane oxidations

Table 5.3 Oxidation of alkanes with H_2O_2 catalyzed by different iron(II) complexes

		Cyclohexane	*cis*-1,2-DMCH	Adamantane		
Entry	Complex	A + K (A/K)[a]	KIE	RC (%)[b]	3°/2°[c]	Ref
1	$[Fe^{II}(tpa)(CH_3CN)_2]^{2+}$	3.2 (5)	3.5	100	17	[81]
2		29 (5.9)	3.1			[82]
3	$[Fe^{II}(5Me_3\text{-}tpa)(CH_3CN)_2]^{2+}$	4.0 (9)	3.8	100	21	[81]
4	$[Fe^{II}(6Me_3\text{-}tpa)(CH_3CN)_2]^{2+}$	2.9 (2)	3.3	54	15	[81]
5	$[Fe^{II}(mep)(CH_3CN)_2]^{2+}$	6.3 (8)	3.2	96	15	[81]
6		48 (2.5)[d]				[82]
7	$[Fe^{II}(bqen)(CH_3CN)_2]^{2+}$	5.1 (5)	–	–	–	[83]
8		30 (2.3)[d]				[83]
9	$[Fe^{II}(MeOPhep)(CH_3CN)_2]^{2+e}$	3.8 (8)	–	82	–	[87]
10	$[Fe^{II}Cl_2(MeOPhep)]^{e}$	0.6 (1)	–	0	–	[87]
11	α-$[Fe^{II}(OTf)_2(mcp)]$	5.9 (9)	3.2	>99	15	[89]
12	β-$[Fe^{II}(OTf)_2(mcp)]$	1.9 (0.9)	4.0	68	17	[89]
13	$[Fe^{II}(OTf)_2(^{Me,H}Pytacn)]$	6.5 (12)	4.3	93	30	[86]
14		39 (2.6)[d]				[86]
15	$[Fe^{II}(OTf)_2(^{Me,Me}Pytacn)]$	7.6 (10)	3.4	94	20	[86]
16		64 (4.3)[d]				[86]
17	$[Fe^{II}(BpdL_1)(CH_3CN)_2]^{2+}$	24 (1.5)	5.2	–	17	[79]
18	$[Fe^{II}(OTf)_2(iso\text{-}mep)]$	3.2 (6.8)	3.4	–	–	[83]
19	$[Fe^{II}(OTf)_2(Me_4\text{-}benpa)]$	0.34 (3.7)	2.1	–	–	[83]
20	$[Fe^{II}(OTf)_2(Me_6\text{-}tren)]$	0.32 (1.3)	1.8	–	–	[83]
21	$[Fe^{II}(OTf)_2(bpmfcl)]$	6.2 (2.4)	–	–	–	[84]
22		23 (2.2)[d]				[84]
23	$[Fe^{II}(OTf)_2(bpmp)]$	4.2 (1.4)	–	–	–	[84]
24		6 (1.4)[d]				[84]
25	$[Fe^{II}(OTf)_2(bpmb)]$	0	–	–	–	[84]
26	$[Fe^{II}(OTf)_2(mbnp)]$	0.95 (2.1)	–	–	–	[88]

[a] Catalyst:H_2O_2:alkane = 1:10:1000. Turnover number (TN, mols of product/mols of catalyst), A = cyclohexanol, K = cyclohexanone. A/K = (mols A/mols K)
[b] Retention of configuration in the oxidation of *cis*-1,2-DMCH
[c] 3°/2° = 3x(1-adamantanol)/(2-adamantanol + 2-adamantanone)
[d] 100 equiv. H_2O_2
[e] 1100 equiv. substrate

ligands derived from 1,4,7-triazacyclononane (tacn) was reported, which showed remarkable efficiencies and evidences of metal-based oxidants (Table 5.3) [85, 86].

Table 5.3 collects data corresponding to alkane oxidation reactions mediated by iron complexes containing N-based ligands. Reactions were performed with conditions where H_2O_2 was the limiting reagent (10–100 equiv. with respect to catalyst), in the presence of a large excess of substrate (1000 equiv.). This large excess was employed to minimize overoxidation reactions of the alcohol product,

which is more easily oxidized than the alkane substrate. In addition, since H_2O_2 can be easily oxidized at faster reaction rates than alkanes, H_2O_2 was added by a syringe pump to minimize its concentration in solution and avoid its disproportionation.

Analysis of the data collected on the table allows to extract some structure–activity correlations:

- Iron complexes that can mediate stereospecific hydroxylation of alkanes contain an Fe^{II} center bound to a tetradentate N-based ligand, leaving two coordination positions in a *cis* relative disposition. The two *cis*-positions are occupied by weakly bound ligands such as CH_3CN, H_2O and CF_3SO_3. Reactions are commonly performed in acetonitrile solvent, and in these conditions, two acetonitrile molecules occupy the labile sites. Fast ligand exchange at these positions allow for fast reaction with H_2O_2. When strong binding ligands such as halides are present at these positions, catalytic activity is very much limited and indicative of Fenton type reactions (compare entries 9 and 10 in Table 5.3) [87]. The reason is that ligand exchange allowing for peroxide binding to the metal center is a prerequisite for generation of a metal centered oxidant.
- Ligands must be oxidatively robust and form very stable complexes under oxidative and acidic reaction conditions. Most efficient complexes contain ligands that form several five-member chelate metalocycles. Ligands that form less stable 4, 6 and larger member chelates do not form efficient C–H oxidation catalysts presumably because of fast catalyst decomposition under reaction conditions (compare entries 5–6 and 22–26) [81, 82, 84, 88].
- The activity and selectivity of the catalysts has also been proposed to be related to the strength of the ligand field [84, 89]. Somewhat, most efficient catalysts contain ligands that exert strong ligand fields.
- At least one pyridine ring (or a pyrazine [90]) is apparently necessary to have catalysts that give rise to metal centered C–H oxidation reactions. Substitutions at the 6th position of the pyridine have a very profound impact in the activity of the catalysts and also in the reaction mechanisms. In general, introduction of methyl groups in this position gives rise to less active catalysts, which also exhibit reactivity patterns characteristic of free-radical type of transformations. As a prototypical example, differently to tpa, $6Me_3$-tpa (entry 4 in Table 5.3) generates a catalyst with some non-metal based character as evidenced by the low percentage of retention of configuration (RC) in the oxidation of *cis*-1,2-DMCH and the large percentage of O_2 incorporation into products [81]. The origin of the effect of this substitution is not completely understood and may be complex [91]. In one hand, steric clashing between 6-Me positions and the iron center leads to longer Fe–N distances. That translates into weaker ligand fields, and also weaker metal–ligand bonds.
- Alteration of the electronic properties of the pyridine rings in tpa and mep ligands does not substantially impact on the catalyst efficiencies [81, 90].
- As shown by the aforementioned studies, catalyst stability under the harsh oxidizing conditions required to oxidize alkanes is a major factor in determining

the catalytic efficiency of a given catalyst. As proof of concept, very robust ligand scaffolds like mep and Pytacn (entries 5–6, 13–16) give rise to especially active catalysts. Replacement of the N-Me groups in mep by an O or S atom completely kills catalytic activity [90].

5.2.5 *Synthetically Useful Stereospecific C–H Oxidation Catalysts*

The metal-based nature of stereospecific C–H oxidation reactions mediate by selected iron catalysts in combination with H_2O_2 could offer a unique chemical technology for selectively functionalizing non-activated alkyl sp^3 C–H bonds. The potential use of these reactions with synthetic purposes was, however, hampered by the large excesses of substrate relative to oxidant that was necessarily employed to limit overoxidation reactions. A breakthrough in the field occurred in 2007 when Chen and White described an iron catalyzed predictable selective aliphatic C–H oxidation methodology that afforded synthetically useful yields of oxidized products, and that could also be employed in late-stage oxidation of complex organic molecules [92]. Two major key aspects lay at the basis of the success of this approach. In first place, acetic acid was identified as a key additive to dramatically improve product yields (Table 5.4). In second place, the authors identified the structurally rigid bipyrrolidine-based complex $[Fe^{II}(S,S\text{-bpbp})(CH_3CN)_2](SbF_6)_2$ as a particularly efficient C–H hydroxylation catalyst. Taking pivalate Piv1 as substrate (Table 5.4), and limiting reagent, by making three consecutive additions of catalyst (5 mol %), AcOH (50 mol %), and H_2O_2 (1.2 equiv.) over a period of 30 min at room temperature, the corresponding diastereomerically monohydroxylated product could be obtained in 51 % isolated yield.

This system is tolerant to several functional groups including esters, amides, halides and epoxides, and impressively, it showed predictable selectivity based in electronic (Scheme 5.15), steric (Eq. 5.4), and directing factors (Eq. 5.5),[92], making it very interesting from a synthetic point of view.

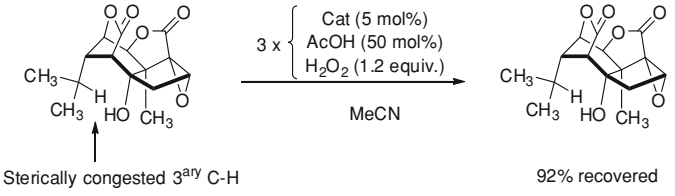

(5.4)

Table 5.4 Optimization of the $[Fe^{II}(S,S\text{-bpbp})(CH_3CN)_2](SbF_6)_2$ system [92]

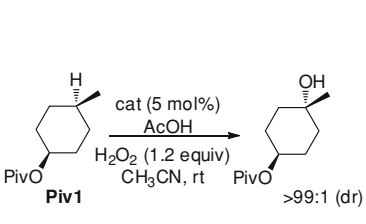

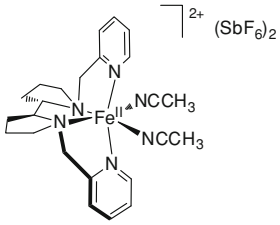

$[Fe(S,S\text{-bpbp})(CH_3CN)_2](SbF_6)_2$

Entry	Catalyst	AcOH(equiv.)	Yield (%)	Conv.(%)[a]	Select (%)[b]
1	$[Fe^{II}(mep)(CH_3CN)_2]^{2+}$	0	7	12	56
2	$[Fe^{II}(S,S\text{-bpbp})(CH_3CN)_2]^{2+}$	0	14	15	92
3	$[Fe^{II}(mep)(CH_3CN)_2]^{2+}$	0.5	26	41	62
4	$[Fe^{II}(S,S\text{-bpbp})(CH_3CN)_2]^{2+}$	0.5	38	42	90
5[c]	$[Fe^{II}(S,S\text{-bpbp})(CH_3CN)_2]^{2+}$	0.5	51	–	–

[a] Conversion of starting material
[b] Selectivity for hydroxylated product (yield/conversion)
[c] Iterative addition protocol (3 x 5 mol % catalyst + AcOH(50 mol %) + H_2O_2 (1.2 equiv. added by syringe pump))

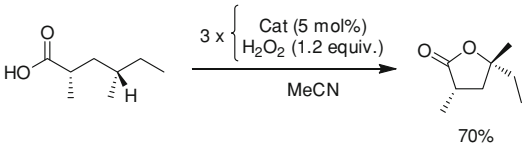

(5.5)

On the basis of electronic factors, when two tertiary C–H bonds are present in the substrate, hydroxylation takes place preferentially at the most remote tertiary C–H from the electron withdrawing group (EWG). For example, the oxidation of 3,7-dimethyl-1X-octane derivates evidences electronic discrimination in the hydroxylation of tertiary C–H bonds (Scheme 5.15). Hydroxylation of 3,7-dimethyloctane affords a 1:1 mixture of the tertiary alcohols. However, when X = F, Cl or OAc, hydroxylation occurs preferentially at the distal site. When the EWG is placed closer to one of the C–H bonds, the electronic discrimination is enhanced (Scheme 5.15).

Steric effects also discriminate reactivity. Because of the steric hindrance of the tertiary C–H bond in (-)-α-dihydropicrotoxinin (Eq. 5.4), this substrate is not effectively oxidized by the catalyst, and the substrate is recovered in 92 % yield. Finally, a carboxylate group can be used to site-direct C–H oxidation, presumably via binding to the iron catalyst (Eq. 5.5). In this case, rapid lactonization follows carboxylate directed C–H hydroxylation of a dimethylhexanoic acid substrate.

Most impressively, selective oxidation in complex molecules with multiple tertiary C–H sites was achieved obtaining synthetically useful yields. This was demonstrated in the carboxylate-directed lactonization of tetrahydrogibberellic acid, and in the hydroxylation of (+)-artemisin (Scheme 5.16). In the first case, the

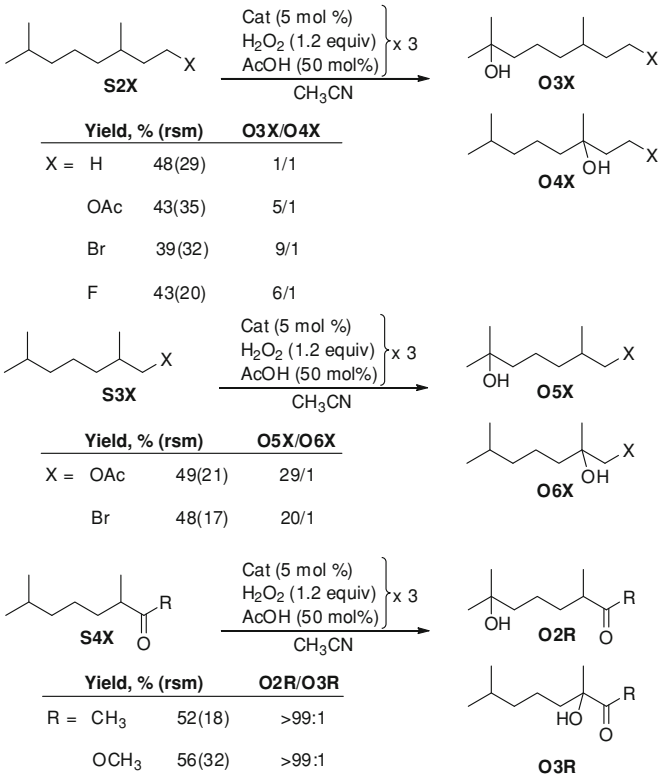

Scheme 5.15 Electronic discrimination in the hydroxylation of C–H bonds catalyzed by $[Fe^{II}(S,S\text{-bpbp})(CH_3CN)_2](SbF_6)_2$ [92]

lactone product was obtained in 52 % isolated yield. In the second case, oxidation occurs preferentially at the most electron-rich and the least sterically hindered 3° C–H bond in 54 % isolated yield. Interestingly, this method compares favorable in terms of reaction times, reaction volume and isolated yields with respect to the enzymatic oxidation of (+)-artemisin with microbial cultures (47 % yield after 4 days, and a tenfold volume throughput using *Cunninghamella echinulata*) [93].

White and Chen landmark system uses 15 % catalyst loading, via an elaborate synthetic protocol that involved iterative addition of reagents, and substrate recycling in some cases. In a subsequent study, the authors described experimental procedures that avoid substrate recycling. In the same study, the authors conclude that formation of oxo-bridged oligomeric species is one of the reasons for catalyst deactivation [94].

The factors that determine the C–H site selectivity in the oxidation reactions catalyzed by $[Fe^{II}(S,S\text{-bpbp})(CH_3CN)_2](SbF_6)_2$ have been explored, with the aim of targeting synthetically more challenging methylene sites [95]. C–H bond strength is a major factor that directs reactivity in the relative order 3° C–H > 2° C–H > 1° C–H bonds. However, from a steric point of view the order is inverted,

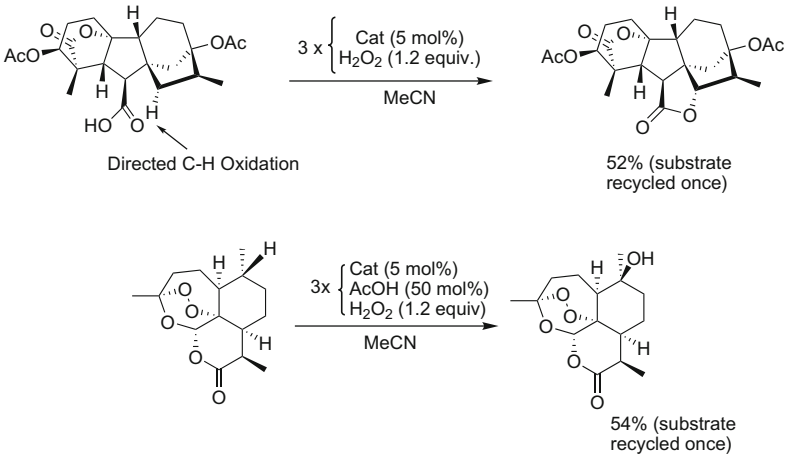

Scheme 5.16 Selective C–H oxidation of complex organic molecules; top) Carboxylate-directed C–H oxidation followed by lactonization of tetrahydrogibberellic acid, and bottom) hydroxylation of (+)-artemisin by $[Fe^{II}(S,S\text{-bpbp})(CH_3CN)_2](SbF_6)_2$ [92]

and 3° C–H bonds are the sterically least accessible. Oxidation of tertiary C–H bonds could be also limited by steric crowding due to vicinal groups. A third factor that could be used in order to direct C–H reactivity is the presence of EWG such as carbonyl moieties, which disfavors oxidation at proximal positions. On the contrary, hydroxylation at adjacent C–H bonds of cyclopropane rings and ether groups is favored because of hyperconjugation effects. As early established for dioxirane mediated oxidations [10], and later recognized in Fe-based oxidations [96], White et al. also show that stereoelectronic factors also need to be considered. For example equatorial C–H bonds in cyclohexane skeletons are more readily oxidized than axial counterparts because in the former, C–H breakage in the transition state liberates tension of 1,3-diaxial interactions.

In structurally simple substrates, when only one of the factors is analyzed, modest selectivity among different C–H bonds is usually attained. However, in complex organic molecules, when several of the effects play in a concerted manner, exquisite site selective C–H oxidation can take place. Most remarkably, combined effects allow selective oxidation of secondary C–H bonds in the presence of tertiary C–H bonds. As illustrative example, selective oxidation of methylene groups of several terpenoids was accomplished with impressive selectivity (Scheme 5.17).

The very modest turnover numbers attained with $[Fe^{II}(bpbp)(CH_3CN)_2](SbF_6)_2$ prompts the design of more efficient catalysts. However, innovative strategies for improvement need to be developed, and are challenged by the dramatic dependence between catalytic activity and iron complex arquitectures. Inspiration towards this goal was taken by Costas, Ribas et al. from well-established principles in oxidation catalysis with heme complexes [97, 98]. Site-isolation in porphyrins limits bimolecular self-decomposition pathways and precludes formation of

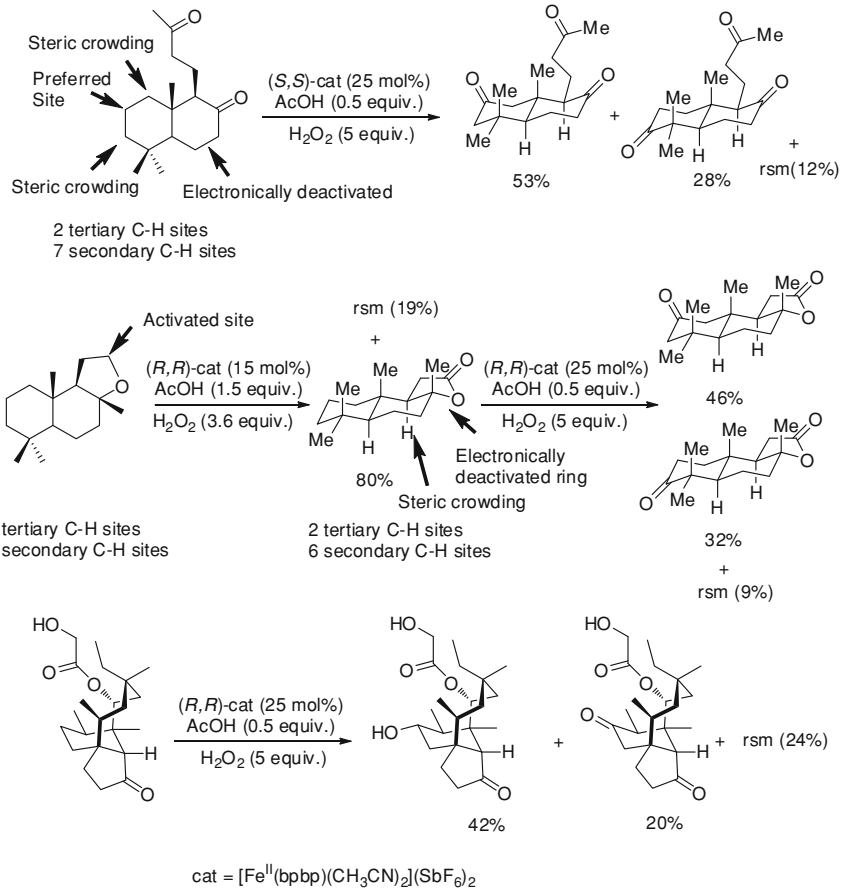

Scheme 5.17 Selective oxidation of methylene groups by $[Fe^{II}(S,S\text{-bpbp})(CH_3CN)_2]$ $(SbF_6)_2$ [95]

catalytically non competent oxo-dimers. As a result, isolation of the metal site causes an enhancement of the metaloporphyrin catalytic activity.

In an attempt to apply this principle to non-heme iron complexes, bulky pinene groups were attached to positions 4 and 5 of the pyridine rings of a tetradentate bis-amine-bis-pyridine ligand [99]. In addition, a rigid chiral *trans*-1,2-cyclohexane diamine backbone was used with the aim of controlling the chirality at the metal, and also to set the relative orientation of the oxidatively most robust pinene CH_3 groups with respect to the metal site. This structural aspect aims at limiting ligand self-oxidation reactions that could lead to deactivation paths.

The novel catalyst $[Fe^{II}(OTf)_2(S,S,R\text{-mcpp})]$ (Scheme 5.18) affords comparable yields and C–H site selectivities with $[Fe^{II}(bpbp)(CH_3CN)_2](SbF_6)_2$ in C–H oxidation reactions, albeit the former requires lower catalyst loadings (1–3 mol %). The profound effect that site isolation has in the relative efficiency and stability of

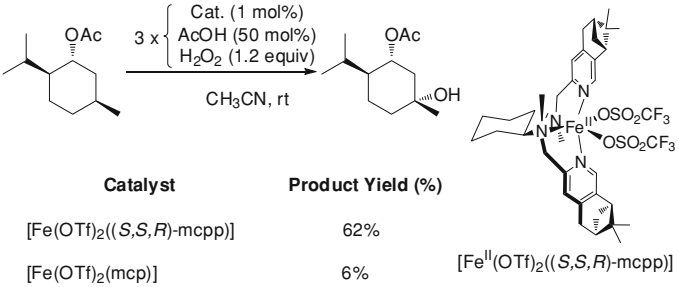

Scheme 5.18 Chemical diagram of [$Fe^{II}(OTf)_2$(*S*,*S*,*R*-mcpp)], and comparative performance with [$Fe^{II}(OTf)_2$(mcp)] in the hydroxylation of p-acetoxymenthane [99]

the catalysts was evidenced by performing a comparative time profile analysis of the oxidation of p-acetoxymenthane catalyzed by [$Fe^{II}(OTf)_2$(mcp)] and [$Fe^{II}(OTf)_2$(*S*,*S*,*R*-mcpp)]. The experiment indicated that unlike [$Fe^{II}(OTf)_2$(mcp)], [$Fe^{II}(OTf)_2$(*S*,*S*,*R*-mcpp)] is not substantially deactivated during the reaction. A second addition of H_2O_2 and substrate resumes the catalytic activity of the latter, but not of the former [99].

5.2.6 *Reaction Mechanisms for C–H Hydroxylation Reactions Mediated by Iron Complexes with N-Rich Ligands*

Mechanistic studies on alkane oxidation reactions catalyzed by iron complexes containing N-rich ligands have shown a rich and subtle mechanistic scenario. Fenton-type free-diffusing radical processes dominate the chemistry in most of the cases. As a prototypical example, reactions with TBHP are dominated by the iron-mediated generation of ^{t}Butoxyl radicals [22]. However, convincing experimental evidence have built up over the last decade that selected iron complexes, in combination with H_2O_2 mediate C–H hydroxylation reactions via metal-centered paths that do not involve the implication of long-lived carbon-centered radicals.

Stereospecific C–H hydroxylation reactivity has been observed for a limited number of H_2O_2-oxidation reactions catalyzed by iron catalysts containing N_4-tetradentate ligands (Table 5.5). The most studied and best understood reactions are those of $[Fe(L)(CH_3CN)_2]^{2+}$ (where L stands for tpa, mep and derivatives) [80, 81]. More recently, a family of [$Fe(OTf)_2$(^{X,Y}Pytacn)] complexes, where ^{X,Y}Pytacn stands for a tetradentate ligand based on a triazacyclononane ring, have also proven to be capable of mediating efficient stereospecific hydroxylation of alkanes [85, 86].

The reactivity patterns associated with the oxidation reactions catalyzed by these families of complexes (Table 5.5) are indicative of the implication of a selective oxidant. But most important is the observation that the oxidation of *cis*-1,2-dimethylcyclohexane is stereospecific, demonstrating that free-diffusing carbon-centered radicals are not involved in the reaction. This conclusion is further

Table 5.5 Oxidation of alkanes with H_2O_2 catalyzed by Fe^{II} complexes

	Cyclohexane		*cis*-1,2-DMCH	Adamantane	Oxygen-source	
Catalyst	A + K (A/K)[a]	KIE	RC (%)[b]	3°/2°[c]	$H_2O/H_2O_2/O_2$[f]	Ref.
$[Fe^{II}(tpa)(CH_3CN)_2]^{2+}$	3.2 (5)	3.5	100	17	27/70/3	[80]
$[Fe^{II}(OTf)_2(mep)]$	6.3 (8)	3.2	96	15	18/84/0	[80, 81]
$[Fe^{II}(5Me_3\text{-}tpa)(CH_3CN)_2]^{2+}$	4.0 (9)	3.8	100	21	38/69/0	[81]
$[Fe^{II}(6Me_3\text{-}tpa)(CH_3CN)_2]^{2+}$	2.9 (2)	3.3	54	15	1/22/77	[81]
$[Fe^{II}(OTf)_2(^{Me,H}Pytacn)]$	6.5 (12)	4.3	93	30	45/47/8	[85, 86]
$[Fe^{II}(OTf)_2(^{Me,Me}Pytacn)]$	7.6 (10)	3.4	94	20	11/85/4	[86]
$[Fe^{II}(OTf)_2(^{iPr,H}Pytacn)]$	2.4 (4)	4.8	86	14	8/59/33	[86]

Catalyst:H_2O_2:alkane = 1:10:1000

[a] Turnover number (TN, mols of product/mols of catalyst), A = cyclohexanol, K = cyclohexanone. A/K = (mols A/mols K)

[b] Retention of configuration in the oxidation of *cis*-1,2-DMCH

[c] 3°/2° = 3x(1-adamantanol)/(2-adamantanol + 2-adamantanone)

[f] Origin of the oxygen atom (%): from water/hydrogen peroxide/O_2

substantiated by isotopic labeling experiments, which indicate minimum incorporation of O_2 in the oxidation products. Instead, the origin of the oxygen atoms incorporated into products is the oxidant (H_2O_2) and water. Since peroxide type of species cannot exchange their oxygen atoms with water, the incorporation of oxygen from water into the alcohol product derived from alkane oxidation is taken as an indication for the involvement of a high-valent iron-oxo species [22, 80, 81, 85, 86].

Reaction mechanisms appear to be highly susceptible to small structural changes in the compexes. Alteration of positions 4 or 5 of the pyridine rings of the ligands has no substantial effect on the mechanistic reaction patterns (Table 5.5) [81]. Instead, C–H oxidation reactions mediated by $[Fe^{II}(6Me_3\text{-tpa})(CH_3CN)_2]^{2+}$, which contain methyl groups in the 6th position of the pyridine rings, evidence some radical character, as shown by the low percentage of retention of configuration (RC) in the oxidation of *cis*-1,2-dimethylcyclohexane (*cis*-1,2-DMCH) and by the high level of O_2 incorporation, a clear indication that free radical processes take place. On the bases of these observations, the proposed mechanism for the oxidation of alkanes is shown in Scheme 5.19.

(Step 1) The initial Fenton process from Fe^{II} to Fe^{III}. Reaction of the starting Fe^{II} $[Fe^{II}(L)(CH_3CN)_2]^{2+}$ complex in acetonitrile with H_2O_2 leads to rapid formation of $[Fe^{III}(OH)(L)]^{2+}$ species, which can be in equilibrium with dimeric $[Fe^{III}{}_2(\mu\text{-}O)(L)_2]^{2+}$ species [81]. The initial reaction of a Fe^{II} center with H_2O_2 most likely generates a hydroxyl radical, which in principle is susceptible to engage in C–H oxidation reactions. However, the selective reaction patterns observed are inconsistent with this scenario. Instead, reaction of the ·OH with a second ferrous center forms a second $[Fe^{III}(OH)(L)]^{2+}$ equivalent.

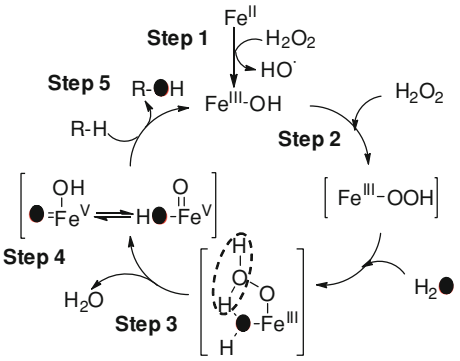

Scheme 5.19 Mechanistic scheme for the stereospecific hydroxylation of alkanes catalyzed by iron complexes with N_4-tetradentate ligands [81]. For clarity reasons, the four coordination sites occupied by the ligand have been omitted from the diagram

Formation (step 2) and fate (step 3) of the Fe^{III} OOH species. Further reaction of the Fe^{III}-OH species with a second molecule of H_2O_2 generates a metastable $[Fe^{III}(OOH)(L)]^{2+}$ intermediate that in the specific case of L = tpa has been spectroscopically characterized by means of UV–Vis, EPR, Resonance Raman, and also by electrospray mass spectrometry [81, 100–102]. Such highly reactive species are interesting *per se* because they are proposed as key intermediates in the catalytic cycle of several iron-based enzymes involved in oxidation reactions such as Cpd 0 in cytochrome P450 [103, 104], or Rieske dioxygesases [105]. Spectroscopic and theoretical studies provide key information to understand the chemistry of these species. EPR analyses indicate that the ferric site in $[Fe^{III}(OOH)(tpa)]^{2+}$ is in the low spin S = 1/2 state [81, 100–102]. Vibrational frequencies corresponding to Fe–O and O–O bond stretching in the resonance Raman spectra can be directly correlated to the strength of the corresponding bond [101, 102]; the low ν(O–O) reported for the low-spin $[Fe^{III}(OOH)(tpa)]^{2+}$ indicates that the O–O bond is weak, while a high energy feature corresponding to the ν(Fe–O) indicates a strong iron-oxygen bond [101, 102]. Indeed, detailed inspection of the resonance Raman spectra of several iron-peroxo species reported in the literature leads to the conclusion that the low-spin iron(III) centers present a weak O–O bond and a strong Fe–O [106].

Homolytic O–O bond cleavage in $[Fe^{III}(OOH)(tpa)]^{2+}$ will lead to the formation of a Fe^{IV}=O compound together with a hydroxyl radical (OH·), while the heterolytic breakage would generate a formally Fe^{V}=O compound and a hydroxide (OH^-). The selective and efficient reactivity observed for selected non-heme iron catalysts (Tables 5.5 and 5.4) is not consistent with the rather indiscriminate chemistry of hydroxyl radicals [25]. Furthermore, synthetic Fe^{IV}=O complexes with nitrogen rich ligands have been prepared over the last years and have been shown to be capable of breaking the strong C–H bond of cyclohexane [107, 108]. However, reactions are slow, incompatible with the fast catalytic activity, and are characterized by small A/K values. Thus, a Fe^{IV}=O species can not account for the fast stereospecific hydroxylation of alkanes.

Alternatively selectivity properties are better described by assuming O–O bond heterolysis to generate Fe^{V}= O species [109]. Heterolytic cleavage of the O–O bond is proposed to result in the formation of highly electrophilic $[Fe^{V}(O)(OH)(L)]^{2+}$ species. In this line, theoretical studies on the hydroperoxo complex $[Fe^{III}(OOH)(tpa)(H_2O)]^{2+}$

indicates that both the heterolytic and the homolytic pathways are feasible and have barriers of comparable size [110]. DFT studies also indicate that a water ligand, in *cis*-relative position with respect to the hydroperoxide unit, assists the heterolytic cleavage of the O–O bond in $[Fe^{III}(OOH)(mep)(H_2O)]^{2+}$, and that the reaction has a small energy barrier [111]. Further indirect evidence of the importance of the water ligand in promoting the heterolytic cleavage of the O–O bond derives from the observation that iron complexes with nitrogen rich pentadentate ligands do not elicit stereospecific C–H hydroxylation [78, 81], despite forming analogous low spin Fe^{III}-OOH species. Indeed, stereospecific C–H hydroxylation strictly requires the presence of two labile sites at the iron center, in *cis*-relative position.

$Fe^{III}OOH$ are not C–H hydroxylating species. The ability of iron(III) hydroperoxides to carry out oxidation reactions has been recently discarded on the basis of a recent work by Nam and co-workers. $[Fe^{III}(OOR)(L)]$ species (R = H, ^{t}Bu; L = tpa, N4Py) were prepared and their reaction with cyclooctene monitored by UV–vis spectroscopy. These experiments show that reactions are very slow, and incompatible with the fast reactions that take place under standard catalytic oxidation conditions [112, 113]. In conclusion, alternative species must be responsible for alkane and alkene reactions mediated by Fe(tpa) and related catalytic systems.

Steps 4 and 5. Water incorporation and alkane oxidation by the $Fe^{V}(O)(OH)$ species. Because of the water-assisted mechanism, the high valent $Fe^{V}(O)(OH)$ species initially contains an oxygen atom derived from a water molecule in the hydroxide ligand. This hydroxide ligand can engage in a prototopic equilibrium with the oxo group via a oxo-hydroxo tautomerism, analogous to that occurring in heme systems [114]. Through this mechanism, the reactive oxo ligand contains an oxygen atom that originates from water.

C–H oxidation by the $Fe^{V}(O)(OH)$ species occurs via a P-450-like rebound mechanism [12, 115]. In the first step, the ferryl species abstracts the hydrogen atom from the substrate to form a caged alkyl radical which rapidly rebounds with the newly formed hydroxo group to give the corresponding alcohol (Scheme 5.20). Since the oxo ligand can contain oxygen atoms that come from a water molecule, the observation of substantial amounts of water incorporation into the alcohol products resulting from the stereospecific C–H hydroxylation constitutes strong experimental evidence in favor of this mechanism. In addition, the stereospecific character of the reaction discards the implication of carbocationic intermediates as the origin of the incorporation of water into products.

An alternative rebound mechanism. The P-450 like rebound mechanism predicts a competition between oxo-hydroxo tautomerism and substrate oxidation [114]. Because of that, the extent of water incorporation into products must be inversely related to the strength of the hydroxylated C–H bond, and that was indeed observed in oxidation reactions catalyzed by $[Fe^{II}(L)(CH_3CN)_2]^{2+}$, L = tpa and mep complexes [81].

Key aspects of this rebound-mechanism were reconsidered on the basis of the reaction patterns observed with the $[Fe^{II}(OTf)_2(^{Me,H}Pytacn)]$ catalyst [85]. In C–H oxidation reactions mediated by this catalyst the level of water incorporation into products was found highly dependent on the specific alkane: while secondary C–H bonds afforded 42(2)% of alcohol containing the oxygen from water, this value

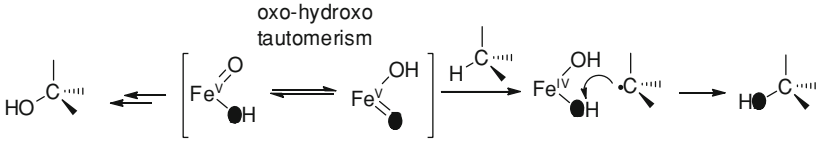

Scheme 5.20 Mechanism of alkane hydroxylation by HO-Fe^{V}=O. One tautomer affords incorporation of oxygen from H_2O_2 into the alcohol product while the other involves incorporation of one oxygen from water (● denotes oxygen atom from water) [81]

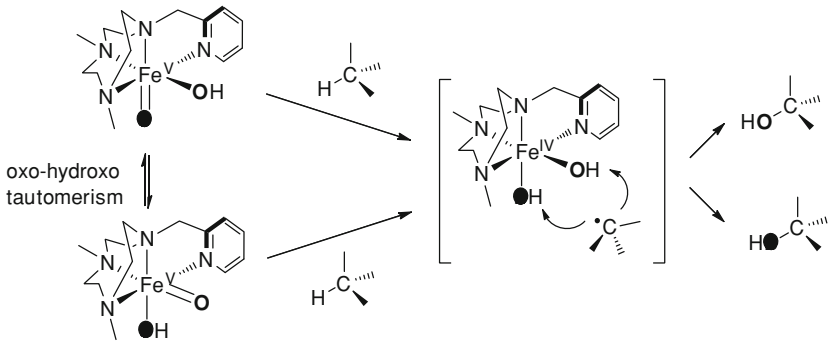

Scheme 5.21 Alternative rebound mechanism for alkane hydroxylation proposed for the Fe(Pytacn) system [85]

increased up to 76(3)% for tertiary C–H bonds. Such high levels of water incorporation into alcohols are unprecedented among the reported bioinspired iron catalysts, but the situation is reminiscent to the results obtained for selected enzymes within the Rieske dioxygenase family. For example the hydroxylation of indane to 1-indanol by toluene dioxygenase [116], occurs with a 68 % level of oxygen from water incorporated into product.

In order to account for these observations, an alternative rebound-like mechanism was proposed [85]. The observation that the levels of water incorporation are independent on substrate concentration led to the proposal that the newly formed alkyl radical (formed by initial hydrogen-atom abstraction) can "rebound" with any of the non-equivalent OH groups in the $Fe^{IV}(OH)_2$ disposed in a relative *cis* configuration (Scheme 5.21). According to the experimental results, 2°-alkyl radicals seem not to discriminate between the two OH groups, but 3°-alkyl radicals favor the rebound with the OH group derived from water. Steric effects may provide a rational for this preference since the sphere surrounding the two *cis* positions is different.

The fundamental origin of the difference between this alternative non-heme rebound mechanism with respect to that of hemes is the presence in the former of a *cis*-labile site, that can be occupied by ligands susceptible to be transferred to the carbon-centered radical. That may actually be a biologically relevant structural feature that can provide non-heme enzymes with a more extense chemical versatility than that of heme oxygenases. Examples of this idea could be reactions

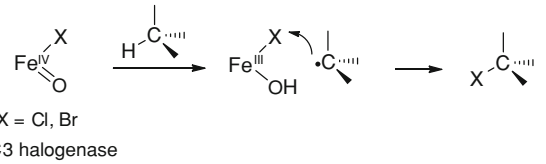

Scheme 5.22 Reaction mechanism for halogenations in α-ketoglutarate dependent halogenases [117]

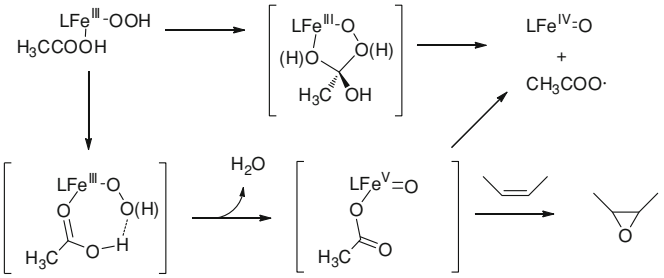

Scheme 5.23 Mechanistic scheme proposed for the AcOH promoted O–O heterolysis in iron catalyzed epoxidations [119]

taking place at α-ketoglutarate dependent halogenases, where hydrogen-atom abstraction by a terminal oxo ligand is followed by rebound with the adjacent Fe–X, X = halide ligand (Scheme 5.22) [117].

5.2.7 The Role of Acetic Acid

Acetic acid has emerged as a very important additive in alkane [92, 95] and alkene [118] oxidation reactions catalyzed by iron complexes containing tetradentate ligands. Its exact role in alkane oxidation reactions has not been explored yet. However, two recent mechanistic studies in the epoxidation of alkenes [119] and in the hydroxylation of arenes [120] have led to the conclusion that one of the key roles of this acid is to promote the heterolytic cleavage of the O–O bond of the Fe^{III}-OOH species (Scheme 5.23), thus generating the highly electrophilic Fe^{V}=O species responsible for substrate oxidation.

5.3 Alkane C–H Oxidation Catalyzed by Chromium Complexes

Chromium derivatives are widely used in organic chemistry as oxidants [121–123]. However, in most cases an stoichiometric amount or excess of this

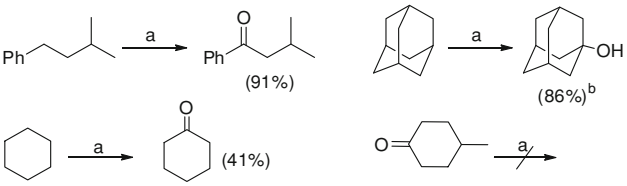

Scheme 5.24 Cr(VI) catalyzed oxidation of alkanes, (Yield). [a]5:300:100:200, $CrO_2(OAc)_2$:H_5IO_6:Substrate:Ac_2O. [b]10 equiv. of H_5IO_6

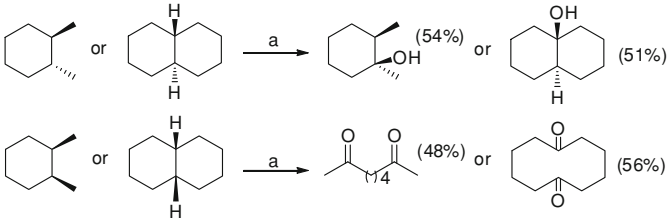

Scheme 5.25 Different reactivity in the oxidation of alkanes with two adjacent tertiary C–H bonds positioned in relative orientation *trans* (*up*) and *cis* (*down*), (Yield). [a]5:300:100:200, $CrO_2(OAc)_2$:H_5IO_6:Substrate:Ac_2O

metal is required for optimal results in alkane oxidation. Only few catalytic systems in chromium have been described for C–H oxidation [124, 125], and most of them are restricted to the oxidation of activated benzylic and allylic C–H bonds [126, 127]. From the point of view of synthetically useful methodologies, the work by Lee and Fuchs stands out. The authors examined the combination of several chromium salts as catalyst in combination with various oxidants [128]. Screening of the chromium catalyst and a series of oxidants led to the selection of $CrO_2(OAc)_2$ and H_5IO_6 as the most optimum combination. For optimal results, 2 equivalents of Ac_2O are also required. Several activated and non-activated C–H bonds are oxidized with up to 96 % yield using 5 mol % of $CrO_2(OAc)_2$ and excess of H_5IO_6 (3 equiv.) in CH_2Cl_2/CH_3CN at −40 °C to 0 °C in 2 h.

The system shows strong preference for benzylic C–H bonds in front of other tertiary or secondary positions (Scheme 5.24). On the other hand, oxidation of tertiary C–H bonds to the corresponding alcohol is performed with stereoretention at the tertiary carbon atom and it is preferred to oxidation at secondary C–H bonds. Interestingly, formation of the corresponding diketone product and breaking of the C–C bond occur (Scheme 5.25) in the oxidation of molecules with two adjacent tertiary C–H bonds in relative *cis* orientation. Monooxygenated product is observed in *trans* analogs.

Noteworthy, the authors reported the efficient α-hydroxylation of the cyclic steroidal ester **ceph1** (Eq. 5.6), related to the north unit of cephalostatin [128]. The oxidation of this structurally complex molecule proceeds selectively at the less

Scheme 5.26 Mechanism of action proposed by Lee and Fuchs [128, 129]

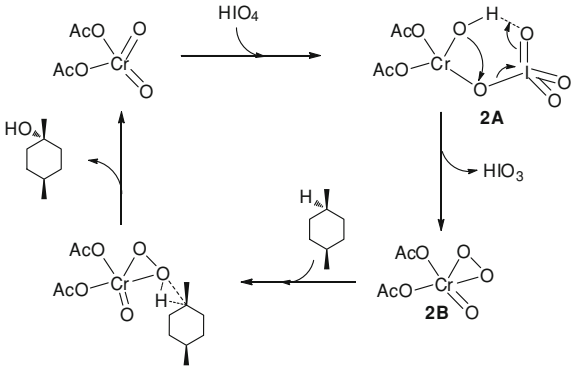

sterically crowded tertiary C–H bond, adjacent to the ether moiety, and in the presence of the a priori more reactive double bound. This unusual chemoselectivity for C–H oxidation over epoxidation is in agreement with a theoretical study showing that Cr(VI) peroxo species have higher calculated activation barriers for oxygen-transfer to ethylene than similar Mo(VI) and W(VI) species, and consequently they are less prone to epoxidation [129].

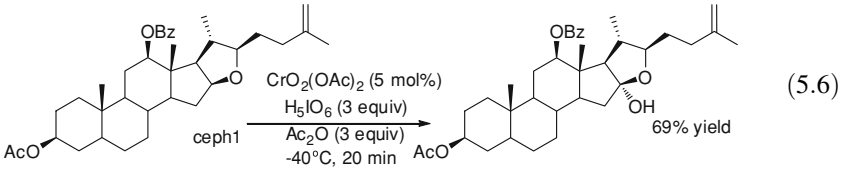

(5.6)

In a subsequent paper the same authors reported that some spiroketal substrates related to **ceph1** underwent decomposition or isomerization due to the strong acidity of H_5IO_6 required in the catalytic protocol [130]. Therefore, stoichiometric oxidation conditions were employed with this type of molecules (CrO_3 (3 equiv.), Bu_4NIO_4 (3 equiv.), CH_3CN/CH_2Cl_2 (3:1, 0.1 M), −40 °C, 10 min). This method resulted chemoselective and compatible with various functional groups including acetate, benzoate, olefin and iodide among others.

As the active C–H oxidant the authors proposed a neutral dioxoperoxy Cr(VI) (**2B**, Scheme 5.26) generated in situ at −40 °C by the reaction of $CrO_2(OAc)_2$ with H_5IO_6 followed by the loss of HIO_3 (Scheme 5.26) [128, 130]. Under these conditions, this orange species (**2B**) is stable for several hours and showed a peroxy stretch (O–O) at 945 cm^{-1} in the IR spectrum. Subsequent concerted "three-centre two-electron" oxenoid insertion into C–H bond is argued based on the retention of configuration observed, which rules out long-lived radical intermediates.

5.4 Alkane C–H Oxidation Catalyzed by Manganese Complexes

Manganese catalysts have been widely applied in epoxidation and even *cis*-hydroxylation of C = C double bonds and although their use in alkane oxygenation is less explored, there are several works that deserve consideration. In this section, reported manganese catalysts involved in C–H oxidation reactions are classified into two main categories depending on their structure: mononuclear complexes and polynuclear systems.

5.4.1 Mononuclear Systems

The use of mononuclear non porphyrinic manganese systems in the oxidation of alkanes was first introduced using a catalyst based on the well-known salen ligand (Scheme 5.27) in combination with TBHP (100 equiv.) as the oxidant [131]. [Mn^{II}(salen)] was applied in the oxidation of cyclohexane (1,000 equiv.) affording preferentially cyclohexanone (53 TN) over cyclohexanol (21 TN) (Table 5.6). Although the authors do not make a detailed mechanistic study, the fact that the presence of O_2 do not affect the reaction outcome and that no free-radical coupling products are detected (such as cyclohexyl ^{t}butyl peroxide or dicyclohexyl) suggests that long-chain radical processes are not involved and instead, it is proposed the intermediacy of a high-valent manganese-oxo species formed by heterolysis of the O–O bond. The manganese(III) analogue of [Mn^{II}(salen)], i. e. [Mn^{III}Cl(salen)], could also be used as catalyst under the same conditions giving a maximum of 76 TN of oxidized products (A/K = 0.6) after 24 h [132].

Nam and coworkers showed that manganese catalysts and peracetic acid constitute a good combination to perform the oxidation of alkanes. In this case, tetradentate neutral nitrogen-based ligands (bqen and mcp, Scheme 5.27) were used for the synthesis of mononuclear complexes [133]. Under conditions of excess of substrate (catalyst:CH_3CO_3H:substrate 1:100:500), cyclohexane could be oxidized to give essentially cyclohexanone (41 or 32 TN respectively) formed by in situ oxidation of the initially generated cyclohexanol (Table 5.6). The high retention of configuration observed in the oxidation of *cis*-1,2-dimethylcyclohexane (>99 %), the very high preference for the oxidation of tertiary C–H bonds over secondary ones in the oxidation of adamantane ($3^\circ/2^\circ = 60$) and the measured kinetic isotope effect (KIE = 2.5) directly point towards the involvement of a metal-based oxidant. Remarkably, no 18-oxygen labeled product was obtained in the presence of $H_2^{18}O$ or $^{18}O_2$, which indicates that the active species cannot exchange the oxygen-atom with water at least at a fast rate and that the oxygen-atom incorporated into the products derives directly from the oxidant and not from atmospheric dioxygen.

Finally, other oxidants such as pentafluoroiodosylbenzene (C_6F_5IO) or the environmentally friendly hydrogen peroxide have also been successfully applied in the oxidation of hydrocarbons (C–H and C = C bonds) using a manganese catalyst

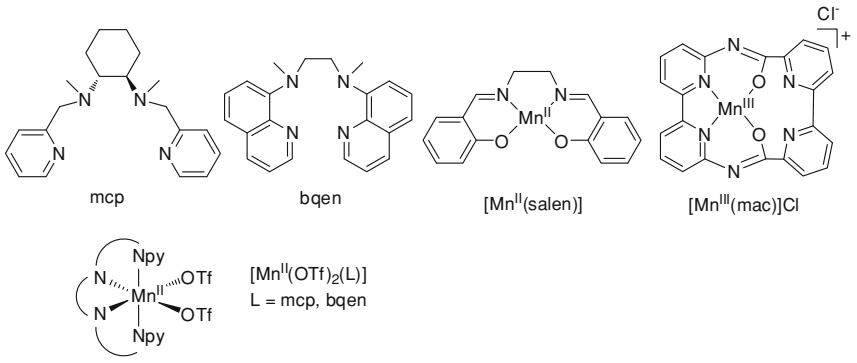

Scheme 5.27 Schematic representation of the reported mononuclear manganese complexes used as catalysts in alkane oxidation

Table 5.6 Cyclohexane oxidation by mononuclear manganese catalysts

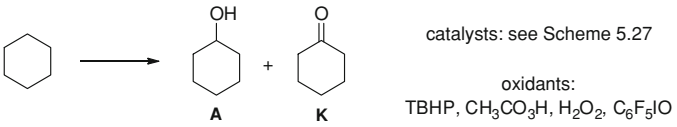

Catalyst	Oxidant	Cat:ox:substrate	A (TN)	K (TN)	Ref
$[Mn^{II}(salen)]$	TBHP	1:100:1000	21	53	[131]
$[Mn^{II}(OTf)_2(bqen)]$	CH_3CO_3H	1:100:500	4	41	[133]
$[Mn^{II}(OTf)_2(mcp)]$	CH_3CO_3H	1:100:500	3	32	[133]
$[Mn^{III}(mac)]Cl$	H_2O_2	1:20:1000	8	1	[134]
$[Mn^{III}(mac)]Cl$	C_6F_5IO	1:60:1000	45	–	[134]

Reactions were run at room temperature without solvent, CH_3CN or a 1:1 mixture CH_3CN:CH_2Cl_2

bearing a tetradentate dianionic asymmetric macrocyclic ligand $[Mn^{III}(mac)]Cl$ (Scheme 5.27) [134]. Under conditions of large excess of cyclohexane, 45 TN of cyclohexanol could be obtained when C_6F_5IO was used as the oxidant, while the combination of the same catalyst with H_2O_2 gave 9 TN of oxidized products (Table 5.6). Cyclooctane, *n*-hexane and even aromatic compounds could also be oxidized under these reaction conditions (e.g. benzene could be oxidized to the corresponding phenol or benzoquinone).

5.4.2 Enantioselective C–H Oxidations

Highly bulky salen complexes also constitute one of the very few examples of non enzymatic catalysts for which stereoselective C–H hydroxylation has been described. These reactions involve oxidation of C–H bonds at benzylic positions,

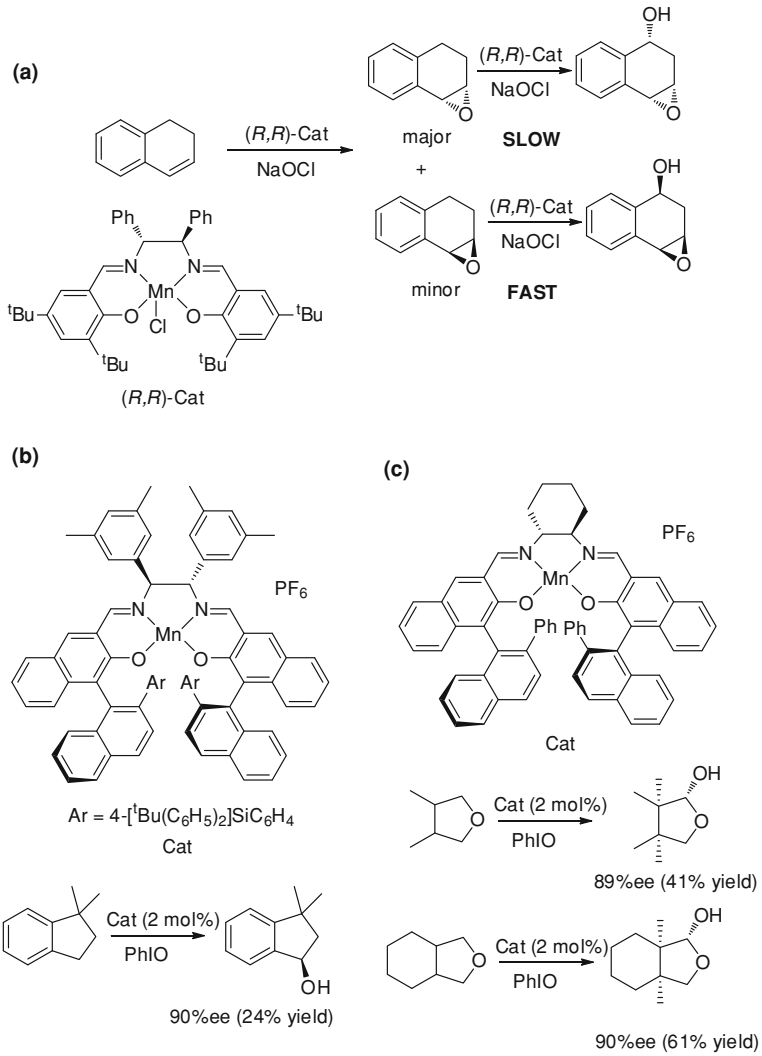

Scheme 5.28 **a** Schematic representation of the asymmetric resolution of epoxides via chiral hydroxylation. **b** Mn-salen catalyst with concave structure and asymmetric hydroxylation of dimethylindane. **c** Desymmetrization of meso-cyclic ethers with a Mn-salen complex

or adjacent to an ether moiety, and therefore can not be considered as representative cases for non activated alkane C–H bonds. Nevertheless, their unique character deserves a special consideration.

Jacobsen and Larrow first described that the kinetic resolution of 1,2-dihydronaphthalene oxide with Mn-salen catalysts was due to an asymmetric C–H hydroxylation (Scheme 5.28a) [135].

Best levels of enantioselectivity have been described by Katsuki et al. by using concave type of manganese complexes. These catalysts were nicely designed to contain cover-like arms that will hang over the two faces of the non-salen bound manganese ion, thus creating a cavity [136, 137]. The authors considered that metal porphyrin [138, 139] and Mn-salen complexes may share a common mechanistic scenario in the hydroxylation of C–H bonds, involving formation of short living "caged" substrate radical intermediates. Difussion of the substrate radical is considered as the main deleterious side reaction to enantioselectivity. To avoid this side reaction, the cavity was aimed at maintaining the substrate in close proximity to the metal ion, and to prevent facile diffusion. By using this strategy, good levels of enantioselectivity up to 90 %,(Scheme 5.28b) were obtained in the hydroxylation of benzylic C–H bonds. Finally, bulky manganese salen complexes have also proven as excellent catalysts for the desymmetrization of *meso*-cyclic ethers, via asymmetric C–H hydroxylation (Scheme 5.28c) [140]. Further oxidation of these alcohol intermediates provides the corresponding chiral lactones.

5.4.3 Polynuclear Systems

The use of polynuclear manganese systems as catalysts in oxidation reactions dates back in the late eighties. Crabtree and coworkers applied the tetranuclear manganese cluster $[Mn^{III}_4(\mu_3\text{-}O)_2(\mu\text{-}AcO)_6(OH)_2]$ (Scheme 5.29a) in combination with TBHP for the oxidation of cyclohexane (catalyst:oxidant:substrate 1:100:100) to give the corresponding alcohol and ketone products (A/K = 0.6) with maximum turnover numbers around 25 after 3 h [141]. The activity of the system could be significantly improved by the partial substitution of the carboxylato bridging ligands by pyridine or bipyridine units (bpy) [142]. For example compound $[Mn^{III}_4(\mu_3\text{-}O)_2(\mu\text{-}O_2CPh)_7(bpy)_2]^+$ (Scheme 5.29b) afforded 127 TN of oxidized products in cyclohexane oxidation (A/K = 1.0) using TBHP as the oxidant (catalyst:oxidant:substrate 1:150:1000) and this number increased up to 580 TN when all the carboxylato units were replaced by bipyridine ligands as in the case of $[Mn^{IV}_3(\mu\text{-}O)_4(bpy)_4(H_2O)_2]^{4+}$ (Scheme 5.29c) (cat:oxidant:substrate 1:8000:4000) [143]. For the latter manganese cluster, an alternative system in which the catalyst was combined with the tetrabutylammonium salt of Oxone (peroxomonosulfate, HSO_5^-) as the oxidant allowed to deepen in the operative mechanism [144]. In comparison with TBHP, the Oxone system afforded higher selectivity for ketone, increased $3^\circ/2^\circ$ ratio in the oxidation of methylcyclohexane as well as a greater degree of stereochemical retention in the oxidation of *cis*-decalin, indicating that free-diffusing alkyl radicals are not involved in the catalysis. The differences obtained between both oxidants highlight that the choice of the oxidant plays a key role in determining the relevant mechanism operating in a specific system and thus, it directly influences the catalytic performance.

Well-defined dinuclear manganese complexes as catalysts in alkane oxidations were developed with the use of the ligands depicted in Scheme 5.30. Fontecave

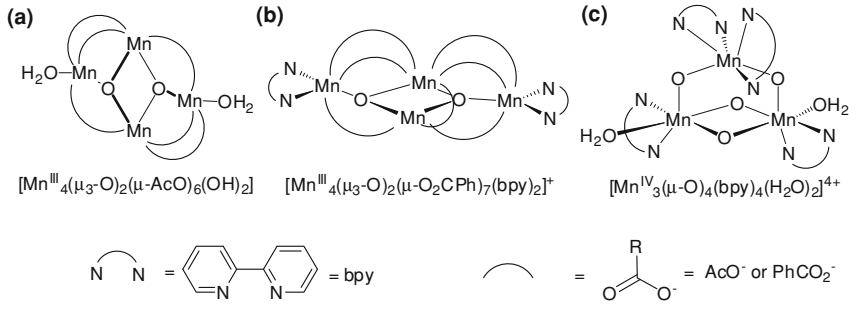

Scheme 5.29 Schematic representation of the manganese clusters used as catalysts in alkane oxidation: **a** cluster with only carboxylato groups, **b** cluster combining carboxylato and bipyridine groups, **c** cluster with bipyridine groups only

et al. found that $Mn(ClO_4)_2{\cdot}6H_2O$, in the presence of TBHP as an oxidant is not able to catalyze the oxidation of cyclohexane [145]. However, addition of bipyridine (bpy) to the manganese salt (ratio bpy:Mn 2:1) in the presence of 140 equiv. TBHP and 1100 equiv. of cyclohexane afforded equimolar amounts of cyclohexanol and cyclohexanone with turnover numbers around 30. Mechanistic studies (Scheme 5.31) indicate that the in situ formed mononuclear $[Mn^{II}(bpy)_3]^{2+}$ reacts with TBHP to give the green bis(μ-oxo) mixed valence complex $[Mn^{III}Mn^{IV}(\mu\text{-}O)_2(bpy)_4]^{3+}$ which is readily recognizable by UV–vis spectroscopy. The involvement of peroxyl radicals in these oxidation reactions is discarded and the formation of a high valent manganese-oxo species formed by O–O bond cleavage of an initially generated Mn-OO^{t}Bu is the proposed mechanistic pathway. In an analogous manner, isolated $[Mn^{III}Mn^{IV}(\mu\text{-}O)_2(L)_2]^{3+}$ (L = mep, bimen, tpa) and $[Mn^{II}{}_2(\mu\text{-}OH)(tpdado)]^{3+}$ (Scheme 5.30) could be applied under similar reaction conditions in the same oxidation processes affording similar results as far as turnover numbers and alcohol:ketone ratios [146, 147]. All the complexes described here proved to be stable under the catalytic conditions and a second addition of TBHP at the end of the reaction reassumed the catalyst activity. In the case of $[Mn^{III}Mn^{IV}(\mu\text{-}O)_2(L)_2]^{3+}$ (L = mep, bimen, tpa, Scheme 5.30) the induction period observed in the catalysis suggests that the mixed-valence $Mn^{III}Mn^{IV}$ species acts merely as a precatalyst and the real active oxidant is postulated to be a dinuclear manganese(III) species probably generated by homolysis of the O–O bond in a putative Mn^{IV}-OOR intermediate.

The selective functionalization of C–H bonds is a major challenge in synthetic chemistry. In biological systems such selectivity is achieved by noncovalent interactions of the substrate with several aminoacids situated in close proximity to the active site. Such recognition is responsible for the selection of a specific substrate and its proper orientation towards the active site to achieve highly selective transformations in well-defined positions. However, noncovalent recognition is hard to implement in synthetic systems because the latter possess a much smaller ligand scaffold that can barely influence substrate orientation. Despite

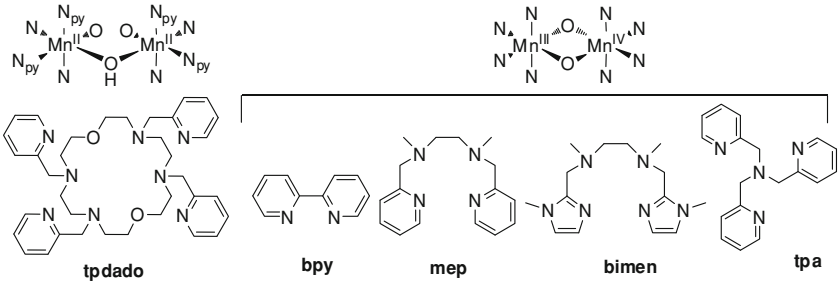

Scheme 5.30 Schematic representation of relevant ligands for the preparation of dinuclear manganese catalysts in oxidation reactions

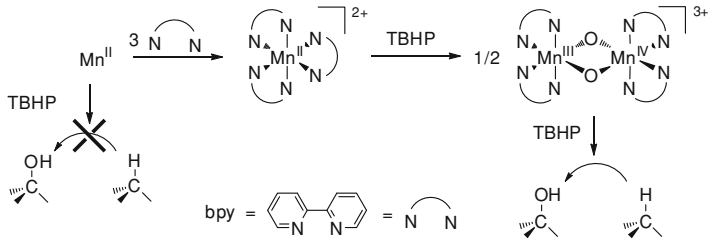

Scheme 5.31 In situ generation of $[Mn^{III}Mn^{IV}(\mu\text{-}O)_2(bpy)_4]^{3+}$ as catalyst for alkane oxidation using TBHP as oxidant

these limitations, Crabtree and coworkers were able to oxygenate C–H bonds with high regioselectivity using a synthetic bis(μ-oxo) dimanganese complex that could non-covalently interact with the substrate by means of hydrogen-bonds [148]. The catalyst (Scheme 5.32) is based on a $Mn^{III}Mn^{IV}(\mu\text{-oxo})_2$ core. Each of the manganese ions is coordinated to a terpyridine structure derivatized with a Kemp's triacid through a phenylene linker (kterpy, Scheme 5.32). The carboxylic acid group of the ligand interacts by means of a double hydrogen-bond with the carboxylic acid group of the substrate (such as ibuprofen) which is selectively oxidized to the C–H bond situated in close proximity to the active site.

Catalytic runs were carried out by mixing 1 equiv. substrate (ibuprofen), 1 mol % of catalyst $[Mn^{III}Mn^{IV}(\mu\text{-}O)_2(OH_2)_2(kterpy)_2]^{3+}$ and 5 equiv. tetrabutylammonium Oxone as oxidant (catalyst:oxidant:substrate 1:500:100). Under these conditions ibuprofen was oxidized in two positions (Scheme 5.33). The regioselective product (**R**) is generated by oxidation of the C–H position situated close to the active manganese bis(μ-oxo) core after ibuprofen docking, while in the alterative product (**A**) oxygenation occurs at the α position of the carboxylic group accompanied with decarboxylation. As can be seen in Table 5.7, substrate docking is essential to achieve high regioselectivities ($\sim$97 %) and the use of simple 4′-phenyl-2,2′:6′,2′′-terpyridine ligand (Phterpy, Scheme 5.32) (where no carboxylic acid can interact with the substrate) significantly decreases the selectivity down to $\sim$77 %. Moreover, the presence of excess acetic acid displaces the ibuprofen

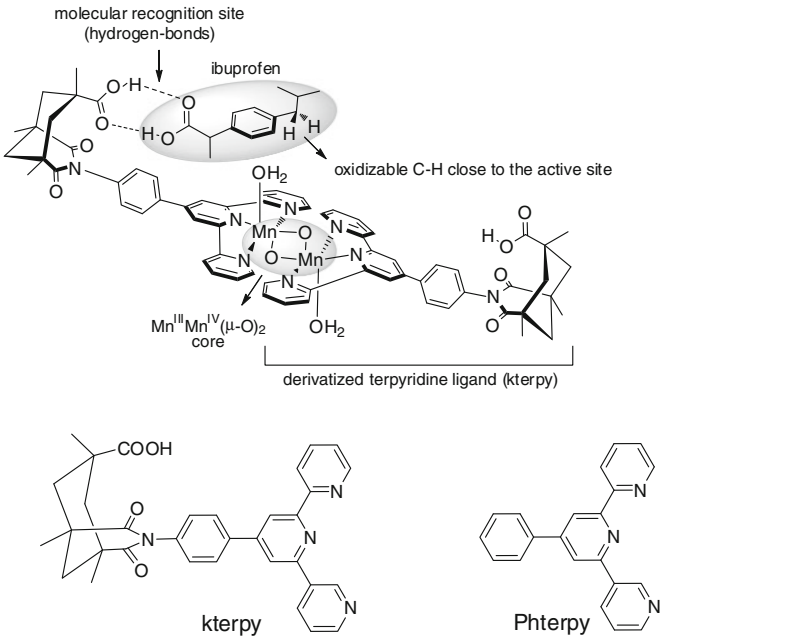

Scheme 5.32 *Top* Schematic representation of catalyst $[Mn^{III}Mn^{IV}(\mu\text{-}O)_2(OH_2)_2(kterpy)_2]^{3+}$ docked with hydrogen-bonded ibuprofen (substrate). *Bottom* Schematic representation of ligands kterpy and Phterpy

from the recognition site and again the **R**:**A** ratio decreases down to the level observed when simple Phterpy ligand is used (where no recognition is possible). Decreasing the catalyst amount down to 0.1 mol % allowed to achieve turnover numbers as high as 710 without any significant decrease in selectivity using CD_3CN as solvent.

The molecular recognition process as well as the oxidation mechanism was studied in detail by means of DFT calculations, being a P-450 like rebound mechanism the most plausible reaction pathway (Scheme 5.34) [149]. Although this particular system is limited to substrates bearing carboxylic groups that can interact with the ligand, it establishes a new strategy that may have a wide range of applications in chemical catalysis.

Finally, trioxo bridged dimanganese complexes derived from 1,4,7-trimethyl-1,4,7-triazacyclononane (tacn) (Scheme 5.35) have also found interesting applications as catalysts in the oxidation of C–H bonds. They were first studied as structural models of the oxygen evolving center of photosystem II [150] but since the disclosure that these compounds were potent low-temperature bleaching catalysts [151], considerable effort has been focused on their development towards the efficient catalytic oxidation of other substrates, principally using the environmentally benign oxidant H_2O_2. In an extensive series of reports, Shul'pin and coworkers reported the application of $[Mn^{IV}{}_2(tacn)_2(\mu\text{-}O)_3](PF_6)_2$ as catalyst in the

Table 5.7 Product distribution in ibuprofen oxidation by $[Mn^{III}Mn^{IV}(\mu\text{-}O)_2(OH_2)_2(kterpy)_2]^{3+}$ and $[Mn^{III}Mn^{IV}(\mu\text{-}O)_2(OH_2)_2(Phterpy)_2]^{3+}$

Catalyst	Additive	Conversion (%)	R[a] (%)	A[b] (%)	TN[c] (%)
$[Mn^{III}Mn^{IV}(\mu\text{-}O)_2(OH_2)_2(kterpy)_2]^{3+}$	–	50	97.5	2.5	50
$[Mn^{III}Mn^{IV}(\mu\text{-}O)_2(OH_2)_2(Phterpy)_2]^{3+}$	–	53	77	23	53
$[Mn^{III}Mn^{IV}(\mu\text{-}O)_2(OH_2)_2(kterpy)_2]^{3+}$	CH_3COOH[d]	56	75	25	56
$[Mn^{III}Mn^{IV}(\mu\text{-}O)_2(OH_2)_2(kterpy)_2]^{3+}$	–	71	96.5	3.5	710[e]

Unless stated, reaction conditions are as follows: catalyst:oxidant:substrate = 1:500:100, oxidant = tetrabutylammonium Oxone, temperature = 20 °C, solvent = CH_3CN

[a] Percentage of the regioselective product **R**

[b] Percentage of the alternative product **A**

[c] Total turnovers = mol products/mol catalyst

[d] Excess acetic acid in the solution (400 % with respect to substrate)

[e] Catalyst:oxidant:substrate = 1:5000:1000 and CD_3CN as solvent instead of CH_3CN

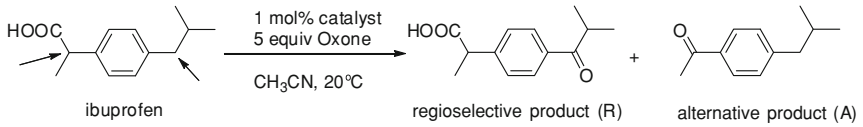

catalyst = $[Mn^{III}Mn^{IV}(\mu\text{-}O)_2(OH_2)_2(kterpy)_2]^{3+}$ or $[Mn^{III}Mn^{IV}(\mu\text{-}O)_2(OH_2)_2(Phterpy)_2]^{3+}$

Scheme 5.33 Oxidation products of ibuprofen with $[Mn^{III}Mn^{IV}(\mu\text{-}O)_2(OH_2)_2(kterpy)_2]^{3+}$ or $[Mn^{III}Mn^{IV}(\mu\text{-}O)_2(OH_2)_2(Phterpy)_2]^{3+}$ as catalysts and Oxone as the oxidant

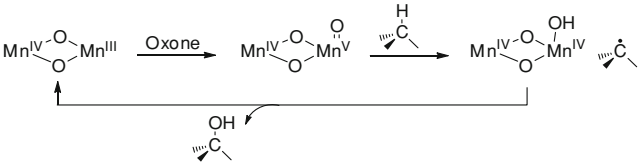

Scheme 5.34 Proposed rebound mechanism in the oxidation of alkanes by $[Mn^{III}Mn^{IV}(\mu\text{-}O)_2(OH_2)_2(kterpy)_2]^{3+}$

Scheme 5.35 Schematic representation of the tacn ligand along with $[Mn^{IV}{}_2(\mu\text{-}O)_3(tacn)_2](PF_6)_2$

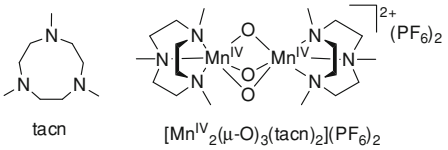

oxidation of alkanes (Scheme 5.35). It was found that several oxidants such as TBHP, MCPBA, PhIO or H_2O_2 could be used to oxidize alkanes but the most remarkable results were obtained with the use of peracetic acid or a combination of H_2O_2 and acetic acid [152–154]. Although several solvents could be applied, the

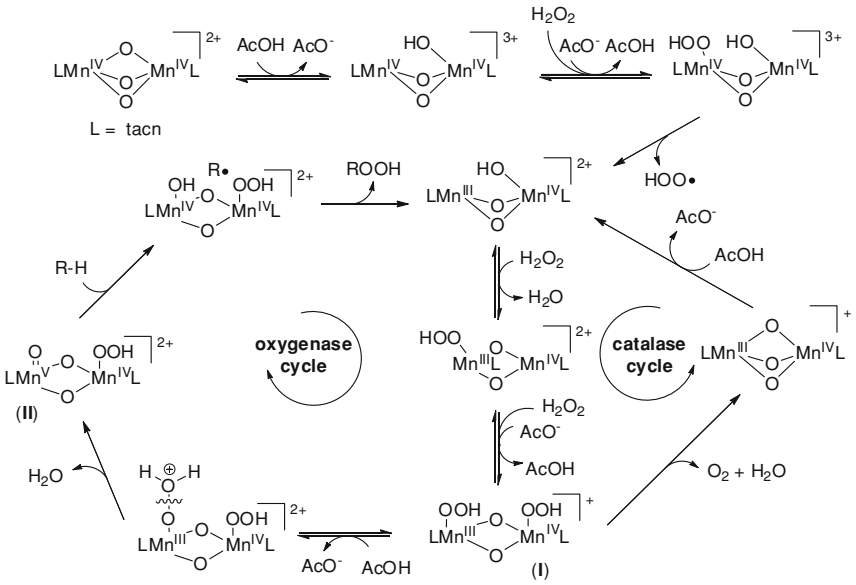

Scheme 5.36 Mechanism proposed for the catalase and oxygenase activity of $[Mn^{IV}{}_2(\mu\text{-}O)_3(tacn)_2](PF_6)_2$ in the presence of acetic acid

best results were obtained with acetonitrile. For example, cyclohexane could be oxidized at room temperature in CH_3CN with turnover numbers as high as 3300 in 2 h when 1:1 H_2O_2:CH_3COOH was used as the oxidant, which accounts for 46 % conversion into oxidized products. Moreover, light alkanes such as propane could be also oxidized under moderate pressures (7 bar) giving turnover numbers around 3100. Mechanistic studies clearly point towards the involvement of alkyl-based radical species as indicated by the generation of bromoalkanes when $BrCCl_3$ is present in the reaction mixture but the mediation of hydroxyl radicals is discarded on the basis of the results obtained in competition oxidation reactions of several cycloalkanes and cyclohexane [153]. The oxidation of these substrates with participation of free hydroxyl radicals is characterized by specific values of their relative reactivities. The results obtained with $[Mn^{IV}{}_2(tacn)_2(\mu\text{-}O)_3](PF_6)_2$ are different enough from the well-established values reported for hydroxyl radicals to affirm that only alkyl radicals and not HO· are involved in the reactions catalyzed by the dinuclear manganese trioxo system.

As stated above, the presence of acetic acid is an essential component to achieve high turnover numbers in alkane oxidation by $[Mn^{IV}{}_2(tacn)_2(\mu\text{-}O)_3](PF_6)_2$ using H_2O_2 as the oxidant and the optimized reaction conditions require the use of an equimolar mixture of H_2O_2 and CH_3COOH. Indeed, at low acetic acid concentrations, $[Mn^{IV}{}_2(\mu\text{-}O)_3(tacn)_2](PF_6)_2$ behaves as a catalase rather than oxygenase and hydrogen peroxide disproportionates to give H_2O and O_2 [155]. Such phenomenon is justified by the mechanistic scenario depicted in Scheme 5.36. Both catalytic cycles share some common intermediates, but the oxygenase cycle

is triggered off by the protonation (by CH_3COOH) of a coordinated hydroperoxo ligand in intermediate (I) accompanied by water release, and generation of the active high-valent manganese(V)-oxo intermediate (**II**). For this reason, high acetic acid concentrations are necessary to ensure that the oxygenase cycle is operative and to minimize the catalase pathway. It is worth mentioning here that the acid co-catalyst is not restricted to acetic acid and even aminoacids (in particular pirazine-2,3-dicarboxylic acid) have been successfully applied in combination with H_2O_2 to achieve alkane oxidation [156]. Oxalic acid has also been used together with H_2O_2 using the same $[Mn^{IV}_2(\mu\text{-}O)_3(tacn)_2](PF_6)_2$ catalyst in the oxidation of alkanes in water at 10–50 °C [157]. In this specific case, apart from the common cycloalkanes even methane (6 bar) could be oxidized to give methanol and formaldehyde (total turnover number = 9).

5.5 Alkane C–H Oxidation Catalyzed by Cobalt Complexes

The use of cobalt-based catalysts in the oxidation of alkanes has found a few industrial applications such as the Mid-Century/Amoco process for the synthesis of terephthalic acid [158] or the DuPont process for adipic acid synthesis [159]. In both systems, molecular O_2 is used as the oxidant, which poses important advantages compared to other oxidants as far as environmental costs are concerned. In these processes, a cobalt catalyst is involved in radical autooxidation chains initiated by decomposition of alkylhydroperoxides generated in the reaction mixture. Despite their industrial application, the systems bear important drawbacks that include elevated pressures and temperatures, indicating the need to find alternative and more efficient catalysts [160].

In this line, the works by Ishii et al. show how a catalytic system combining N-hydroxyphthalimide (NHPI) and $Co(acac)_2$ can be efficiently used in the oxidation of alkanes and alkylbenzenes (Scheme 5.37) [161–163]. Cyclohexane is converted to cyclohexanone and adipic acid, adamantane is oxidized to a mixture of alcohol and ketone products with 93 % conversion, while toluene is efficiently transformed to benzaldehyde and benzoic acid. Remarkably, such transformations take place under relatively mild reaction conditions, i.e. relatively low temperatures and only 1 atm O_2.

From a mechanistic point of view, the active species involved in these oxidative transformations is thought to be the phthalimide N-oxyl radical (PINO) formed through a hydrogen-atom abstraction from NHPI by the cobalt(II) compound that acts as co-catalyst (Scheme 5.38). The crucial role of the cobalt salt in the generation of the PINO radical has been experimentally proved by electron paramagnetic resonance (EPR) spectroscopy: [163] when an acetonitrile solution of NHPI in toluene was exposed to a dioxygen atmosphere at room temperature, no EPR signal was observed over a 10 h period. However, when a very small amount of Co^{II} was added to this solution under ambient conditions, an EPR signal characteristic of the PINO radical was clearly observed. Remarkably, no signal appeared under an argon atmosphere or when Co^{III} was added instead of Co^{II}. These observations suggest that

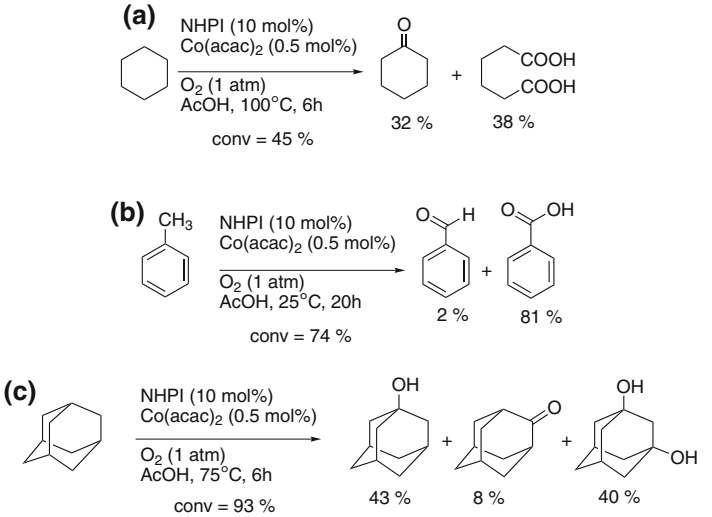

Scheme 5.37 Oxidation of **a** cyclohexane, **b** toluene and **c** adamantane by $Co(acac)_2$/NHPI using molecular O_2 as the oxidant. The yield (%) of each product is based on the amount of reacted substrate (conv = conversion)

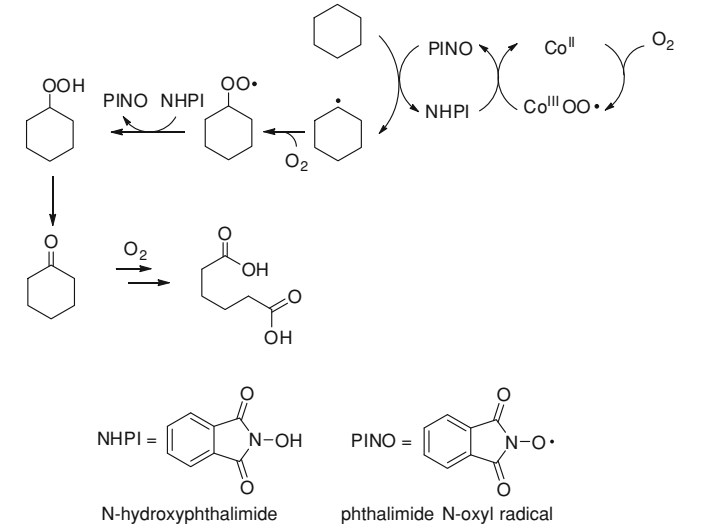

Scheme 5.38 Proposed mechanism of cyclohexane oxidation by the NHPI/$Co(acac)_2$ system using molecular O_2 as the oxidant

the cobalt(II) center reacts with dioxygen to generate a superoxocobalt(III) intermediate that assists the generation of the PINO radical from NHPI, which is the real executor of the oxidation process. The feasibility of the generation of cobalt-

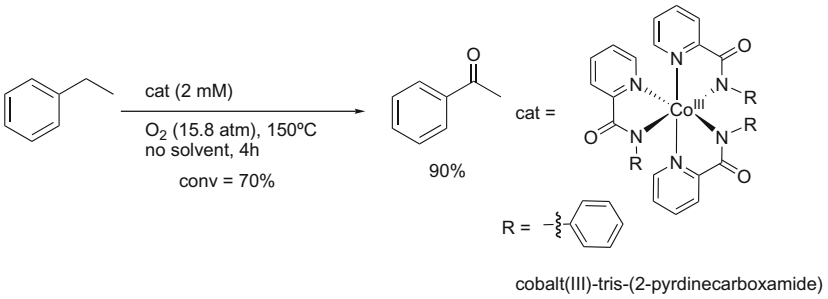

Scheme 5.39 Selective oxidation of ethylbenzene to acetophenone using cobalt(III)-tris-(2-pyrdinecarboxamide) as catalyst

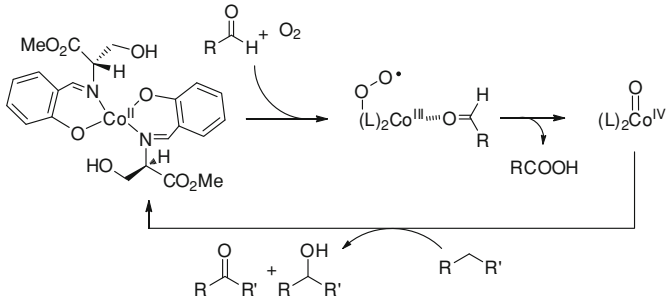

Scheme 5.40 Carbonyl assisted oxidation of alkanes catalyzed by Schiff-base cobalt(II) complexes with molecular O_2

superoxo species by a $1e^-$ reduction of O_2 and their ability to perform hydrogen-atom abstraction has been previously reported [164]. To exemplify the proposed mechanism of the oxidation process, in Scheme 5.38 it is represented the oxidation of cyclohexane by the NHPI/Co(acac)$_2$ system. The newly generated PINO radical performs a hydrogen-atom abstraction form cyclohexane, to generate an alkyl radical that spontaneously reacts with dioxygen to give cyclohexyl hydroperoxide which decomposes to cyclohexanone or adipic acid by further oxidation.

Another interesting system combining cobalt and O_2 as the oxidant is constituted by the cobalt(III)-tris(2-pyridinecarboxamide), which oxidizes alkanes under solvent-free conditions (Scheme 5.39) [165]. Ethylbenzene is converted in 70 % yield in 4 h and acetophenone is produced with high selectivity (90 %). However, some disadvantages of the system include high O_2-pressures (15.8 atm) and temperatures (150 °C) required for catalysis.

Some cobalt(II) Schiff-base complexes can also perform the oxidation of alkanes in the presence of O_2 and aliphatic aldehydes as co-catalysts (Scheme 5.40) [166]. In these particular systems, a cobalt(III)-superoxo species was experimentally detected by EPR spectroscopy under catalytic conditions. The authors suggest that aldehyde coordination modifies the properties of the metal center so that formation of the metal-superoxo species (which is not observed in

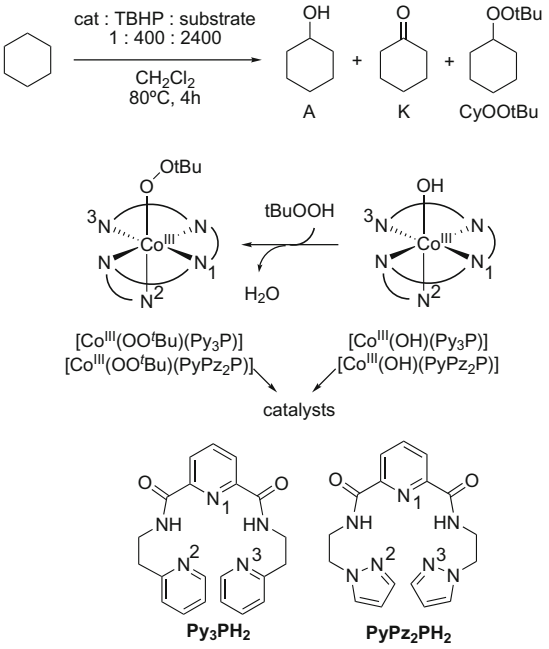

Scheme 5.41 Schematic representation of the cobalt(II)-alkylhydroperoxo complexes used as catalysts in cyclohexane oxidation using TBHP as the oxidant

the absence of the carbonyl compound) becomes feasible but it also assists the posterior homolytic O–O bond cleavage, that leads to the formation of a carboxylic compound and a high valent cobalt(IV)-oxo species, considered to be the active species responsible for the oxidation process. Thus, the aldehyde used as co-catalyst has two crucial functions: on one hand it becomes oxidized in an oxygen-atom transfer event from the cobalt(III)-superoxo to form a cobalt(IV)-oxo compound, and on the other hand its coordination to the metal center finely tunes the electronic and steric properties of the cobalt center enabling the formation of the initial cobalt-superoxo species. The use of TBHP together with cobalt complexes constitutes also a good combination to perform alkane oxidation [160]. In this line, the groups of Mascharak and Mimoun could isolate and structurally characterize a series of Co^{III}-alkylperoxo species by reaction of Co^{III}-hydroxo precursors with ROOH [167–170]. Although several ligand structures have been applied for such studies, the most successful systems include dianionic ligands combining three N-heterocyclic groups and two amido units, that, upon coordination of the akyl-peroxide unit, generate well-characterized octahedral complexes with the general formula $[Co^{III}(OOR)(L)]$ (L = Py_3P, $PyPz_2P$) (Scheme 5.41). Direct reaction of these isolated cobalt-alkylperoxo species (in the absence of any external oxidant) with alkanes gave the corresponding oxidized products (alcohol and ketones) together with $[Co^{III}(OH)(L)]$ as the final metal compound. The fact that the cobalt(III)-hydroxo starting material was recovered at the end of the oxidation reaction suggested that these compounds could be potentially applied catalytically, which prompted the authors to design catalytic systems based on the combination

Table 5.8 Catalytic results obtained in the oxidation of cyclohexane using TBHP as the oxidant and cobalt(III)-alkylhydroperoxo or cobalt(III)-hydroxo complexes as catalysts (reaction conditions as described in Scheme 5.41)

Catalyst	A (TN)[a]	K (TN)[a]	CyOO^{t}Bu (TN)[a]
[Co^{III}(OH)(Py_3P)]	57	66	7
[Co^{III}(OH)($PyPz_2P$)]	61	73	7
[Co^{III}(OO^{t}Bu)(Py_3P)]	53	61	6
[Co^{III}(OO^{t}Bu)($PyPz_2P$)]	58	71	7

[a] TN = (mols oxidized products)/(mols catalyst)

of [Co^{III}(OOR)(L)] or [Co^{III}(OH)(L)] and excess TBHP [168]. Oxidation of cyclohexane was achieved with turnover numbers as high as 140 (Table 5.8). From a mechanistic point of view, it is proposed that [Co^{III}(OOR)(L)] initiates radical-based autooxidation processes by preferential homolytic scission of the O–O bond, which explains the low alcohol/ketone (A/K) ratios and the presence of cyclohexyl ^{t}butyl hydroperoxide (CyOO^{t}Bu) as a minor oxidation product.

5.6 Alkane C–H Oxidation Catalyzed by Nickel Complexes

The use of nickel complexes as catalysts in the oxidation of alkanes is scare compared to other first row transition metals such as iron and manganese. However, selected works deserve to be highlighted as they have succeeded in using nickel-based systems in such oxidative transformations.

[Ni^{II}(OAc)(tpa)(H_2O)](BPh_4) has been used as catalyst in the oxidation of cyclohexane in combination with MCPBA as the oxidant (Scheme 5.42) [171]. Turnover numbers as high as 656 can be achieved at room temperature in 1 h under conditions of limiting oxidant (catalyst:oxidant:substrate 1:1000:7500). Unfortunately, the use of other oxidants which are much more appealing from an environmental point of view (H_2O_2 or TBHP) resulted in a complete loss of oxidation activity. Systematic studies performed by modifying the primary tpa ligand architecture concluded that the replacement of two pyridine units by 2,4-di-*tert*-butylphenol groups resulted in nickel catalysts with enhanced reactivity (860 TN) [172, 173].

The mechanism operating in this nickel tpa-based system seems to involve a metal-based oxidant as suggested by the mechanistic probes that show high alcohol:ketone ratio (A/K = 8.5), significant kinetic isotope effect (KIE = 2.3) and also a high preference for the oxidation of tertiary C–H bonds over secondary ones in the oxidation of adamantane ($3^\circ/2^\circ$ = 12.5). The proposed catalytic pathway requires the O–O homolytic cleavage of a putative [Ni^{II}(OOC(O)Ar)(X)(tpa)] intermediate to give a nickel-oxo species (Ni^{III} = O or its isomer Ni^{II}-O·) which is directly responsible for substrate oxidation (Scheme 5.43). Although, nickel-oxo species are highly elusive, their potential oxidizing ability has been directly experimentally proved in the gas-phase. Schröder and Schwarz demonstrated that methane can be selectively oxidized to generate methanol by NiO^+ under ion cyclotron resonance

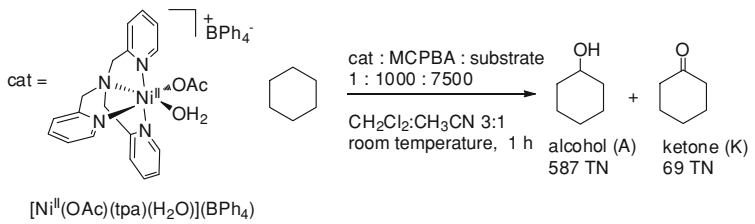

Scheme 5.42 Oxidation of cyclohexane by $[Ni^{II}(OAc)(tpa)(H_2O)](BPh_4)$ using MCPBA as the oxidant

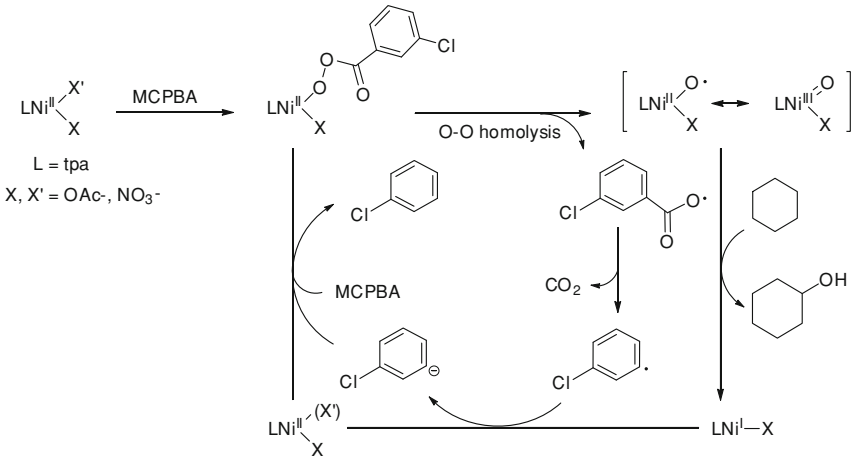

Scheme 5.43 Proposed reaction mechanism for the catalytic oxidation of cyclohexane by $[Ni^{II}(OAc)(tpa)(H_2O)](BPh_4)$ using MCPBA as the oxidant [172]

conditions [174]. Indeed, NiO^+ proved to be the most efficient and selective oxidant from all the metal-oxo species used in the study.

Oxidation of cyclohexane has also been observed for a selected structurally characterized $[Ni^{II}(OO^tBu)(Tp^{iPr})]$ complex (Tp^{iPr} = hydro-tris(3,5-di-2-propyl-pyrazolyl)borate) (Scheme 5.44) [175]. Nevertheless, the small turnover number achieved (TN = 2) indicates a poor catalytic performance of the system and the low alcohol:ketone ratio (1:2) suggests the involvement of free-diffusing radical species rather than a metal-based oxidant, which may be generated during the decomposition of the nickel-alkylperoxo compound.

5.7 Alkane C–H Oxidation Catalyzed by Copper Complexes

Copper is found at the active site of a number of enzymes that perform C–H oxidation reactions. This is clearly exemplified by the well-known enzyme pMMO (particulate methane monooxygenase) which performs the oxidation of methane to

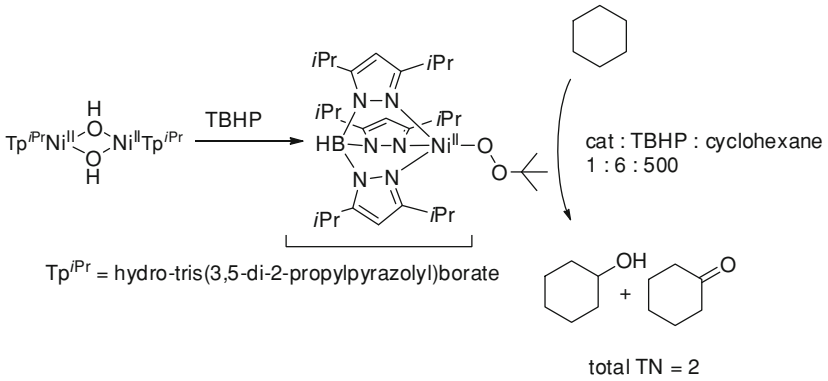

Scheme 5.44 Synthesis of [Ni^{II}(OOtBu)(Tp^{iPr})] complex along with its cyclohexane oxidation activity

methanol using O_2 as the oxidant. Despite the fact that the structure of its active site has been a matter of intense debate in the last 20 years, a recent crystallographic study establishes the presence of a dicopper active site [176]. The fact that copper is used in biological systems for the oxidation of hydrocarbons suggests that it might be a good candidate to perform analogous transformations in synthetic systems. In fact, in the literature several studies deal with the use of this metal in alkane oxidation reactions. A general overview of these systems is given below.

Pioneer works by Geletii in the 80s made use of copper perchlorate in combination with pyridine in acid medium for the oxidation of cyclohexane into cyclohexanone using hydrogen peroxide as the oxidant [177]. Shortly afterwards, this copper system was studied by Barton in the frame of the so-called Gif chemistry [178]. Both cyclic (cyclohexane, cyclododecane, adamantane) and acyclic (n-hexane) alkanes were tested as substrates in these reactions under different reaction conditions. However, in all cases the yields were below 30 % and the reactions were barely selective affording a mixture of oxidized products including alcohols and ketones. Molecular dioxygen [179] or TBHP [180] have also been used as oxidants in combination with several copper salts, albeit affording limited yields and turnover numbers.

In 1993 a contribution by Murahashi and coworkers constituted a significant advance in the field. The combination of $Cu(OH)_2$ and acetaldehyde afforded the oxidation of several alkanes in high yields using molecular O_2 (1 atm). For example, indane was oxidized to a mixture of indanol and indanone in a 97 % overall yield [181]. From a thoroughly screening of copper salts and aldehydes, an extraordinarily active system arouse [182, 183]. It consisted in the combination of $CuCl_2$ and 18-crown-6 in the presence of acetaldeyde and using molecular oxygen as the oxidant at 70 °C. The system exhibited turnover numbers in the 10^4 range for all the alkanes tested (Scheme 5.45). A clear preference for the formation of the ketone product over the alcohol was observed (ketone/alcohol rations ranged

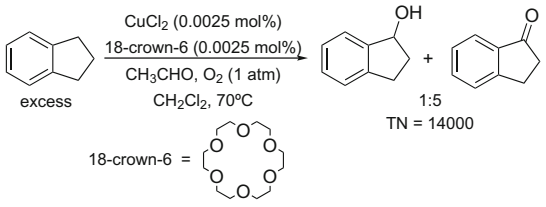

Scheme 5.45 Oxidation of indane by $CuCl_2$ in combination with 18-crown-6 and acetaldehyde

from 5 to 20). The authors suggested that under the reaction conditions a peracid was formed in situ through the copper-assisted reaction of the aldehyde with O_2, and indeed they did observe the presence of peracetic acid by ^{1}H-NMR. Despite the fact that a copper-oxo species derived from the interaction of the peracid with copper(II) was suggested as the key intermediate, this idea was afterwards discarded and a radical-based mechanism was proposed instead [184].

Within the frame of providing understanding for the nature of oxidizing species in Fenton chemistry, Sawyer, Llobet and co-workers studied the combination of copper salts and N-based ligands as catalysts for the oxidation of alkanes and alkylaromatics using H_2O_2 and TBHP as oxidant [185, 186]. Modest efficiencies were obtained with H_2O_2, but TBHP oxidations provided good yields in terms of oxidant transformed into products. The authors propose a rather complex mechanistic scenario based on the formation of high valent copper species. However, reaction patterns are very similar to those obtained in free radical transformations where tBuO· and tBuOO· radicals are involved.

The use of well defined copper complexes instead of copper salts opened the door to the development of systems with new reactivities. In the late 90s, Nishida reported the use of $[Cu^{II}(bpdg)Cl]^+$ (Scheme 5.46a) in combination with H_2O_2 to afford the oxidation of cyclohexane with very modest turnover numbers ($\sim$10) [187], while Schuchardt used $[Cu^{II}(en)_2]^{2+}$ (Scheme 5.46b) in combination with TBHP in the same reaction but with a significantly increased activity (TN $\sim$ 100) [188]. Kitagawa also described mononuclear and dinuclear copper(I) complexes as catalysts in the oxidation of alkanes (Scheme 5.46: $[Cu^{I}(SPy_2)]^+$ and $[Cu^{I}_2(Py_2SSPy_2)]^{2+}$). A supporting ligand combining nitrogen and sulphur as donors was used in this case. Both H_2O_2 and TBHP were used as oxidants for the oxidation of cyclohexane affording a mixture of alcohol and ketone products with maximal turnovers around 70 [189]. In this work the authors detected and characterized the formation of a copper(II)-hydroperoxo intermediate which was regarded as either the active species or the precursor that led to the real oxidant by homolytic or heterolytic O–O bond cleavage. In another work, Itoh et al. described the involvement of a dicopper-bis(μ-oxo) species in the oxidation of alkanes with hydrogen peroxide [190]. In this case, mononuclear copper(II) complexes bearing a β-diketiminato ligand $[Cu^{II}(^{R}L)(OAc)]$ (Scheme 5.46c) were used as precatalysts. However, the system showed limited activity with turnover numbers around 26 in the oxidation of cyclohexane.

Ligands combining N and O-atom donors have also been successfully used for the preparation of active copper catalysts in the oxidation of alkanes. Punniyamurthy and coworkers described the high activity of a hydrogenated version of the salen-

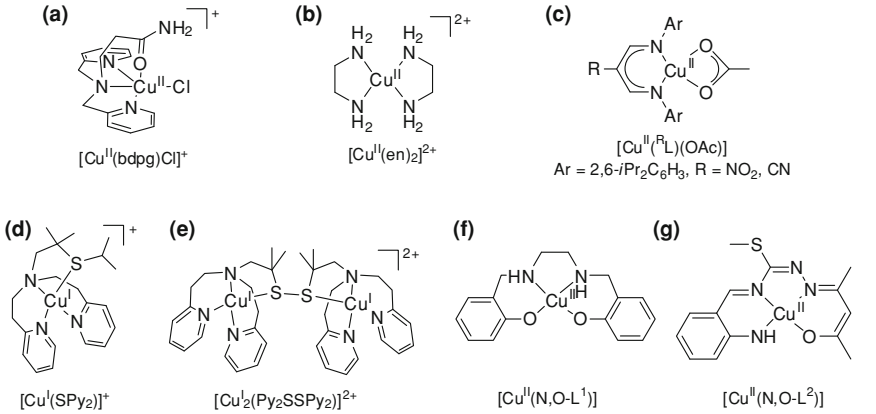

Scheme 5.46 Copper complexes used for the oxidation of alkanes

Scheme 5.47 Oxidation of alkanes using H_2O_2 and TBHP as oxidants, catalyzed by copper complexes

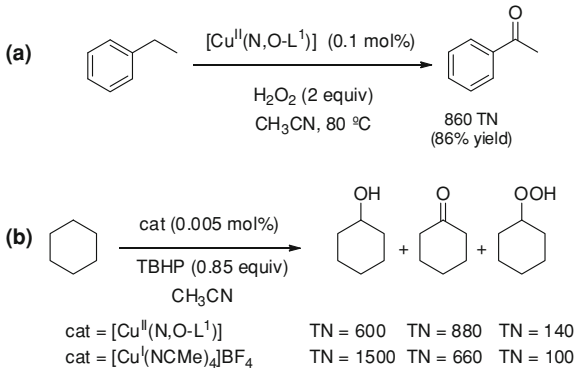

copper(II) complex, that is $[Cu^{II}(N,O\text{-}L^1)]$ (Scheme 5.46f), in the oxidation of alkylbenzenes with H_2O_2 as the oxidant under conditions of limiting substrate [191]. For example, ethylbenzene could be oxidized to acetophenone with turnover numbers as high as 860 (86 % yield) (Scheme 5.47a). Remarkably, the stronger C–H bonds of cyclohexane proved to be a difficult target for the system and only 18 % yield was achieved in this case. In the same line, Shul'pin and coworkers used copper(II) complexes with N,O-ligands in combination with several oxidants including H_2O_2, TBHP and peracetic acid. The most active catalyst in this series, $[Cu^{II}(N,O\text{-}L^2)]$ (Scheme 5.46g), was very efficient affording 480 TN in the oxidation of cyclohexane to give cyclohexyl hydroperoxide as the main product along with cyclohexanol and cyclohexanone [192]. Under certain conditions and using TBHP as oxidant the turnover number reached 1600, but this number could be increased up to 2200 with simple copper(I) salts as catalysts such as $[Cu^{I}(CH_3CN)_4]BF_4$ (Scheme 5.47b). A free diffusing radical path involving oxygen- or carbon-centered radicals was the most plausible mechanism for these transformations.

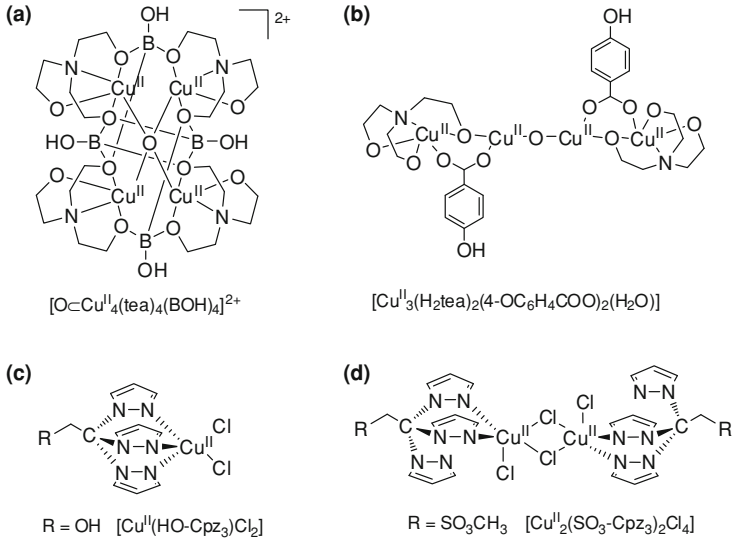

Scheme 5.48 Copper complexes developed by Pombeiro and coworkers for the oxidation of alkanes

Despite the variety of the systems described above, it was not until 2005 when Pombeiro and coworkers described a copper system that could even oxidize the strong C–H bonds of methane [193, 194]. A series of dimeric, trimeric, tetrameric and polymeric copper(II) complexes based on the triethanolamine ligand (H_3tea) were synthesized and initially tested in the oxidation of cyclohexane. The trimeric and tetrameric complexes (Scheme 5.48: $[Cu^{II}_3(H_2tea)_2(4\text{-}OC_6H_4COO)_2(H_2O)]$ and $[O \subset Cu^{II}_4(tea)_4(BOH)_4]^{2+}$) proved to be specially active affording yields up to 32 % with respect to substrate and turnover numbers around 400 when large excess of oxidant was used. Moreover, the catalysts could be recovered at the end of the reaction and reused at least 5 times [195]. The presence of the tripodal tea ligand was essential for the activity because the use of a simple salts such as $Cu(NO_3)_2$ gave significantly lower turnover numbers. The most active tetrameric complex, $[O \subset Cu^{II}_4(tea)_4(BOH)_4]^{2+}$, could even oxidize methane and ethane to the corresponding alcohols with turnover numbers of 47 and 23, respectively (Scheme 5.49a). The reaction conditions required the use of excess H_2O_2 and the presence of acid (cat:H_2O_2:HNO_3 = 1:1000:20) at 30 atm and 40 °C. Although the overall yields were very low (~2 %) the performance in the oxidation of these strong C–H bonds converts the system in a functional model for the natural enzyme pMMO. The same tetracopper catalyst was used with TBHP in the oxidation of cyclohexane [196] and alkyl benzenes giving remarkable turnover numbers (~300 TN) (Scheme 5.49b) [197].

Posterior systems reported by the same group did not afford any improvement with respect to the catalysts described above in terms of yields and turnover numbers [198, 199]. However, the authors did develop an interesting soluble

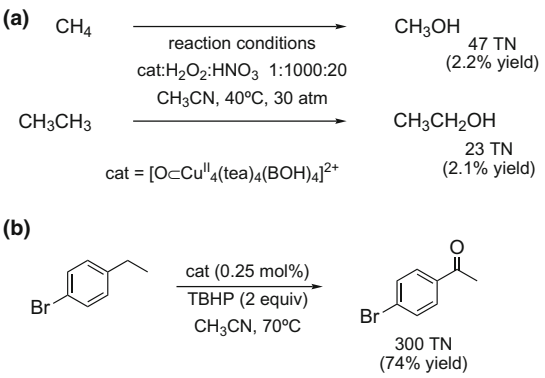

Scheme 5.49 Application of the tetrameric copper complex $[O\subset Cu^{II}_4(tea)_4(BOH)_4]^{2+}$ for the oxidation of alkanes: **a** light alkanes, **b** alkyl benzenes

version of copper complexes based on an scorpionate ligand [200]. Both the mononuclear $[Cu^{II}(HO\text{-}Cpz_3)Cl_2]$ (Scheme 5.48c) and dinuclear $[Cu^{II}_2(SO_3\text{-}Cpz_3)_2Cl_4]$ (Scheme 5.48d) catalysts were very efficient for the oxidation of cyclohexane with hydrogen peroxide in acetonitrile giving turnover numbers up to 190. The replacement of acetonitrile by water caused a remarkable decrease in the activity but still some conversion into oxidized products was achieved and $[Cu^{II}_2(SO_3\text{-}Cpz_3)_2Cl_4]$ performed 23 catalytic cycles.

5.8 Alkane C–H Oxidation Catalyzed by Ruthenium Complexes

5.8.1 RuO_4 as Oxidant

Ruthenium-oxo species from oxidation states IV to VIII are powerful oxidants, capable of oxidizing C–H bonds with different hybridations (sp-sp^3). One of the first reported useful organic synthetic methods using stoichiometric or catalytic ruthenium reagents was the oxidation of organic substrates by RuO_4 [201–203]. The extreme reactivity of the higher valent and highly electrophilic RuO_4 does not require polydentate ligands which are needed to stabilize the corresponding oxo-iron or oxo-manganese species to obtain a distinctive level of efficiency and selectivity (*vide infra*). Stoichiometric or catalytic α-hydrogen transformation on activated C–H bonds such as alcohols, ethers and amines through high oxidation state ruthenium-oxo compounds ("in situ" generated, ex. catalytic amount of $RuCl_2PPh_3$ treated with TBHP or $(n\text{-}Pr_4N)(RuO_4)$ [204–207] combined with *N*-methylmorpholine *N*-oxide) affords the corresponding carbonyl or iminium ion. In these reactions the heteroatom-containing compounds such as ethers [208, 209], amines [210–215] and amides [206, 207], are transformed into esters or lactones and amides or imides, respectively. These transformations are illustrated by the examples depicted in the Scheme 5.50, Scheme 5.51 showing the in situ preparation of the oxidant.

Scheme 5.50 Selected oxidations of activated C–H bonds by ruthenium tetraoxide

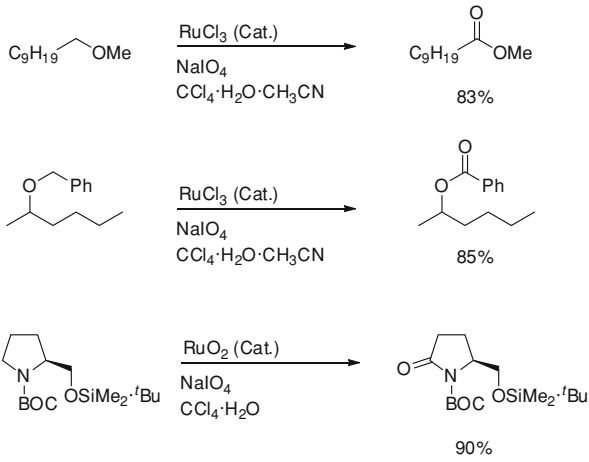

The oxidation of non-functionalized alkenes by high valent ruthenium-oxo species become of interest since 1953 when Djerassi and Engle studied the activity of RuO_4 in order to replace OsO_4 as stoichiometric oxidant agent for olefins [216]. The extraordinary capacity of the ruthenium tetraoxide to oxidize organic compounds was revealed. However, the danger of explosions needed to be avoided by using halogenated solvents. The difference in C–H oxidation reactivity between RuO_4 and OsO_4 was appreciated by its reaction with phenantrene. Osmium tetraoxide in benzene solution slowly affords (after 2–7 days) the osmate ester in good yield, which upon cleavage leads to the crystalline 9,10-dihydrophenanthrene-9,10-diol. Instead, ruthenium tetraoxide in CCl_4 at 0 °C leads rapidly to the formation of 9,10-phenanthrenequinone as the main compound.

5.8.2 *Catalytic Systems Based on RuO_4*

The first attempts to perform a catalytic oxidation of a C–H bond using a biphasic system with a catalytic amount of ruthenium ($RuCl_3$ or RuO_2) dates on late 60s. Oxidants such as NaOCl [217–219] $NaBrO_3$ [220–222] HIO_4 [223], $NaIO_4$[224–235], as well as electro-oxidation conditions [236–238] have been also employed as oxidants. Nonetheless, very slow and incomplete reactions have been frequently observed in the oxidations with RuO_4. The formation of low-valence ruthenium carboxylate complexes was identified as the most plausible pathway of catalysts deactivation. In 1981, Sharpless et al. introduced a broadly applicable catalytic biphasic system (CCl_4:CH_3CN:H_2O; 2:3:2) where $RuCl_3$ (5 %) is "in situ" oxidized to RuO_4 by periodate (IO_4^-). In the initial report, the catalytic system was shown useful in the C–H oxidation of ethers to esters [208, 209]. Seminal studies by Bakke [239–243] and Waegel [244–246] have shown that the combination of $RuCl_3$ (2–4 mol %) and $NaIO_4$ in the same tertiary solvent mixture introduced by

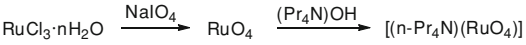

Scheme 5.51 In situ preparation of RuO_4^- oxidizing species

Table 5.9 Oxidation products of unactivated alkanes

Entry	Substrate	Time	T (°C)	Product	Yield (%)[f]
1[a]		26 h	40	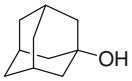	81
2[b]	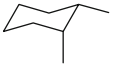	–	rt	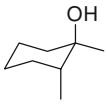	100[c]
3[d]	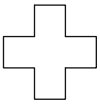	3–7 h	Reflux	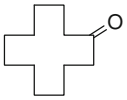	49
4[d]		3–7 h	Reflux	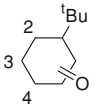	C2, C3 56 C4 17
5[a]		96 h	40	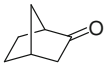	60
6[e]	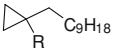	R = H 18 h R = CH_3 28 h	rt	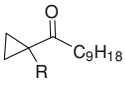	R = H 41 R = CH_3 53

[a] Reactions were performed in a 2/2/3 mixture of CCl_4/acetonitrile/H_2O using $NaIO_4$ 4 equivalents and $RuCl_3{\cdot}3H_2O$ 2 %

[b] Kinetic experiment carried out in 2/1/2 mixture of CCl_4/acetonitrile/H_2O with $NaIO_4 > 10$ equivalents and different amounts of $RuCl_3{\cdot}3H_2O$

[c] GC Yield

[d] 4/2/3 mixture of CCl_4/acetonitrile/H_2O, $NaIO_4$ 2.3 equivalents and $RuCl_3{\cdot}3H_2O$ 2%

[e] Reaction condition used in (a) but using 3 equiv of $NaIO_4$

[f] Isolated yields

Sharpless (CCl_4:CH_3CN:H_2O) is capable of hydroxylating tertiary C–H bonds of simple substrates (Table 5.9), and the natural product cedrane and related compounds (Table 5.10) [242–245, 247].

Basic aspects of the hydroxylation of alkanes when generating in situ the RuO_4 catalyst under biphasic conditions are illustrated in the series of substrates collected in Tables 5.9, 5.10, 5.11, 5.12. The general trend is that tertiary C–H bonds are more reactive than the secondary C–H, being almost inert the primary C–H bonds. Chemoselective hydroxylation of tertiary C–H bonds has been achieved in a significant number of examples, affording the corresponding tertiary alcohols (ex. adamantane) [244, 245, 247]. Interestingly, some selected examples indicate that the reaction takes place in a stereospecific manner. Under identical conditions, secondary carbons are transformed into ketones through a hydroxylated intermediate (Table 5.9 entry 3–6) [248].

Table 5.10 Selectivity patterns found in the oxidation of unactivated alkanes by RuO_4[a]

Entry	Substrate	Time	T (°C)	Product	Yield (%)[b]
1	 endo/exo 3:1	20 h	55	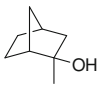	68 (90)
2		48 h	40	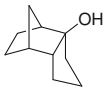	85
3	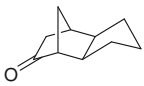	22 h	85	No reaction	
4	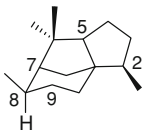	30 h	25	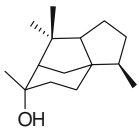 epi-cedrol	69
5	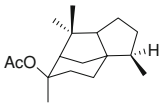	24 h	55	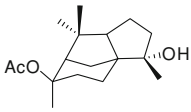	53
6	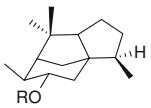	24 h	55	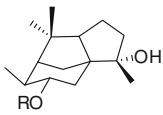	53

[a] Reactions were performed in a 2/2/3 mixture of CCl_4/acetonitrile/H_2O using $NaIO_4$ 4 equivalents and $RuCl_3 \cdot 3H_2O$ 2 %

[b] Isolated yields

Table 5.11 Selection of elaborate substrates with a cyclopropane functional group

Entry	Substrate	Time	T (°C)	Product	Yield (%)
1[a]	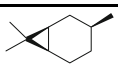 (-)-Carane	24 h	rt	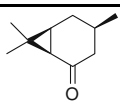	75
2[b]	 2-methylspiro[2.5]octane	8 h	60	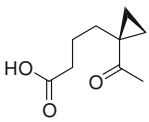	44
3[a]	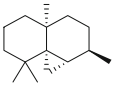 Thujopsane	24 h	rt	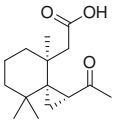	30

Reactions were performed in a 2/2/3 mixture of CCl_4/acetonitrile/H_2O using

[a] $NaIO_4$ 3 equivalents and $RuCl_3 \cdot 3H_2O$ 20 %,

[b] $NaIO_4$ 4 equivalents and $RuCl_3 \cdot 3H_2O$ 2 %

Table 5.12 Reactivity of *cis*— and *trans*—pinane

Entry	Substrate[a]	Oxidant	Main products[b]	
1	 *cis*-pinane	4 $NaIO_4$	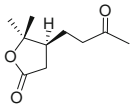 48%	 10%
2	 *cis*-pinane	2.1 $Ca(OCl)_2$	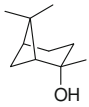 42%	
3	 *trans*-pinane	4 $NaIO_4$	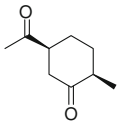 26%	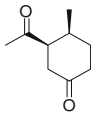 29%

[a] Reactions were performed at 60°C for 1 h in a 2/2/3 mixture of CCl_4/acetonitrile/H_2O using $RuCl_3 \cdot 3H_2O$ 6 %

[b] Isolated yields

In specific cases, (entries 4–6 from Table 5.9) there is an inversion of the expected selectivity: secondary carbons become preferentially oxidized in front of tertiary C–H bonds. Preferential methylene oxidation of ^{t}butylcyclohexane, most likely indicates that the steric hindrance of the ^{t}butyl group directs the C–H selectivity. Another general rule is that the tertiary C–H in a bridge-head position (fused norbornanes) are not oxidized [244–246]. An illustrative example is reported in entry 5, the methylene groups of the norbornane undergo oxidation without affecting the tertiary C–H bonds [235]. Stereoelectronic effects also affect C–H oxidation selectivity. Entry 6 of Table 5.9 illustrates the chemoselective oxidation of the methylene group in the α position to the cyclopropane ring. The selective oxidation of the -CH_2- occurs not only in presence of the bridgehead tertiary C–H bonds of the cyclopropane but also in the presence of other tertiary C–H bonds (Table 5.11 entry 1) [249, 250].

Oxidation of tertiary C–H bonds occur with stereoretention as it is illustrated in the examples of Table 5.9 (entry 2) and in Table 5.10. Furthermore, endo/exo selectivity is also observed in bicyclic [2, 21] alkanes, cedrane skeleton and related substrates [235, 244–246, 251]. The selectivity is highly marked towards the oxidation of the endo 3° C–H bond in a competition experiment by a 3/1 endo/exo mixture of 2-methyl-norbonane (Table 5.10 entry 1). The only hydroxylated compound detected was the endo 2-methyl-exo-2-norbornanol in 90 % yield, leaving the exo isomer intact. Likewise, the oxidation of endo-tetrahydrodicyclopentadiene affords efficiently the hydroxylated product in an isolated 85 % yield. In contrast, no reaction was observed for the exo-isomer of entry 3 under identical conditions. The complex cedrane skeletons (Table 5.10 entries 4–6) are hydroxylated at the tertiary positions with high selectivity. The basic structure

Scheme 5.52 Proposed mechanism of 4-methylspiro[2.5]octane oxidation

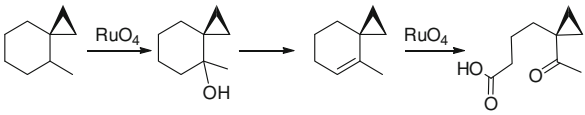

(entry 4) has 4 tertiary, 10 secondary and 12 primary C–H bonds. However, only the ternary C(8), the less hindered carbon, is oxidized leading to epi-cedrol in 69 % isolated yield. Introducing an acetate group on the C(9) block, the oxidation in C(8) transfers into carbon C(2).

The direct derivatization of cyclopropane terpenoids via oxidation using ruthenium tetraoxide has been recently reported by T. Kusumi et al. [252]. Selected examples are depicted in Table 5.11 Straightforward oxidation under standard oxidation conditions leads to the transformation of (-)-Carene into 5-carenone with 75 % yield.

Even more interesting is the transformation observed in some other cases: 4-methylspiro[2.5]octane, thujopsane and (+)-cyclosativene (Table 5.11 and scheme 5.53). When using ruthenium, the oxidation of 4-methylspiro[2.5]octane and thujopsane results in the unusual cleavage of the sp^3-sp^3 σ bond β to the cyclopropane ring to form the corresponding ketocarboxylic acid derivative. The mechanism of these remarkable transformations has been proposed for 4-methylspiro[2.5]octane (Scheme 5.52). The first step is expected to be the oxidation of the more activated C–H; the tertiary C–H bond α to the cyclopropane. Following, dehydratation favored by the formation of the double bond leaves an olefinic intermediate. Subsequent oxidation of the olefin drives to the obtained product [249, 250].

Related examples of a sp^3-sp^3 σ bond cleavage were found in the oxidation of *cis*-pinane and *trans*-pinane with RuO_4 generated in situ (Table 5.12). As it is expected, oxidation into the tertiary equatorial C–H on the *cis*-pinane is proposed as starting point to explain the final product. Experimental observations indicate the formation of an olefin as intermediate. Additionally, the independent oxidation of the olefin proposed intermediate leads to the same final product with higher yields (55 %) [253]. In contrast, the oxidation of the homologous axial tertiary C–H in the *trans*-pinane is not the mayor oxidation pathway. Instead, the oxidation of the bridgehead hydrogen could explain the found products. Bridgehead hydroxylation by ruthenium tetraoxide is highly unusual.

Another example of a complex transformation is found in the cyclopropane terpenoid oxidation of (+)-cyclosativene (Scheme 5.53). On the bases of the observed reactivity, the more activated C–H bond is expected to be located on the α-carbon to the cyclopropane (C10). However, none of the isolated compounds could be ascribed to the initial C10 oxidation. In this regard, it was suggested that the inertness of the methylene C10 of (+)-cyclosativene against oxidation may be associated to the steric hindrance by the surrounding aliphatic moieties [252].

As general trend, primary C–H bonds do not react with RuO_4. However, activated methyl groups such as toluene or ring substituted toluenes with electron withdrawing groups, are converted to carboxylic acids in only 2 h (Scheme 5.54) [254]. In contrast to other substrates, the presence of a quaternary phase transfer

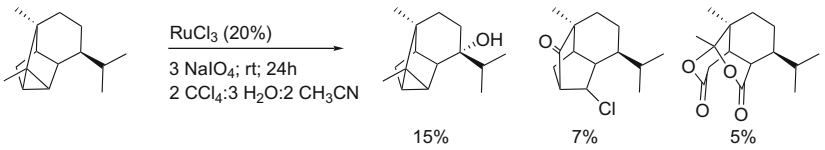

Scheme 5.53 Isolated products on the oxidation of the cyclopropane terpenoid (+)-cyclosativene

Scheme 5.54 Oxidation of the methyl group in substituted methylbenzenes

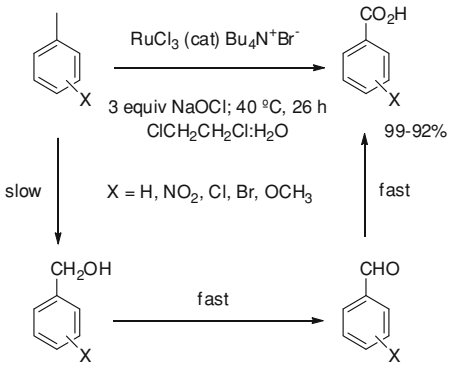

salt ($Bu_4N^+Br^-$) is a necessary prerequisite for the reaction. Kinetic studies show that the reaction is first order in the substrate and catalyst and zero order in the oxidant. Additionally, the absence of detectable intermediates suggests that the first stage of the oxidation is the rate-determining step [254].

An interesting application of the RuO_4 hydroxylation is the selective hydroxylation of steroids in 100 g scale. The family of steroids which was studied presented carbon C16 as an accessible and activated C–H bond (Scheme 5.55). Hydroxylation of the acid sensitive steroids is done in a phosphate buffer (pH 7.5) to inhibit the formation of unwanted transketalized side products. Additionally, the selective oxidation with a cheaper oxidant such as potassium bromate gives the opportunity to develop economically more viable C–H hydroxylation processes [255].

Recently, a new catalytic protocol for tertiary C–H bond hydroxylation involving RuO_4 has been developed by J. Du Bois et al. This represents a significant improvement over the previous protocols (Table 5.13) [256]. The combination of catalytic $RuCl_3$ (5 mol %) and $KBrO_3$ as the stoichiometric oxidant (3 equiv.) promotes the formation of RuO_4, which in the presence of pyridine (10 % mol) undergoes the efficient hydroxylation of unactivated tertiary C–H bonds. The combination of $KBrO_3$ and pyridine is crucial, other oxidants such as $NaIO_4$, NaOCl and Oxone and other bases such as quinuclidine, imidazole, pyridazine, pyrazine, 2,2-bipyridine and pyridine *N*-oxide were examined but significant lower conversions were obtained.

The functional groups included in the substrate scope study demonstrate the compatibility of the method with substrates that include different polar substituents such as an ester, an epoxide, a sulfone, an oxazolidinone, a carbamate, and a sulfamate (Table 5.14).

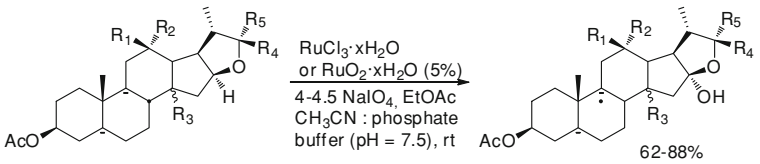

Scheme 5.55 Oxidation of the activated tertiary C–H in steroids

Table 5.13 Comparison among different catalytic systems based on RuO_4

Entry	Substrate	Product	Yield (%)[a]		
			A[b]	B[a]	C[d]
1	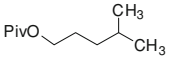	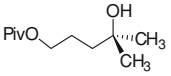	52	40	12
2	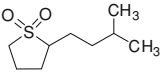	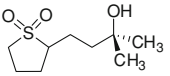	63	48	22
3	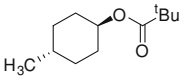	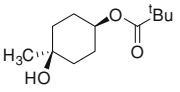	54	29	20

Reactions were performed at 60 °C with 5 mol % $RuCl_3 \cdot xH_2O$ and 3 equiv. of oxidant
[a] Isolated yield of chromatographed product
[b] Acetonitrile/H_2O 1:1, $KBrO_3$ 3 equiv., 10 % pyridine
[c] Acetonitrile/H_2O 1:1, $KBrO_3$ 3 equiv., no pyridine
[d] Acetonitrile/H_2O/CCl_4 1:2:1, $NaIO_4$ 3 equiv., no pyridine

Table 5.14 Selected ruthenium catalyzed hydroxylation of tertiary C–H bonds[a]

Ent.	Substrate	Oxid.	Solvent	Add.	Product	Yield (%)[b]
1		$NaIO_4$	CCl_4/ CH_3CN/H_2O	None		25
2	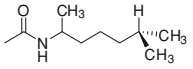	$KBrO_3$	CH_3OAc/ CH_3CN/H_2O	Pyridine	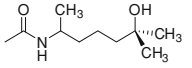	73
3		$KBrO_3$	CH_3CN/H_2O	Pyridine		74
4	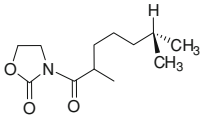	$KBrO_3$	CH_3CN/H_2O	Pyridine	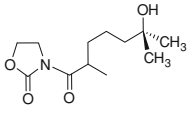	73
5	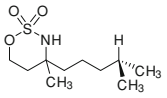	$KBrO_3$	CH_3CN/H_2O	Pyridine	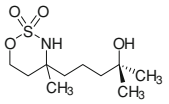	42

[a] Reactions were performed at 60 °C with 5 mol % $RuCl_3xH_2O$, 10 mol % pyridine, and 3 equiv. of oxidant
[b] Isolated yields of chromatographed product
[c] No other tertiary alcohol products were obtained

5.8.3 Reaction Mechanisms for the Catalytic Systems Based on RuO_4

Waegell [244–246, 249–251, 253], Bakke et al. [224–234, 239–243, 257] early studies on the oxidation of C–H bonds by RuO_4 led to the initial proposal of a ionic mechanism in 1986 [247]. Since then, several mechanisms have been postulated. Nowadays, it is believed that the activation of the C–H bond in alkanes follows a (3 + 2) pathway.

Kinetic investigations on the oxidation of saturated hydrocarbons when using RuO_4 shows pseudo-first order kinetics with respect to the substrate and the ruthenium catalyst. The same result is obtained independently of the solvent mixture used (H_2O:acetone or H_2O:CCl_4:acetonitrile). The polarity of the reaction medium has low influence on the reaction rate. Additionally, the activation parameters obtained are consistent with a bimolecular associative process. Therefore, the studies on the effect of the solvent in the reaction rate indicate a small degree of charge separation in the transition state. Besides, a correlation between the rate dependency with the substrates and the Taft constants σ^* provided reaction constants ρ^* of -2.5 in CCl_4:acetonitrile suggesting a considerable development of a positive charge in the TS. Kinetic isotopic effects (KIE) obtained in CCl_4:acetonitrile show a large primary KIE (as example *cis*-decaline 4.8), negligible secondary KIE, and no solvent effect on KIE. There are important experimental observations that support the postulated mechanism. The reactions are stereospecific. The introduction of chloride atoms into products when using CCl_4:acetonitrile as the solvent mixture is usually not observed. The only exception is an example where phase-transfer conditions (H_2O:CCl_4:acetonitrile) are employed. All over, no introduction of nucleophiles has been detected so far. All these findings are consistent with a (3 + 2) addition. However, a P-450 like rebound-like mechanism will also account for the observations, provided the radical pair collapses at a rate faster than 10^{-8}.

Recently, Strassner et al. [257] have studied the RuO_4 catalyzed C–H oxidation of adamantane, *cis*-, *trans*-decaline through a mechanism based on a (3 + 2) addition using DFT methods. Computed energies are on the range of those experimentally obtained by Bakker and co. Moreover, computed KIEs in gas phase are in good agreement with the values observed when performing the reactions in polar solvents. Finally, the authors propose that the hydroxide adduct $RuO_4(OH)^-$ could play an active role in the substrate oxidation when using basic conditions (Scheme 5.56).

5.8.4 Catalytic Systems Based on Coordination Ruthenium Complexes

The in situ generation of RuO_4 leads to Ru(VIII)-based systems for the oxidation of alkanes which are highly selective and efficient. On the other hand, the use of ligands to stabilize the ruthenium in other oxidation states opens up different opportunities to modulate the reactivity.

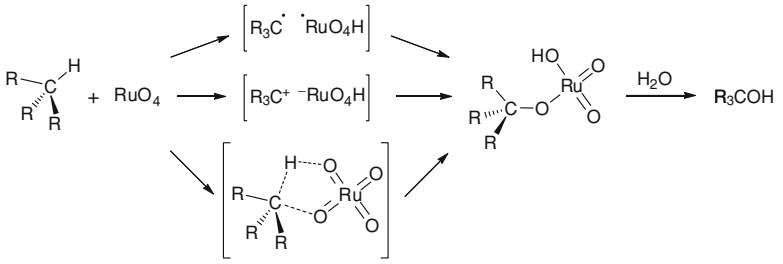

Scheme 5.56 Proposed mechanism for the oxidation of C–H bonds by RuO_4

Scheme 5.57 Examples of high-valent ruthenium complexes studied as stochiometric oxidants

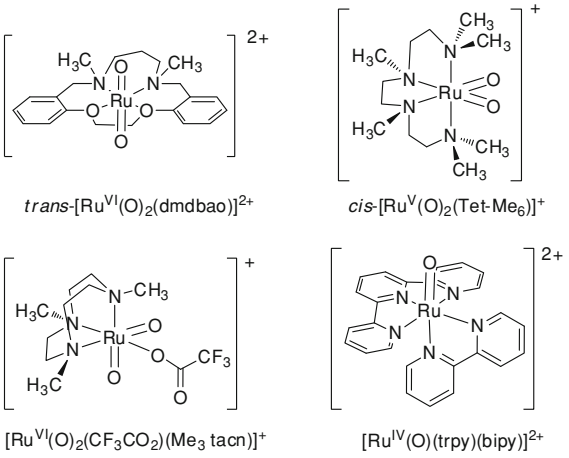

Ruthenium complexes in which the ruthenium is in lower oxidation state than VIII (IV, V and VI) are known to be stabilized by nitrogen-ligands. Among others (Scheme 5.57), $BaRu^{VII}(O)_2(OH)_3$ [258, 259], *trans*-$[Ru^{VI}(O)_2(dmdbao)]^{2+}$ [260], *cis*-$[Ru^{V}(O)_2(Tet\text{-}Me_6)]^{+}$ [261], $[Ru^{VI}(O)_2(CF_3CO_2)(Me_3tacn)]^{+}$ [262], *cis*-$[Ru^{VI}(O)_2(6,6'\text{-dichloro-}2,2'\text{-bpy})_2]^{2+}$ [263], and $[Ru^{IV}(O)(trpy)(bpy)]^{2+}$ [264], have been found to be active in the oxidation of alkanes when used in stochiometric amounts. It was suggested that in many of these high-valent ruthenium complexes, the oxidation of the C–H bond by the Ru = O moiety takes place through an H-atom abstraction mechanism [202, 265–269].

Ruthenium complexes with either 2,2′-bipyridines or 1,10-phenanthrolines are attractive systems to study due to their robustness and the easy availability of [Ru = O] complexes [270]. Pioneer studies by Che et al. reported the catalytic oxidation of cyclohexane to cyclohexanol and cyclohexanone when using *cis*-$[Ru(L)_2(OH_2)_2]^{2+}$ complexes (L = substituted 2,2′-bipyridines or 1,10-phenanthrolines) and TBHP as oxidant. The complexes also showed high efficiency in the oxidation of hexane and pentane. The formation of the ketone product was preferred over the hydroxylation. As an example, the oxidation of cyclohexane

Scheme 5.58 Selected ruthenium bipyridyl systems

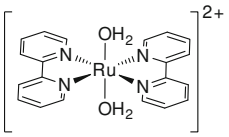

trans-$[Ru(H_2O)_2(bipy)_2]^{2+}$

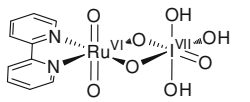

$[RuO_2(bipy)\{IO_3(OH)_3\}]\cdot 1.5\ H_2O$

Scheme 5.59 $K[Ru^{III}(EDTA\text{-}H)]$ and $K[Ru^{III}(PDTA\text{-}H)]$ as examples of the Ru(III) complexes studied in oxidation catalysis

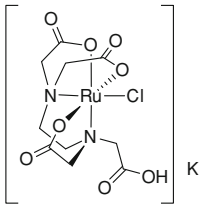

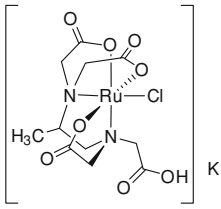

with the complex *cis*-$[Ru(6,6\text{-}Cl_2bpy)_2(OH_2)_2](OTf)_2$ and TBHP in acetone at 20 °C for 2 h, yields 420 TONs with a A/K ratio of 0.65 [202, 263, 265–269, 271].

Trans-$[Ru(H_2O)_2(bipy)_2]^{2+}$ (Scheme 5.58) catalyzes the hydroxylation of a large variety of alkanes using TBHP as oxidant at room temperature for 5 h in benzene with much modest results: cyclopentane (5 % yield, 10 TON), cyclohexane (13 % yield, 26 TON), cycloheptane (13 % yield, 26 TON), pentane (8 % yield, 16 TON), adamantane (1 % yield, 2 TON). However, a remarkable activity is observed in the oxidation of toluene into benzaldehyde (90 % yield, 180 TON). Nevertheless, the yields are relatively low in comparison to $[Ru^{VI}(O)_2(bipy)(IO_3(OH)_3)]\cdot 1.5H_2O$. This ruthenium complex leads to high product yields under refluxing conditions using a biphasic water-CH_2Cl_2 system, periodate as oxidant and 15 h of reaction time. In particular, the hydroxylation of cyclopentane (91 % yield, 114 TON), cyclohexane (87 % yield, 110 TON), cycloheptane (60 % yield, 75 TON), pentane (67 % yield, 84 TON), adamantane (45 % yield, 56 TON) are particularly efficient [272].

Mechanistic insights are provided by the observation that chlorinated products were obtained when the oxidation of cyclohexane was performed in acetone/CCl_4 (9:1 v/v). This observation, together with the KIE observed in the case of cyclohexane ($k_H/k_D = 4.8$) and the lack of stereoretention obtained in the hydroxylation of *cis*-decaline (*cis*-/*trans*-9-decanol 15/62) suggest that following C–H bond breakage, free diffusing radicals are generated [273].

In parallel, Khan et al. introduced the ruthenium(III)-EDTA-ascorbate-H_2O_2 system. The study of its activity in the catalytic oxidation of cyclohexane reveals comparable activity with regard to the iron(III)-EDTA-ascorbate system. Additionally, complexes $K[Ru^V(O)(EDTA)]\cdot 3H_2O$ and $K[Ru^V(O)(PDTA)]\cdot 3H_2O$ (Scheme 5.59) were also synthesized by oxidation of $K[Ru^{III}(EDTA\text{-}H)Cl]$ and $K[Ru^{III}(PDTA\text{-}H)Cl]$ with PhIO or NaOCl. The oxidation of the inactivated secondary C–H bonds of cyclohexane and the primary C–H bonds of toluene were investigated when using the $Ru^V = O$ complexes mentioned above. The reaction rate was found to be first-order on the ruthenium complex and on the substrate. However, the reaction rate turned to be

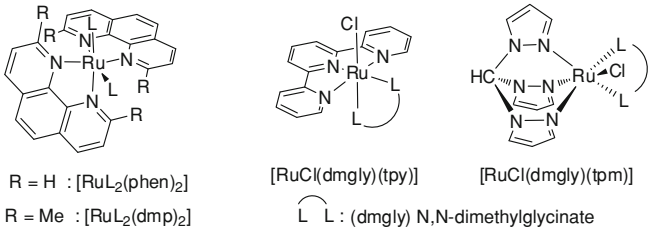

Scheme 5.60 Selected ruthenium catalyst systems based on non-porphyrinic ligands

zero-order on the ruthenium complex when higher concentrations of the substrates were employed. Based on these results, a very intriguing pre-equilibrium involving formation of a substrate-Ru= O complex was proposed [274–277].

In 1989, Morvillo et al. introduced non-porphyrinic ruthenium complexes (*trans*-$[RuCl_2(dpp)_2]$; dpp: 1,3-bis(diphenylphosphino)propane), (*cis*-$[RuCl_2(DMSO)_4]$) and (*cis*-$[RuCl_2(phen)_2]$; phen: 1,10-phenantroline), as alkane oxidation catalysts. A significant activity was observed in the oxidation of adamantane (>50 TON in 20 h) when using biphasic conditions such as CH_2Cl_2 and an aqueous solution of LiClO. A free diffusing radical pathway was proposed to operate in these reactions. This hypothesis is supported by the experimental observation that considerable amounts of chlorinated hydrocarbons (<10 %) are obtained when the reaction is performed using chlorinated solvents [278].

Drago et al. reported that the use of sterically demanding ligands such as 2,9-dimethyl-1,10-phenantroline (dmp) leads to catalysts for the oxidation of methane, ethane and propane. In complexes like *cis*-$[Ru(H_2O)_2(dmp)_2]$, the oxo ligands are forced to be *cis* (Scheme 5.60). According to the experimental evidences reported by Drago, Cundari and Che, the *cis*-dioxoruthenium complexes are significantly more active than the corresponding *trans*-dioxoruthenium complexes. Only mild conditions are usually required: aqueous H_2O_2 30 % as oxidant and relatively low pressure of the hydrocarbon (4 bars). After 1 day, the hydroxylation of methane leads to 1.7 % (TON 125) when using water as a solvent and to 1.9 % (TON 140) of conversion when employing acetonitrile. The reaction can be inhibited by a radical inhibitor, and chloride incorporation into products can be detected when CCl_4 is employed as a solvent. On these bases, the authors propose that reactions involve a hydrogen-atom abstraction that initiate a free-diffusing radical mechanism [279, 280].

Structurally different type of systems is the μ_3-oxo trinuclear carboxylate complex $[Ru_3(\mu_3\text{-}O)(pfb)_6(EtO_2)_3]^+$ (where pfb = $CF_3CF_2CF_2CO_2^-$) which catalyzes the hydroxylation of alkanes using O_2 as oxidant (75 °C, 3 atm). Cyclohexane was oxidized to a mixture 5:1 cyclohexanol:cyclohexanone achieving 15:3 TONs. The oxidation of methylcyclohexane yielded 10 TONs of 1-cyclohexanol, and significant amounts of 2- and 3-cyclohexanol were also detected (4 TONs). The mechanism proposed involves a free-diffusing radical pathway [281].

The μ_3-oxo trinuclear carboxylate complex $[Ru_3(\mu_3\text{-}O)(CH_3COO_2)_6(Py)_2L]^+$ where L is CH_3OH or dmso, both of which are good leaving groups under catalytic

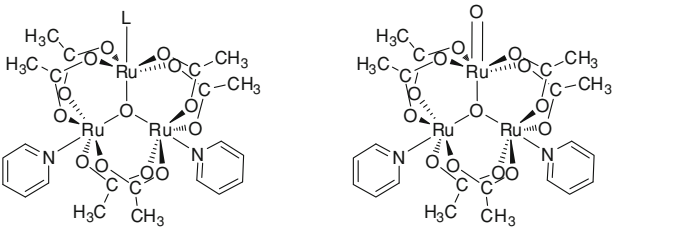

Scheme 5.61 μ_3-Oxo trinuclear carboxylate complexes studied in oxidation catalysis

oxidation conditions, was also tested in the oxygenation of alkanes. The use of TBHP or PhIO as oxidants generates the proposed catalytically active intermediates $[Ru_3^{IV,IV,III} = O]^+$(Scheme 5.61). Oxidation of cyclohexane was carried out leading to modest conversions and activities [282, 283].

An uncharacterized catalytic system has been developed using $BaRuO_3(OH)_2$ in combination with trifluoroacetic acid and CH_2Cl_2. The system is able to oxidize alkanes at room temperature. Presumably, beyond acidification of the reaction mixture, the trifluoroacetic acid is also a ligand for the ruthenium ion. PhIO is the oxidant effective for the hydroxylation of cyclohexane under these reaction conditions. Other oxidants such as nBu_4IO_4, MCPBA, TBHP or H_2O_2 lead to lower activity and yields [259]. Additionally, the use of a CF_3CO_2H-CH_2Cl_2 mixture has been also investigated either using $RuCl_3 \cdot nH_2O$ as pre-catalyst and CH_3CO_3H as oxidant, or a $RuCl_2(PPh_3)_3$-TBHP system. Although the catalyst is undefined under these conditions, the simple experimental protocol leads to an attractive highly efficient and selective system for the oxidation of hydrocarbons [284].

Tripodal polypyridine structures based in tris(2-pyridylmethyl)amine (tpa) have been also evaluated as possible ligands for the development of ruthenium oxidation catalysts (Scheme 5.62). Jitsukawa and Yamaguchi, amongst others, studied the influence on the reactivity when modifying the 6th, 5th or 4th-position of the pyridine in the tpa substructure. In addition, the replacement of one of the pyridyl arms by a carboxylic acid or the exchange of the pyridines by quinolines or benzimidazoles substructures was also evaluated [285–289]. Results are collected in Table 5.15. These comparative studies indicate that the simplest tpa ligand provides the most efficient catalysts.

Yamagishi et al. analyzed the differences in reactivity of *cis*-[RuCl(dmso)(tpa)]PF_6 and *trans*-[RuCl(dmso)(tpa)]PF_6 complexes (where *cis* and *trans* refer to the relative orientation of the Cl ligand with respect to the non-pyridinic nitrogen ligand), in the hydroxylation of adamantane, using MCPBA as oxidant. The experimental results revealed significant differences: 1-adamantanol was formed in 88 % when using the *trans*(Cl, N_{amino}) complex and in 63 % when using the *cis*(Cl, N_{amino}) complex (Scheme 5.57). In both cases, high selectivities in the oxidation of 3°/2° C–H bonds were observed and only traces of 2-adamantanol and

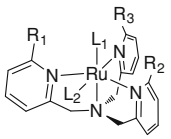

R_1:R_2:R_3 = H : [Ru(tpa)Cl_2]

R_1:R_2:R_3 = H : [Ru(tpa)Cl](PF_6)

R_1:R_2:R_3 = Me : [Ru(6-Me_3tpa)Cl](PF_6)

R_1:R_2:R_3 = CO_2Me : [Ru((6-MeO_2C)$_3$tpa)Cl](PF_6)

R_1:R_2:R_3 = ^{t}BuCONH : [Ru(tppa)Cl](PF_6)

R_1:R_2:R_3 = ^{t}BuCH_2NH : [Ru(tnpa)Cl_2](PF_6)

R_1:R_2 = H; R_3 = ^{t}BuCONH : [Ru(bnpa)Cl](PF_6)

R_1:R_2 = H; R_3 = ^{t}BuCH_2NH : [Ru(mnpa)Cl_2](PF_6)

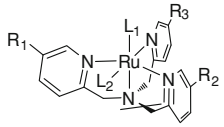

R_1:R_2:R_3 = Me : [Ru(5-Me_3tpa)Cl_2]

R_1:R_2:R_3 = CO_2Me : [Ru(5-MeO_2C-tpa)Cl](PF_6)

R_1:R_2 = H; R_3 = $(CH_3)_2$NCO : [Ru(5-$(CH_3)_2$NCO-tpa)Cl_2]

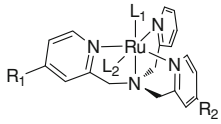

R_1 = H; R_2 = EtOOC : [Ru(4-(COOEt)-tpa)Cl_2]

R_1 : R_2 = EtOOC : [Ru(4-$(COOEt)_2$-tpa)Cl_2]

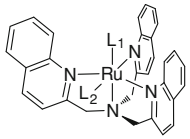

[RuCl(tqa)](PF_6)

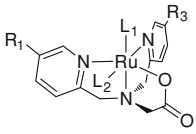

[RuCl(dpca)](PF_6)

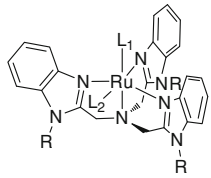

R = H; [RuCl(tHba)](PF_6)

R = Me; [RuCl(tMeba)](PF_6)

Scheme 5.62 Ruthenium catalyst systems based on the tpa framework structure

1-chloroadamane were detected. Surprisingly, the hydroxylation of *cis*-decalin was achieved with complete retention of configuration. Yamaguchi suggests a metal-based oxidation via short-lived alkyl radicals [285–288]. The replacement of MCPBA by other oxidants such as TBHP or PhIO led to less effective systems. A general trend is also that the hydroxylation of alkanes (ex. adamantane) with ruthenium-tpa complexes is more efficient in chlorinated solvents than in acetonitrile.

Electrochemical studies were performed by Kojima and Fukuzumi in order to elucidate if either Ru^{II}/Ru^{III} or Ru^{III}/Ru^{IV} couples are operative when employing [$RuCl_2$(L)]-tpa based catalysts. The complexes studied were [$RuCl_2$(5Me_3tpa)], [$RuCl_2$(tpa)], [$RuCl_2$(5-$CONMe_2$-tpa)], [$RuCl_2$(4-MeO_2C-tpa)] and [$RuCl_2$((4-MeO_2C)$_2$-tpa)] (Scheme 5.62). The results reveal that the redox properties can be significantly influenced by the substituent on the tpa substructure. The Ru^{III}/Ru^{IV} pair has a relatively large ρ value of +0.150 on the linear Hammett plot. As expected, electron withdrawing substituents such as carboxylic methyl esters and dimethyl amidate stabilize the lower oxidation states with respect to complexes with the methyl substituted or non-substituted tpa substructures. These observations translate into important differences in reactivity. In fact, sharp divergences in time dependent product distribution are observed depending on the ruthenium complex employed in the oxidation of cyclohexane with MCPBA. In the case of

Table 5.15 Ruthenium-catalyzed hydroxylation of adamantane using tpa-derivatives as ligands

Entry	Catalyst	Oxid.	Product[a]				
			1-ol	2-ol	2-one	Cl	Diol
1[b]	*cis*-[RuCl(dmso)(tpa)]PF_6	MCPBA	63	Trace	trace	6	24
2[b]	*trans*-[RuCl(dmso)(tpa)]PF_6	MCPBA	88	2	trace	4	Trace
3[c]	[$RuCl_2$(tpa)]PF_6	PhIO	8	0.7	0.4	0.8	nr[e]
4[c]	[RuCl(tppa)]PF_6	PhIO	9	0.4	0.7	1.2	nr[e]
5[c]	[$RuCl_2$(tnpa)]PF_6	PhIO	10	0.2	0.5	1.0	nr[e]
6[c]	[RuCl(bnpa)]PF_6	PhIO	22	Trace	1.1	0.7	nr[e]
7[c]	[$RuCl_2$(mnpa)]PF_6	PhIO	28	0.2	1.2	0.8	nr[e]
8_b	[RuCl(5MeO_2C-tpa)]PF_6	MCPBA	76	0	2	2	1
9_b	[$RuCl_2$(tqa)]PF_6	MCPBA	63	4	1	2	nd[f]
10_d	[RuCl(dmgly)(tpy)]PF_6	MCPBA	66	3	2	5	nr[e]
11_d	[RuCl(dmgly)(tmp)]PF_6	MCPBA	39	3	2	7	nr[e]

[a] abbreviations: 1-ol = 1-adamantanol, 2-ol = 2-adamantanol, 2-one = 2-adamantanone, Cl chlorinated-adamantanes, diol = adamantane-1,3-diol
[b] The reaction was carry out in $CHCl_3$ at r.t. for 24 h. [substrate] = 4×10^{-2} mol/L, [catalyst] = 2×10^{-4} mol/L, [MCPBA] = 6×10^{-2} mol/L
[c] The reaction was carry out in 1,2-dichloroethane at 40 °C for 1 h. [substrate] = 1×10^{-1} mol/L, [PhIO] = 1×10^{-1} mol/L, [catalyst] = 1×10^{-3} mol/L
[d] The reaction was carry out at rt for 24 h. [substrate] = 4×10^{-2} mol/L, [catalyst] = 4×10^{-4} mol/L, [MCPBA] = 6×10^{-2} mol/L
[e] not reported
[f] not determined

[$RuCl_2$(tpa)], the formation of cyclohexanol, cyclohexanone and chlorobenzene follows a parallel increment over time. The concomitant formation of cyclohexanol and cyclohexanone is attributed to an autoxidation process of the cyclohexane via a free-radical chain. However, [$RuCl_2$((4-MeO_2C)$_2$-tpa)] seems to promote the oxidation of cyclohexane to cyclohexanol which is continuously consumed to give cyclohexanone. In second place, when oxidation reactions are performed in the presence of $H_2^{18}O$, only 9 % of ^{18}O is incorporated into products when using [$RuCl_2$(tpa)] but 100 % of ^{18}O incorporation is obtained if [$RuCl_2$((4-MeO_2C)$_2$-tpa)] is employed. This high ratio of ^{18}O inclusion strongly suggests that high-valent metal-oxo species are the responsible intermediates for the hydroxylation of cyclohexane in the case of [$RuCl_2$((4-MeO_2C)$_2$-tpa)]. However, the use of [$RuCl_2$(tpa)] promotes the formation of free radicals via a Haber–Weiss mechanism in which an electron transfer from MCPBA to Ru^{III} leads to Ru^{II} species and an acylperocyl radical (Scheme 5.63). Instead, the higher redox potential of the Ru^{II}/Ru^{III} pair of the [$RuCl_2$((4-MeO_2C)$_2$-tpa)] complex blocks the electron transfer from MCPBA to Ru^{III}. Therefore, a free radical chain is not possible but the formation of [Ru^{IV} = O] species is expected instead [290].

The bis-μ-chloro Ru^{II} dimmers [Ru^{II}Cl(tpa)]$_2$($ClO)_2$ and [Ru^{II}Cl(5-Me_3t-pa)]$_2$($ClO)_2$ (Scheme 5.64) also catalyze the oxidation of cyclohexane and adamantane with TBHP or CHP (cumene hydroperoxide) as oxidants at 40 °C [291–294]. The addition of an excess of NEt_4Br gives rise to the formation of bromocyclohexane as unique product. Reactions performed under an O_2 atmosphere

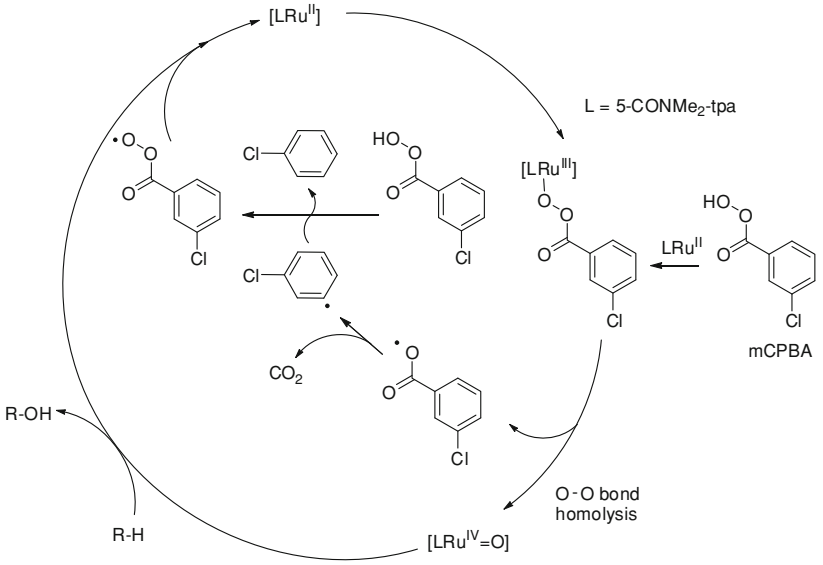

Scheme 5.63 Proposed catalytic cycle for the oxidation of substrates by $[RuCl_2((4\text{-}MeO_2C)_2\text{-tpa})]$

Scheme 5.64 Dimeric ruthenium catalyst systems based on the tpa framework structure

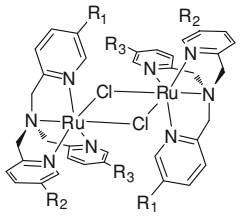

$R_1{:}R_2{:}R_3$ = Me : $[Ru(5Me\text{-}tpa)Cl](PF_6)$

exhibit reaction rates higher than under a N_2 atmosphere. These facts are attributed mainly to a radical chain mechanism initiated by an electron-transfer reaction to generate alkoxo ($RO^{\bullet}$) and alkylperoxo ($ROO^{\bullet}$) radicals as reactive species (Scheme 5.65) [295, 296].

On the other hand, $[Ru(tpa)(H_2O)_2](PF_6)_2$ has been oxidized in the presence of water with $(NH_4)_2[Ce(NO_3)_6]$ to form a Ru^{IV}–oxo complex, which proved to be catalytically reactive species in oxidation reactions. This strategy results into a catalytic oxygenation system in which water acts as both the solvent and as the oxygen source [297].

Chatterjee and Shepherd et al. studied series of ruthenium(III) complexes bearing a tridentate Schiff-base ligands (see Scheme 5.66) and bidentate ligands as bipy or 2-picolinate (pic). These systems were successfully employed for the oxidation of alkanes (cyclohexane, toluene, THF) when using TBHP as oxidant. However, only modest yields were reported. The authors suggest the formation of Ru^{V}=O as the catalytic active intermediates [298–300].

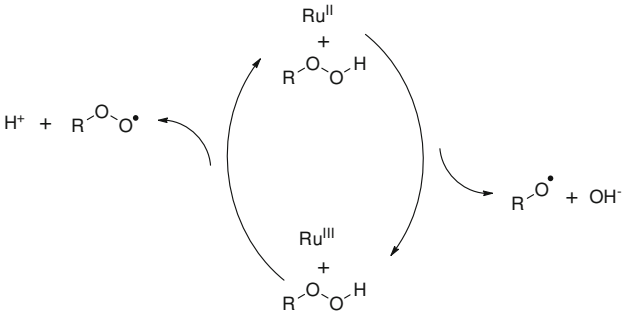

Scheme 5.65 Ruthenium catalyzed formation of radical species from the oxidant

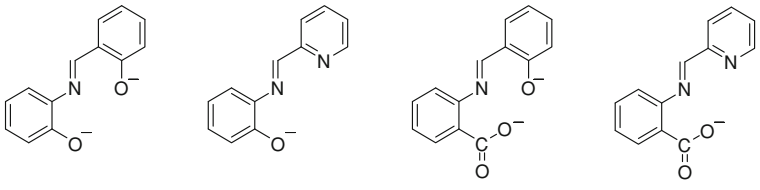

Scheme 5.66 Tridentate Schiff base ligands used by Chatterjee to form ruthenium based oxidation catalysts

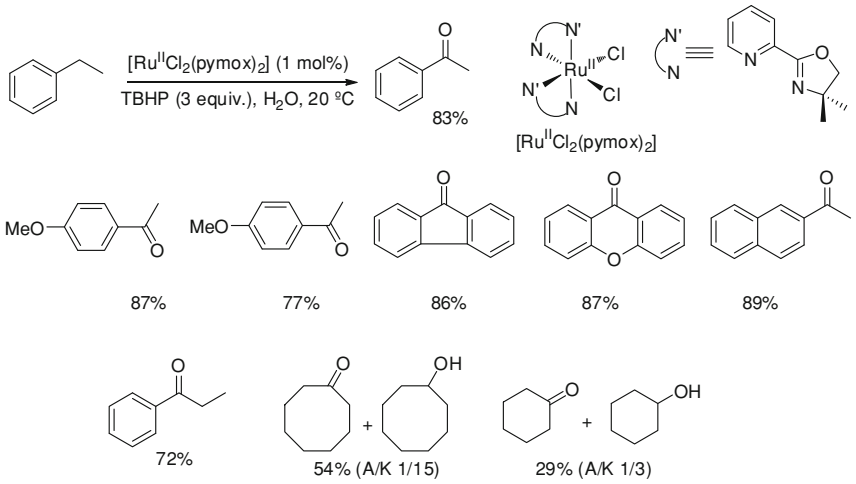

Scheme 5.67 Catalytic oxidation of alkylarenes and cycloalkanes by $[RuCl_2(pymox)_2]$ and TBHP in water

Finally, the water soluble cationic Ru^{III}-complex $[RuCl_2(pymox\text{-}Me_2)_2]BF_4$ (Scheme 5.67) has been established as a highly useful catalyst for the C–H bond oxidation of alkylarenes and alkanes in water when using TBHP as oxidant.

Table 5.16 Catalytic oxidation of alkanes by MTO [311]

Entry	Substrate	Time (h)	T (°C)	Product	Yield (%)[a]
1[b]		48	60		88
2[b]		48	60		60
3[c]		72	40	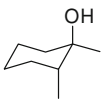	98
4[c]		72	40	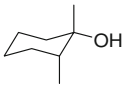	20
5[c]		72	40	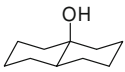	20
6[c]		72	40	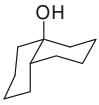	90

Reactions were performed in a molecular ratio of substrate/H_2O_2/MTO (6/150/1)
[a] Calculated using an internal standard
[b] EtOH was used as a solvent
[c] ^{t}BuOH was used as a solvent

Ketone products are predominantly obtained while alcohols are detected in low ratios. In this particular system, a solvent-caged P-450 like oxygen rebound mechanism via a Ru^{IV}-oxo active species was proposed to account for a large KIE in the oxidation of ethylbenzene ($k_H/k_D = 14$), an electrophilic character ascertained by the Hammett analysis ($\rho = -1.1$), and the lack of reaction inhibition when radical traps such as TEMPO are added to the reaction mixture [301].

5.9 Alkane C–H Oxidation Catalyzed by Rhenium Complexes

Herrmann and Espenson groups were the pioneers to explore the catalytic activity of oxo-rhenium compounds such as Re_2O_7, ReO_4^- and $(CH_3)Re(O)_3$ (MTO) as catalysts in oxidation reactions. Among all of them, MTO emerged as the most active species for oxidizing unsaturated compounds [302–305].

The first report that explores the capacity of MTO for oxidizing alkanes when combined with H_2O_2 as ultimate oxidant was published by Murray et al. in 1995. Under catalytic reaction conditions (MTO/alkane/H_2O_2 ratio of 1/6/150), the system formed by MTO/H_2O_2 slowly reacts with tertiary C–H bonds of saturated alkanes to yield hydroxylation products (see Table 5.16). Remarkable high yields and complete stereoselectivity was observed in the oxidation of substrates like *cis*-1,2-dimethylcyclohexane or *cis*-decaline (Table 5.16, entries 3–6). High

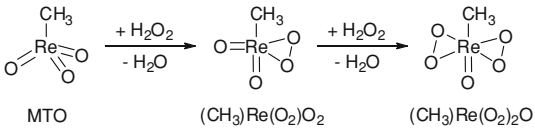

Scheme 5.68 MTO reaction with H_2O_2 to form $((CH_3)Re(O_2)O_2)$ and $((CH_3)Re(O_2)_2O)$

selectivity for the tertiary against secondary C–H bonds was attained in the case oxidation of adamantane (Table 5.16, entry 1). These observations are indicative of a metal center hydroxylation. However, later on a discrepancy in the results derived form the oxidation of triphenylmethane was noted. Murray obtained triphenylcarbinol from the catalytic oxidation of triphenylmethane (Table 5.16 entry 2), while Crucianelli and Saladino reported the formation of benzophenone as a mayor product (73 %) together with a small amount of benzoate (8 %) under the same experimental conditions [306, 307]. Despite of the high selectivity, a drawback of this methodology is that reaction rates are low, even in the presence of relatively high catalyst loadings (16.7 %). Other rhenium (VII) complexes such as $K[ReO_4]$ and Re_2O_7 showed lower reactivity than MTO [308].

Attempts to modify the activity of the organorhenium catalyst MTO by the addition of ligands, such as pyrazine-2-carboxylic acid, generated a less selective catalytic system. In fact, when the reaction was performed in refluxing acetonitrile solution at 80 °C with an alkane:H_2O_2:ligand:MTO ratio of 4700:2000:4:1 the oxidation of cyclohexane, cyclooctane and n-heptane was achieved at 3 times faster than in absence of the ligand. However, a complex distribution of alcohol, ketones and hydroperoxide derivates were obtained [309]. In contrast, when the reaction was performed in a subs:H_2O_2:MTO ratio of 500:500:1 (subs = cyclopentane and cyclohexane) at room temperature only alcohol and ketone products were obtained [308]. Interestingly, η^1- or η^2-(benzoylhydrazido) rhenium complexes in oxidation state III and V showed also catalytic activity under high H_2O_2 loadings as oxidant (ratio subs:H_2O_2:Cat of 16000:32000:1). Selective hydroxylation of cyclopentane was observed. Instead, under the same experimental conditions, Pombeiro and co-workers reported the oxidation of cyclohexane affords alcohol/ketone rations in the range of 1.44 – 1.69 [310].

The MTO/H_2O_2 system is mechanistically very intricate. Indeed, Herrmann [312] and Espenson[313] groups in 1993 found that reacting MTO with H_2O_2 gives two higher oxidized rhenium compounds, the peroxo- $((CH_3)Re(O_2)O_2)$ and bisperoxo- $((CH_3)Re(O_2)_2O)$ complexes, both of which could be involved in the catalytic processes (Scheme 5.68).

With the aim to clarify the somewhat different collection of results Pombeiro et al. studied computationally with DFT methods the plausible routes that may produce $HO^{\bullet}$ and $HOO^{\bullet}$ radicals from the MTO/H_2O_2/H_2O-CH_3CN system [314]. Calculations were performed at level of theory (B3LYP/6-311G(d,p)) using CPCM model to account for the solvent effects. On the basis of these calculations, the authors described a possible catalytic cycle with two reaction steps as responsible for the $HO^{\bullet}$ and $HOO^{\bullet}$ radical generation; homolytic Re-OOH cleavage in a $[MeRe^{VII}O_2(\eta^2\text{-}OOH)(OOH)(H_2O)]$ intermediate gives a $HOO^{\bullet}$

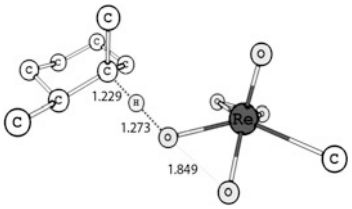

Fig. 5.1 Transition state proposed for the oxidation of ethers, alcohols and unsaturated hydrocarbons by the MTO/H_2O_2 system

radical and the reduction of the rhenium metal center to Re(VI) (Fig. 5.1). In addition, [MeRe^{VI}O(OOH)(OOH)(OH)] intermediates can also undergo homolytic O-OH cleavage forming HO$^{\bullet}$ radicals and the regeneration of the rhenium VII. This mechanism will provide a computational support for the formation of radicals, as it was inferred from the experimental observations under low catalyst loadings.

On the other hand, the high selectivity observed in the oxidation of alkanes by Murray et al. clearly indicates the absence of HO$^{\bullet}$ and HOO$^{\bullet}$ radicals. In fact, a computational study at DFT level of theory (B3LYP/lacvp**-6-31G(d,p) using PB-SCRF as solvent model) focus on the C–H activation by the peroxo- ((CH_3)Re(O_2)O_2) and bisperoxo- ((CH_3)Re(O_2)$_2$O) complexes. This study unravels a plausible C–H insertion reaction via a concerted but highly asynchronous mechanism that proceeds by initial asynchronous hydride transfer, that then turns into hydroxide transfer/rebound [315]. The energy barriers calculated for the reaction between bisperoxo- ((CH_3)Re(O_2)$_2$O), and *cis*-1,2-dimethylcyclohexane and toluene, have free energy barriers of 20.2 and 23.1 kcal·mol^{-1}, respectively. On the other hand, the free energy activation energy barrier corresponding to the reaction of the peroxo-complex ((CH_3)Re(O_2)O_2) with *cis*-1,2-dimethylcyclohexane was almost 10 kcal·mol^{-1} higher in energy. The concerted mechanism, confirmed by the intrinsic reaction coordinate (IRC) method, was invariant irrespective of the solvent.

5.10 Alkane C–H Oxidation Catalyzed by Osmium Complexes

The reactivity of high oxidation states of osmium is best illustrated by the well-known alkene *cis*-dihydroxylation with OsO_4 [316]. Osmium-Oxo complexes in high oxidation states present modest reactivity in alkane oxidation reactions [317–319]. OsO_4 is inactive as stochiometric oxidant of alkanes [320]. However, basic aqueous reaction media (pH = 12.1 by sodium phosphate buffer) or catalytic conditions employing $NaIO_4$ as oxidant (periodate acts as a buffer, 0.1 M gives pH = 4.3) enable the oxidation of different alkanes [317].

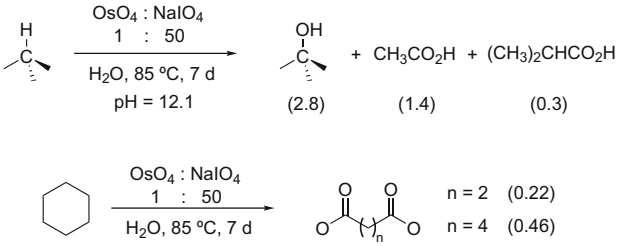

Scheme 5.69 Catalytic hydroxylation of isobutane and cyclohexane. Numbers in parentheses indicates TONs

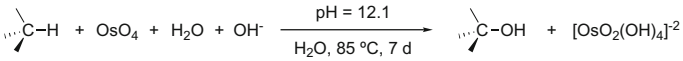

(5.7)

OsO_4 reacts with isobutane (10 bars) when using a basic aqueous reaction medium (pH = 12.1) at 85 °C during 7 days forming ^{t}BuOH in 30 ± 3 % yield with respect to the initial amount of the OsO_4, (Eq. 5.7). 30 ± 1 % of the initial OsO_4 was transformed in $[Os^{VI}O_2(OH)_4]^{-2}$. Oxidation of cycloalkanes such as cyclopentane, cyclohexane, 2-cyclopropylpropane, *cis*- and *trans*-decaline were studied. 2-cyclopropylpropane forms 2-cyclopropyl-2-propanol in low yield. Likewise, the hydroxylation of *cis*-decaline is stereospecific and affords *cis*-9-decalol [321]. Cyclopentane and cyclohexane oxidation reactions only yield over oxidation products.

Ethane and propane were also proven reactive giving acetate as a product in both cases. The lack of formation of propionate was most likely due to the higher reactivity of the secondary C–H bond rather than the primary, which rapidly gives acetone which in turn undergoes further oxidation.

Remarkably, the hydroxylation of isobutane could be carried out catalytically by using $NaIO_4$ as an oxidant (Scheme 5.69). Under these conditions ^{t}BuOH (2.8 TON), acetic acid (1.4 TON) and iso-butyric acid (0.3) were formed. In contrast, when cyclohexane was used as substrate lower amounts of 1 TON of oxidation products were obtained. Nevertheless, these conditions provide higher yields than in the stoichiometric version.

Based on the selectivity reported (OH radicals react rapidly with ^{t}BuOH and exhibit a characteristic competitive reaction between primary and tertiary C–H bonds) and DFT calculations, a concerted [3 + 2] mechanism, was suggested (Scheme 5.70). This mechanism is analogous to that proposed for RuO_4 oxidations of alkanes. However, the proposed active species was most likely the compound $OsO_4(OH)^-$ which is formed under basic conditions (Scheme 5.70).

Previous attempts to produce in situ a selective catalytic system based on osmium was reported by Shul'pin et al. By reacting $OsCl_3$ alone or in presence of nitrogenated ligands (ex. 2,5-dichloropyridine or 2,2′-bipyridine, among others)

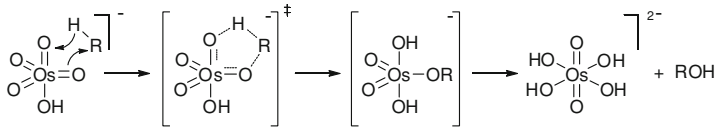

Scheme 5.70 Proposed [3+2] mechanism for the hydroxylation by $[Os^{VIII}O_4(OH)]^-$

with H_2O_2 as ultimate oxidant provides a catalytic system for alkane oxidation. The hydroxylation of *cis*-decaline leads to a modest *trans*/*cis*-9-decalinol ratio of 0.26, indicating that substantial epimerization occurs during the reaction. The authors suggest that the systems H_2O_2-$OsCl_3$ abstracts a hydrogen atom from the alkane via an oxo-osmium complex [322].

Lau et al. explored the $[Os^{VIII}(N)(O)_3]^-$ anion, in combination with a Lewis acid ($FeCl_3$ and $Sr(OTf)_3$) in a CH_2Cl_2/CH_3CO_2H solvent mixture as stochiometric alkane oxidant. The system can also be used as a catalytic oxidation system, when combined with different oxidants (H_2O_2, TBPC, 2,6-Cl_2PyNO and MPPH), allowing for the oxidation of alkanes such as cyclohexane, adamantane, n-pentane, n-hexane, n-heptane and n-octane among others [319]. Indeed, the catalytic was extraordinary efficient in the oxidation of cyclohexane when adding TBHP as oxidant by syringe pump (up to 7500 TON). Under the same experimental conditions OsO_4 was inactive. Replacement of the oxo ligand in (O^{2-}) in $Os^{VIII}O_4$ by the stronger electron donating nitride ion (N^{3-}) leads to the $[Os^{VIII}(N)(O)_3]^-$ anion, in which the electrophylicity of the oxo ion (O^{2-}) is reduced, which translates into a reduced oxidizing capacity. In fact, $[^nBu_4N][Os^{VIII}(N)(O)_3]$ alone was found inactive as stoichiometric oxidant of alkanes (Table 5.17, entry 1) [319].

Stopped-flow kinetic studies on the stochiometric oxidation of cyclohexane by the $[^nBu_4N][Os^{VIII}(N)(O)_3]/FeCl_3$ system reveal that a $[^nBu_4N][Os^{VIII}(N)(O)_3]$-$FeCl_3$ intermediate is rapidly formed. Electrospray Ionization mass spectroscopy studies suggest that reaction of $[^nBu_4N][Os^{VIII}(N)(O)_3]$ with $FeCl_3$ leads to the formation of the bimetallic $[Fe^{III}\text{-}N \equiv Os^{VIII}(O)_3)]$ adduct. Related X-ray diffraction structures, between $[Os^{VIII}(N)(O)_3]^-$ and Au, Pt, Rh and Ru complexes, gives support to the formation of the iron-nitride unit [323, 324]. The decomposition rate of the proposed heterobimetallic intermediate was determined to be directly dependent on substrate (cyclohexane) concentration, but a saturation was observed at high substrate concentration. After reaction, 80 % of the initial osmium complex was recovered as $[^nBu_4N][Os^{VI}(N)(Cl)_4]$, while the Fe species retain the initial oxidation state. Consequently, the osmium species were suggested to act as a 2-electron oxidant. Control experiments discard Cl_2 as a part of the reaction.

The reaction mechanism proposed by the authors (Scheme 5.71) was based on the following observations. No differences in product distribution were obtained when performing the reaction under air instead of Ar atmosphere, or when performing the reactions in the presence of $BrCCl_3$. Remarkably, high efficiency in the oxidation of cyclohexane was also obtained when replacing $FeCl_3$ by $Sc(OTf)_3$ as Lewis acid. (Table 5.17) Additionally, $[^nBu_4N][Os^{VI}(N)(Cl)_4]$ and $[^nBu_4N][Os^{VIII}(N)(O)_3]$ provide identical product distribution. On top of that, 80 % of the initial osmium

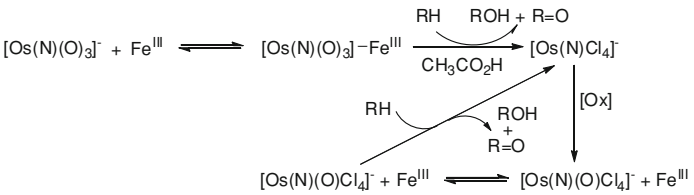

Scheme 5.71 Reactivity of $[Os(N)(O)_3]$-Fe^{III} system as stoichiometric and precatalyts oxidant of alkanes

Table 5.17 Stoichiometric and catalytic oxidation of cyclohexane by $[^nBu_4N][Os^{VIII}(N)(O)_3]$ or $[^nBu_4N][Os^{VI}(N)Cl_4]$

Entry	$FeCl_3$ (molar equiv.)	Conditions (Oxidant)	Time	$C_6H_{11}OH$	Product Yields (%) c-$C_6H_{10}O$	c-$C_6H_{11}Cl$
1	0	S.	24 h	–	–	–
2	2	S.	30 s	2	63	1
3	8	S.	30 s	19	51	4
4	0	C. (TBHP)	5 min	<1	<1	<1
5	0	C. (TBHP)	8 h	25	20	3
6	2	C. (TBHP)	5 h	56	24	2
7	8	C. (TBHP)	5 min	67	21	3
8[a]	8	C. (TBHP)	5 min	69	21	3
9[b]	8	C. (TBHP)	5 min	68	19	3
10	2[c] ($Sc(OTf)_3$)	C. (TBHP)	10 min	57	31	2
11	8	C. (H_2O_2)	5 min	60	26	2
12	1	C. (MPPH)	5 min	49	2	2
13[d]	1	C. (MPPH)	40 min	69	4	3
14[d]	1[c] ($Sc(OTf)_3$)	C. (MPPH)	40 min	61	2	1

*Condition (*S., *Stochiometric)*: the reaction was carried out in CH_3CO_2H:CH_2Cl_2, (2:5 mL) at 23 °C with $[^n Bu_4N][Os(N)(O)_3] = 5.0 \times 10^{-3}$ mol/L and cyclohexane = 1.2 mol/L; Yields were calculated based on $[^n Bu_4N][Os(N)(O)_3]$ as two-electron oxidant. Condition (C.1, Catalytic): the reaction was carried out in CH_3CO_2H:CH_2Cl_2, (2:5 mL) at 23 °C with $[^n Bu_4N][Os(N)Cl_4] = 1.25 \times 10^{-3}$ mol/L, cyclohexane = 1.2 mol/L and Oxidant = 0.1 M; Yields were calculated based on TBHP consumed

[a] Reaction in air

[b] 0.1 M $BrCCl_3$ was added

[c] $FeCl_3$ was replaced by $Sc(OTf)_3$

[d] The oxidant was added by slow syringe pump addition, flow rate = 25 $\mu L \cdot min^{-1}$

complex was recovered as $[^nBu_4N][Os^{VI}(N)(Cl)_4]$, while the Fe species retained the original oxidation state. It was then concluded that both precatalysts should form the same type of reaction intermediate. The oxidation of adamantane leads to a high tertiary/secondary ratio of 28. Stereospecificity was observed in the oxidation of *trans*- or *cis*-1,2-dimethylcyclohexane. MPPH have been used as oxidant to differentiate between free radical and metal-based hydrocarbon oxidations (see iron section). Oxidation reactions catalyzed by $[^nBu_4N][Os^{VI}(N)(Cl)_4]$/Lewis acid and MPPH added by syringe pump gives less than 4 % of products arising from the

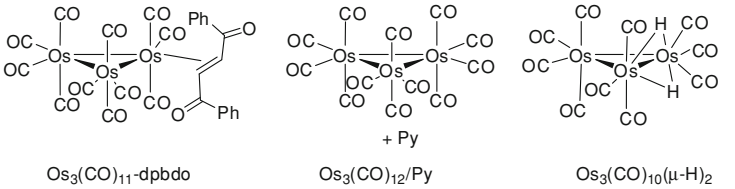

Scheme 5.72 Precatalytic osmium carbonyl clusters

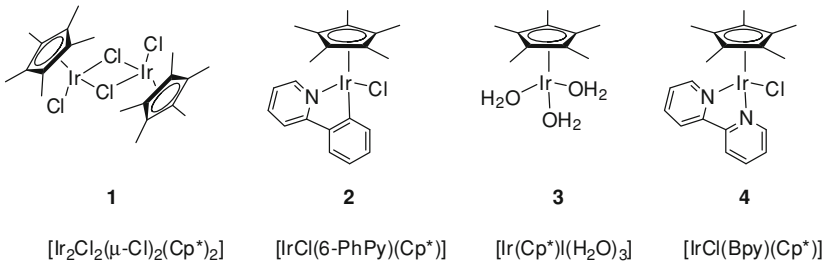

Scheme 5.73 Cyclopentadienyl Iridium complexes active in C–H hydroxylation

homolytic breakage of the O–O bond. Yields of cyclohexanol up to 69 % were obtained in 40 min when the MPPH oxidant was added via syringe pump.

Isotopic labeling experiments with $H_2^{18}O$ on the oxidation of cyclohexane leads to the same ^{18}O incorporation (6 % for 2,6-Cl_2PyNO and none for H_2O_2) independently of the precatalyst used; [$^nBu_4N$][$Os^{VI}(N)(Cl)_4$] or [$^nBu_4N$][$Os^{VIII}(N)(O)_3$]. In contrast, under stoichiometric conditions the use of [$^nBu_4N$][$Os^{VIII}(N)(O)_3$] as oxidant gives 61 % ^{18}O enriched cyclohexanol. Consequently, the hydroxylation most probably proceed by the same [FeL_n-$NOs^{VIII}(O)(Cl)_4$] species where the Os^{VIII} = O unit is activated by the Lewis acid.

Shul′pin et al. studied the oxidation performance of carbonyl osmium clusters as precatalysts (Scheme 5.72) [322, 325, 326]. Intriguingly, the low valent $Os_3(CO)_{11}$-dpbdo and $Os_3(CO)_{12}$/Py are very effective generators of hydroxyl radicals. In particular, the $Os_3(CO)_{12}$/Py/H_2O_2 system oxidized alkanes with an efficiency up to 60,000 TON and 24,000 h^{-1} TOF. In the case of $Os_3(CO)_{10}(\mu\text{-H})_2$ the authors propose that the main pathway is the oxidation through metal-oxo complexes but hydroxyl radicals are also present.

5.11 Alkane C–H Oxidation Catalyzed by Iridium Complexes

The catalytic C–H hydroxylation reaction using iridium complexes was recently reported by Crabtree et al. [327]. The treatment of alkanes and related substrates in a mixture of ^{t}BuOH:H_2O (1:1) with cerium ammonium nitrate as oxidant (CAN) and [Cp*Ir] complexes as catalysts (shown in Scheme 5.73, Table 5.18) leads to

Table 5.18 Hydroxylated Substrates by Cp* iridium complexes

Substrate	Product	Catalyst (Loading per metal)	CAN	Time (h)	Yield[b]
		$[Ir_2Cl_2(\mu\text{-}Cl)_2(Cp^*)_2]$ (4 %)	16	–	27 %[a]
		$[Ir_2Cl_2(\mu\text{-}Cl)_2(Cp^*)_2]$ (4 %)	5.5	12	23 % (91 %)[a] [d]
		[IrCl(6-PhPy)(Cp*)] (4 %)	5.5	12	9 % (79 %)[a] [d]
		$[Ir(Cp^*)(H_2O)_3]$ (4 %)	5.5	21	17 % (95 %)[a] [e]
		$[Ir_2Cl_2(\mu\text{-}Cl)_2(Cp^*)_2]$ (1 %)	9	20	29 %[a]
		[IrCl(6-PhPy)(Cp*)] (3 %)	18	20	55 % (56 %)[a]
		[IrCl(Bpy)(Cp*)] (11 %)	18	24	26 %[a]
		[IrCl(6-PhPy)(Cp*)] (2 %)	3	2	48 %[c]
		$[Ir(Cp^*)(H_2O)_3]$ (1 %)	8	1/3	72 % (72 %)[c]

[a] Reactions were run at 21°C under nitrogen or argon in 1:1 ^{t} BuOH:H_2O

[b] The yield, obtained by NMR, is base on total starting material; yield base on converted starting material in parentheses

[c] D_2O as solvent yield obtained by NMR

[d] Isolated yield

[e] Isolated yield

the C–H hydroxylation from good to moderate yields in the case of inactivated substrates. These complexes also proved to be highly active as catalysts for the oxidation of water [328, 329]

Interestingly, the C–H oxidation of *cis*-1,4-dimethylcyclohexane and *cis*-decalin proceeds with complete retention of stereochemistry. Additionally, use of ^{18}O labeled water in the hydroxylation of *cis*-decaline leads to the quantitative incorporation of ^{18}O into the *cis*-decanol. Activated secondary C–H bonds, like in the case of ethylbenzene and tetrahydrofurane, are oxidized in higher yields than non-activated alkanes. Further oxidation of the initially hydroxylated product yields the final ketone product. Some recent studies suggest the $Ir^V = O$ complexes are the key intermediates in the C–H hydroxylation of alkanes and in water oxidation processes [328, 329]. However, a well defined Ir^V-oxo complex [330], $[Ir^V(O)(mes)_3]$, mes = mesityl, can only oxidize PPh_3, $AsPh_3$ and NMe_3, but not alkanes [331].

5.12 Future Prospects

Alkane C–H bond oxidation remains as a very challenging chemical problem, and the significance of this transformation in biological chemistry and in chemical synthesis will likely continue to drive the attention of chemists during the next decade. On the positive side, the large efforts that are being dedicated to this problem have resulted in the discovery of selected metal based reagents that allow for alkane oxidation under relatively mild conditions, and that in some cases also attain satisfactory yields. In addition, we start to have now an understanding of the major factors that govern selectivity among different C–H bonds in oxidation

reactions [332]. However, these factors exert only subtle and sometimes contraposed influences, and we still have to admit that this understanding is fragile and, with beautiful exceptions, far from allowing predictability when complex organic settings are subjected to oxidation. From a mechanistic perspective, we also have very reliable methods to discern mechanistic paths involved in these reactions, and implication of free-diffusing radical paths can be easily traced and in some cases avoided or limited.

Despite of the advances already made over the last years, discovery of novel practical methods for selective alkane C–H oxidation under mild conditions will continue to be a topic of major interest. But the major challenge in the field remains at designing methods that introduce novel selectivities. Our understanding is that with very few exceptions, regioselective C–H oxidation by currently available reagents is basically dominated by the intrinsic properies of C–H bonds, and so far little diversity is currently attainable irrespective of the oxidizing agent. That is quite a limiting scenario considering that most of organic molecules contain multiple and different types of C–H bonds. Therefore, the full potential of this reaction is very far from being satisfactorily reached. Development of novel reagents that operate with C–H selectivities distinct from those inherently dictated by the spatial and chemical properties of C–H bonds will be a valuous goal because they will open novel synthetic paths and fast building-up of chemical complexity from simple alkane reagents. Stereoselective C–H oxidation reactions can also be included in this general quest for selective C–H bond oxidations. So far, enantioselective C–H oxidations are almost exclusively limited to enzymatic systems, and remains as a holy grial for synthetic catalysts.

Transition metal catalysts are called into playing a major role in this endeavour towards selectivity, since their tunable electronic and structural properties are especially suitable for inducing tailored reactivity patterns. Because of that, it is envisioned that major research efforts will be devoted over the next years to the design of these very unique selective C–H oxidation catalysts.

Acknowledgments Anna Company and Julio Lloret thank MICINN for Ramon Y Cajal Contracts. Financial support via ICREA-Academia Award to MC, Catalan SGR 2009-SGR637, MICINN-Spain (CTQ2009-08464/BQU), the European Research Foundation for Project ERC-2009-StG-239910 and Consolider Ingenio/CSD2010-00065.

References

1. Dyker G (2005) Handbook of C–H transformations. Wiley Weinheim, vol 1–2
2. Olah GA, Molnár Á (2003) Hydrocarbon chemistry, 2nd edn. Wiley, New York, p 871
3. Shilov AE, Shul'pin GB (2000) Activation and catalytic reactions of saturated hydrocarbons in the presence of metal complexes. Springer, Boston
4. Sheldon RA, Kochi JA (1981) Metal-catalyzed oxidations of organic compounds. Academic Press, New York
5. Labinger JA, Bercaw JE (2002) Nature 417:507–514
6. Godula K, Sames D (2006) Science 312:67–72

7. Chen K, Baran PS (2009) Nature 459:824–828
8. James MM (2000) Thermodynamic influences on C-H bond oxidation. In: Meunier B (ed) biomimetic oxidations catalyzed by transition metal complexes. Imperial College Press, London, pp 1–43
9. Ingold KU, MacFaul PA (2000) Distinguishing biomimetic oxidations from oxidations mediated by freely diffusing radicals. In: Meunier B (ed) Biomimetic oxidations catalyzed by transition metal complexes. Imperial College Press, London, pp 45–89
10. Curci R, D'Accolti L, Fusco C (2006) Acc Chem Res 39:1–9
11. Davies HML, Manning JR (2008) Nature 451:417–424
12. Ortiz de Montellano PR (2010) Chem Rev 110:932–948
13. Meunier B, de Visser SP, Shaik S (2004) Chem Rev 104:3947–3980
14. Mansuy D (1993) Coord Chem Rev 125:129–141
15. Perkins MJ (1996) Chem Soc Rev 25:229–236
16. Barton DHR (1998) Tetrahedron 54:5805–5817
17. Stavropoulos P, Celenligil-Cetin R, Tapper AE (2001) Acc Chem Res 34:745–752
18. Correa A, Mancheño OG, Bolm C (2008) Chem Soc Rev 8:1108–1117
19. Enthaler S, Junge K, Beller M (2008) Angew Chem Int Ed 47:3317–3321
20. Plietker B (2008) Iron catalysis in organic chemistry. Wiley, Weinheim
21. Biomimetic Oxidations Catalyzed by Transition Metal Complexes (2000) Imperial College Press, London
22. Costas M, Chen K, Que L Jr (2000) Coord Chem Rev 200–202:517–544
23. Que L Jr, Tolman WB (2008) Nature 455:333–340
24. Fenton HJH (1894) J Chem Soc Trans 65:899–910
25. Walling C (1975) Acc Chem Res 8:125–131
26. Halliwell B, Gutteridge JMC (1999) Free radicals in biology and medicine. Oxford University Press, Oxford
27. Valko M, Morris H, Cronin MTD (2005) Curr Med Chem 12:1161–1208
28. Kell DB (2010) Arch Toxicol 84:825–889
29. Gogate PR, Pandit AB (2004) Adv Environ Res 8:501–551
30. Pignatello JJ, Oliveros E, MacKay A (2006) Crit Rev Environ Sci Technol 36:1–84
31. Brillas E, Sires I A., O. M., (2009) Chem. Rev. 109:6570–6631
32. Gozzo F (2001) J Mol Cat A-Chem 171:1–22
33. Fokin AA, Schreiner PR (2002) Chem Rev 102:1551–1594
34. Masarwa A, Rachmilovich-Calis S, Meyerstein N, Meyerstein D (2005) Coord Chem Rev 249:1937–1943
35. Haber F, Weiss JJ (1934) Proc Roy Soc London Ser A 147:332–351
36. Russell GA (1957) J Am Chem Soc 79:3871–3877
37. Dunford HB (2002) Coord Chem Rev 233–234:311–318
38. Goldstein S, Meyerstein D (1999) Acc Chem Res 32:547–550
39. Walling C (1998) Acc Chem Res 31:155–157
40. Sawyer DT (1997) Coord Chem Rev 165:297–313
41. Bray WC, Gorin MH (1932) J Am Chem Soc 54:2124–2125
42. Nakanishi M, Bolm C (2007) Adv Synth Catal 861–864
43. Pavan C, Legros J, Bolm C (2005) Adv Synth Catal 347:703–705
44. Retcher B, Costa JS, Tang JK, Hage R, Gamez P, Reedijk J (2008) J Mol Cat A-Chem 286:1–5
45. Tang J, Gamez P, Reedijk J (2007) Dalton Trans 4644–4646
46. Shul'pin GB, Golfeto CC, Süss-Fink G, Shul'pina LS, Mandelli D (2005) Tetrahedron Lett 46:4563–4567
47. Li D, Schröder K, Bitterlich B, Tse MK, Beller M (2008) Tetrahedron Lett 49:5976–5979
48. Merkx M, Kopp DA, Sazinsky MH, Blazyk JL, Müller J, Lippard SJ (2001) Angew Chem Int Ed 40:2782–2807
49. Friedle S, Reisner E, Lippard SJ (2010) Chem Soc Rev 39:2768–2779
50. Siewert I, Limberg C (2009) Chem Eur J 15:10316–10328

51. Wang X, Wang S, Li L, Sundberg EB, Gacho GP (2003) Inorg Chem 42:7799–7808
52. Trettenhahn G, Nagl M, Neuwirth N, Arion VB, Jary W, Pöchlauer P, Schmid W (2006) Angew Chem Int Ed 45:2794–2798
53. Esmelindro MC, Oestreicher EG, Márquez-Alvarez H, Dariva C, Egues SM, Fernandes C, Bortoluzzi AJ, Drago V, Antunes OA (2005) J Inorg Biochem 99:2054–2061
54. Romakh VB, Therrien B, Süss-Fink G, Shul'pin GB (2007) Inorg Chem 46:3166–3175
55. Visvaganesan K, Suresh E, Palaniandavar M (2009) Dalton Trans 3814–3823
56. Mayilmurugan R, Stoeckli-Evans H, Suresh E, Palaniandavar M (2009) Dalton Trans 5101–5114
57. Nagataki T, Tachi Y, Itoh S (2005) J Mol Cat A-Chem 225:103–109
58. Kulikova VS, Gritsenko ON, Shteinman AA (1996) Mendeleev Commun 119–120
59. Kitajima N, Ito M, Fukui H, Moro-oka Y (1991) J Chem Soc Chem Commun 102–104
60. Mukerjee S, Stassinopoulos A, Caradonna JP (1997) J Am Chem Soc 119:8097–8098
61. Foster TL, Caradonna JP (2003) J Am Chem Soc 125:3678–3679
62. Rowe GT, Rybak-Akimova EV, Caradonna JP (2008) Chem Eur J 14:8303–8311
63. Rowe GT, Rybak-Akimova EV, Caradonna JP (2007) Inorg Chem 46:10594–10606
64. Mekmouche Y, Duboc-Toia C, Ménage S, Lambeaux C, Fontecave M (2000) J Mol Catal A: Chem 156:85–89
65. Sorokin AB, Kudrika EV, Bouchub D (2008) Chem Commun 22:2562–2564
66. Nizova GV, Krebs B, Süss-Fink G, Schindler S, Westerheide L, Cuervo LG, Shul'pin GB (2002) Tetrahedron 58:9231–9237
67. Mayer AC, Bolm C (2008) Iron-catalyzed Oxidation Reactions. Oxidation of C-H and C = C bonds. In: Plietker B (ed) Iron Catalysis in Organic Chemistry Wiley Weinheim pp 73–92
68. Britovsek GJP, England J, Spitzmesser SK, White AJP, Williams DJ (2005) Dalton Trans 5:945–955
69. Balogh-Hergovich É, Speier G, Réglier M, Giorgi M, Kuzmann E, Vértes A (2003) Eur J Inorg Chem 1735–1740
70. Nguyen C, Guajardo RJ, Mascharak PK (1996) Inorg Chem 35:6273–6281
71. Rowland JM, Olmstead MM, Mascharak PK (2001) Inorg Chem 40:2810–2817
72. Gosiewska S, Permentier HP, Bruins AP Koten Gv, Gebbink RJMK (2007) Dalton Trans 31:3365–3368
73. Lee Y-M, Dhuri SN, Sawant SC, Cho J, Kubo M, Ogura T, Fukuzumi S, Nam W (2009) Angew Chem Int Ed 48:1803–1806
74. Burger RM (1998) Chem Rev 98:1153–1169
75. Li F, Wang M, Ma C, Gao A, Chen H, Sun L (2006) Dalton Trans 2427–2434
76. van den Berg TA, de Boer JW, Browne WR, Roelfes G, Feringa BL (2004) Chem Commun 22:2550–2551
77. Roelfes G, Lubben M, Hage R, Que L Jr, Feringa BL (2000) Chem Eur J 6:2152–2159
78. Roelfes G, Lubben M, Chen K, Ho RYN, Meetsma A, Genseberger S, Hermant RM, Hage R, Mandal SK, Young VG Jr, Zang Y, Kooijman H, Spek A, Que L Jr, Feringa BL (1999) Inorg Chem 38:1929–1936
79. Comba P, Maurer M, Vadivelu P (2009) Inorg Chem 48:10389–10396
80. Chen K, Que L Jr (1999) Chem Commun 1375–1376
81. Chen K, Que L Jr (2001) J Am Chem Soc 123:6327–6337
82. Britovsek GJP, England J, White AJP (2005) Inorg Chem 44:8125–8134
83. England J, Britovsek GJP, Rabadia N, White AJP (2007) Inorg Chem 46:3752–3767
84. England J, Davies CR, Banaru M, White AJP, Britovsek GJP (2008) Adv Synth Catal 350:883–897
85. Company A, Gómez L, Güell M, Ribas X, Luis JM, Que L Jr, Costas M (2007) J Am Chem Soc 129:15766–15767
86. Company A, Gómez L, Fontrodona X, Ribas X, Costas M (2008) Chem Eur J 14:5727–5731
87. Mekmouche Y, Ménage S, Toia-Duboc C, Fontecave M, Galey J-B, Lebrun C, Pecaut J (2001) Angew Chem Int Ed 40:949–952

88. Britovsek GJP, England J, White AJP (2006) Dalton Trans 11:1399–1408
89. Costas M, Que L Jr (2002) Angew Chem Int Ed 12:2179–2181
90. England J, Gondhia R, Bigorra-Lopez L, Petersen AR, White AJP, Britovsek GJP (2009) Dalton Trans 5319–5334
91. Zang Y, Kim J, Dong Y, Wilkinson EC, Appelman EH, Que L Jr (1997) J Am Chem Soc 119:4197–4205
92. Chen MS, White MC (2007) Science 318:783–787
93. Bautz J, Comba P, Laorden CLd, Menzel M, Rajaraman G (2007) Angew Chem Int Ed 46:8067–8070
94. Vermeulen NA, Chen MS, White MC (2009) Tetrahedron 65:3078–3084
95. Chen MS, White MC (2010) Science 327:566–571
96. Chen K, Eschenmoser A, Baran PS (2009) Angew Chem Int Ed 48:9705–9708
97. Meunier B (1992) Chem Rev 92:1411–1456
98. McLain JL, Lee J, Groves JT (2000) Biomimetic oxygenations related to cytochrome P-450: metal-Oxo and Metal-Peroxo Intermediates. In: Meunier B (ed) Biomimetic oxidations catalyzed by transition metal complexes. Imperial College Press, London, pp 91–169
99. Gomez L, Garcia-Bosch I, Company A, Benet-Buchholz J, Polo A, Sala X, Ribas X, Costas M (2009) Angew Chem Int Ed 48:5720–5723
100. Kim C, Chen K, Kim J, Que L Jr (1997) J Am Chem Soc 119:5964–5965
101. Ho RYN, Roelfes G, Feringa BL, Que L Jr (1999) J Am Chem Soc 121:264–265
102. Lehnert N, Neese F, Ho RYN, Que L Jr, Solomon EI (2002) J Am Chem Soc 124:10810–10822
103. Ortiz de Montellano PR (2005) Cytochrome P450: structure, mechanism and biochemistry. 3rd edn. Kluwer Academic/Plenum Publishers, New York
104. Ortiz de Montellano PR, De Voss JJ (2002) Nat Prod Rep 19:477–493
105. Karlsson A, Parales JV, Parales RE, Gibson DT, Eklund H, Ramaswamy S (2003) Science 299:1039–1042
106. Costas M, Mehn MP, Jensen MP, Que L Jr (2004) Chem Rev 104:939–986
107. Kaizer J, Klinker EJ, Oh NY, Rohde J-U, Song WJ, Stubna A, Kim J, Munck E, Nam W, Que L Jr (2004) J Am Chem Soc 126:472–473
108. Company A, Prat I, Frisch JR, Ballesté RM, Güell M, Juhász G, Ribas X, Münck E, Luis JM, Que L Jr, Costas M (2011) Chem Eur J 17:1622–1634
109. Chen K, Costas M, Kim J, Tipton AK, Que L Jr (2002) J Am Chem Soc 124:3026–3035
110. Bassan A, Blomberg MRA, Siegbahn PEM, Que L Jr (2002) J Am Chem Soc 124:11056–11063
111. Quinonero D, Morokuma K, Musaev DG, Mas-Balleste R, Que L Jr (2005) J Am Chem Soc 127:6548–6549
112. Seo MS, Kamachi T, Kouno T, Murata K, Park MJ, Yoshizawa K, Nam W (2007) Angew Chem Int Ed 46:2291–2294
113. Park MJ, Lee J, Suh Y, Kim J, Nam W (2006) J Am Chem Soc 128:2630–2634
114. Bernadou J, Meunier B (1998) Chem Commun 2167–2173
115. Groves JT (2005) Models and mechanisms of cytochrome P450 action. In cytochrome P450: structure, mechanism and biochemistry. 3rd edn, Ortiz de Montellano, P. R., Ed. Kluwer Academic/Plenum Publishers, New York, pp 1–42
116. Wackett LP, Kwart LD, Gibson DT (1988) Biochemistry 27:1360–1367
117. Galonić DP, Barr EW, Walsh CT, Bollinger JM, Krebs C (2007) Nat Chem Biol 3:113–116
118. White MC, Doyle AG, Jacobsen EN (2001) J Am Chem Soc 123:7194–7195
119. Mas-Balleste R, Que L Jr (2007) J Am Chem Soc 129:15964–15972
120. Makhlynets OV, Rybak-Akimova EV (2010) Chem Eur J 16:13995–14006
121. Cainelli G, Cardillo G (1984) Chromium oxidations in organic chemistry. Springer, Berlin
122. Hudlicky M (1990) Oxidations in organic chemistry. Am Chem Soc, Washington
123. Tojo G, Fernández MI (2006) Oxidation of alcohols to aldehydes and ketones. Springer, Berlin, p 1–97
124. Muzart J (1992) Chem Rev 92:113–140

125. Shilov AE, Shul'pin GB (1997) Chem Rev 97:2879–2932
126. Yamazaki S (1999) Org Lett 1:2129–2132 and references herein
127. Muzart J, Aït-Mohand S (1995) Tetrahedron Lett 36:5735–5736
128. Lee S, Fuchs PL (2002) J Am Chem Soc 124:13978–13979
129. di Valentin C, Gisdakis P, Yudanov IV, Rösch N (2000) J Org Chem 65:2996–3004
130. Lee S, Fuchs PL (2004) Org Lett 6:1437–1440
131. Ganeshpure PA, Tembe GL, Satish S (1996) J Mol Cat A-Chem 113:L423–L425
132. Salomao GS, Olsen MHN, Drago V, Fernandes C, Filho LC, Antunes OAC (2007) Catal Commun 8:69–72
133. Nehru K, Kim SJ, Kim IY, Seo MS, Kim Y, Kim S-J, Kim J, Nam W (2007) Chem Commun 4623–4625
134. Nakayama N, Tsuchiya S, Ogawa S (2007) J Mol Catal A-Chem 277:61–71
135. Larrow JF, Jacobsen EN (1994) J Am Chem Soc 116:12129–12130
136. Hamachi K, Irie R, Katsuki T (1996) Tetrahedron Lett 37:4979–4982
137. Hamada T, Irie R, Mihara J, Hamachi K, Katsuki T (1998) Tetrahedron 54:10017–10028
138. Groves JT, McCluskey GA (1976) J Am Chem Soc 98:859–861
139. Groves JT, Viski P (1989) J Am Chem Soc 111:8537–8538
140. Miyafuji A, Katsuki T (1998) Tetrahedron 54:10339–10348
141. Taft KL, Kulawiec RJ, Sarneski JE, Crabtree RH (1989) Tetrahedron Lett 30:5689–5692
142. Fish RH, Fong RH, Vincent JB, Christou G (1988) J Chem Soc Chem Commun 1504–1506
143. Sarneski JE, Michos D, Thorp HH, Didiuk M, Poon T, Blewitt J, Brudvig GW, Crabtree RH (1991) Tetrahedron Lett 32:1153–1156
144. Wessel J, Crabtree RH (1996) J Mol Cat A-Chem 113:13–22
145. Ménage S, Collomb-Dunand-Sauthier M-N, Lambeaux C, Fontecave M (1994) J Chem Soc Chem Commun 1885–1886
146. Tétard D, Rabion A, Verlhac J-B, Guilhem J (1995) J Chem Soc Chem Commun 531–532
147. Tetard D, Verlhac J-B (1996) J Mol Catal A-Chem 113:223–230
148. Das S, Incarvito CD, Crabtree RH, Brudvig GW (2006) Science 312:1941–1943
149. Balcells D, Moles P, Blakemore JD, Raynaud C, Brudvig GW, Crabtree RH, Eisenstein O (2009) Dalton Trans 5989–6000
150. Wieghardt K, Bossek U, Nuber B, Weiss J, Bonvoisin J, Corbella M, Vitols SE, Girerd JJ (1988) J Am Chem Soc 110:7398–7411
151. Hage R, Iburg JE, Kerschner J, Koek JH, Lempers ELM, Martens RJ, Racherla US, Russell SW, Swarthoff T, Vliet MRPv, Warnaar JB, Wolf Lvd, Krijnen B (1994) Nature 369:637–639
152. Lindsay-Smith JR, Shul'pin GB (1998) Tetrahedron Lett 39:4909–4912
153. Shul'pin GB, Lindsay-Smith JR (1998) Russ Chem Bull 47:2379–2386
154. Shul'pin GB, Süss-Fink G, Lindsay-Smith JR (1999) Tetrahedron 55:5345–5358
155. Shul'pin GB, Nizova GV, Kozlov YN, Pechenkina IG (2002) New J Chem 26:1238–1245
156. Nizova GV, Shul'pin GB (2007) Tetrahedron 63:7997–8001
157. Shul'pin GB, Nizova GV, Kozlov YN, Arutyunov VS, Santos ACMd, Ferreira ACT, Mandelli D (2005) J Organomet Chem 690:4498–4504
158. Saffer A, Babyside NY (1958) Barker RS Preparation of aromatic polycarboxylic acids. US Patent 2,833,816
159. Srinivas D, Chavan SA, Ratnasamy P (2001) Process for the preparation of adipic acid. US Patent 6,521,789 B1, 2001
160. Chavez FA, Mascharak PK (2000) Acc Chem Res 33:539–545
161. Ishii Y, Iwahama T, Sakaguchi S, Nakayama K, Nishiyama Y (1996) J Org Chem 61:4520–4526
162. Ishii Y, Kato S, Iwahama T, Sakaguchi S (1996) Tetrahedron Lett 37:4993–4996
163. Yoshino Y, Hayashi Y, Iwahama T, Sakaguchi S, Ishii Y (1997) J Org Chem 62:6810–6813
164. Nishinaga A, Tomita H, Nishizawa K, Matsuura T, Ooi S, Hirotsu K (1981) J Chem Soc Dalton Trans 7:1504–1514
165. Qi J-Y, Ma H-X, Li X-J, Zhou Z-Y, Choi MCK, Chan ASC, Yang Q-Y (2003) Chem Commun 1294–1295

166. Punniyamurthy T, Reddy MM, Kalra SJS, Iqbal J (1996) Pure Appl Chem 68:619–622
167. Chavez FA, Briones JA, Olmstead MM, Mascharak PK (1999) Inorg Chem 38:1603–1608
168. Chavez FA, Rowland JM, Olmstead MM (1998) J Am Chem Soc 120:9015–9027
169. Chavez FA, Nguyen CV, Olmstead MM, Mascharak PK (1996) Inorg Chem 35:6282–6291
170. Saussine L, Brazi E, Robine A, Mimoun H, Fischer J, Weiss R (1985) J Am Chem Soc 107:3534–3540
171. Nagataki T, Tachi Y, Itoh S (2006) Chem Commun 4016–4018
172. Nagataki T, Ishii K, Tachi Y, Itoh S (2007) Dalton Trans 1120–1128
173. Nagataki T, Itoh S (2007) Chem Lett 36:748–749
174. Schröder D, Schwarz H (1995) Angew Chem Int Ed 34:1973–1995
175. Hikichi S, Okuda H, Ohzu Y, Akita M (2009) Angew Chem Int Ed 48:188–191
176. Balasubramanian R, Smith SM, Rawat S, Yatsunyk L, Stemmler TL, Rosenzweig AC (2010) Nature 465:115–131
177. Geletii YV, Lavrushko VV, Lubimova GV (1988) J Chem Soc Chem Commun 936–937
178. Barton DHR, Csuhai E, Doller D, Geletii YV (1991) Tetrahedron 47:6561–6570
179. Shul'pin GB, Bochkova MM, Nizova GV (1995) J Chem Soc Perkin Trans 2:1465–1469
180. Rothenberg G, Feldberg L, Wiener H, Sasson Y (1998) J Chem Soc Perkin Trans 2:2429–2434
181. Murahashi S-I, Oda Y, Naota T, Komiya N (1993) J Chem Soc Chem Commun 139–140
182. Komiya N, Naota T, Murahashi S-I (1996) Tetrahedron Lett 37:1633–1636
183. Komiya N, Naota T, Oda Y, Murahashi S-I (1997) J Mol Catal A-Chem 117:21–37
184. Rudler H, Denise B (2000) J Mol Catal A-Chem 154:277–279
185. Sobkowiak A, Qui A, Liu X, Llobet A, Sawyer DT (1993) J Am Chem Soc 115:609–614
186. Costas M, Llobet A (1999) J Mol Cat A Chem 142:113–124
187. Okuno T, Ohba S, Nishida Y (1997) Polyhedron 16:3765–3774
188. Schuchardt U, Pereira R, Rufo M (1998) J Mol Catal A-Chem 135:257–262
189. Ohta T, Tachiyama T, Yoshizawa K, Yamabe T, Uchida T, Kitagawa T (2000) Inorg Chem 39:4358–4369
190. Shimokawa C, Tetraoka J, Tachi Y, Itoh S (2006) J Inorg Biochem 100:1118–1127
191. Velusamy S, Punniyamurthy T (2003) Tetrahedron Let 44:8955–8957
192. Shul'pin GB, Gradinaru J, Kozlov YN (2003) Org Biomol Chem 1:3611–3617
193. Kirillov AM, Kopylovich MN, Kirillova MV, Haukka M, Silva MFCGd, Pombeiro AJL (2005) Angew Chem Int Ed 44:4345–4348
194. Kirillova MV, Kozlov YN, Shul'pina LS, Lyakin OY, Kirillov AM, Talsi EP, Pombeiro AJL, Shul'pin GB (2009) J Catal 268:26–38
195. Kopylovich MN, Kirillova MV, Karabach EY, Haukka M, Silva MFCGd, Pombeiro AJL (2006) Adv Synth Catal 348:159–174
196. Kirillova MV, Kirillov AM, Mandelli D, Carvalho WA, Pombeiro AJL, Shul'pin GB (2010) J Catal 272:9–17
197. Zhu M, Wei X, Li B, Yuan Y (2007) Tetrahedron Lett 48:9108–9111
198. Nicola CD, Karabach YY, Kirillov AM, Monari M, Pandolfo L, Pettinari C, Pombeiro AJL (2007) Inorg Chem 46:221–230
199. Alegria ECBA, Martins LMDRS, Pombeiro AJL (2008) Adv Synth Catal 350:706–716
200. Silva TFS, Mishra GS, Silva MFGd, Wanke R, Martins LMDRS, Pombeiro AJL (2009) Dalton Trans 9207–9215
201. Lee DG, van den Engh M (1973) Chapter 4. In Oxidation in Organic Chemistry, Part B, Trahanovsky,WS,(ed) Academic Press, New York
202. Courtney JL (1986) In Organic synthesis by oxidation with metal compounds, Mijs, WJ, de Jonge CRH. I., Eds. Plenum Press, New York, pp 445–467
203. Martín VS, Palazón JM, Rodríguez CM (1996) Encyclopedia of Reagents for Organic Synthesis. In Paquette LA (ed) Wiley, Chichester vol 6, p 4415
204. Perrone R, Bettoni G, Tortorella V (1976) Synthesis 598–600
205. Bettoni G, Carbonara G, Franchini C, Tortorella V (1981) Tetrahedron 37:4159–4164
206. Ley SV, Norman J, Griffith WP, Marsden SP (1994) Synthesis 639–666

207. Griffith WP, Ley SV (1990) Aldrichimica Acta 23:13–19
208. Carlsen PHJ, Katsuki T, Martin VS, Sharpless KB (1981) J Org Chem 46:3936–3938
209. Schuda PF, Cichowicz MB, Heimann MR (1983) Tetrahedron Lett 24:3829–3830
210. Sheehan JC, Tulis RW (1974) J Org Chem 39:2264–2267
211. Yoshifuji S, Tanaka K, Nitta Y (1985) Chem Pharm Bull 33:1749–1751
212. Yoshifuji S, Tanaka K, Kawai T, Nitta Y (1985) Chem Pharm Bull 33:5515–5521
213. Yoshifuji S, Tanaka K, Kawai T, Nitta Y (1986) Chem Pharm Bull 34:3873–3878
214. Tanaka K, Yoshifuji S, Nitta Y (1986) Chem Pharm Bull 34:3879–3884
215. Tanaka K, Yoshifuji S, Nitta Y (1987) Chem Pharm Bull 35:364–369
216. Djeressi C, Engle RR (1953) J Am Chem Soc 75:3838–3840
217. Wolfe S, Hasan SK, Campbell JR (1970) J Chem Soc Chem Commun 1420–1421
218. Spitzer UA, Lee DG (1974) J Org Chem 39:2468–2469
219. Orita H, Hayakawa T, Takehira K (1986) Bull Chem Soc Jpn 59:2637–2638
220. Yamamoto Y, Suzuki H, Moromoka Y (1985) Tetrahedron Lett 26:2107–2108
221. Kanemoto S, Tomioka H, Oshima K, Nozaki H (1986) Bull Chem Soc Jpn 59:105–108
222. Giddings S, Mills A (1988) J Org Chem 53:1103–1107
223. Nuñez MT, Martín VS (1928) J Org Chem 55:1928–1932
224. Morris PEJ, Kiely DE (1987) J Org Chem 52:1149–1152
225. Torii S, Inokuchi T, Kondo K (1985) J Org Chem 50:4980–4982
226. Webster FX, Rivas-Enterrios J, Silverstein RM (1987) J Org Chem 52:689–691
227. Albarella L, Giordano F, Lasalvia M, Piccialli V, Sica D (1995) Tetrahedron Lett 36:5267–5270
228. Denisenko MV, Pokhilo ND, Odinokova LE, Denisenko VA, Uvarova NI (1996) Tetrahedron Lett 37:5187–5190
229. Shing TKM, Tai VW-F, Tam EKW (1994) Angew Chem Int Ed 33:2312–2313
230. Caputo, JA, Fuchs, R (1967) Tetrahedron Lett 4729–4731
231. Piatak DM, Herbst G, Wicha J, Caspi E (1969) J Org Chem 34:116–120
232. Chakraborti AK, Ghatak UR (1983) Synthesis 746–748
233. Kasai M, Ziffer H (1983) J Org Chem 48:2346–2349
234. Ranganathan D, Vaish NK, Shah K (1994) J Am Chem Soc 116:6545–6557
235. Spitzer UA, Lee DG (1975) J Org Chem 40:2539–2540
236. Torii S, Inokuchi T, Hirata Y (1987) Synthesis 377–378
237. Torii S, Inokuchi T, Sugiura T (1986) J Org Chem 51:155–161
238. Zibuck R, Seebach D (1988) Helv Chim Acta 71:237–241
239. Bakke JM, Bethell D (1992) Acta Chem Scand 46:644–649
240. Bakke JM, Brænden JE (1991) Acta Chem Scand 45:418–423
241. Bakke JM, Frøhaug AE (1994) Acta Chem Scand 48:160–164
242. Bakke JM, Frohaug AE (1996) J Phys Org Chem 9:310–318
243. Bakke JM, Frohaug AE (1996) J Phys Org Chem 9:507–513
244. Tenaglia A, Terranova E, Waegell B (1989) Tetrahedron Lett 30:5271–5274
245. Tenaglia A, Terranova E, Waegell B (1992) J Org Chem 57:5523–5523
246. Tenaglia A, Terranova E, Waegell B (1990) J Chem Soc Chem Commun 1344–1345
247. Bakke JM, Lundquist M (1986) Acta Chem Scand B 40:430–433
248. Carlsen PHJ (1997) Synth Commun 17:19–23
249. Hasegawa T, Niwa H, Yamada K (1985) Chem Lett 1385–1386
250. Coudret JL, Zöllner S, Ravoo BJ, Malara L, Hanisch C, Dörre K, de Meijere A, Waegell B (1996) Tetrahedron Lett 37:2425–2428
251. Teneglia A, Terranova E, Waegell B (1989) Tetrahedron Lett 30:5275–5276
252. Kawai T, Ooi T, Kusumi T (2003) Chem Pharm Bull 51(3):291–294
253. Coudret JL, Waegell B (1994) Inorg Chim Acta 222:115–122
254. Sasson Y, Zappi GD, Neumann R (1986) J Org Chem 51:2880–2883
255. Fuchs PL (2007) J Org Chem 72:5820–5823
256. McNeill E, Bois JD (2010) J Am Chem Soc 132:10202–10204
257. Drees M, Strassner T (2006) J Org Chem 71:1755–1760

258. Lau T-C, Mak C-K (1993) J Chem Soc Chem Commun 766–767
259. Lau T-C, Mak C-K (1995) J Chem Soc Chem Commun 943–944
260. Che C-M, Tang W-T, Wong W-T, Lai T-F (1989) J Am Chem Soc 111:9048–9056
261. Li C-K, Che C-M, Tong W-F, Tang W-T, Wong K-Y, Lai T-F (1992) J Chem Soc Dalton Trans 2109–2116
262. Cheng W-C, Yu W-Y, Cheung K–K, Che C-M (1994) J Chem Soc Chem Commun 1063–1064
263. Che C-M, Leung W-H (1987) J Chem Soc Chem Commun 1376–1377
264. Thompson MS, Meyer TJ (1982) J Am Chem Soc 104:5070–5076
265. Che C-M (1995) Pure Appl Chem 67:225–232
266. Che CK, Lau TC (2004) In Comprehensive coordination chemistry II. In: Constable EC, Dilworth JR (eds) Elsevier Pergamon, Amsterdam, vol 5, pp 733–847
267. Murahashi SI, Komiya N (2004) In Ruthenium in organic synthesis. In: Murahashi SI (ed) Wiley, Weinheim, pp 345–366
268. Murahashi SI; Komiya N (2004) In Modern oxidation methods. In: Bäckwall JE (ed) Wiley, Weinheim pp 165–191
269. Haines AH (1985) Methods for the oxidation of organic compounds: alkanes, alkenes, alkynes and arenas. Academic Press, London
270. Roecker L, Meyer TJ (1987) J Am Chem Soc 109:746–754
271. Lau T-C, Che C-M, Lee W-O, Poon C-K (1988) J Chem Soc Chem Commun 1406–1407
272. Bailey AJ, Griffith WP, Savage PD (1995) J Chem Soc Dalton Trans 3537–3542
273. Che C-M, Cheng K-W, Chan MCW, Lau T-C, Mak C-K (2000) J Org Chem 65:7996–8000
274. Khan MMT, Siddiqui MRH, Hussain A, Moiz MA (1986) Inorg Chem 25:2765–2771
275. Khan MMT, Shukla RS (1988) J Mol Cat A-Chem 44:73–83
276. Khan MMT, Shukla RS (1989) J Mol Cat A-Chem 51:171–180
277. Khan MMT, Chatterjee D, Merchant RR, Paul P, Abdi SHR, Srinivas D, Siddiqui MRH, Moiz MA, Bhadbhade MM, Venkatasubramaian K (1992) Inorg Chem 31:2711–2718
278. Bresaan M, Morvillo A (1989) J Chem Soc Chem Commun 421–423
279. Glodstein AS, Drago RS (1991) J Chem Soc Chem Comm 21–22
280. Goldstein AS, Beer RH, Drago RS (1994) J Am Chem Soc 116:2424–2429
281. Davis S, Drago RS (1990) J Chem Soc Chem Commun 250–251
282. Tembe GL, Ganeshpure PA (1999) React Kinet Catal Lett 67:83–88
283. Nunes GS, Alexiou ADP, Toma HE (2008) J Catal 206:188–192
284. Murahashi S-I, Komiya N, Oda Y, Kuwabara T, Naota T (2000) J Org Chem 65:9186–9193
285. Kojima T (1996) Chem Lett 121–122
286. Yamaguchi M, Kousaka H, Yamagishi T (1997) J Inorg Biochem 67:236
287. Yamaguchi M, Kousaka H, Yamagishi T (1997) Chem Lett 769–770
288. Yamaguchi M, Kosusaka H, Izawa S, Ichii Y, Kumano T, Masui D, Yamagishi T (2006) Inorg Chem 45:8342–8354
289. Murali M, Mayilmurugan R, Palaniandavar M (2009) Eur J Inorg Chem 3238–3249
290. Kojima T, Hayashi K, Iizuka S, Tani F, Naruta Y, Kawano M, Ohashi Y, Hirai Y, Ohokubo K, Matsuda Y, Fukuzumi S (2007) Chem Eur J 13:8212–8222
291. Che C-M, Yam VW-W, Mak TCW (1990) J Am Chem Soc 112:2284–2291
292. Che C-M, Ho C, Lau T-C (1991) J. Chem. Soc. Dalton Trans 1259–1263
293. Jitsukama K, Oka Y, Einaga H, Masuda H (2001) Tetrahedron Lett 42:3467–3469
294. Jitsukama K, Oka Y, Yamaguchi S, Masuda H (2004) Inorg Chem 43:8119–8129
295. Kojima T, Amano T, Ishii Y, Ohba M, Okaue Y, Matsuda Y (1998) Inorg Chem 37:4076–4085
296. Kojima T, Matsuo H, Matsuda Y (2000) Inorg Chim Acta 300–302:661–607
297. Hirai Y, Kojima T, Mizutani Y, Shiota Y, Yoshizawa K, Fukuzumi S (2008) Angew Chem Int Ed 47:5772–5776
298. Chatterjee D, Mitra A, Shepherd RE (2004) Inorg Chim Acta 357:980–990
299. Chatterjeea D, Mitra A, Roy BC (2000) J Mol Catal A-Chem 161:17–21
300. Chatterjeea D, Mitra A, Mukherjee S (1999) Polyhedron 18:2659–2663

301. Yi CS, Kwon KH, Lee DW (2009) Org Lett 11:1567–1569
302. Herrmann WA, Kühn FE (1997) Acc Chem Res 30:169–180
303. Espenson JH (1999) Chem Commun 479–488
304. Romão CC, Kühn FE, Herrmann WA (1997) Chem Rev 97:3197–3246
305. Conley BL, Tenn III WJIII, Young KJH, Ganesh SK, Meier SK, Ziatdinov VR, Mironov O, Oxgaard J, Gonzales J, Goddard III WA, Periana RA (2006) J Mol Catal A:Chem 251:8–23
306. Bianchini G, Crucianelli M, Angelis FD, Neri V, Saladino R (2004) Tetrahedron Lett 45:2351–2353
307. Bianchini G, Crucianelli M, Angelis FD, Neri V, Saladino R (2005) Tetrahedron Lett 46:2427–2432
308. Kirillova MV, Kirillov AM, Reis PM, Silva JAL, Silva JJRFd, Pombeiro AJL (2007) J Mol Catal A: Chem 248:130–136
309. Schuchardt U, Mandelli D, Shui'pin GB (1996) Tetrahedron Lett 37:6487–6649
310. Kirillov AM, Haukka M, Silva MFCGd, Pombeiro AJL (2005) Eur J Inorg Chem 2071–2080
311. Murray RW, Iyanar K, Chen J, Wearing JT (1995) Tetrahedron Lett 36:6415–6418
312. Herrmann WA, Ficher RW, Scherer W, Rauch MU (1993) Angew Chem Int Ed Engl 32:1157–1160
313. Yamazaki S, Espenson JH, Huston P (1993) Inorg Chem 32:4683–4687
314. Kuznetsov ML, Pombeiro AJL (2009) Inorg Chem 48:307–318
315. Karlsson EA, Privalov T (2009) Chem Eur J 15:1862–1869
316. Schröder M (1980) Chem Rev 80:187–213
317. Bales BC, Brown P, Dehestani A, Mayer JM (2005) J Am Chem Soc 127:2832–2833
318. Yiu S-M, Lam WWY, Lau T-C (2008) J Am Chem Soc 130:10821–10827
319. Yiu S-M, Wu Z-B, Mak C-K, Lau T-C (2004) J Am Chem Soc 126:14921–14929
320. Singh HS (1986) Organic synthesis by oxidation with metal compounds. In: Mijs WJ, de Jonge CRHI (eds) Organic synthesis by oxidation with metal compounds. Plenum Press, New York, pp 633–693
321. Mehta SPS, Mehrotra RN (1991) Trans Met Chem 16:402–406
322. Shul'pin GB, Kudinov AR, Shul'pina LS, Petrovskaya EA (2006) J Organomet Chem 691:837–845
323. Leung WH, Chim JLC, Lai W, Lam L, Wong WT, Chan WH, Yeung CH (1999) Inorg Chim Acta 290:28–35
324. Zheng H, Leung WH, Chim JLC, Lai W, Lam C-H, Williams ID, Wong WT (2000) Inorg Chim Acta 306:184–192
325. Shul'pin GB, Kozlov YN, Shul'pina LS, Kudinov AR, Mandelli D (2009) Inorg Chem 48:10480–10482
326. Shul'pin GB, Kozlov YN, Shul'pina LS, Petrovskiy PV (2010) Appl Organomet Chem 24:464–472
327. Zhou M, Schley ND, Crabtree RH (2010) J Am Chem Soc 132:12550–12551
328. Hull JF, Balcells D, Blakemore JD, Incarvito CD, Eisenstein O, Brudvig GW, Crabtree RH (2009) J Am Chem Soc 131:8730–8731
329. Blakemore JD, Schley ND, Balcells D, Hull JF, Olack GW, Incarvito CD, Eisenstein O, Brudvig GW, Crabtree RH (2010) J Am Chem Soc 132:16017–16029
330. Hay-Motherwell RS, Wilkinson G, Hussain-Bates B, Hursthouse MB (1993) Polyhedron 12:2009–2012
331. Jacobi BG, Laitar DS, Pu LH, Wargocki MF, DiPasquale AG, Fortner KC, Schuck SM, Brown SN (2002) Inorg Chem 41:4815–4823
332. Newhouse T, Baran PS (2011) Angew Chem Int Ed 50:3362–3374

Chapter 6
Alkane Catalytic Functionalization by Carbene or Nitrene Insertion Reactions

M. Mar Díaz-Requejo, Ana Caballero, Manuel R. Fructos and Pedro J. Pérez

Abstract The functionalization of carbon-hydrogen bonds of alkanes by means of the insertion of carbene (CR_2) or nitrene (NR) units are presented in this chapter. Developed at different extends, the former methodology has received much attention, probably due to the use of available diazo compounds as the carbene source. For the NR case, the sources are usually based in hypervalent iodine compounds. In both cases, a yet reduced number of catalytic systems have been reported for the conversion of plain, non-activated alkanes into value added products. The development of these methodologies, current state of the art, including asymmetric systems and mechanistic considerations are described.

6.1 Introduction

As already mentioned in the previous chapters, the neat catalytic functionalization of alkanes is yet far to be considered a developed area in chemistry [1–3]. Scheme 6.1 shows a general view of what it is considered as a functionalization reaction for these molecules. Given a R-H substrate, three major reactions can be thought to convert a hydrocarbon into another molecule: (a) replacement of H by another group; (b) formation of a double C=C bond, with loss of two H atoms and (c) functionalization of the C–H bond by insertion of a X fragment, the H atom being maintained. The few reactions known to proceed to a certain extend under catalytic conditions with plain alkanes are those shown in the previous chapters of

M. M. Díaz-Requejo · A. Caballero · M. R. Fructos · P. J. Pérez (✉)
Laboratorio de Catálisis Homogénea, Departamento de Química y Ciencia de los Materiales, Unidad Asociada al CSIC, Centro de Investigación en Química Sostenible, Universidad de Huelva, Campus de El Carmen, 21007 Huelva, Spain
e-mail: perez@dqcm.uhu.es

P. J. Pérez (ed.), *Alkane C–H Activation by Single-Site Metal Catalysis*, Catalysis by Metal Complexes 38, DOI: 10.1007/978-90-481-3698-8_6,
© Springer Science+Business Media Dordrecht 2012

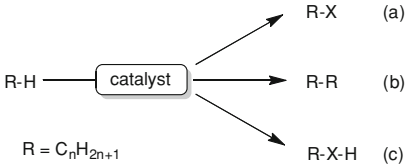

Scheme 6.1 Different catalytic reactions for alkane functionalization

this book. The alkane borylation (Chap. 3) and dehydrogenation (Chap. 4) processes correspond to type (a) and (b), whereas the electrophilic activation (Chap. 2) and the alkane oxygenation (Chap. 5) are classified into type (c).

Just as a general reminder, the electrophilic activation as well as the borylation and dehydrogenation of alkanes very often require the use of high temperatures or harsh conditions such as highly acidic reaction media. On the other hand the oxygenation of alkanes takes places under relatively mild conditions. This difference stands on the mechanism that governs those transformations. In the first three cases, intermediates involving the formation of metal–carbon and/or metal-hydrogen bonds are stable enough to preclude a catalytic cycle or, at least, impelling the need of high temperatures or harsh conditions. Scheme 6.2 shows two possible catalytic cycles that would lead to the neat C–H bond functionalization [4–6]. All the steps shown in cycles I and II are known from a stoichiometric point of view. However, the coexistence of those accounting for each cycle in the same chemical system is quite rare, and when possible, with productivities far from those that could be considered within a practical value, at least at the lab scale. The reason has been just mentioned: the relative stability of some of the intermediates in the above catalytic cycles, which in many cases constitute a thermodynamic sink from which the reaction does not proceed further. However, a somewhat different picture is observed for the oxygenation reaction. In this case, it has been proposed that no M-C–H interaction takes place along the reaction mechanism (see Chap. 5). The transformation would occur by the approach of the C–H bond to a coordinated oxo (or other O-containing species). This route avoids the formation of stable organometallic intermediates and therefore favors the catalytic cycle to close. This strategy can also be applied in a general manner to achieve the insertion of a given X group into a carbon-hydrogen bond, with X standing for oxo, carbene or nitrene moieties. The interaction of the alkylic C–H bond with the unsaturated intermediate [M]=X can take place either in a concerted or in a stepwise manner (Scheme 6.3). The requirements that favor this route instead of the organometallic pathway are the following: (i) an electrophilic character of the L_nM=X intermediate, since a low electronic density located at the X group would enhance the reactivity of the C–H bond toward this intermediate; and (ii) the use of L_nM catalyst precursors with low propensity to undergo C–H oxidative addition reactions, i.e. low electron density at metal and/or coordination spheres that would preclude such reaction. Once accomplished them, the alkane C–H bond behaves as a (poor) nucleophile and interact with the electrophile L_nM=X to trigger the functionalization reaction.

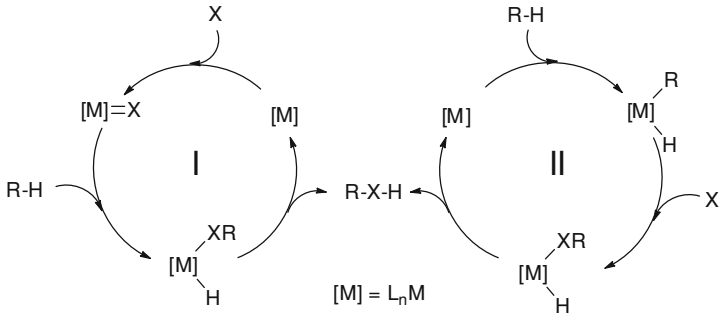

Scheme 6.2 Possible catalytic cycles for alkane functionalization based on organometallic activation

Scheme 6.3 A catalytic cycle for alkane functionalization that avoids organometallic activation

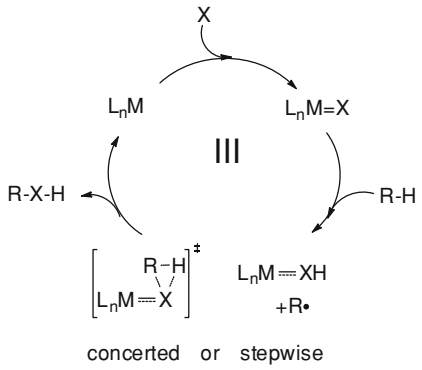

The relative reactivity of the alkane C–H bonds in the above transformations deserves some comments. As already explained in Chap. 1, the organometallic activation involving C–H oxidative addition follows the order of reactivity CH_3-H > RCH_2-H > R_2CH-H > R_3C-H, that fits the order of bond dissociation energies [7, 8]. This means that in the organometallic activation the stronger bonds are readily activated in comparison with the weaker ones. Most examples are based in electron-rich metal centers, with metals in a low oxidation state, therefore favoring that a poor donor such as the C–H bond can coordinate the metal center in the first step of the activation process [9]. On the other hand, the route shown in Scheme 6.3 does not involve any interaction of the C–H bond with the metal center, and the observed trend (see Chap. 5 for the oxygenation reaction) is the opposite to that shown above, i.e., R_3C-H > R_2CH-H > RCH_2-H > CH_3-H. Such trend is very often observed even in the case of sterically hindered C–H bonds and catalytic centers, evidencing that electronic effects play a crucial role in this transformation. This order follows the bond dissociation energy of the C–H bonds. Actually, it would be more appropriate to use the nucleophilicity of the bonds to explain this behavior. Given that the [M] = X intermediate acts as an electrophile, it is clear that the nucleophilia of the C–H bonds enhances the reactivity in these catalytic processes [10].

Scheme 6.4 C–H functionalization by carbene and nitrene insertion

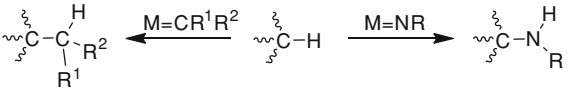

The functionalization of alkane C–H bonds by means of the insertion of carbene (CR^1R^2) or nitrene (NR) moieties constitutes the scope of this chapter. The definition as an insertion process stands on the fact that the final products derive from the neat cleavage of the C–H bond and the insertion of the carbene or nitrene fragment in between (Scheme 6.4). This methodology has been applied in both the intra- and intermolecular fashions, as well as to a range of C–H bonds. On the basis of the general aim of this book, we have exclusively focused in the intermolecular version and with alkanes as the substrates. Those bearing activating groups (allylic, benzylic, ethers…) have been excluded although review articles cited herein contain relevant information about their use [11–19].

6.2 Alkane Functionalization by Carbene Insertion

6.2.1 Fundamentals

As explained above, this methodology is based in the transfer of a carbene unit from an unsaturated intermediate $L_nM{=}CR^1R^2$. Therefore, we first might consider a route to generate such species under catalytic conditions. The answer stands on the well-known capabilities of transition metal complexes to decompose diazocompounds and to generate such metallocarbenes intermediates [20]. All metals from group 8 to group 11 are known to react with diazocompounds in this manner (Scheme 6.5) [21–27], in some cases the metallocarbene being detected or isolated. The presence of a given nucleophile in the reaction mixture originates the interaction with the electrophilic metallocarbene to release the desired product as well as the catalyst to restart the catalytic cycle. The group of twelve metals shown in Scheme 6.5 has demonstrated their capabilities to react with a diazocompound and to transfer the carbene fragment to olefins in the olefin cyclopropanation reaction. Other nucleophiles such as alkynes, N–H or O–H bonds have also been functionalized in the same manner by many of those metals. However, the functionalization of C–H bonds by this methodology is reduced to some of them, as will be discussed in the next section.

Metallocarbene intermediates from the direct reaction of a transition metal complex and a diazocompound have been detected (and structurally characterized in a few cases) with Fe, Ru, Os, Co, Rh and Cu. Group 8 as well as Rh carbene complexes have been detected or isolated when bearing porphyrin ligands. Kodadek first demonstrated [28–30] the coordination of the diazocompound and nitrogen extrusion to give a rhodium-carbene intermediate (Scheme 6.6a). A series

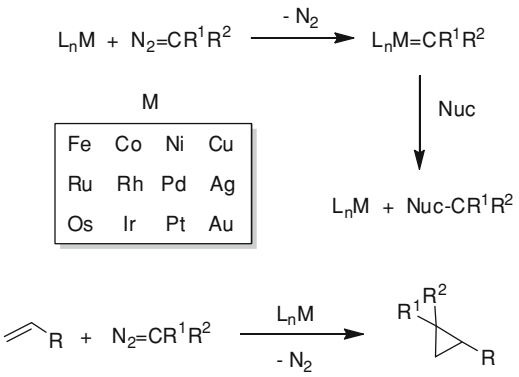

Scheme 6.5 The metal-catalyzed diazocompound decomposition and carbene transfer (*top*) and the olefin cyclopropanation reaction (*bottom*)

of Fe, Ru and Os carbene complexes have been reported by the groups of Collman [31], Woo [32–34], Che [35–37], Simonneaux [38] (Scheme 6.6b). Nishiyama (Scheme 6.6c) [39] and Bianchini (Scheme 6.6d) [40] independently reported the formation of ruthenium and osmium carbene complexes with pybox and triphosphine ligands, respectively. Mezzetti has employed a PNNP ligand to detect a ruthenium-carbene complex (Scheme 6.6e) [41] involved in the imine aziridination reaction. Very recently, a radical cobalt-carbene has been described by Zhang and co-workers (Scheme 6.6f) [41-43]. Copper has also provided some examples for this class of catalytic intermediates. Hofmann first described [44, 45, 46] the formation in solution of such species upon reacting a Cu(I)-containing iminophosphanamide complex with $PhC(N_2)CO_2Et$ (Scheme 6.7a). Later, Warren [47] employed the same strategy starting from a β-diketiminate Cu(I) ethylene complex and diphenyldiazomethane: dinuclear and mononuclear copper-carbene (Scheme 6.7b) complexes were obtained. Identical diazocompound led to a bis-phosphinoboratecopper(I) carbene complex in a recent contribution from Peters' group (Scheme 6.7c) [48].

Since the formation of the metallocarbene intermediate takes place upon direct reaction of the catalyst precursor and the diazo compound, the coordination of the latter to the metal center has been proposed as the first step in most cases, followed by nitrogen loss and metallocarbene formation. To favor coordination, the metal center should display a certain electrophilic character, usually favored by the existence in the coordination sphere of other ligands bearing electron-withdrawing groups (EWG) [11–15, 20]. In fact, the latter feature also affects the reactivity of the metallocarbene that will be then more prone to react with the incoming nucleophile. Since the metal-carbene interaction can be explained as the result of two components (Scheme 6.8), the σ-donation to metal and the π-back donation to the carbene, an increase of electrophilicity at the carbon atom of the carbene ligand would require that π-back donation is diminished as much as possible, an effect that is also promoted by ligands with low donation capabilities.

The nature of the diazo compound also deserves some comments. Diazo compounds can be classified into three types according to the groups attached to

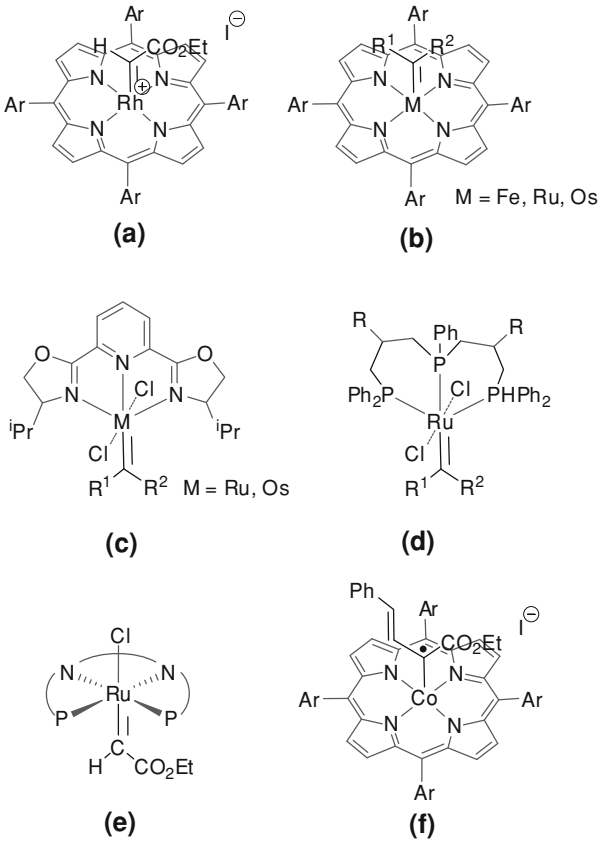

Scheme 6.6 Groups 8 and 9 metallocarbene intermediates formed by direct reaction with diazo compounds

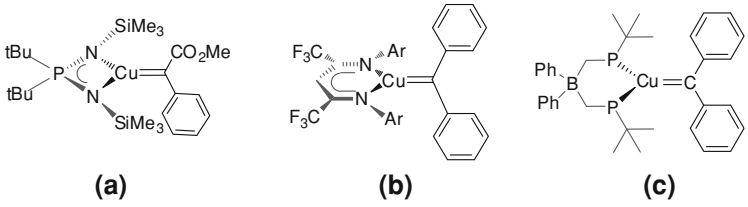

Scheme 6.7 Copper metallocarbene intermediates formed by direct reaction with diazo compounds

the diazo functionality: acceptor, acceptor-acceptor and donor–acceptor [11–15, 20]. The existence of acceptor groups (carbonyl or carboxylate have been the most employed) helps in the aforementioned requirement of an electrophilic carbene

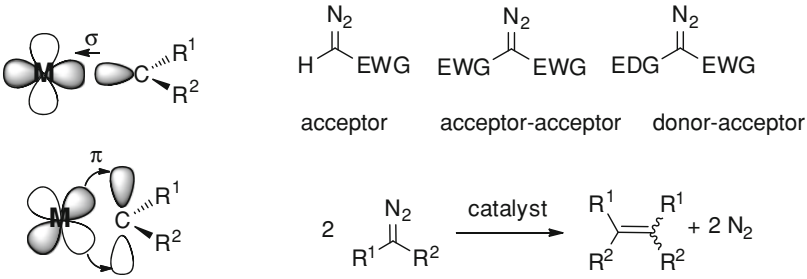

Scheme 6.8 The bonding of the metallocarbene unit (*left*), the different types of diazocompounds (*top*, *right*) and the undesired coupling reaction of diazocompounds (*bottom*, *right*)

ligand. However, it has been found that certain combinations of donor–acceptor substituents also favors some of these transformations (vide infra) [11–15].

The functionalization of organic substrates by this methodology usually competes with the collateral, non-desired reaction of diazo coupling in which olefins are formed (Scheme 6.8). The formation of these side-products can be diminished by using slow addition devices: a very low concentration of the diazo compound in the reaction mixture favors the desired functionalization. Therefore, the chemoselectivity of these processes is defined as the fraction of functionalized products (i.e., functionalized alkanes) referred to the initial amount of diazocompound.

6.2.2 Early Examples

The metal-catalyzed decomposition of diazocompounds and subsequent transfer of the carbene moiety to an organic compound was first described by Novak, Sorm and co-workers in 1957 for the intermolecular reaction of diazoketones with olefins [49]. Although many examples of inter- and intramolecular transformations were later reported, it was not only until 1974 that the first example involving the functionalization of a C–H bond of cyclohexane was reported by Scott using copper sulfate as the catalyst (Scheme 6.9) [50]. Although yield was moderate, it constituted the starting point for the intermolecular functionalization of a non-activated C–H bond by this methodology. A second example was given by Wulfman shortly after [51], in which the allylic C–H bond of cyclohexene was also functionalized at a low yield in the presence of $Cu(acac)_2$ (Scheme 6.9).

It is surprising that in spite of the historical interest in the development of catalytic methods for the functionalization of hydrocarbons, due to their availability, the above examples rested for several years until in 1981, Noels and co-workers discovered [52–55] that dirhodium tetraacetate $Rh_2(OAc)_4$ and related complexes $Rh_2(L)_4$ catalyzed this transformation at a noticeable extend. When cyclohexane was reacted with ethyl diazoacetate (N_2CHCO_2Et, EDA) at room temperature in the presence of $Rh_2(OOCCF_3)$, 75 % of the diazocompound

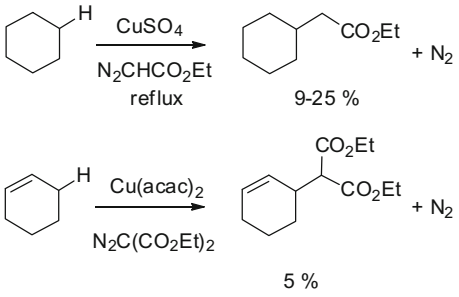

Scheme 6.9 Early examples of C-H bond functionalization by carbene insertion with copper-based catalysts

incorporated into the cycloalkane, the remaining 25 % converting into a mixture of diethyl fumarate and maleate. As already mentioned, this is a common feature of this catalytic systems, the amount of the coupling products being diminished by the use of a large substrate:diazocompound ratio (200:3 in this rhodium system) and in many cases with the aid of slow addition devices to control the ratio of incorporation of the diazocompound into the solution containing both the alkane and the catalyst. In the case of n-pentane (Scheme 6.10), the same group reported the formation of a mixture of three products derived from the formal insertion of the carbene unit into the C–H bonds of the primary as well as of the two distinct secondary sites. Analogously, the use of 2,3-dimethylbutane as the reactant yielded a mixture of two products upon reaction of the primary and tertiary C–H bonds. As shown in Scheme 6.10, the normalized regioselectivity, calculated considering the number of available C–H bonds of the same type in each substrate, follows the trend tertiary > secondary > primary C–H bonds.

6.2.3 Catalyst Development

After the above discovery, a number of groups have focused in the development of catalytic systems capable of inducing the functionalization of C–H bonds by the methodology of carbene insertion from diazocompounds [11–15]. Although different carbon-hydrogen bonds, i.e., benzylic, allylic, vicinal to heteroatom, etc., have been transformed in this manner, this chapter is restricted to the most unreactive ones, those of alkanes. Scheme 6.5 showed that all metals from group 8–11 are known to transfer carbene fragments from diazocompounds. However, regarding the transformation of alkanes with this strategy, only rhodium, copper, silver and gold-based catalysts have been described, along with scarce examples based on iron and ruthenium. The ligands commonly employed are shown in Scheme 6.11. For rhodium, both bidentate anionic ligands such as acetate and derivatives as well as porphyrin macrocycles have been employed. The latter has also been reported with iron and ruthenium. In the case of the three group 11 metals, most of the work in the field has been developed using trispyrazolylborate ligands, with some other results based in complexes bearing N-heterocyclic carbene or polypyridyl-ligands.

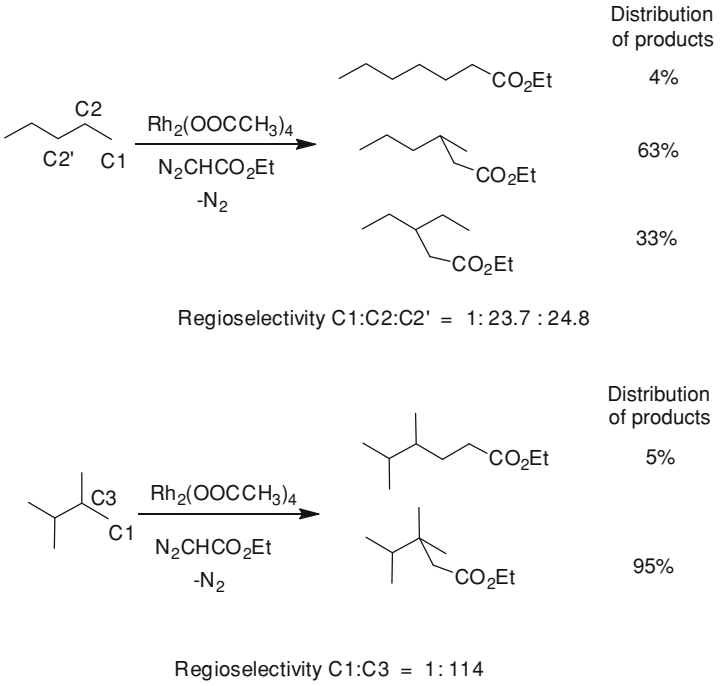

Scheme 6.10 Noels' seminal discovery of the rhodium-catalyzed alkane functionalization by carbene insertion

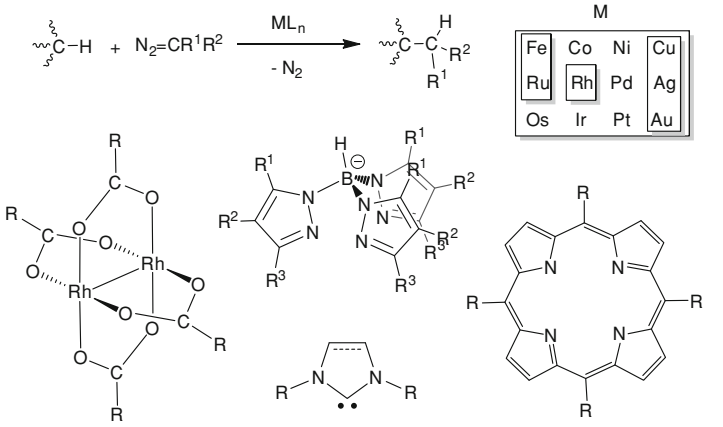

Scheme 6.11 Metals and ligands commonly employed in alkane C–H bond functionalization by carbene insertion

In order to compare the activity of the catalyst described for this transformation, three reactions have been chosen for such discussion: the functionalization of a cyclic alkane (cyclohexane), a linear alkane (n-pentane or n-hexane) and a branched alkane

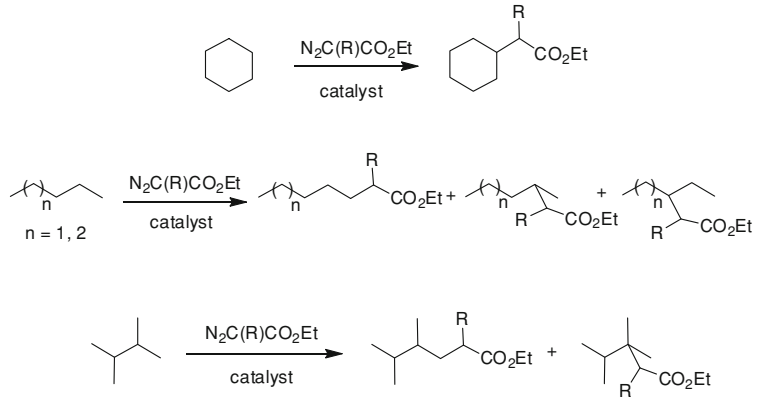

Scheme 6.12 Model cyclic, linear and branched alkanes to evaluate catalyst activity

Table 6.1 Metal-catalyzed functionalization of cyclohexane with diazocompounds[a]

Entry	Catalyst	Diazocompound	Yield[b]	Reference
1	$CuSO_4$	$N_2C(H)CO_2Et$	24	[50]
2	$Rh_2(OOCCF_3)_4$	$N_2C(H)CO_2Et$	75	[52, 53]
3	RhTPPI	$N_2C(H)CO_2Et$	71	[56]
4	$Rh_2(S\text{-}DOSP)_4$	$N_2C(Ar)CO_2Et$	80	[57–59]
5	$Tp^{Ms}Cu(thf)$	$N_2C(H)CO_2Et$	54	[60]
6	$Tp^{Br3}Cu(NCMe)$	$N_2C(H)CO_2Et$	90	[61, 62]
7	$Tp^{(CF3)2}Cu(thf)$	$N_2C(H)CO_2Et$	58	[23–24,63]
8	$Tp^{(CF3)2}Ag(thf)$	$N_2C(H)CO_2Et$	99	[23–24,63]
9	$[IPrCu(NCMe)]BF_4$	$N_2C(H)CO_2Et$	80	[27]
10	$[IPrAu(NCMe)]BAr'_4$	$N_2C(H)CO_2Et$	84	[27]
11	$Tp^{F21}Cu(OCMe_2)$	$N_2C(H)CO_2Et$	99	[64]
12	$Tp^{F21}Ag(OCMe_2)$	$N_2C(H)CO_2Et$	97	[64]
13	$(TPN)Cu(thf)BAr'_4$	$N_2C(H)CO_2Et$	85	[65]
14	$Tp^{(CF3)2}Ag(thf)$	$N_2C(Me)CO_2Et$	76	[66]
15	$Tp^{(CF3)2}Ag(thf)$	$N_2C(Ph)CO_2Et$	77	[66]
16	$Rh_2(OOCR_F)_4$	$N_2C(Ar)CO_2Et$	78	[67]
17	$[Tpm^*Cu(NCMe)]BF_4$	$N_2C(H)CO_2Et$	77	[68]
18	Fe(TTP)Cl	$N_2C(Ar)CO_2Et$	78	[69]
19	Rh(ttppp)(Me)(MeOH)	$N_2C(Ar)CO_2Et$	80	[70]
20	nano-Ru-polym	$N_2C(Ph)CO_2Et$	60	[71]

[a] As in Scheme 6.12

[b] As percentage of functionalized products, carbene coupling products $R^1R^2C{=}CR^1R^2$ accounted for 100 % of initial diazocompound

(2, 3-dimethylbutane). Most of the results have been described with ethyl diazoacetate as the carbene source, although in some cases a different, more substituted diazo reagent has been employed. Scheme 6.12 shows the three model reactions that allow evaluation of activities as well as comparison of regioselectivities. Tables 6.1,

Table 6.2 Metal-catalyzed functionalization of pentane/hexane with diazocompounds[a]

Entry	Catalyst	Diazocompound	n[a]	Yield[b]	Selectivity[c]			Reference
					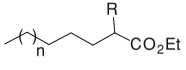	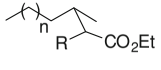	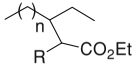	
1	$Rh_2(OOCCF_3)_4$	$N_2C(H)CO_2Et$	1	n.r.[d]	1.0	14.1	11.6	[53]
2	$Rh_2(OOCTC)_4$	$N_2C(H)CO_2Et$	1	n.r.[d]	1.0	3.1	0.9	[53]
3	RhTPPI	$N_2C(H)CO_2Et$	2	86	1.0	13.4	4.0	[56]
4	RhTMPI	$N_2C(H)CO_2Et$	2	36	1.0	3.7	0.8	[56]
5	$Rh_2(OOCR_F)_4$[f]	$N_2C(H)CO_2Et$	2	92	1.0	14.4	6.9	[67]
6	$Tp^{Br3}Cu(NCMe)$	$N_2C(H)CO_2Et$	2	60	n.d.	3.0	1.0	[61-62]
7	$Tp^{Br3}Ag(thf)$	$N_2C(H)CO_2Et$	2	98	1.0	3.7	1.4	[25]
8	$Tp^{(CF3)2}Ag(thf)$	$N_2C(H)CO_2Et$	1	81	1.0	1.7	0.9	[23-24]
9	$[IPrCu(NCMe)]BF_4$	$N_2C(H)CO_2Et$	1	75	n.d.	3.5	1.0	[27]
10	$[IPrAu(NCMe)]BAr'_4$	$N_2C(H)CO_2Et$	1	82	1.0	2.9	1.8	[27]
11	$Tp^{F21}Cu(OCMe_2)$	$N_2C(H)CO_2Et$	1	47	1.0	18.5	7.0	[64]
12	$Tp^{F21}Ag(OCMe_2)$	$N_2C(H)CO_2Et$	1	86	2.3	4.6	1.0	[64]
13	$(TPN)Cu(THF)BAr_4$	$N_2C(H)CO_2Et$	2	62	n.d.	1	1.0	[65]
14	Rh(ttppp)(Me)(MeOH)	$N_2C(Ar)CO_2Et$	2	66	3.5	1.21[e]		[70]
15	nano-Ru-polym	$N_2C(Ph)CO_2Et$	2	50	1	1[e]		[71]

[a] As in Scheme 6.12

[b] As percentage of functionalized products, carbene coupling products R^1R^2 $C{=}CR^1R^2$ accounted for 100 % of initial diazocompound

[c] Normalized by the number of hydrogen atoms of each type

[d] not reported

[e] Overall secondary sites regioselectivity

[f] R_F fluorinated chain

Table 6.3 Metal-catalyzed functionalization of 2,3-dimethylbutane with diazocompounds

Entry	Catalyst	Diazocompound	Yield[b]	Selectivity[c]		Reference
				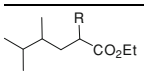	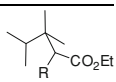	
1	$Rh_2(OOCCH_3)_4$	$N_2C(H)CO_2Et$	n.r.[d]	1.0	114	[53]
2	$Rh_2(OOCCF_3)_4$	$N_2C(H)CO_2Et$	n.r.[d]	1.0	44	[53]
3	$Rh_2(OOCTC)_4$[e]	$N_2C(H)CO_2Et$	n.r.[d]	1.0	12	[53]
4	$Rh_2(S\text{-}DOSP)_4$	$N_2C(Ar)CO_2Et$	27	n.d.	1.0	[57-59]
5	$Tp^{Br3}Cu(NCMe)$	$N_2C(H)CO_2Et$	56	n.d.	1.0	[61-62]
6	$Tp^{Br3}Ag(thf)$	$N_2C(H)CO_2Et$	98	1.0	3.7	[25]
7	$Tp^{(CF3)2}Ag(thf)$	$N_2C(H)CO_2Et$	85	1.0	1.5	[23-24]
8	$[IPrCu(NCMe)]BF_4$	$N_2C(H)CO_2Et$	65	1.0	40	[27]
9	$[IPrAu(NCMe)]BAr'_4$	$N_2C(H)CO_2Et$	95	1.0	0.9	[27]
10	$Tp^{F21}Cu(OCMe_2)$	$N_2C(H)CO_2Et$	16	1.0	94	[64]
11	$Tp^{F21}Ag(OCMe_2)$	$N_2C(H)CO_2Et$	96	1.0	2.0	[64]
12	$(TPN)Cu(THF)BAr_4$	$N_2C(H)CO_2Et$	69	n.d.	1.0	[65]
13	$Tp^{(CF3)2}Ag(thf)$	$N_2C(Ph)CO_2Et$	66	n.d.	1.0	[66]

[a] As in Scheme 6.12
[b] As percentage of functionalized products, carbene coupling products $R^1R^2C=CR^1R^2$ accounted for 100 % of initial diazocompound
[c] Normalized by the number of hydrogen atoms of each type
[d] Not reported
[e] TC trypticyl

6.2 and 6.3 contain the data available with the catalysts reported for these transformations that have induced a noticeable degree of functionalization.

The reaction of cyclohexane and a diazocompound has been usually employed as a first probe to test the catalytic capabilities of a given complex. As shown in Table 6.1, all reported metals (Rh, Cu, Ag, Au, Fe, Ru) provided moderate to high degree of conversions. It is worth noting that those experiments were carried out under distinct reaction conditions, and therefore the direct comparison is somewhat difficult. As already mentioned, the substrate to diazocompound ratio or the use (or not) of slow addition devices strongly affect the outcome of these reactions. In any case, most of the catalysts have induced high to very high yields (based in the initial diazocompound, usually the limiting reagent), and probably those with the lower values could be improved with the aid of the above reaction conditions. With ethyl diazoacetate as the carbene source, the silver-based catalysts containing trispyrazolylborate or trisindadozylborate ligands (entries 8 and 12) gave quantitative conversions. Disubstituted diazoacetates of general formula $N_2{=}C(R)CO_2Et$ have also been utilized with success (entries 4, 14–16, 18–20).

The previous systems operate under homogeneous conditions. In order to achieve the well-known advantages of heterogeneous catalysis for catalyst separation and recycling, three systems have been reported that accomplish with that feature. A fluorinated rhodium catalyst (entry 16) was described to induce cyclohexane functionalization although high levels of deterioration precluded a reasonable degree

Scheme 6.13 Meso-tetrakis (2,4,6-triphenyl)porphyrinato ligand (ttppp)

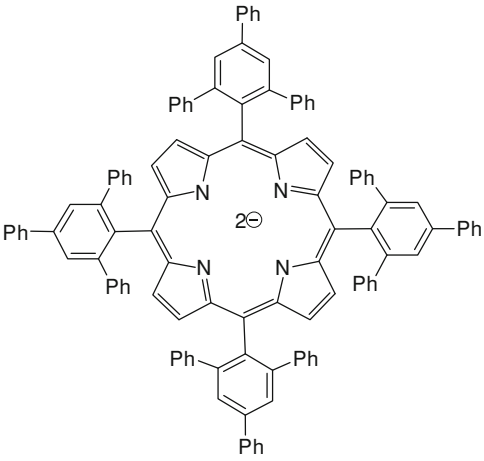

of catalyst recycling. The copper catalyst [Tpm*Cu(NCMe)]BF_4 (entry 17) was employed using an ionic liquid/hydrocarbon heterogeneous mixture as the reaction medium, allowing the recycling of the catalyst for five cycles without significant loss of the catalytic activity. A recyclable ruthenium-based system, where Ru nanoparticles were supported on non-cross-linked soluble polystyrene, induced the functionalization of cyclohexane (entry 20). Iron and rhodium complexes bearing porphyrin ligands have also been employed for this transformation (entries 18 and 19). The latter constitutes a particular example since it is related to an exceptional regioselectivity toward primary sites as well as in the asymmetric version, and will be discussed in detail later on.

Table 6.2 shows the different catalytic systems reported for the functionalization of pentane or hexane using ethyl diazoacetate as well as other N_2=C(R)(CO_2Et) as the carbene source. First examples (entries 1 and 2) demonstrated the importance of the presence of electron withdrawing ligands in the coordination sphere of the metal center, therefore decreasing the electron density at metal and increasing the electrophilia of the metallocarbene intermediate. Thus, just by using the fluorinated version of the acetate ligand, the yield was dramatically enhanced (entry 5). A second feature is the use of bulky ligands that protect that intermediate from bimolecular decomposition pathways. This is exemplified with the rhodium catalyst containing trypticyl substituents (entry 3), that increased the yield up to 86 %. Also, the steric hindrance disfavored the functionalization of the secondary sites with the subsequent enhancement of the regioselectivity toward the primary sites.

Most of the catalysts led to mixtures of products derived from the preference of secondary sites over primary ones. Actually, those based in copper did not affect the latter (entries 6, 9, 11and 13). Silver- and gold-based catalysts did functionalize the primary sites, the complex $Tp^{F21}Ag(OCMe_2)$ providing the highest selectivity toward the C–H bonds of the terminal methyl group in pentane or hexane with ethyl diazoacetate (1:2.4, primary:secondary sites). The sole exception to this trend

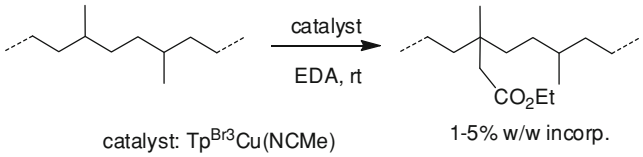

Scheme 6.14 Polyolefin functionalization by carbene insertion

has been reported with a highly hindered porphyrin ligand bonded to a rhodium center (Scheme 6.13), but with $N_2C(Ph)CO_2Et$ as the diazo compound. In this case, a preferential functionalization of the primary sites has been observed, with an overall 9.8:1, primary:secondary sites regioselectivity (entry 14).

The above trends can be also found when 2, 3-dimethylbutane was employed as the reactant. This molecule allows the direct comparison of primary and tertiary sites. The aforementioned effects of the R substituent in terms of electron donation capabilities and steric pressure in the catalysts $Rh_2(OOCR)_4$ also applied in this case (Table 6.3, entries 1–3). Exclusive tertiary C–H functionalization was obtained with $Tp^{Br3}Cu(NCMe)$ and EDA. The silver complex $Tp^{(CF3)2}Ag(thf)$ along with the diazocompounds $N_2C(R)CO_2Me$ (R = Me, Styryl) also gave the product derived from the insertion of the $:C(R)CO_2Me$ group into the tertiary C–H bond (Table 6.3, entries 7 and 13). On the other hand, the highest selectivity toward the primary sites have been obtained with the gold complex [IPrAu(NCMe)]BAr'$_4$ (Table 6.3, entry 9).

This methodology has been applied to the insertion of polar ester groups into polyolefin chains [72]. This is an interesting transformation since polymer materials bearing polar groups constitute a target in polymer industry and their direct synthesis from polar monomers is not straightforward. Polyethylene and polypropylene were treated with EDA in the presence of $Tp^{Br3}Cu(NCMe)$ as the catalyst to yield functionalized polyolefins with a 1–5 % degree of incorporation of $CHCO_2Et$ groups (Scheme 6.14). Interestingly, the new materials showed similar hydrodynamic properties than the starting polymers, demonstrating that the process takes place without chain scission and maintaining the polymer structure.

6.2.4 Methane Functionalization

The previous section have shown that non-activated carbon-hydrogen bonds of plain alkanes as well as those of polyolefins can be functionalized by the carbene insertion methodology using diazocompounds as the carbene source with an array of metal-based catalyst. The extreme case of methane has also been recently included in the list of substrates [73]; therefore all the possible alkane C–H bonds being now known to be modified with the strategy. To achieve such goal, supercritical carbon dioxide ($scCO_2$) was employed as the reaction solvent. The use of any other solvent containing other carbon-hydrogen bonds would lead to the functionalization of the latter. Halosolvents such as CCl_4 were not an option since the C-X bonds are also functionalized by this methodology [74].

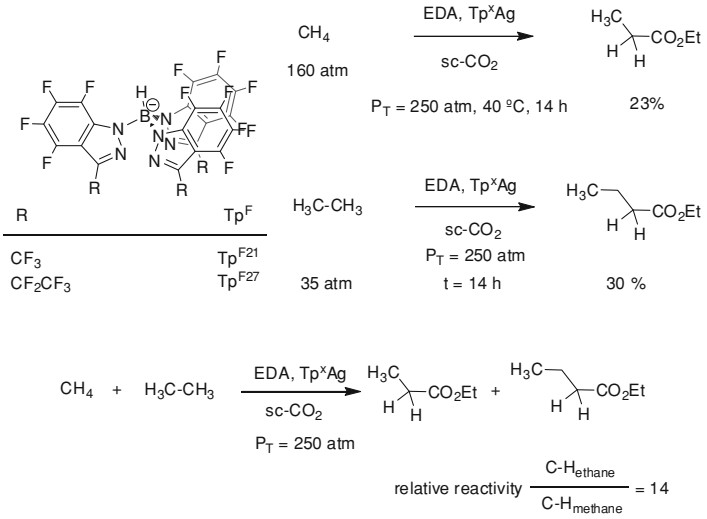

Scheme 6.15 Methane and ethane functionalization by carbene insertion

Methane was converted [73] into ethyl propionate by direct reaction with EDA at 40 °C and using $scCO_2$ as the solvent (Scheme 6.15). Nearly 500 TON were achieved using a completely fluorinated trisindazolylborate-containing silver catalyst, with a maximum of 23 % yield based on the initial diazocompound. The remaining initial EDA was converted into a mixture of diethyl fumarate and maleate.

Ethane was also converted into ethyl butyrate using the same catalyst. A competition experiment using both alkanes, methane and ethane, provided a direct comparison of the relative reactivity of their C–H bonds, that of ethane being favoured by a 14-fold factor.

6.2.5 The Asymmetric Version

In some cases, the insertion of a carbene group into a C–H bond of a hydrocarbon generates the formation of one (or more) stereocenter. Therefore, the use of chiral catalysts could induce the appearance of enantiomeric excesses during the transformation. To date, only two catalytic systems have been reported to achieve such results, both based on rhodium (Scheme 6.16). At the end of the 90's, dirhodium tetrakis(*S*-(N-dodecylbenzenesulfonyl)prolinate) (I, Scheme 6.16), Rh_2(S-DOSP)$_4$ was found to induce the asymmetric functionalization of some non-activated hydrocarbons [57–59]. Ee values were moderate to high, methyl aryldiazoacetates being employed as the carbene source. As shown in Scheme 6.17, ca 90 % ee were achieved with cyclohexane (secondary C–H) and adamantane (tertiary C–H), whereas only 60 % ee was reached with 2-methylbutane. Ten years later, a rhodium-

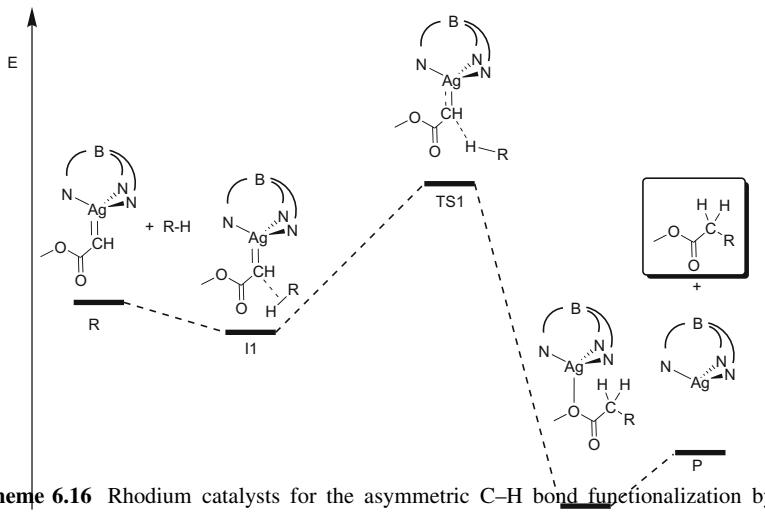

Scheme 6.16 Rhodium catalysts for the asymmetric C–H bond funetionalization by carbene insertion

porphyrin catalyst [70] (II, Scheme 6.16) was described to give similar degrees of enantioselection, as well as the already mentioned high regioselection toward primary sites. Thus, hexane or 2,2-dimethylbutane were preferentially functionalized in the primary sites with the subsequent generation of the stereocenter.

In spite of the use of ethyl diazoacetate in most of the reported system for hydrocarbon functionalization (Tables 6.1, 6.2, 6.3), no example of asymmetric induction using this diazocompound has been yet reported: such transformation would originate a stereocenter, as shown in Scheme 6.17e.

6.2.6 Mechanistic Considerations

The general picture of the mechanism that governs this transformation is given in Scheme 6.18 [20]. The direct interaction of the diazocompound with a metal complex, electrophilic in nature, provides a metallocarbene intermediate that further react with the C–H bond through a concerted step. Such proposal was establish on the basis of experimental data from several groups using dirhodium carboxylate catalysts. Thus, the rate limiting step was established as that of nitrogen extrusion and metallocarbene insertion [74]. In addition, kinetic isotope effect depended of the catalyst [75, 76]. It has also been mentioned that the trend in reactivity follows the order tertiary > secondary ≫ primary [77, 78]. With the appropriate substrate, it was demonstrated that the insertion reaction proceeded with retention of the configuration at the carbon atom where the carbon-hydrogen functionalization takes place, an evidence of the concerted nature of the process [79]. The effect of the catalyst structure in the regio- and stereoselectivity was also demonstrated with an array of dirhodium carboxylate catalysts [80-82].

Scheme 6.17 Asymmetric functionalization of several hydrocarbons

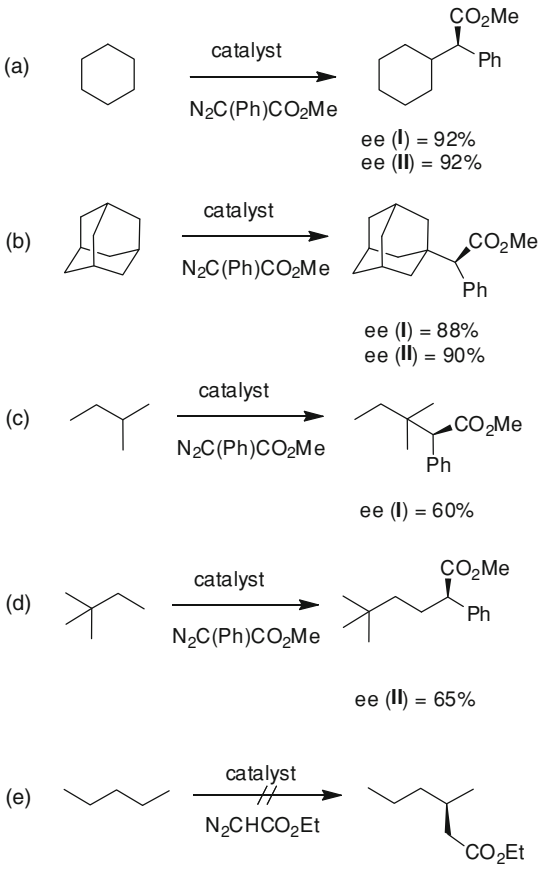

Scheme 6.18 Mechanistic picture of the metal-mediated carbon-hydrogen bond functionalization by carbene insertion from diazocompounds

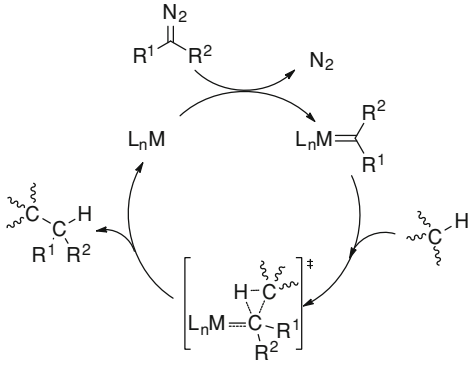

An interesting experimental feature was shown with dirhodium tetraacetates that depending of the nature of the diazocompound could induce the functionalization of alkanes by metallocarbene species or by free carbenes [75]. As shown in

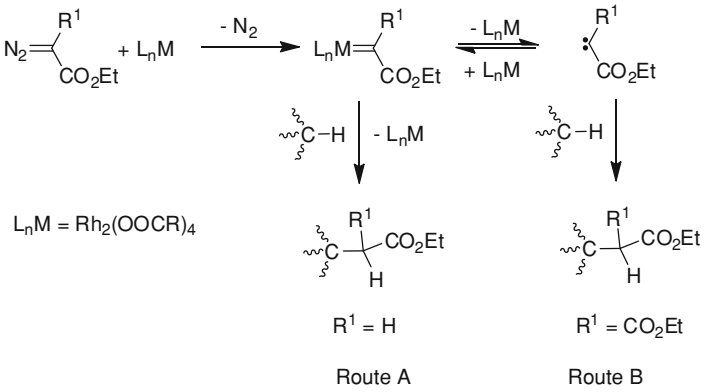

Scheme 6.19 Carbene transfer to C–H bonds from the metal center (*route A*) and by free carbenes (*route B*)

Scheme 6.19, the metal center decomposes the diazo reagent to give a metallocarbene that is in equilibrium with the dissociated carbene. With ethyl diazoacetate, the reaction takes place through route A whereas with diethyl diazomalonate route B was preferred. The distinction between both pathways was established on the basis of the different selectivities observed. This is the only example known in which the participation of free carbenes was proposed in a C–H functionalization reaction by carbene insertion with metal-based catalysts.

A theoretical study delivered a mechanism in agreement with the above experimental data [83]. As shown in Scheme 6.20, the reaction starts with the attack of the diazocompound to one rhodium atom, inducing the breaking of the Rh-Rh bond and the formation of two Rh(I)-Rh(III) centers, the reaction proceeding on the latter. Nitrogen extrusion followed by carbene formation takes place prior to the interaction of the C–H bond with the carbon metallocarbenic atom throughout a late transition state in which the cleavage of the Rh-C bond is involved. This is in contrast with the olefin cyclopropanation reaction that is proposed to proceed through an early transition state in which the metal-carbene bond does not undergo cleavage. In the C–H functionalization, the process is concerted but asynchronous (the TS are shown as two resonance structures) and due to the low nucleophilia of the substrate, both the metal-carbene lability as well as the high electrophilicity of the carbene carbon atom are relevant.

The catalytic systems based in group 11 metal complexes bearing tris-pyrazolylborate ligands have also been modelled [84, 85]. The metallocarbene intermediate interacts with the C–H bond to give a weak van der Waals intermediate that evolves toward products by means of a low barrier transition state (Scheme 6.21). In the latter, the hydrogen atom of the hydrocarbon interacts with the carbenic carbon atom. When different types of C–H compete for the metallocarbene, the selectivity is decided by the barriers of that transition state, the process operating under kinetic control. The tridentate ligand maintains such

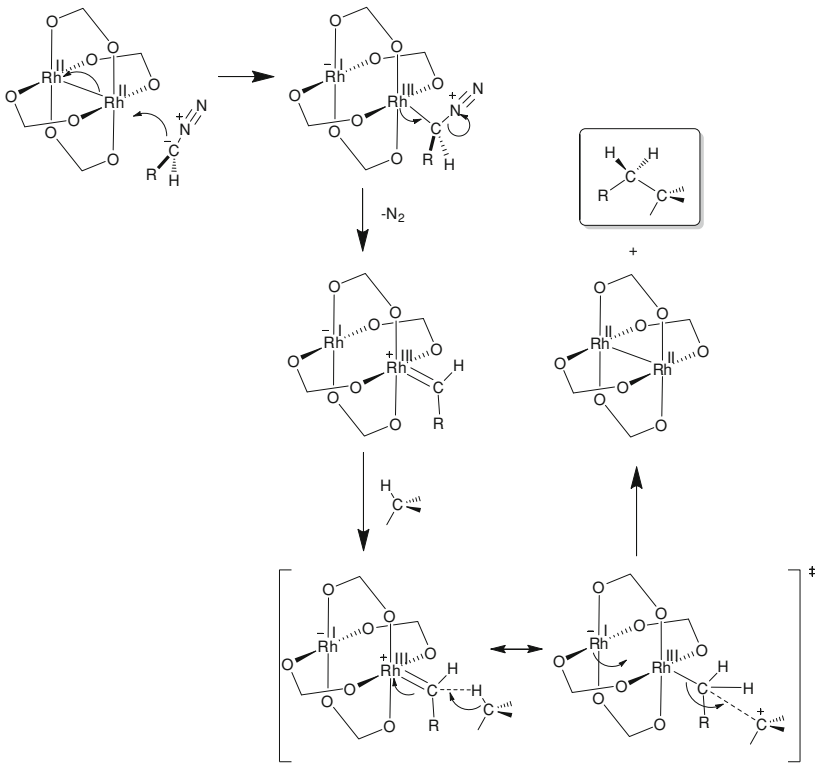

Scheme 6.20 Mechanism proposed from theoretical calculations for the rhodium-mediated C–H bond functionalization by carbene insertion

coordination mode along the reaction coordinate. This study provided comparative values for the activation barriers for different ligands, metals and substrates.

One particular characteristic of the Tp^xM system is the observance of an inhibitor effect when large amounts of diazocompounds are employed, in the case of silver. This is not the case with Tp^xCu catalysts, for which the addition of EDA in whatever amounts, provided high yields of the diazo coupling products, unless slow addition devices are employed. But with the silver analogs, the diazocompound can be added in one portion at the beginning of the reaction to give very high yield of the alkane functionalized products. However, at a certain EDA concentration the reaction rate slows down dramatically. Theoretical studies [85] have shown that this is the result of the formation of a species derived from metallocarbene trapping with a second molecule of EDA (Scheme 6.22). That species would act as the catalyst resting state, the equilibrium with the metallocarbene driving the reaction rate toward the functionalized products given the higher barrier calculated for the formation of diethyl fumarate and maleate from this intermediate.

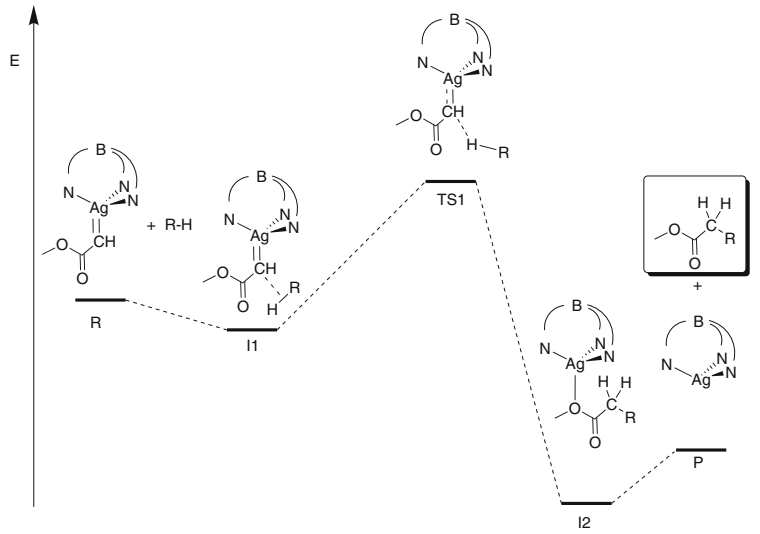

Scheme 6.21 Mechanism proposed from theoretical calculations for the silver (as well as copper) mediated C–H bond functionalization by carbene insertion. The BN3 ligand represents trispyrazolylborate, Tp^x

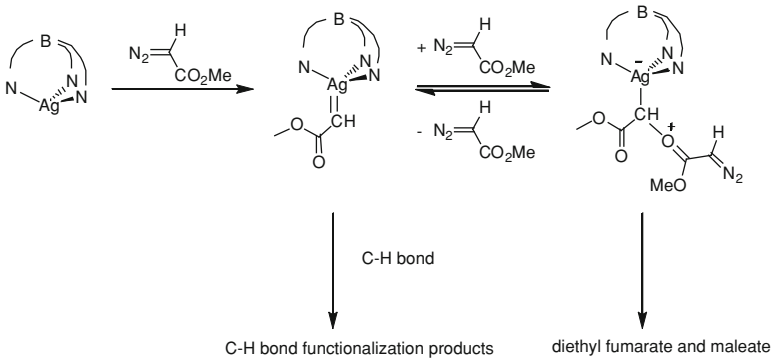

Scheme 6.22 The silver-mediated alkane functionalization with ethyl diazoacetate involves an intermediate derived from two molecules of the carbene precursor

In a simple approach, the general mechanism for this transformation can be explained as the attack of a strong electrophile (the carbenic carbon) onto a (poor) nucleophile, the C–H bond. The interaction of the σ-bonding molecular orbital of the latter with the empty 2p orbital of the metallocarbene carbon constitutes the crucial step in this transformation (Scheme 6.23). Therefore, the catalytic activity is controlled by the electrophilicity of the metallocarbene and the nucleophilicity of the C–H bond. It has already been discussed that the former is enhanced using electron deficient metal centers, a feature favored with poor donating ligands. As

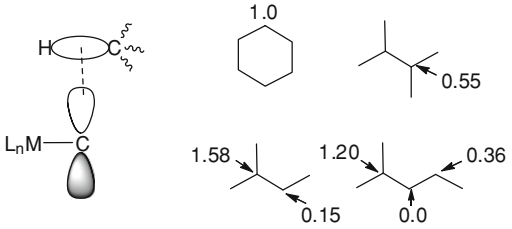

Scheme 6.23 The C–H-carbene interaction (*left*) and the relative reactivity of several C–H bonds of alkanes toward the functionalization by carbene insertion from EDA using $Tp^{Br3}Cu$ as the catalyst

mentioned before, the order of reactivity found in these transformation matches the bond dissociation energy order, that is, tertiary C–H bonds are more prone to be functionalized that secondary sites, and these more than primary C–H bonds. Scheme 6.23 shows the relative reactivity, obtained from competition experiments, of distinct C–H bonds of alkanes, with $Tp^{Br3}Cu$ as the catalyst, using the cyclohexane C–H bonds as the reference [62]. Interestingly, the tertiary sites of 2,3-dimethylbutane were found to be less reactive than cyclohexane whereas that site in 2-methylbutane was more reactive than cyclohexane. The bond dissociation energy for a tertiary C–H bond is slightly lower than for cyclohexane (by 1 kcal/mol). Therefore, the steric pressure of an additional methyl group seems to disfavour the functionalization, in spite of a higher electron density (due to inductive effects) of such reaction site. The same behavior is observed when comparing the secondary sites of 2-methylbutane and 2-methylpentane. The C–H bonds vicinal to the isopropyl groups show a different reactivity due to steric effects of the other substituent (methyl vs ethyl). In both cases, the tertiary site is more reactive, as expected. Similar trends were found with $Rh_2(S\text{-DOSP})_4$ as the catalyst and $N_2C(Ph)CO_2Me$ as the diazo compound [59]. The selectivity of this transformation is mainly governed by electronic factors although when dealing with C–H bonds with similar electron densities, steric factors seem to be decisive.

6.3 Alkane Functionalization by Nitrene Insertion

6.3.1 The Reaction

The transfer of a nitrene (NR) unit to a given substrate from the coordination sphere of a metal complex has been already mentioned in Sect. 6.2.1. The first example of this methodology was described by Kwart and Khan in the late 60's in the past century [86], using azides as the NR source and copper powder as the catalyst to induce the aziridination of cyclohexene (Scheme 6.24a). Since then, the transition-metal catalyzed nitrene transfer reaction has been extended to saturated (C–H amination) and unsaturated (olefin aziridination) substrates (Scheme 6.24b), both in the inter- and intramolecular fashions [16–19, 87–89].

On the basis of the aim of this volume, this subchapter is focussed in the functionalization of alkane C–H bonds by means of the (formal) insertion of a NR

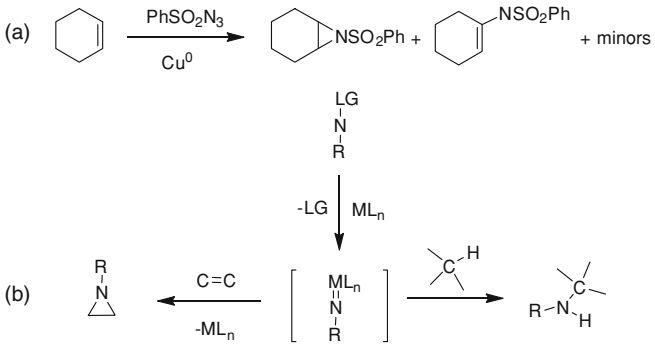

Scheme 6.24 **a** Seminal work by Kwart and Khan showing the nitrene transfer reaction with copper as catalyst. **b** The general metal-mediated nitrene transfer reaction: the metallonitrene intermediate, electrophilic in nature, can react with saturated or unsaturated substrates

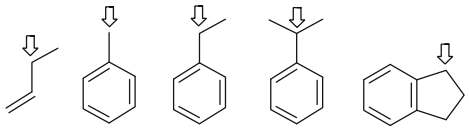

Scheme 6.25 Most frequently employed substrates for the evaluation of catalysts in the nitrene insertion reaction. *Arrow* indicates the preferential, activated reaction site

unit into such bond. At this point it is important to define the nature of the substrates to be presented in the following sections. The above two transformations have been developed to date in different degree, the aziridination reaction having been by far more studied than the C–H functionalization by nitrene insertion. This is the result of the electrophilic nature of the metallonitrene intermediate proposed for both reactions (Scheme 6.24b), that will preferentially react with good nucleophiles such as olefins, instead of C–H bonds. But it is also true that, when targeting the amination reaction, such carbon-hydrogen bonds are not all the same in terms of nucleophilicity. Thus, the reactivity of a benzylic C–H bond is far from that of n-hexane, for instance, with a ca 8 kcal/mol gap in their bond dissociation energies [90–92]. Not surprisingly, many of the catalytic systems described for C–H aminations are based on allylic or benzylic functionalizations, or related activated sites (indane, toluene), as shown in Scheme 6.25. For the purpose of this book, only plain alkanes (including cycloalkanes) without any activating group will be considered along this subchapter. As a consequence of that, the intramolecular activation processes, that constitutes an area of interest in the field, will not be discussed either [93].

The nitrene source also deserves some comments. Initial work was carried out with sulfonylazides [86, 94], until Yamada and co-workers described the hypervalent iodine (III) reagent PhINTs (Scheme 6.26) [95]. Since then, the majority of the work involving the addition or insertion of NR groups to unsaturated or

Scheme 6.26 Nitrene precursors (LG-NR in Scheme 6.24)

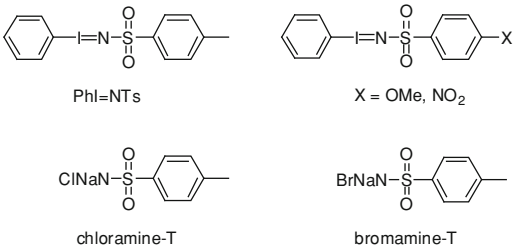

Scheme 6.27 First examples of non-activated C–H bonds by nitrene insertion. TPP = tetrakisphenyl-porphyrin

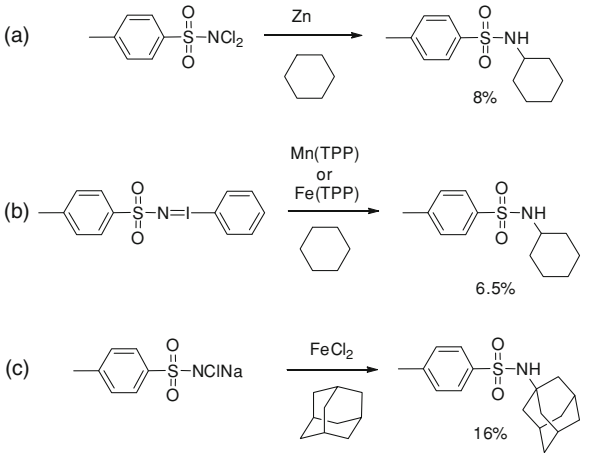

saturated substrates has been performed with PhI=NTs such reagent. Similar derivatives with other substituents in the *para* position of the arylsulfonyl group have been used for the same purpose [96]. Also chloramine-T (NaClNTs) [97, 98] and bromamine-T (NaBrNTs) [99, 100] have been tested as the nitrene sources. All those reagents are quite unsoluble in most organic solvents, therefore conditioning the reaction rate of the overall process to their dissolution rate. Recent catalytic development has focussed in the in situ generation of the active nitrene source upon mixing the precursors $PhI(OAc)_2$ and $TsNH_2$.

Therefore, in the subsequent sections an account of the state of the art of the functionalization of alkane C–H bonds by means of the metal-catalyzed nitrene insertion will be presented, with the restrictions already noted about the nature of the reaction site: non-activated C–H bonds and in the intermolecular case only.

6.3.2 Early Examples

The first report of an alkane C–H bond functionalization by this methodology was described by Breslow [94] using cyclohexane as the substrate, dichloramine-T as the nitrene source and zinc powder as the catalyst, to provide a 8 % yield into the

cycloalkane functionalization product (Scheme 6.27a). Nearly fifteen years after that report, the same author described the use of Mn(III)- and Fe(III)-based catalysts for the tosylamidation of cyclohexane (Scheme 6.27b), yet using the PhINTs reagent. Although yields were also low, this work is commonly accepted as the seminal work in metal-catalyzed C–H bond amidation reactions [101]. Shortly after, Barton described the use of an iron-based system for the functionalization of adamantane with chloramine-T (Scheme 6.27c) [102].

6.3.3 Cycloalkanes as Substrates

Cycloalkanes and adamantane have been the most frequently non-activated hydrocarbons employed within this methodology. Tables 6.4 and 6.5 enumerate the catalytic systems described for their conversion into amines upon nitrene transfer processes, that are yet short in number, with only a few metals having proven their capabilities to promote such transformation: Mn (group 7), Fe, Ru (group 8), Rh (group 9), Cu, Ag (group 11) and Zn (group 12).

In spite of the interest of the conversion of alkane C–H bonds into value added products and the report in the early 80s of the past century by Breslow and Gellman of the tosylamidation of cyclohexane with porphyrin-containing Mn- or Fe-based catalysts (Table 6.4, entry 2), it has not been until this century that a certain, hitherto insufficient, development in this area has been observed. Before that, Müller reported [103] the use of $Rh_2(OAc)_4$ with the nitrene source NsNIPh, bearing a NO_2 group (Ns = p-nitrobenzenesulfonyl), to give a 30 % conversion of cyclohexane into the amine derivative (Table 6.4, entry 3). Later, $Tp^{Br3}Cu(NCMe)$ (Tp^{Br3} = hydrotris(3,4,5-tribromopyrazolyl)borate) was reported by Pérez and co-workers to induce a certain degree of functionalization of cyclohexane (Table 6.4, entry 4) [104, 105]. Shortly after, Du Bois's group described a Rh-based catalyst for the functionalization of cyclooctane in high yield (Table 6.4, entry 5). The nitrene source in this case was generated in situ upon mixing iodobenzeenediacetate and the amine $Cl_3CCH_2SO_3NH_2$ [106]. Silver was introduced as catalyst by He and co-workers [107], with a disilver complex containing the bathophenantroline ligand (4, 7-diphenyl,1-10-phenantroline). Several cycloalkanes (Table 6.4, entries 6–8) were functionalized in 35–40 % yield with NsNIPh. An elegant work by Warren and co-workers [108], also relevant for mechanistic considerations (see below) showed the transfer of a NAd (Ad = adamantyl) group from adamantylazide to cyclohexane (Table 6.4, entry 9). A trispyrazolylborate-containing silver complex improved the catalytic activity of the related copper catalyst (Table 6.4, entries 10, 11) [109]. Finally, Dauban, Müller, Dodd and co-workers described [110, 111] a catalytic system formed by a dirhodium complex containing a chiral dicarboxylate bridging ligand (nta) in conjunction with a chiral sulfonimidamide to generate the nitrene precursor in situ. The C_5–C_8 series of cycloalkanes were converted into amines in 85–96 % yield, and with a moderate excess of the hydrocarbon (Table 6.4, entries 12–15).

Table 6.4 Metal-catalyzed functionalization of cycloalkanes by nitrene insertion[a]

Entry	Substrate	Nitrene source	Catalyst	Temperature (°C)	Yield (%)	Reference
1	Cyclohexane	$TsNCl_2$	Zn	85	8	94
2	Cyclohexane	TsNIPh	Mn(TPP) or Fe(TPP)	rt	6.5	101
3	Cyclohexane	NsNIPh	$Rh_2(OAc)_4$	83	30	103
4	Cyclohexane	TsNIPh	$Tp^{Br3}Cu(NCMe)$	rt	65	104, 105
5	Cyclooctane	$PhI(OAc)_2/H_2NR$	$Rh_2(esp)_4$	rt	84	106
6	Cyclopentane	NsNIPh	(bp)AgOTf	50	35	107
7	Cyclohexane	NsNIPh	(bp)AgOTf	50	40	107
8	Cyclooctane	NsNIPh	(bp)AgOTf	50	33	107
9	Cyclohexane	AdN_3	$[(Me_3NN)Cu]_2(\mu\text{-}C_6H_6)$	80	40	108
10	Cyclopentane	TsNIPh	$[Tp^{*,Br}Ag]_2$	80	80	109
11	Cyclohexane	TsNIPh	$[Tp^{*,Br}Ag]_2$	90	90	109
12	Cyclopentane	$PhI(OCO^tBu)_2/H_2NR^*$	$Rh_2\text{-}\{(S)\text{-nta}\}_4$	rt	85	110, 111
13	Cyclohexane	$PhI(OCO^tBu)_2/H_2NR^*$	$Rh_2\text{-}\{(S)\text{-nta}\}_4$	rt	85	110, 111
14	Cycloheptane	$PhI(OCO^tBu)_2/H_2NR^*$	$Rh_2\text{-}\{(S)\text{- nta}\}_4$	rt	96	110, 111
15	Cyclooctane	$PhI(OCO^tBu)_2/H_2NR^*$	$Rh_2\text{-}\{(S)\text{- nta}\}_4$	rt	92	110, 111

[a] Abbreviations: Ts = tosyl (p-toluenesulfonyl); TPP = tetrakisphenylporphyrin; Tp^{Br3} = hydrotris(3,4,5-tribromopyrazolyl)borate); esp = dicarboxylate bridging ligand; R = $Cl_3CCH_2SO_3$; Ns = nosyl (p-nitrobenzenesulfonyl); bp = 4,7-diphenyl,1-10-phenantroline; Ad = adamantyl; Me_3NN = β-diketiminate; $Tp^{*,Br}$ = hydrotris (3,5-dimethyl-4-bromopyrazolyl)borate); *R** = S(=O)(NTs)(p-Tol)

Table 6.5 Metal-catalyzed functionalization of adamantane by nitrene insertion

Entry	Nitrene source	Catalyst	Temperature (°C)	Yield (%)	Reference
1	TsNClNa	$FeCl_2$	16	16	[102]
2	NsNIPh	$Rh_2(OAc)_4$	83	76	[103]
3	TsNIPh	Ru(TPFPP)(CO)	40	74	[112]
4	TsNIPh	Mn(TPFPP)Cl	40	80	[112]
5	TsNIPh	$Ru(Me_3tacn)(L_3)$	rt	57	[113]
6	TsNIPh	$ZnBr_2$	50	22	[114]
7	$PhI(OCO^tBu)_2/H_2NR^*$	Rh_2-{(*S*)-nta}$_4$	rt	94	[110,111]

[a] Abbreviations: Ts = tosyl (p-toluenesulfonyl); TPFPP = tetrakis(pentafluorophenyl)porphyrin; Me_3tacn = N, N′, N″-trimethyl-1,4,7-triazacyclononane. R* = S(=O)(NTs)(p-Tol)

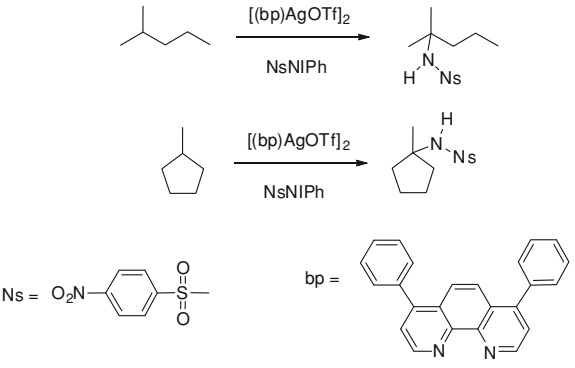

Scheme 6.28 Alkane functionalization with the disilver catalyst precursor [(bp) $AgOTf]_2$

The results shown in Table 6.5 regarding the use of adamantane are somewhat those expected, since the reaction site, a tertiary C–H bond, is more prone to undergo the insertion that the secondary C–H bonds of cyclohexane. Muller's work provided 76 % of the amine derivatives, as a mixture (71:5) of the products formed from the functionalization of tertiary and secondary sites, respectively (Table 6.5, entry 2) [103]. Catalytic systems described by Che (Ru, Mn) [112, 113], and Nicholas [114] (Zn) were similar in activity, but at lower temperatures (Table 6.5, entries 3–6). The already mentioned chiral system by Dauban et al. gave higher conversions for adamantane than for cyclohexane (compare Table 6.4, entry 13 with Table 6.5 entry 7) [110, 111].

6.3.4 Linear and Branched Alkanes

The extension of this methodology to plain, linear or branched alkanes is yet scarce, and very few examples have appeared in the literature. He and co-workers described with their di-silver catalyst, along with the above data for cycloalkanes, the use of 2-methylpentane as well as methylcyclopentane (Scheme 6.28) [107]. Yields were moderate (22–29 %), with a preferential functionalization of the tertiary sites, with NsNIPh as the NR precursor.

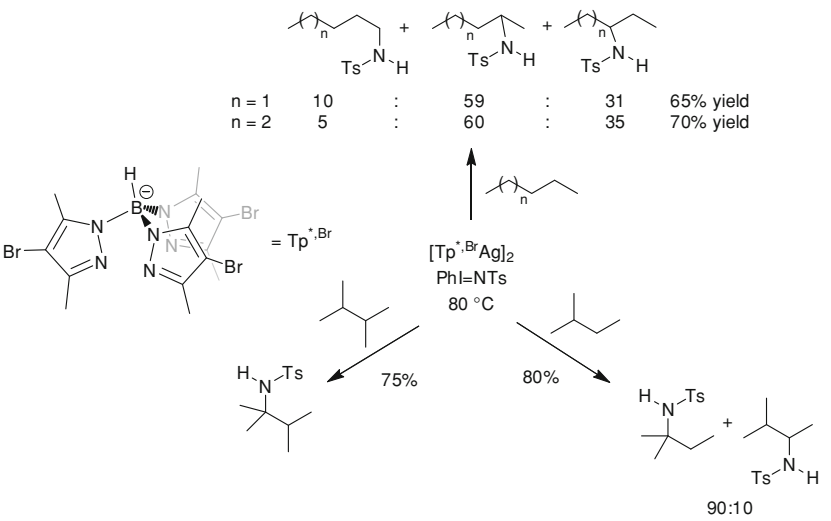

Scheme 6.29 $Tp^{*,Br}Ag$-catalyzed alkane functionalization by nitrene insertion

Scheme 6.30 Rhodium-catalyzed functionalization of an open-chain alkane by nitrene insertion

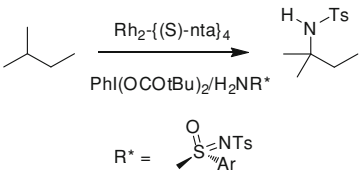

The second silver-based catalytic system described by Pérez group, that contains a $Tp^{*,Br}$ ligand, has been applied to a number of alkanes, as shown in Scheme 6.29 [109]. Linear (pentane, hexane) or branched (2-methylbutane, 2,3-dimethylbutane) saturated hydrocarbons were converted into mixtures of amines, with observed yields within the range 65-80 %. This system has also provided a comparison between the distinct reaction sites in a given substrate. Thus, as inferred from the relative ratio of products, a clear trend in reactivity of 3ry C–H > 2ry C–H > 1ry C–H was extracted. Although this is similar to the trend also observed in the already discussed C–H bond functionalization by carbene insertion processes, both transformations are not as similar as one could think (see the subchapter about mechanistic considerations).

The sulfonimidamide-based catalytic system has also been described [110, 111] to modify 2-methylbutane in moderate yield, again only the tertiary C–H bond being the preferred reaction site (Scheme 6.30).

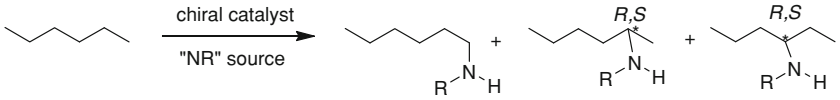

Scheme 6.31 Ideal asymmetric functionalization of n-hexane by nitrene insertion

6.3.5 Asymmetric Functionalization by Nitrene Insertion

Following the results shown in Scheme 6.29, it could be envisaged that with an appropriate chiral catalyst a certain enantiomeric excess could be induced in the formation of the C2- and C3- C–H bonds of n-hexane. However, this reaction, i.e., the asymmetric insertion of a nitrene unit into a C–H bond of an alkane (Scheme 6.31), remains undiscovered.

There are a few reports in the literature in which a C–H bond of a hydrocarbon molecule has been modified upon NR insertion. In all case, the substrates correspond to those shown in Scheme 6.25, the functionalization taking place in somewhat activated positions such as benzylic or allylic sites. For the sake of completeness, and as a possible guide to future development toward plain alkanes, the results described with indane are presented in this section. Other substrates such as ethylbenzene or tetrahydronaphtalenes displayed similar yields and ees to that, and need no further comments.

The first example of the asymmetric amination of indane (Table 6.6) upon nitrene insertion was reported by Müller, with a dirhodium complex bearing a binaphtol-derived ligand and NsNIPh (entry 1). [103] The modest 31 % ee was later reproduced by Che with chiral Ru- and Mn-based porphyrin complexes and PhINTs (entry 2) [115], before Katsuki would describe with the same nitrene source the use of a Mn(Salen) catalyst for this transformation, with a 44 % ee (entry 1) [116]. A noticeable increase in enantioselection was introduced by Hashimoto, that rediscovered dirhodium complexes [117], with leucinate-derived ligands, reaching 70 % of ee (entry 4). Subsequent improvement was based in the variation of the ancillary, chiral ligand onto dirhodium complexes. Thus, Davies showed that adamantylglycine chelating ligands promoted the insertion of nitrene groups in the benzylic position of adamantane with a 94% ee, in a protocol in which the nitrene precursor was generated in situ upon mixing $NsNH_2$ and $PhI(OAc)_2$ (entry 5) [118].

The last example has been developed by Dauban and co-workers using a chiral nitrene source [110, 111]. When a pure sulfonimidamide was employed along with $PhI(OCO^tBu)_2$ in the presence of a chiral rhodium complex as the catalyst, very high diastereomeric excesses were obtained with several activated hydrocarbons. In the particular case of indane >98 % de were obtained, as the consequence of a nearly complete control of the enantioselectivity by the metal center (Scheme 6.32, 6.33). Unfortunately, this system does not seem to promote the transformation shown in Scheme 6.31 with linear alkanes.

Table 6.6 Asymmetric amination of indane by nitrene insertion[a]

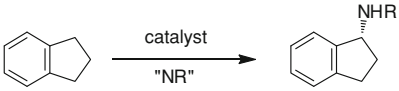

Entry	Nitrene source	Catalyst	Yield (%)	ee (%)	Reference
1	NsNIPh	$Rh_2(L_1{}^*)_4$	71	31	[103]
2	TsNIPh	M(por*) (M = Ru, Mn)	47	31	[115]
3	TsNIPh	$Mn(salen)PF_6$	63	44	[116]
4	NsNIPh	Rh_2(*S*-TCPTTL)$_4$	82	70	[117]
5	$NsNH_2/PhI(OAc)_2$	Rh_2(*S*-TCPTAD)$_4$	95	94	[118]

[a] See Scheme 6.32 for ligands in entries 1, 3, 4 and 5; see Scheme 6.16, II, for ligand por*

Scheme 6.32 Chiral ligands and complexes employed in the asymmetric amination of indane by nitrene insertion

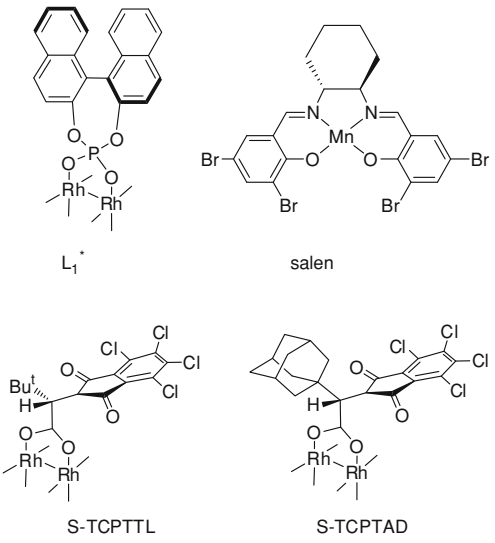

6.3.6 *Mechanistic Considerations*

The catalytic data presented in the previous section have been obtained with several metal-based complexes: ruthenium, rhodium, iron, manganese, copper and silver provided the more relevant results. Due to the lack of a number of catalytic systems that operate with plain alkanes, most mechanistic studies have been performed with somewhat activated C–H bonds. However, in this case it seems reasonable to assume that the reaction pathways should be common for both activated and non-activated hydrocarbons.

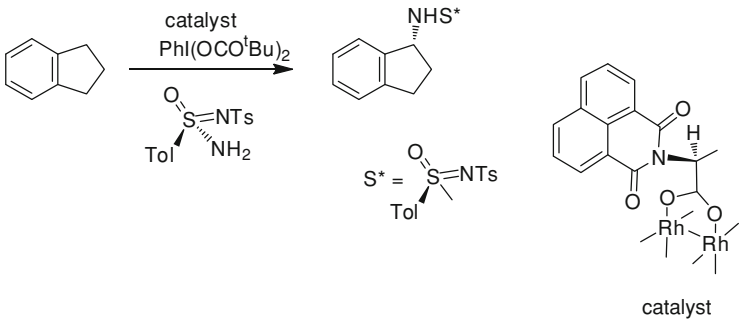

Scheme 6.33 Diastereoselective functionalization of indane with Dauban′s sulfinimidamides

Scheme 6.34 Structurally characterized nitrene complexes relevant for nitrene transfer reactions to C–H bonds

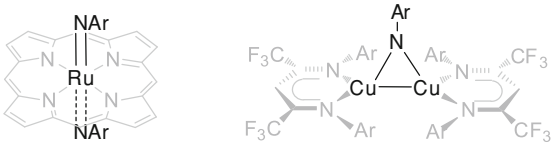

(a) **(b)**

6.3.6.1 Metallonitrene Species as Intermediates

The formation of unsaturated metallonitrenes $L_nM{=}NR$ as intermediates in this process is well-documented, due to the isolation in some cases of complexes with such moiety that serve as NR transfer agents. Che and co-workers first isolated ruthenium-nitrene complexes upon reacting a ruthenium (II)-porphyrin complex with PhI=NTs [119, 120]. The resulting bis (imido) complex underwent stoichiometric transfer of the NTs group to olefins as well as to benzylic C–H bonds (Scheme 6.34a). A similar bis (imido) complex with nearly identical reactivity has been reported by Gallo and co-workers [121] with an aryl azide as the nitrene source. Warren's group [122] have also demonstrated the presence of nitrene intermediates in the copper-catalyzed C–H amination reaction. In this case, a dinuclear, nitrene-bridged structure was obtained from an azide an a Cu (I) source (Scheme 6.34b). Rhodium-nitrene intermediates have resulted elusive to date.

At variance with the already discussed nature of the carbene transfer reaction, in which the CR^1R^2 is transferred from the metal center to the C–H bond through a concerted pathway (see Schemes 6.20 and 6.21), the nitrene reaction has brought some controversy among the researchers in the field. This is due to the existence of two possible reaction pathways depending of the electronic nature of the metallonitrene intermediate, that could be either a singlet nitrene or a triplet nitrene (Scheme 6.35) [123]. It could be thought that the former should behave in a similar manner to the carbene transfer process, operating as a concerted mechanism. On the other hand, the participation of triplet nitrenes should favor a stepwise mechanism, with radical species being involved. The available mechanistic data are presented in the following section.

Scheme 6.35 The metallonitrene singlet and triplet states and the respectively derived concerted or stepwise reaction pathways

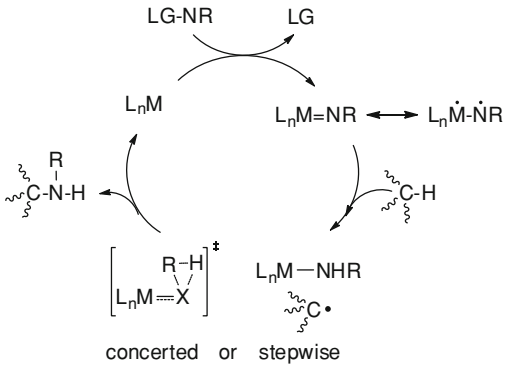

6.3.6.2 Concerted or Step-Wise? That is the Question

To discern about this two possibilities, a number of experiments have systematically been employed (Scheme 6.36). For example, competition experiments with p-substituted ethyl benzenes would provide relative reactivities that depend of the electronic nature of the X group. Data analysis with Hammett's equation usually gives information about the electrophilic nature of the intermediate, as well as about the concerted/stepwise routes by analogy with the well-known carbene transfer process (Scheme 6.36a). A second type of experiment is based in the use of radical-clocks that contain functional groups (e.g. cyclopropane rings) that could react if radical species are involved (Scheme 6.36b). The addition of radical traps constitutes an additional tool in these studies. However, the last two experiments should be carefully performed, since the observance of any effect depends of the relativity rates with the coupling of the R-radical and the L_nM–NHR species. If the latter proceeds at a very high rate, then effect of radical-clocks or radical inhibitors could be masked. The use of an enantiomeric pure substrate to analyse whether or not the reaction proceeds with retention or inversion (total or partial) of the configuration has also been invoked to respectively support concerted or stepwise processes (Scheme 6.36c). Kinetic isotope effects have also been employed (Scheme 6.36d), since both routes have been described with a large different in KIEs (1–2 for concerted, >6 for step-wise).

With data arisen from the above experiments, mechanistic proposals have been built for the catalytic systems reported to date. The ruthenium- [119, 120], cobalt- [124, 125] and silver-based [109] catalysts behave in the expected manner for a stepwise reaction pathway. The reaction proceeds from the nitrene intermediate upon hydrogen abstraction from the hydrocarbon, generating a carbon radical. This species further attacks the nitrogen atom, in a process similar to the so-called *rebound* mechanism that has been explained in Chap. 5 for the C–H bond oxygenation reaction. The rate at which this interaction takes place is usually very high, since the radical does not diffuse to the reaction mixture and stays very close

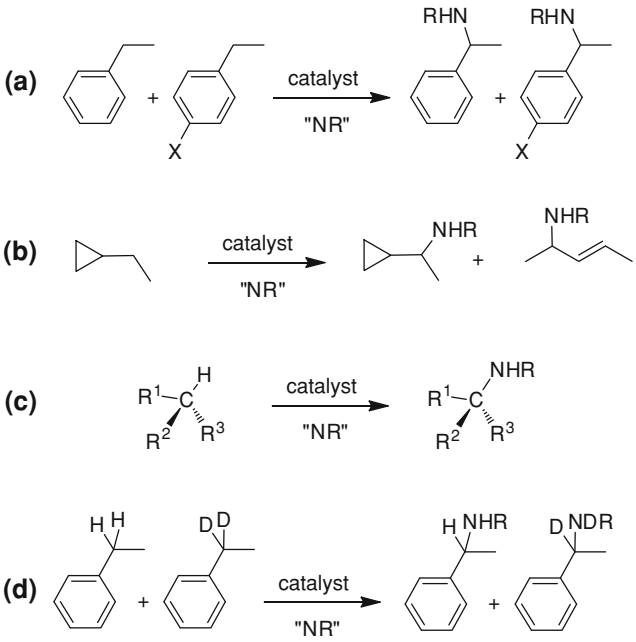

Scheme 6.36 Frequently employed experiments to ascertain between concerted and stepwise mechanisms

to the catalyst. Because of this, it is common that some experiments directed to the support of the presence of radicals (radical clocks, retention/inversion of the configuration, radical traps) do not provide that information.

In the rhodium case, some authors have proposed the concerted pathway, although not all the experimental evidences are in complete accord with this. For instance, work by Müller [103, 126] proposed the one step mechanism on the basis of several experiments (also supported by Du Bois' studies) [127, 128] whereas Dauban has shown some doubts due to the collection of contradictory data: [129] Hammett analyses supported the concerted pathway but KIE studies did not. DFT studies have shown that singlet and triplet states for Rh_2-$^{II,\,II}$-NR are very close in energy [130], and therefore small changes in the catalytic system could influence the reaction pathway. One of the factors could be the nature of the nitrene source that is probably far to be innocent. Thus, it has been proposed that the use of –NAr sources with an electron withdrawing group accelerates the NR transfer due to an enlargement of the M-N (nitrene) distance [119, 120, 131]. Such effect would also affect the relative reactivity toward the reaction probes, again altering the competition experiments. In accord with this, it has to be pointed out that Müller's work was done with NsNIPh, whereas Dauban's studies were carried out with chiral sulfinimidamides.

6.4 Work Ahead

It seems clear that the functionalization of C–H bonds of alkanes, intended as non-activated hydrocarbons, is achievable from both the carbene or nitrene insertion processes. However, catalyst development is yet necessary to afford the following goals:

(a) Improvement of the regioselectivity, exerting the control of the C–H bond to be modified in a given substrate. Of particular interest is the exclusive functionalization of primary sites.
(b) More efficient chiral catalysts. Just a few examples for both reactions are known, from an asymmetric point of view. In the nitrene case, the use of plain alkanes is yet unreported.
(c) Development of heterogeneous systems that would allow easy catalyst and products separation as well as catalyst recycling is also desirable, once the above goals have been achieved.
(d) Extensive mechanistic studies in the nitrene transfer case, since the mechanism is yet far to be completely understood and it is excessively system-dependent.

Overall, this methodology is yet far to be considered exhausted, and future work will for sure provide breakthroughs in the area of alkane functionalization.

Acknowledgments We thank all the past and present members of the Laboratorio de Catálisis Homogénea (Universidad de Huelva) for their contributions to the chemistry related to the topic of chapter. We also wish to thank the continuous funding by the Subdirección General de Proyectos de Investigación since 2000 (R&D National Plan), and particularly the current grant (CTQ2011-28942-CO2-O1). We also thank Junta de Andalucía (P10-FQM-6292) and Universidad de Huelva (Plan Propio de Investigación) for funding along the years.

References

1. Goldberg KI, Goldman AS (eds) (2004) Activation and functionalization of C–H bonds, ACS symposium series 885, American Chemical Society, Washington
2. Dyker G (ed) (2005) Handbook of C–H transformations, vol 1, Wiley–VCH, Weinheim
3. Shilov AE, Shul'pin GB (2000) Activation and catalytic reactions of saturated hydrocarbons in the presence of metal complexes. Kluwer, Dordrecht
4. Bergman RG (2007) Nature 446:391–393
5. Labinger JA, Bercaw JE (2002) Nature 417:507–513
6. Arndtsen BA, Bergman RG, Mobley TA, Peterson TH (1995) Acc Chem Res 28:154–162
7. Janowicz AH, Bergman RG (1982) J Am Chem Soc 104:352–354
8. Hartwig JF (2009) Organotransition metal chemistry: from bonding to catalysis, University Science books, Sausalito
9. Bernskoetter WH, Schauer CK, Goldberg KI, Brookhart M (2009) Science 326:553–556
10. Newhouse T, Baran PS (2011) Angew Chem Int Ed 50:3362–3374
11. Davies HML, Dick AR (2010) Top Curr Chem 292:303–345
12. Doyle MP, Duffy R, Ratnikov M, Zhou L (2010) Chem Rev 110:704–724
13. Díaz-Requejo MM, Pérez PJ (2008) Chem Rev 108:3379–3394

14. Díaz-Requejo MM, Belderraín TR, Nicasio MC, Pérez PJ (2006) Dalton Trans 5559–5566
15. Davies HML, Beckwith REJ (2003) Chem Rev 103:2861–2903
16. Davies HML, Manning JR (2008) Nature 451:417–424
17. Zalatan DN, Du Bois J (2010) Top Curr Chem 292:347–378
18. Halfen JA (2005) Curr Org Chem 9:657–669
19. Müller P, Fruit C (2003) Chem Rev 103:2905–2919
20. Doyle MP, McKervey MA, Ye T (1998) Modern catalytic methods for organic synthesis with diazo compounds. Wiley, New York
21. See reference 20 for examples based on Fe, Ru, Os, Co, Rh, Ni, Pd, Pt and Cu
22. For iridium as catalyst: Kubo T, Sakagushi S, Ishii Y (2000) Chem Commun 625–626
23. For silver as catalyst: Dias HVR, Browning RG, Richey SA, Lovely CJ (2004) Organometallics 23:1200–1202
24. For silver as catalyst: Dias HVR, Browning RG, Richey SA, Lovely CJ (2005) Organometallics 24:5784
25. For silver as catalyst: Urbano J, Belderrain TR, Nicasio MC, Trofimenko S, Díaz-Requejo MM, Pérez PJ (2005) Organometallics 24:1528–1532
26. For gold-based catalyst: Fructos MR, Belderrain TR, Frémont P, Scott NM, Nolan SP, Díaz-Requejo MM, Pérez PJ (2005). Angew Chem Int Ed 44:5284–5288
27. For gold as catalyst: Fructos MR, de Frémont P, Nolan SP, Díaz-Requejo MM, Pérez PJ (2006) Organometallics 25:2237–2241
28. Maxwell JL, Brown KC, Bartley DW, Kodadek T (1992) Science 256:1544–1547
29. Bartley DW, Kodadek T (1993) J Am Chem Soc 115:1656–1660
30. Maxwell JL, O′Malley S, Brown KC, Bartley DW, Kodadek T (1992) Organometallics 11:645–652
31. Collman JP, Rose E, Venburg GD (1993) J Chem Soc Chem Commun 934–935
32. Woo LK, Smith DA (1992) Organometallics 11:2344–2346
33. Smith DA, Reynolds DN, Woo LK (1993) J Am Chem Soc 115:2511–2513
34. Djukic J-P, Smith DA, Young VG, Woo LK (1994) Organometallics 13:3020–3026
35. Li Y, Huang J-S, Zhou Z-Y, Che C-M (2001) J Am Chem Soc 123:4843–4844
36. Che C-M, Huang J-S, Lee F-W, Li Y, Lai T-S, Kwong H-L, Teng P-F, Lee W-S, Lo W-C, Peng S-M, Zhou Z-Y (2001) J Am Chem Soc 123:4119–4129
37. Deng Q-H, Chen J, Huang J-S, Chui SS-Y, Zhu N, Li G-Y, Che C-M (2009) Chem Eur J 15:10707–10712
38. Galardon E, Le Maux P, Toupet L, Simonneaux G (1998) Organometallics 17:565–569
39. Park S-B, Sakata N, Nishiyama H (1996) Chem Eur J 2:303–306
40. Lee H-M, Bianchini C, Jia G, Barbaro P (1999) Organometallics 18:1961–1966
41. Ranocchiari M, Mezzetti A (2009) Organometallics 28:3611–3613
42. Lu H, Dzik WI, Xu X, Wojtas L, de Bruin B, Zhang XP (2011) J Am Chem Soc 133:8518–8521
43. Kirmse W (2003) Angew Chem Int Ed 42:1088–1093
44. Straub BF, Hofmann P (2001) Angew Chem Int Ed Engl 40:1288–1290
45. Hofmann P, Shishkov IV, Rominger F (2008) Inorg Chem 47:11755–11762
46. Shishkov IV, Rominger F, Hofmann P (2009) Organometallics 28:1049–1059
47. Dai XL, Warren TH (2004) J Am Chem Soc 126:10085–10094
48. Mankad NP, Peters JC (2009) Chem Commun 1061–1063
49. Novak J, Ratusky J, Sneberk V, Sorm F (1957) Collect Czech Chem C 22:1836–1851
50. Scott LT, DeCicco GJ (1974) J Am Chem Soc 96:322–323
51. Wulfman DS, McDaniel RS, Peace BW (1976) Tetrahedron 32:1241–1249
52. Demonceau A, Noels AF, Hubert A, Teyssié P (1981) J Chem Soc Chem Commun 688–689
53. Demonceau A, Noels AF, Hubert A, Teyssié P (1984) Bull Soc Chim Belg 93:945–948
54. Demonceau A, Noels AF, Teyssié P, Hubert A (1988) J Mol Catal 49:L13–L17
55. Demonceau A, Noels AF, Hubert A (1989) J Mol Catal 57:149–152
56. Callot HJ, Metz F (1982) Tetrahedron Lett 23:4321–4324
57. Davies HML, Hansen T, Churchill MRJ (2000) J Am Chem Soc 122:3063–3070

58. Davies HML, Hansen T (1997) J Am Chem Soc 119:9075–9076
59. Davies HML, Antoulinakis EG (2001) J Organomet Chem 617–618:47–55
60. Díaz-Requejo MM, Belderrain TR, Nicasio MC, Trofimenko S, Pérez P (2002) J Am Chem Soc 124:896–897
61. Caballero A, Díaz-Requejo MM, Belderrain TR, Nicasio MC, Trofimenko S, Pérez P (2003) J Am Chem Soc 125:1446–1447
62. Caballero A, Díaz-Requejo MM, Belderrain TR, Nicasio MC, Trofimenko S, Pérez PJ (2003) Organometallics 22:4145–4150
63. Rangan K, Fianchini M, Singh S, Dias HVR (2009) Inorg Chim Acta 362:4347–4352
64. Despagnet-Ayoub E, Jacob K, Vendier L, Etienne M, Álvarez E, Caballero A, Díaz-Requejo MM, Pérez PJ (2008) Organometallics 27:4779–4787
65. Pérez J, Morales D, García Escudero LA, Martínez-García H, Miguel D, Bernad P (2009) Dalton Trans 375–382
66. Lovely CJ, Flores JA, Meng X, Dias HVR (2009) Synlett 129–132
67. Endres A, Maas G (2002) J Organomet Chem 643:174–180
68. Rodríguez P, Álvarez E, Nicasio MC, Pérez PJ (2007) Organometallics 26:6661–6668
69. Mbuvi HM, Woo LK (2008) Organometallics 27:637–645
70. Thu H-Y, Tong GS-M, Huang J-S, Chan SL-F, Deng Q-H, Che C-M (2008) Angew Chem Int Ed 47:9747–9751
71. Choi MK-W, Yu W-Y, So M-H, Zhou C-Y, Deng Q-H, Che C-M (2008) Chem Asian J 3:1256–1265
72. Díaz-Requejo MM, Wehrmann P, Leatherman MD, Trofimenko S, Mecking S, Brookhart M, Pérez PJ (2005) Macromolecules 38:4966–4969
73. Caballero A, Despagnet-Ayoub E, Díaz-Requejo MM, Díaz-Rodríguez A, González-Núñez ME, Mello R, Muñoz BK, Ojo W-S, Asensio G, Etienne M, Pérez PJ (2011) Science 332:835–838
74. Alonso ME, García MC (1989) Tetrahedron 45:69–76
75. Demonceau A, Noels AF, Costa JL, Hubert A (1990) J Mol Catal 58:21–26
76. Wang P, Adams J (1994) J Am Chem Soc 116:3296–3305
77. Doyle MP, Westrum LJ, Wolthuis WNE, See MM, Boone WP, Bagheri V, Pearson MM (1993) J Am Chem Soc 115:958–964
78. Tauber DF, Rucle RE Jr (1986) J Am Chem Soc 108:7686–7693
79. Tauber DF, Petty EH, Raman K (1985) J Am Chem Soc 107:196–199
80. Padwa A, Austin DJ, Price AT, Semones MA, Doyle MP, Protopopova MN, Winchester WR, Tran A, Tauber DF, Rucle RE Jr (1993) J Am Chem Soc 115:8669–8680
81. Pirrung MC, Morehead AT Jr, Tauber DF, Rucle RE Jr (1994) J Am Chem Soc 116:8991–9000
82. Wang J, Chen B, Bao J (1998) J Org Chem 63:1853–1862
83. Nakamura E, Yoshikai N, Yamanaka M (2002) J Am Chem Soc 124:7181–7192
84. Braga AAC, Maseras F, Urbano J, Caballero A, Díaz-Requejo MM, Pérez PJ (2006) Organometallics 25:5292–5300
85. Braga AAC, Caballero A, Urbano J, Díaz-Requejo MM, Pérez PJ, Maseras F (2011) Chemcatchem 3:1646–1652
86. Kwart H, Khan AA (1967) J Am Chem Soc 89:1951–1953
87. Chang JWW, Ton TMU, Chan PWH (2011) Chem Rec 11:331–357
88. Collet F, Dodd RH, Dauban P (2009) Chem Commun 5061–5064
89. Collet F, Lescot C, Dauban P (2011) Chem Soc Rev 40:1926–1936
90. Blanksby SJ, Ellison GB (2003) Acc Chem Res 36:255–263
91. Tian Z, Fattahi A, Lis L, Kass SR (2006) J Am Chem Soc 128:17087–17092
92. Burkey TJ, Castelhano AL, Griller D, Lossing FP (1983) J Am Chem Soc 105:4701–4703
93. Davies HML, Long MS (2005) Angew Chem Int Ed 44:3518–3520
94. Breslow DS, Sloan MF (1968) Tetrahedron Lett. 5349–5352
95. Yamada Y, Yamamoto T, Okawara M (1975) Chem. Lett 361–362

96. Södergren MJ, Alonso DA, Bedekar AV, Andersson PG (1997) Tetrahedron Lett 38:6897–6900
97. Barman DN, Liu P, Houk KN, Nicholas KN (2010) Organometallics 29:3404–3412
98. Albone DP, Challenger S, Derrick AM, Fillery SM, Irwin JL, Parsons CM, Takada H, Taylor PC, Wilson DJ (2005) Org Biomol Chem 3:107–111
99. Harden JD, Ruppel JV, Gao G-Y, Zhang XP (2007) Chem Commun 4644–4646
100. Vhanda BM, Vyas R, Bedekar AV (2001) J Org Chem 66:30–34
101. Breslow R, Gellman SH (1982) J Chem Soc Chem Commun 1400–1401
102. Barton DHR, Hay-Motherwell RS, Motherwell WB (1983) J Chem Soc Perkin Trans I 445–451
103. Nageli I, Baud C, Bernardelli G, Jacquier Y, Moran M, Muller P (1997) Helv Chim Acta 80:1087–1105
104. Díaz-Requejo MM, Belderrain TR, Nicasio MC, Trofimenko S, Pérez P J(2003) J Am Chem Soc 125:12078–12079
105. Fructos MR, Trofimenko S, Díaz-Requejo MM, Pérez PJ (2006) J Am Chem Soc 128:11784–11791
106. Espino CG, Fiori KW, Kim M, Du Bois J (2004) J Am Chem Soc 126:15378–15379
107. Li Z, Capretto DA, Rahaman RO, He C (2007) Angew Chem Int Ed 46:5184–5186
108. Baidei YM, Dinescu A, Dai X, Palomino RM, Heinemann FW, Cundari TR, Warren TH (2008) Angew Chem Int Ed 47:9961–9964
109. Gómez-Emeterio BP, Urbano J, Díaz-Requejo MM, Pérez PJ (2008) Organometallics 27:4126–4130
110. Liang C, Collet F, Robert-Peillard F, Müller P, Dodd RH, Dauban P (2008) J Am Chem Soc 130:343–350
111. Liang C, Robert-Peillard F, Fruit C, Müller P, Dodd RH, Dauban P (2006) Angew Chem Int Ed 45:4641–4644
112. Yu X-Q, Huang J-S, Zhou X-G, Che C-M (2000) Org Lett 2:2233–2236
113. Au S-M, Huang J-S, Che C-M, Yu W-Y (2000) J Org Chem 65: 7858–7854
114. Kalita B, Lamar AA, Nicholas KM (2008) Chem Commun 4291–4293
115. Zhou X-G, Yu X-Q, Huang J-S, Che C-M (1999) Chem Commun 2377–2378
116. Kohmura Y, Katsuki T (2001) Tetrahedron Lett 42:3339–3342
117. Yamawaki M, Tsutsui H, Kitakagi S, Anada M, Hashimoto S (2002) Tetrahedron Lett 43:9561–9564
118. Reddy RP, Davies HML (2006) Org Lett 8:5013–5016
119. Au S-M, Huang J-S, Yu W-Y, Fung W-H, Che C-M (1999) J Am Chem Soc 121:9120–9132
120. Leun SK-Y, Tsui W-M, Huang J-S, Che C-M, Liang J-L, Zhu N (2005) J Am Chem Soc 127:16629–16640
121. Fantauzzi S, Gallo E, Caselli A, Ragaini F, Casati N, Macchi P, Cenini S (2009) Chem Commun 3952–3954
122. Badiei YM, Krishnaswamy A, Melzer MM, Warren TH (2006) J Am Chem Soc 128:15056–15057
123. Cundari TR, Dinescu A, Kazi AB (2008) Inorg Chem 47:10067–10072
124. Lyaskovskyy V, Olivos Suarez AI, Lu H, Jiang H, Zhang XP, de Bruin B (2011) J Am Chem Soc 133:12264–12273
125. Ragaini F, Penoni A, Gallo E, Tollari S, Li Gotti C, Lapadula M, Mangioni E, Cenini S (2003) Chem Eur J 9:249–259
126. Müller P, Baud C, Naegeli I (1998) J Phys Org Chem 11:597–601
127. Zalatan DN, Du Bois J (2008) J Am Chem Soc 130:9220–9221
128. Fiori KW, Du Bois J (2007) J Am Chem Soc 129:562–568
129. Collet F, Lescot C, Dauban P (2010) Dalton Trans 39:10401–10413
130. Lin X, Zhao C, Che C-M, Ke Z, Phillips DL (2007) Chem Asian J 2:1101–1108
131. Moreau Y, Chen H, Derat E, Hirao H, Bolm C, Shaik S (2007) J Phys Chem B 111:10288–10299

Index

P. J. Pérez (ed.), *Alkane C–H Activation by Single-Site Metal Catalysis*, Catalysis by Metal Complexes 38, DOI: 10.1007/978-90-481-3698-8,

© Springer Science+Business Media Dordrecht 2012